AD NUMBER
AD822520

NEW LIMITATION CHANGE

TO

Approved for public release, distribution unlimited

FROM

Distribution authorized to U.S. Gov't. agencies and their contractors; Critical Technology; SEP 1967. Other requests shall be referred to Air Force Materials Laboratory, Wright-Patterson AFB, OH 45433.

AUTHORITY

AFSC ltr dtd 26 May 1972

AD822520

SEMI-RIGID OR NON-RIGID STRUCTURES FOR RE-ENTRY APPLICATIONS

J. F. Keville

Space-General, a Division of
Aerojet-General Corporation

September 1967

FINAL TECHNICAL REPORT AFML-TR-67-310

Project No. 7-943b

Part 2 Fabrication and Test

Air Force Materials Laboratory
Research and Technology Division
Air Force Systems Command
Wright-Patterson Air Force Base, Ohio

AFML-TR-67-310

SEMI-RIGID OR NON-RIGID STRUCTURES
FOR RE-ENTRY APPLICATIONS

J. F. Keville

Space-General, a Division of
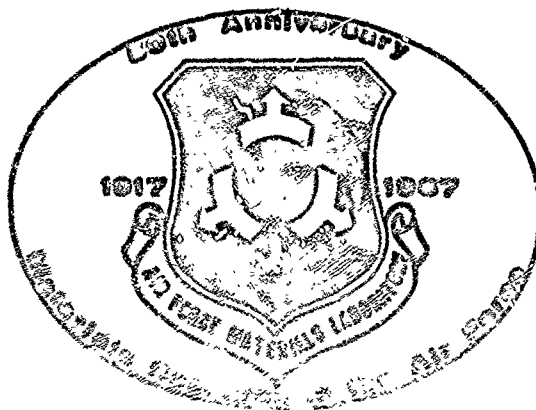Aerojet-General Corporation

September 1967

FINAL TECHNICAL REPORT AFML-TR-67-310

Project No. 7-943b

Part 2 Fabrication and Test

This document is subject to special export controls and each
transmittal to foreign governments or foreign nationals may
be made only with prior approval of the Air Force Materials
Laboratory (MATF) Wright-Patterson Air Force Base, Ohio
45433.

Air Force Materials Laboratory
Research and Technology Division
Air Force Systems Command
Wright-Patterson Air Force Base, Ohio

FOREWORD

This Final Technical Report covers all work performed under contract AF 33(657)-10252 from 15 January 1963 to 15 January 1967. The manuscript was released by the author September 1967 for publication as an RTD Technical Report.

This contract with the Space-General Plant, Aerojet-General Corporation, El Monte, California, was initiated under ASD (subsequently RTD) Project Number 7-943b, entitled "Semi-Rigid or Non-Rigid Structures for Re-entry Applications." It was accomplished under the technical direction of Mr. Thomas Campbell, MATF (now ASKMM), of the Manufacturing Technology Division, Air Force Materials Laboratory, Wright-Fatterson Air Force Base, Ohio.

Mr. J. F. Keville was the Program Manager for Space-General. Others who participated in the development, fabrication, and test work in this project were:

A. F. Baca, Stress and Loads Analyst
M. K. Barsh, Materials Systems Specialist
C. J. Barton, Vehicle Design Engineer
C. R. Burnett, Materials Engineer
J. E. Crawford, Manager, Expandable Structures Department
G. H. Fredy Jr., Test Engineering Supervisor
W. A. Grant, Welding Engineering
J. G. Guidero, Project Staff Engineer
W. Hatalsky, Aerodynamicist
J. S. Haynes, Test Engineer
C. S. Horine, Senior Engineer
J. C. Huisking, Manufacturing Engineer
J. D. McNerney, Aerodynamicist
J. V. Miller, Design Specialist
J. E. Misselhorn, Thermodynamicist
R. A. Morrison, Design Specialist
A. H. Olsen, Senior Engineer
R. B. Robinson, Materials and Processes Engineer
J. R. Schrink, Manufacturing Engineer
S. L. Tomkinson, Project Staff Engineer
F. Warren, Program Management Office
J. A. Wrede, Materials Scientist

In addition to these Space-General technical personnel, numerous other technicians and project support personnel, as well as subcontractor technical personnel, participated significantly in the completion of this work.

FOREWORD (Continued)

This project has been accomplished as a part of the Air Force Manufacturing Methods Program, the primary objective of which is to develop, on a timely basis, manufacturing processes, techniques and equipment for use in economical production of USAF materials and components.

Suggestions concerning additional manufacturing methods development required on this or other subjects will be appreciated.

This technical report has been reviewed and is approved.

C. H. NELSON, Assistant Chief
Manufacturing Technology Division
Air Force Materials Laboratory

ABSTRACT

This study, fabrication and test program was undertaken to determine the most suitable structural design, using available materials, for inflatable re-entry vehicles and space structures, to develop suitable manufacturing processes and techniques, and to perform tests on the resulting components of a typical re-entry paraglider. The results are applicable to other types of structures. This final technical report covers the period 15 January 1963 to 15 January 1967. Materials system development was conducted in conjunction with re-entry, aero-thermodynamic studies and vehicle structural design. A two-ply, ultra-fine, multifilament, nickel-chromium metal fabric, impregnated and coated with two different types of silicone rubber, was chosen as the basic structural and inflatable membrane of the re-entry vehicle. Major areas of technology advancement included development of manufacturing and processing techniques for the utilization of ultra-fine metal filament in the manufacture of special metal fabrics; stress analysis, and confirmation by test, of structures constructed of anisotropic woven materials; design and construction of a special, deep-throat, semi-automatic metal fabric welder capable of producing flexible, welded seams of approximately 90 percent efficiency in two through five layers of metal fabric; techniques for thorough impregnation and coating of metal fabric with high-temperature and ablative silicone elastomers, and fabrication methods for the construction of expandable space structures.

CONTENTS

Part 1   Evaluation and Design

CONTENTS (Continued)

Part 2 Fabrication and Test

Part 3 Appendices

ILLUSTRATIONS

Part 1 Evaluation and Design

ILLUSTRATIONS (Continued)

ILLUSTRATIONS (Continued)

viii

ILLUSTRATIONS (Continued)

ILLUSTRATIONS (Continued)

Part 2 Fabrication and Test

ILLUSTRATIONS (Continued)

ILLUSTRATIONS (Continued)

ILLUSTRATIONS (Continued)

xiii

ILLUSTRATIONS (Continued)

ILLUSTRATIONS (Continued)

ILLUSTRATIONS (Continued)

ILLUSTRATIONS (Continued)

ILLUSTRATIONS (Continued)

ILLUSTRATIONS (Continued)

ILLUSTRATIONS (Continued)

TABLES

Part 1 Evaluation and Design

TABLES (Continued)

Part 2 Fabrication and Test

LIST OF SYMBOLS

A	Reference Area
A_n	Acceleration, Normal
A_t	Acceleration, Tangential
c	Specific Heat of Materials, Btu/lb $^\circ$F
c_p	Specific Heat, Btu/lb $^\circ$F
C_D	Drag Coefficient
C_L	Lift Coefficient
C_n	Normal Force Coefficient
C_p	Pressure Coefficient
D	Boom Diameter, inches
E	Young's Modulus
Fg	Load due to Acceleration, pounds/inch
f_o	Force per Unit Length
f_s	Shear Fiber Load
f_t	Tension Fiber Load Due to Internal Pressure
F	Force
$\bar{i}$	Unit Vector in the x Direction
I	Moment of Inertia
$\bar{j}$	Unit Vector in the y Direction
$\bar{k}$	Unit Vector in the z Direction
k	Thermal Conductivity Btu/hr ft^2 $^\circ$F/ft
Ku	Effective Sharp-Edged Gust Velocity, ft/sec
ℓ	Length of Boom from Apex

L/D	Lift-to-Drag Ratio
$\dot{m}$	Mass Ablation Rate
m	Mass per Unit Length
M_v	Keel Moment, inch-pound
M_y	Moment About the Horizontal Axis, inch-pound
M_z	Moment About the Vertical Axis, inch-pound
M	Bending Moment
n_g	Gust Load Factor, Normal to Flight Path
n_z	Gust Load Factor, Normal to Keel
N'/ql	Normal Span Loading
N_θ	Unit Hoop Load, pounds/inch
N_{ϕ_B}	Unit Longitudinal Bending Load, pounds/inch
N_{ϕ_P}	Unit Longitudinal Force Due to Internal Pressure pounds/inch
p	Internal Pressure, pounds/sq. inch
p_s	Boom Shear Unit Loads, pounds/inch
P_s	Increment of Internal Pressure Applied to a Strand
q	Dynamic Pressure, pounds/sq. ft.
$\dot{q}$	Heat Flux, Btu/sec ft^2
q_{cw}	Cold Wall Heat Flux, Btu/sq. ft., sec
$\dot{q}$	Pseudo Heat Flux, Btu/sq. ft., sec
q_ℓ	Heat Flux on Boom
q_s	Heat Flux on Boom at Stagnation Point

Q	Shear Force
Q_c	Heating Rate, Btu/sq. ft., sec
Q_c^*	Effective Heat of Ablation, Btu/lb
r_1	Radius of Curvature
r_2	Distance from Neutral Axis
R	Apex Radius
R_i	Instantaneous Radius
t	Time, sec., or Wall Thickness, in.
T_{av}	Average Temperature of Material During Time (dt), $^{\circ}R$
T_i	Inside Surface Temperature, $^{\circ}R$
T_i	Effective Average Inside Temperature of Material, $^{\circ}R$
T_m	Ablation Temperature, $^{\circ}F$
T_{psm}	Pseudo Melting Temperature, $^{\circ}F$
T_s	Tension in a Longitudinal Strand
T_i	Inside Surface Temperature, $^{\circ}F$
T_o	Outside Surface Temperature, $^{\circ}R$
T_H	Tension in a Hoop Strand
V	Shear Load, pounds
w	Unit weight pounds/in
W	Weight, Pounds
$W/C_D A$	Ballistic Coefficient
W/s	Wing Loading
x, y, z	Coordinate System
$x'/q\ell$	Axial Span Loading

x/ℓ	Keel Station
y/ℓ	Span Station
α	Angle of Attack - Degrees
γ	Cone Semivertex Angle, Degrees
ϵ	External Emissivity at T_o
δ	Thickness of Material, ft.
η	Angle Between Velocity Vector and the Normal to the Surface
θ	Angular Change
θ_i	Re-entry Angle, Degrees
$\iota(\xi)$	E_ξ/E_{ξ_o}, Normalized to Unity at ξ
ξ	Nondimensional Length Coordinate, x/ℓ
Λ	Sweep Angle of L. E. Boom Relative to y-Axis
ρ	Ambient Air Density, lb/ft^3
ρ_m	Density of Material, lb/ft^3
σ	Stefan-Boltzmann Constant
σ_c	Pressure Stress in Cylindrical Section
σ_p	Pressure Stress
σ_s	Shear Stress
σ_t	Pressure Stress in Toroidal Section
$\varphi(\xi)$	Nondimensional Force Distribution Parameter
ψ	Nondimensional Parameter, $\dfrac{\ell^2 F}{EI_o}$
$\omega''(x)$	Transverse Beam Deflection
η	Nondimensional Frequency Parameter, $\dfrac{\ell^4 \omega^2 m_o}{EI_o}$

LIST OF SYMBOLS (Continued)

Subscripts

a	Aft Station
f	Forward Station
n	Normal Component
o	Apex

3. 9. 3. 4 MONITORING WELDER PERFORMANCE

During this program, all patterns of metal fabric that were cut and cleaned were accompanied by coupons for in-process welder checkout. These coupons were cut from the main bolt of fabric adjacent to the area where the pattern was cut. The coupon experienced the same handling and cleaning operations as the main pattern. On the average, one coupon was made for each two feet of seam that had to be welded. At the beginning and end of welding every segment of fabric, and as often as every two feet on welding large segments, a test coupon was welded without changing any of the welder settings. If this coupon did not show at least 80 percent joint efficiency, all of the adjustments and settings were carefully inspected and an evaluation of the fabric history was made. If the fabric was suspected another coupon from a different batch of fabric was welded. After each new adjustment of welder heads, electrode alignment, or power supply settings, a new coupon was welded. Welding was not continued on main test components until the in-process weld check coupons indicated that an efficiency in excess of 80 percent was being obtained.

Occasionally, it was desirable to disconnect the power leads from the upper electrode holders, one at a time, and make a test coupon with a single-row weld. Two coupons, one made with each electrode, could then be tensile tested to determine which electrode system was causing the difficulty.

3. 10   FABRICATION OF TEST COMPONENTS

3. 10. 1   FABRICATION PLANNING

The fabrication technique for construction of the test components, including the full-scale sections of the paraglider, was adopted after an extensive study of the various means of scaling-up the laboratory processes which appeared most favorable. Based on analysis of the results of development work in this program, fabrication of any inflatable, metal fabric structure would include the following steps: layout and cutting of fabric segments from flat material, cleaning, fitting fabric segments on a form tool to produce proper configuration, basting segments together, welding seams, impregnation and coating with silicone rubber, and curing the entire assembly under heat and pressure.

3. 10. 1. 1 PRELIMINARY INVESTIGATIONS

Laying-up the fabric for impregnation and coating with an elastomer requires considerably more care than for impregnation and coating with a thermosetting plastic. Hard plastic is able to carry loads across local areas where the fabric has been inadvertently distorted and fibers poorly oriented (or broken), and can even overcome fairly gross conditions such as folds in the fabric. In contrast, an elastomer, due to its extremely low modulus of

elasticity, will merely deform while any discontinuity and flaws in the fabric lay-up become weak areas in the structure and will show up as reduced strength under loading.

Special care is required to see that all the yarns or fibers of the fabric are properly oriented and stretched out to normal length as woven. If the fabric is trellised or stretched on the bias, compression will result in the direction perpendicular to the stretch direction. This will cause un-normal bending in the yarns. Care in laying-up the fabric is required especially where there is compound curvature of the form. Shaping a fabric to a compound curvature may be accomplished easily by slight compression in certain areas of the fabric, but this is undesirable. The local areas of pre-compressed fabric will be unable to pick up their share of loads when the structure is pressurized and distortion and stress concentration will result.

To evaluate the various pattern configurations and establish the most desirable locations for seams in the apex (the most complicated structure built in this program), a sub-scale plaster mock-up as shown in Figure 110 was constructed. This mock-up was exactly two-thirds the size of the full-scale apex and was used to fabricate an apex from galvanized wire screen. Observation and studies of how this wire screen apex performed when pressurized and loaded led to substantiation of the location of design joints in the proposed full-scale apex. A photograph of the wire screen apex is shown in Figure 111 wherein the soldered joints may be seen clearly. It may be noted that the joints are not symmetrical; actually, two systems of joint locations were evaluated, one on either half of the apex.

The wire screen apex was inflated by building a thin rubber bladder, using rubber cement adhesive joints and inflating this bladder within the screen structure. The wooden handles and closures shown in Figure 111 were used to create bending moments on the structure simulating the loads which would be exerted by the wings and booms in an actual paraglider vehicle.

The plaster mock-up was also used to determine the size and shape of the fabric segments by laying-up pieces of properly cut paper on the form. Since paper does not easily assume a compound curvature shape without wrinkling, paper patterns were ideal for the determination of the amount of inherent yarn compression that would occur when using actual fabric. A compromise was made between the amount of inherent compression and distortion to be tolerated and the number of fabric segments and weld joints required. The plaster form was then wrapped with strips of paper to simulate the mummy-type wrapping of metal fabric tape which would be used to reinforce the crotch areas. It was apparent that a continuous wrapping could not be developed. The final reinforcing took the form of strips of 1-inch wide fabric which radiated from the inside radius to the forward edge of the apex. The plaster form, wrapped to demonstrate the final configuration, with sufficient paper tapes in place to demonstrate the feasibility, is shown in Figures 112 and 113.

235

Figure 110a.   Sub-Scale Plaster Mock-Up of Apex

Figure 110b.   Plaster Mock-Up with Wire Screen Model Being Assembled

236

Figure 111. Sub-Scale Wire Apex

335/019

Figure 112. Plan View - Apex Mock-Up Wrapped with Cloth Strips

335/027

238

335/026

Figure 113. Side View - Apex Mock-Up Wrapped with Cloth Strips

Figure 117. Basting Frustum Bias-Ply Segment

335/178

246
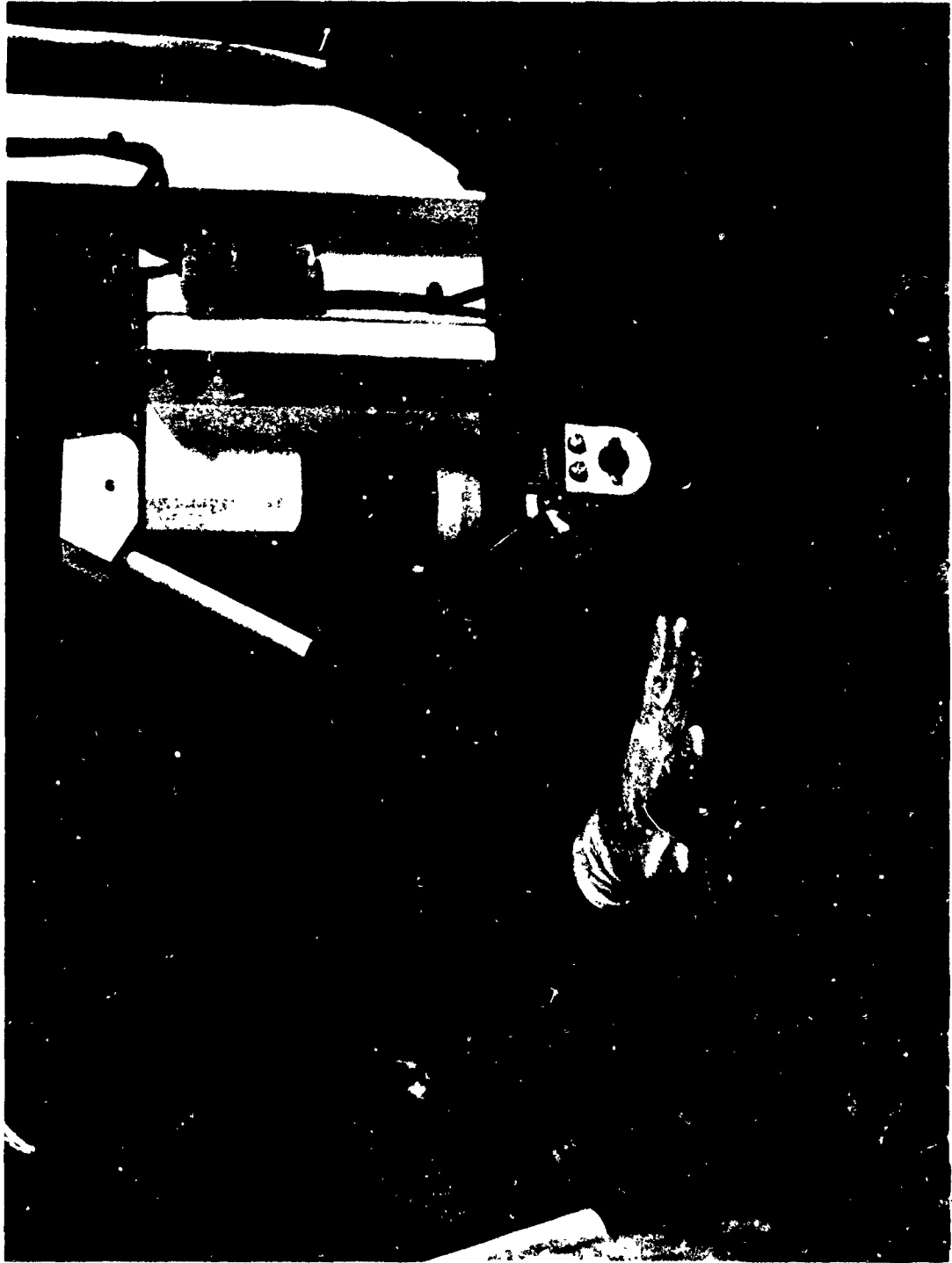
Figure 118. Welding Frustum Cross-Ply Segments

335/.8J

247

f. The best fit of fabric plies is obtained if basting is per-
    formed on a mandrel having copper backup strips inlaid
    in the surface. It is more difficult to obtain satisfactory
    fit between plies when using a protruding conductor strip
    such as a hand-held copper strip (bent "shoehorn").

g. Reinforcing cuffs should be basted with a circumference
    1 to 2 percent less than the actual circumference of the
    main assembly to assure that they will be tight on final
    assembly. This is done by marking the cuff end overlap
    with a ball-point pen as assembled over the two-ply basic
    assembly, and then spot basting the intended joints on the
    slightly smaller circumference after removal from the
    form.

3.10.1.2.4 IMPREGNATION WITH SILICONE RUBBER

The combined bias and cross plies of fabric must be thoroughly
saturated with silicone rubber to prevent voids or bubbles of air that might
cause blistering or delamination when the proposed vehicle is used in space,
to decrease conductive heat transfer through the matrix, and to prevent in-
ternal abrasion between metal filaments.

After priming the fabric by brushing on a methanol solution con-
taining 20 percent stock SS-4120 (General Electric) primer, the two primed
plies of fabric are placed on the form tool which has previously been coated
lightly with Orvus WA release agent. The primer is allowed to dry for a
minimum of one hour. Nylon spacer screen is placed over the form and a
polyvinyl chloride film vacuum bag is laid-up over this. Inlet headers are
connected and the vacuum bag is sealed using chromate paste. The system
is evacuated and checked for leaks. Meanwhile, the liquid RTV 655 silicone
rubber (General Electric) is degassed under vacuum using a shaking tech-
nique to break the resulting foam. While the vacuum is maintained on the
vacuum bag and metal fabric assembly, the liquid RTV silicone rubber is
allowed to flow into the vacuum bags using atmospheric pressure to force
the liquid through the tubing and into the assembly. A pilot scale setup for
the impregnation operation is shown in Figure 119. The impregnation or
saturation of the metal fabric by the liquid rubber can be observed through
the clear vacuum bagging.

After impregnation is complete, the system is held under vacuum
for an additional 15 to 45 minutes, and then it is opened to atmospheric
pressure. This forces the silicone rubber into any small evacuated voids
that may not have been previously filled. After another 15 minutes, the
vacuum bag assembly is stripped from the component and the excess RTV
rubber is wiped from the surface of the metal fabric with clean, lint-free
paper towels. Mylar shrink-tape is then wrapped on the assembly in such a
way as to hold down all edges of fabric and joints. The overlap between the
successive spiraling of the shrink tape is held to about 1/8-inch so that ex-
cess RTV silicone rubber can be squeezed out. The tape is shrunk using a
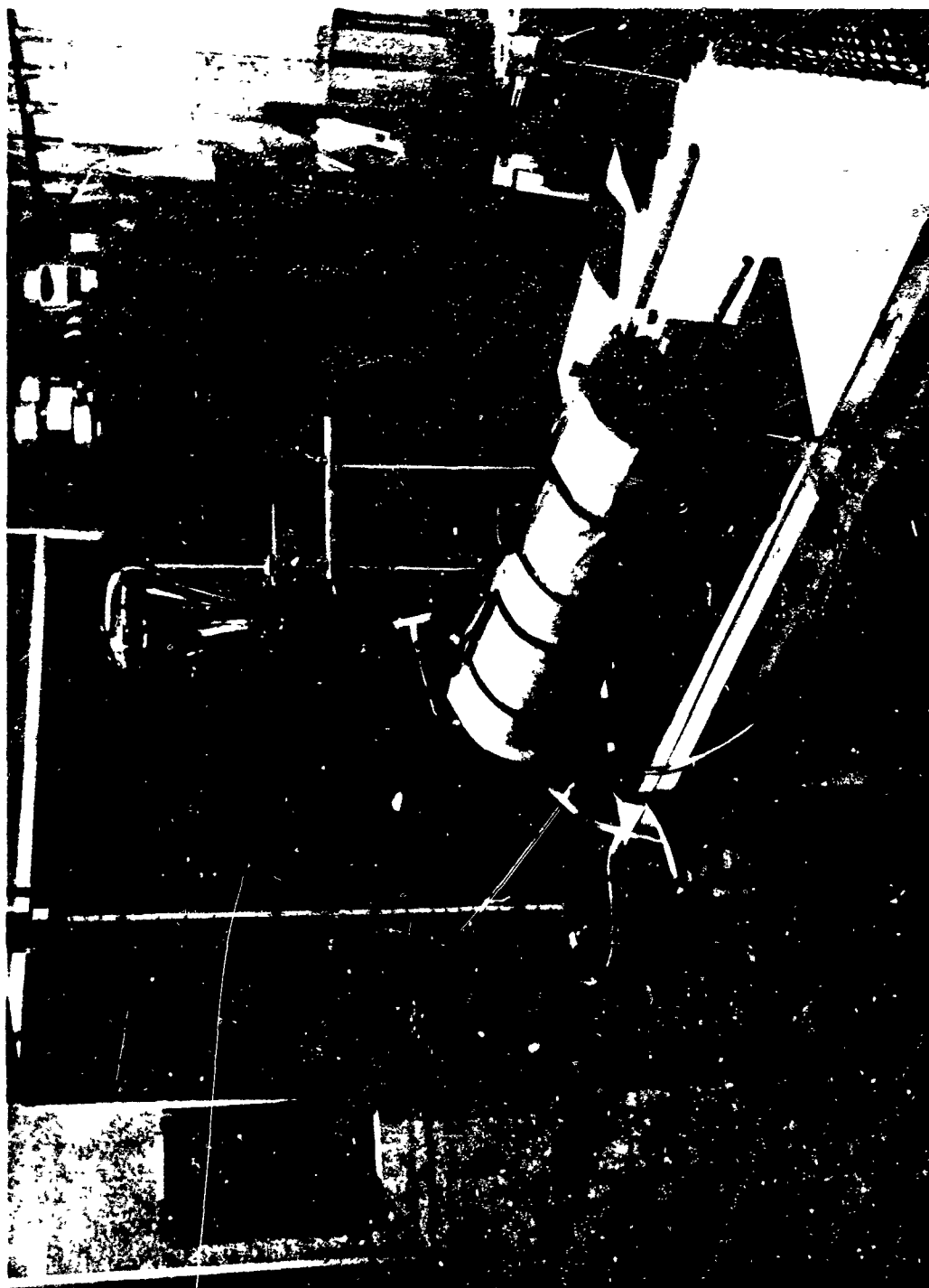
Figure 119. Impregnation of Fiber Glass Frustum

335/121

249

small hot-air blower. Since the RTV 655 silicone rubber is catalyzed, it cures under the shrink tape.

3.10.1.2.5 APPLYING SILICONE RUBBER COATING

After the RTV impregnant has sufficiently set-up, the shrink tape is removed and the surface condition of the impregnated component carefully inspected. Before the RTV has cured completely and while still in a tacky condition, thin calendered sheets of gum-type silicone rubber (S-6510 from Dow Corning) are carefully laid in place. Any depressions in the cuff areas due to multiple layers of fabric and irregularities at seams are filled with additional S-6510 put in place with a spatula. All blisters of entrapped air are removed by lightly puncturing with a sharp needle or knife blade. In the case of the frustums, the first layer of S-6510 was 0.025-inch thick. Additional layers were laid over this in a shingle-like arrangement to build up the thickness to the maximum of 0.125 inches on the "stagnation line" or most highly heated side of the frustum. After all necessary repairs have been made, the assembly is covered with Teflon-coated fiber glass fabric (such as Temp-R-Glass or equivalent), overlaid with a second thicker layer of type-181 fiber glass bleeder cloth, and finally vacuum bagged with polyvinyl chloride film and sealed with chromate paste. Vacuum connections are also fastened in place with chromate paste

The assembly is then placed in an autoclave and vacuum applied to the bag. All leaks are sealed. The autoclave is then closed and pressurized to 100 psig with nitrogen or carbon dioxide. The port in the autoclave is then heated, using forced circulation, to 250°F for 30 minutes to accomplish the pre-cure. One or more monitoring thermocouples should be affixed to the rubber coating within the vacuum bag to determine the cure temperatures.

Following pre-cure, the autoclave is cooled to at least 125°F before the pressure and vacuum are changed. The pressure in the autoclave is then reduced slowly (approximately 30 minutes) to atmospheric pressure and the vacuum pump is disconnected. Upon opening the autoclave the part is stripped of its vacuum bag and bleeder cloth and then carefully inspected. If any small fissures or irregularities in the silicone rubber coating are found, they may be repaired with fresh silicone gum rubber, in small areas, at this time.

The final curing is accomplished by heating the part (without bag or covering) in a ventilated, forced-circulation oven at atmospheric pressure, to 400°F for 14 to 18 hours. After the final curing, part should be cream or near-white in color. Darkening indicates improper ventilation or possible error in catalyst compounding.

3.10.2   FORM TOOLING

3.10.2.1   CYLINDER AND FRUSTUM TOOLS

A form tool, which was used in the early part of the program for constructing the 7-inch-diameter by 15-inch-long cylinders, is shown in Figure 120. Due to difficulty in removing cylindrical structures from cylindrical form tools after impregnation with rubber (in spite of the use of release agents), a split form tool for the 7-inch cylinders was made from Transite pipe and is illustrated in Figure 121. One of the welded 7-inch-diameter cylinders, including reinforcing end cuffs, is shown in this view in addition to the split mandrel, tapered end plugs, and supports. This type of form tool was made vacuum tight during impregnation by use of internal vacuum bagging affixed with chromate paste.

Several tapered, welded-aluminum form tools were fabricated for the 30-inch-long frustums tapering from 10-inch-diameter to 7-inch-diameter. In all cases the form tools were made in such a manner that they would extend one to two inches beyond the open end of the metal fabric part to accommodate affixing of vacuum bags, etc. The use of the tapered aluminum form and supporting stand during an actual impregnation of a frustum is shown in Figure 119. In some later work with impregnation of frustums considerable difficulty was encountered in removing the tapered metal fabr from the tapered form. Rolled aluminum forms, without end plates, were made up and the longitudinal joint was tack-welded and epoxy-sealed. These open-ended forms were supported by wooden end plugs. When difficulty was encountered in removing the frustum the small tack welds c the inside and the epoxy seams were broken allowing the sheet metal form to be collapsed slightly and permitting easy removal of the impregnated metal fabric structure.

3.10.2.2   RELEASE AGENT EVALUATION

Since difficulty was anticipated in removing the rubber-impregnated fabric from the form tools and since the form tool material must be compatible with any type of release coating, an evaluation of potential release coatings was made as part of the form tool evaluation program. A number of materials were considered as a release coat on the form tool material selected. A set of lap shear test specimens was prepared with the fabric impregnant, RTV 655, cured in contact with the release coating. In addition, the resistance of the release coat materials to solvent attack by the methanol primer solvent was explored by exposing coated specimens to the solvent at ambient temperature for two hours. The results, which are summarized in Table XXIX, indicate that either the common detergent, Dreft, or Orvus WA (both manufactured by Proctor and Gamble), would be satisfactory as release coat materials for the indicated use. Actually, the Orvus WA solution was used to coat all of the aluminum forms for the 7-inch cylinders and 10-inch frustums.

Because of great concern that the boom structure could not be easily removed from the large boom form tool, two layers of thin Teflon film were

251
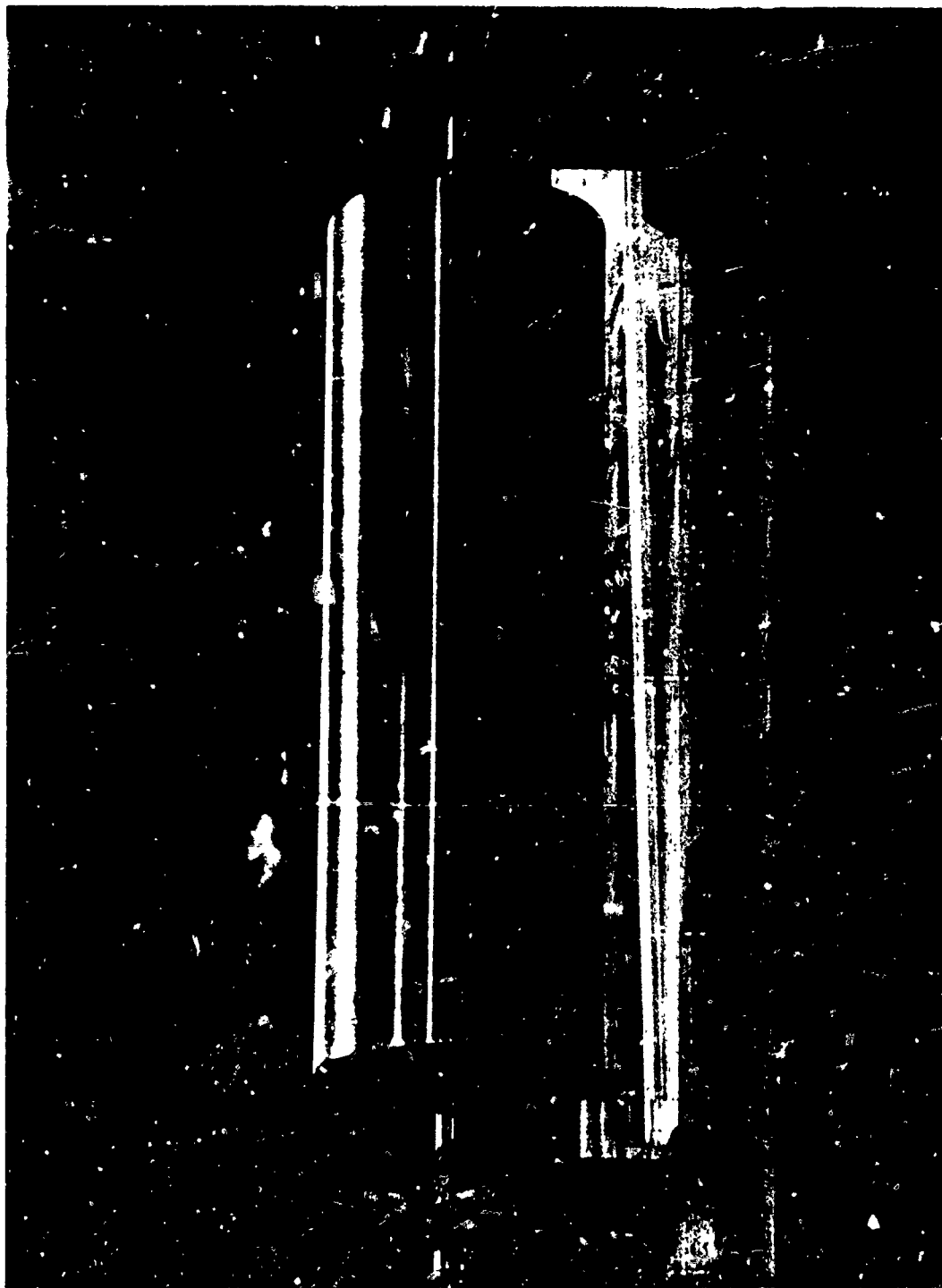
Figure 120. Building Form for Seven-Inch Cylinder

SGC/540

252

335/227

Figure 121. Welded Cylinder and Mandrel Prior to Impregnation

253

Table XXIX

RELEASE COAT MATERIAL EVALUATION

Material	Lap Shear Test (lb/in.)*	Solvent Effects**
1. Uncoated Reference Sample	3	None
2. Miller-Stephenson - S122 (Spray Coat) - Teflon	5	Coating Slough Off
3. Proctor and Gamble - Dreft (5% solution in H_2O)	1+	None
4. Proctor and Gamble - Orvus WA (10% solution in H_2O)	0	None

 * Average of four specimens
** Two-hour soak in methanol

254

pre-placed on the form tool and small air lines were led to small holes in the wall of the form tool. This technique, which is discussed in detail in the Fabrication Section, permitted removal of the impregnated and coated boom structure from the form tool without difficulty.

Since the apex form tool was segmented and the pieces could be disassembled by unbolting internal clips, release agents were not believed to be required for the apex form tool. Actually, difficulty was encountered with the patched areas of the tool sticking to the impregnant and a release agent may have been beneficial.

To increase the likelihood of success in removing the 10-inch by 30-inch-long frustums from their form tools (after difficulty was experienced with the removal of the early frustums) a small-scale process development was carried out. Three miniature forms about two inches in diameter at the large end and six inches long were constructed using different surface finishes. Two small metal fabric-impregnated and coated frustums, of one and two plies, respectively, were made on these forms to help solve the form removal problem. This work indicated that removal of the part from the form after pre-cure, but before post-cure, was easily done. This procedure was then established for use on the remaining frustums as well as on the larger components.

One of these small mandrels was polished to a four to five micro-inch surface condition. This provided the basis for evaluating a miniature, welded-fabric tapered frustum (bias ply only) impregnated with RTV 655 and overlaid with one layer of 0.025-inch S-6510. The tool was previously coated with Orvus WA and the metal fabric fitted tightly on the tool. The system was cured at 250°F for one hour and the cylinder was found to release easily from the tool with gentle force from one finger and thumb. Figure 122 shows the small mandrel and miniature frustum used in this experiment.

A little more Orvus WA was applied to the tool, the part was again fitted closely on the mandrel, and the system was post-cured at 450°F for eighteen hours. This time much more effort was required to release the part from the tool. This tended to support the theory that the post-cure on the tool caused sufficient shrinkage of the silicone rubber to make release difficult.

To insure that the release technique was satisfactory, another of the miniature tool forms was finished with a 25 to 30 micro-inch surface condition. This is rougher than the finish of the full-scale tool forms for the 10-inch by 30-inch frustums which are 10 to 15 micro-inches. A miniature two-ply (bias and cross) frustum was welded and then impregnated and coated on this small form tool. After pre-curing, but prior to post-curing, it was found that no difficulty was experienced in removing this impregnated and coated miniature part from the tool, even though it was rougher than the tools which would be used for the larger scale frustums. Although the miniature tools were of the same taper as the larger frustum tools, results of these small-scale experiments indicated that no difficulty would be encountered in removing the 10-inch-diameter by 30-inch-long frustums from their tools as long as the release agent was used and the tool was extracted before post-cure.

255
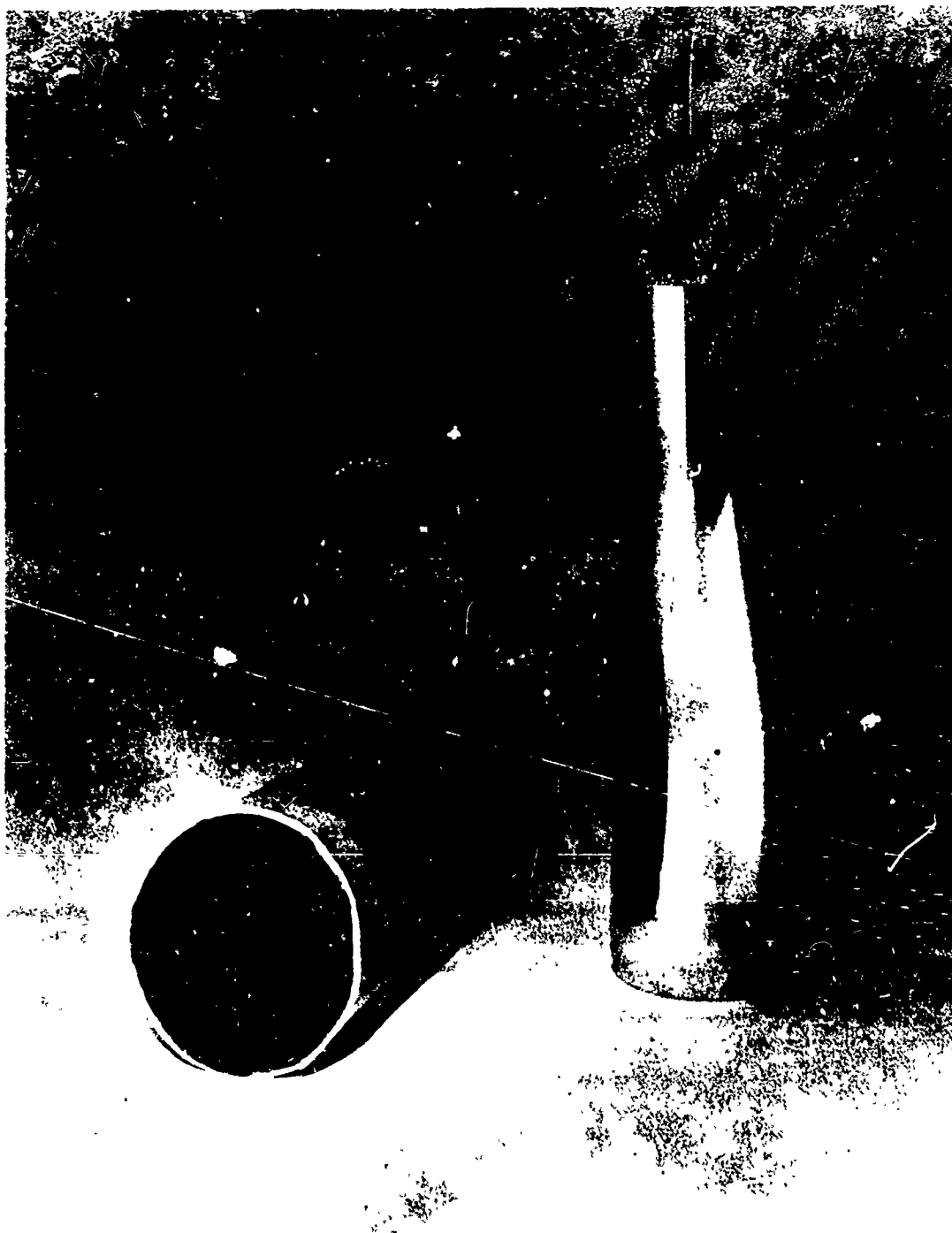
33b/210

Figure 122. Miniature Frustum and Mandrel

256

As discussed in the Fabrication Section, however, some difficulty was still encountered, probably due to the much larger surface area to be released, and it was necessary to go to the collapsible, sheet metal forms.

3.10.2.3 LARGE FORM TOOLS FOR BOOM AND APEX

Work statements were prepared by Space-General for quotations on the large, special form tooling needed to accommodate the full-scale boom and apex components. Because of the compound curvature shape of these large tools and the requirement that the apex tool be able to be taken apart and reassembled from within the fabric structure, fiber glass-reinforced epoxy construction was selected. It was necessary that such form tools be able to withstand the pre-cure conditions involving vacuum bagging and heating to 250°F without degassing or degrading while maintaining impermeability or vacuum tightness and dimensional stability.

After laboratory testing, a fiber glass-reinforced, high-temperature, epoxy resin composite was selected. This composite used Hess-Goldsmith fabric No. 481 and Fibre-Resin FR 40 resin. Samples were made and tested, both under vacuum and in air. No degassing under vacuum was evident and the material appeared to be essentially unaffected by exposure to temperatures up to 450°F for an 8-hour period.

The epoxy-impregnated, laminated fiber glass boom form, Figure 123, was manufactured for Space-General by a plastics fabrication concern. This large tool, which was about 18 feet long, was laid up externally on a form using conventional fiber glass pre-pregnated laminating techniques, and then turned and sanded on a large lathe. Inspection showed that its outside diameter was, at a 17-foot-length, 1.2 percent or 0.4-inch under the specified 32 inches. This error was accepted since any type of repair or correction action would have been uneconomical, although the error did necessitate rework of the paper patterns which had previously been cut for the bias ply.

The apex form tool shown in Figure 124 was manufactured by the same supplier. The discrepancies noted during inspection were that the exterior contour exhibited waviness beyond the allowable tolerances and that mismatch at joints between segments would have caused considerable difficulty during the use and reassembly of the tool. Consequently, the form was returned to the vendor for modification and rework. Low areas or valleys in the exterior contour of the form were filled with conventional, gray-colored, epoxy-type "body putty" which did not conform to Space-General's specification on acceptable materials of construction. However, after it was found that this epoxy putty had been used and the surface resanded to reduce the irregularities, tests were run on the cured epoxy putty to determine its resistance to temperature, solvents, and the vacuum environments utilized in the curing operations. A specimen of RTV 655-impregnated fabric was also allowed to cure in contact with the cured epoxy puttied surface. No detrimental effects were discovered. As discussed in the Fabrication Section, the epoxy putty did cause degradation of the RTV 655 during the final curing of the full-scale apex.

257

Figure 123.   Boom Form

335-195

258
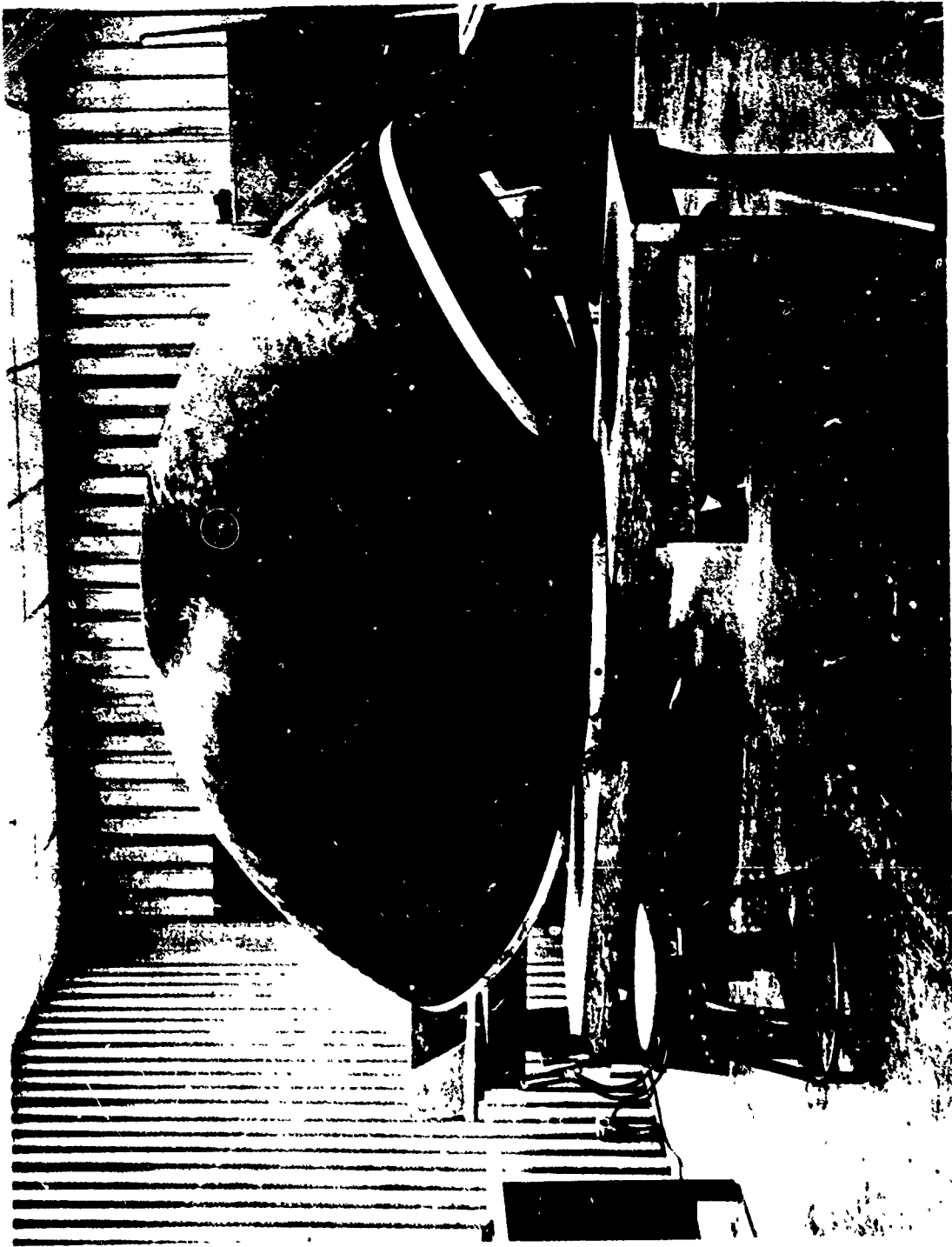
Figure 124. Apex Form

335/198

The apex form tool segments were held together by bolted plastic clips on the inside of the hollow form tool. These clips were inadequate with respect to holding the segments together tightly as well as aligning the segments when working from within. After considerable additional development effort by Space-General, additional clips were affixed with epoxy cement and notches were added to the clip edges to help align the segments. Disassembly and assembly of this form tool proved to be a laborious, time-consuming job, especially when a completed ply of fabric had its last joint basted and the form had to be removed entirely from within the fabric structure. An interior view of the apex form tool on its quardriped support is shown in Figure 125.

During the welding of the boom and apex metal fabric structures, it was necessary to construct economical fabric support forms as work aids to prevent the fabric from becoming unnecessarily creased and to assist in feeding it through the welder. Such forms were made from corrugated cardboard rolled into cylindrical and conical shapes and fastened with masking tape. During the fabrication of the apex, the large sections which had been basted or welded into closed circular shapes were supported by inflating heat-sealed, plastic film bags about 30 inches in diameter.

3.10.3 FABRICATION OF SMALL CYLINDERS

In addition to the cylinders made of monofilament stainless steel cloth (as described in Section 3.7.3.1), three 7-inch diameter by 15-inch-long cylinders were constructed of multifilament Karma fabric from the pilot run of fabric. One of these cylinders was a single-bias ply with the yarns at 45° to the cylinder axis; another cylinder was a single cross ply with the yarns at right-angles and parallel to the cylinder axis; and the other cylinder was a two-ply structure with inner bias ply and outer cross ply. The first attempt to make this two-ply cylinder was unsuccessful. All of these cylinders were equipped with double reinforcing cuffs at each end to help distribute load concentrations that would occur due to the clamped-on closures.

The first cylinder to be attempted using the multifilament fabric was the two-ply structure with the inner, bias ply having three equally spaced circumferential hoop joints. The impregnation method used was that of pressing calendered, uncured RB 141 silicone rubber gum into the fabric using a hand-operated rubber roller. This work was conducted by the B. F. Goodrich Co. under subcontract to Space-General, and the RB 141 elastomer was a silicone rubber compound which Goodrich recommended. The rubber was to be stitched into the fabric, as illustrated in Figure 126. It will be noted that the stitching process was undertaken before the longitudinal closure seam of the cross ply was made.

The cylindrical, aluminum form tool was sprayed with a parting agent (Miller Stephenson S-122) and appeared as shown in Figure 120. Next, two 4-mil layers of RB 141 silicone rubber gum were laid directly on the building form completely around its periphery. A 1-inch-wide by 0.013-inch-thick copper strip for conduction of welding current was applied over the silicone rubber at the location of the intended final longitudinal joint of the bias ply. The
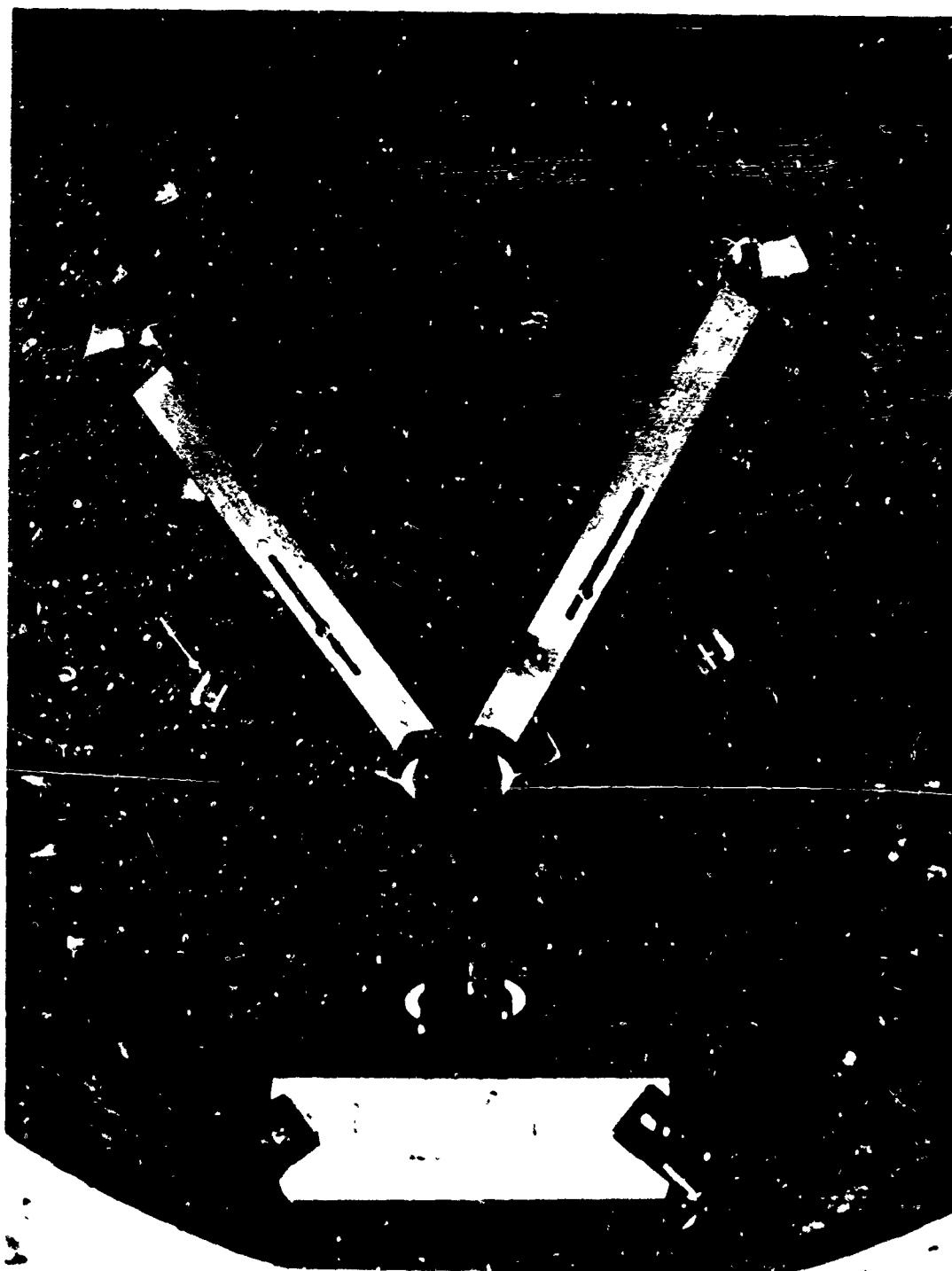
335/580

Figure 125. Interior View of Portion of Apex Form Tool Showing
Bolted Clips and Adjustable Support

261

Figure 126. Stitching Operation, Cross Ply

SGC/537

262

bias ply of fabric was next laid over the form and stitched, as shown in Figure 126. With the hoop seams having been made, but the longitudinal seam unwelded, the part appeared as in Figure 127 in which the fabric is held on the rubber coated form with rubber bands and the copper backup strip is held in place with masking tape. The entire assembly was then placed in a specially constructed box for welding the final longitudinal seam, as illustrated in Figure 128.

The welding on this cylinder was performed with the original portable welding gun discussed in Section 3.7.2.2. The actual welding of the bias ply closure seam is shown in Figure 129. The gun had to be loaded with 160 pounds of dead weight to effect this seam. Figure 129 clearly shows the imprinting of the fabric on the electrode wheels. In spite of the difficulties associated with the use of the welding gun, a satisfactory-appearing cylinder was welded, as shown in Figure 130.

Four-mil thick calendered RB 141 was placed between the reinforcing cuffs and the cross ply, with the cuffs and cross-ply assembly having been previously welded flat. The RB 141 sheet stock was also overlaid on the completed bias ply, the cross ply assembled over it, and the entire assembly stitched together as shown in Figure 126.

Although the resulting cylinder appeared to be satisfactorily welded, it was found that the final longitudinal joint was very weak since it started to pull apart due to normal handling. Unsuccessful attempts were made also to weld the final reinforcing cuff joints. It was observed that the electrode wheels penetrated deeply into the fabric and radically increased the effective electrode-to-fabric contact area under the heavy loading. Another observation made was that the electrode wheel track in the fabric was approximately eight fabric yarns wide while the equivalent width for fabric specimens which had been welded with solid metal backing was approximately four yarns. The 13-mil-thick copper backing strip had two deep grooves where the electrode wheels had passed. All of these observations supported the belief that the relatively soft underlay of silicone gum and metal fabric was responsible for a large proportion of the inability to obtain satisfactory welds in the cross ply and reinforcing cuffs. In the attempts to weld the reinforcing cuffs, more rigid support in the form of a thicker copper strip was provided with no success. It is also possible that the lack of success in welding was due in part to contamination of the fabric by silicone rubber or solvents.

Following development and construction of the semi-automatic welder (see Figure 107) by Space-General, the construction of the 7-inch-diameter cylinders was undertaken again. Using this welder, the three cylinders, referred to at the beginning of this section, were satisfactorily constructed. The two single-ply cylinders were not impregnated or coated with silicone rubber since the purpose of these tests was to study the performance of the reinforcing fabric independent of the effects of the silicone rubber.

The 7-inch bias-ply cylinder and the 7-inch cross-ply cylinder were laid up and held to proper shape on an expandable, split, 7-inch Transite cylinder form tool which had been used approximately two years before the fabrication of the monofilament stainless steel cylinders. The form tool, along with the
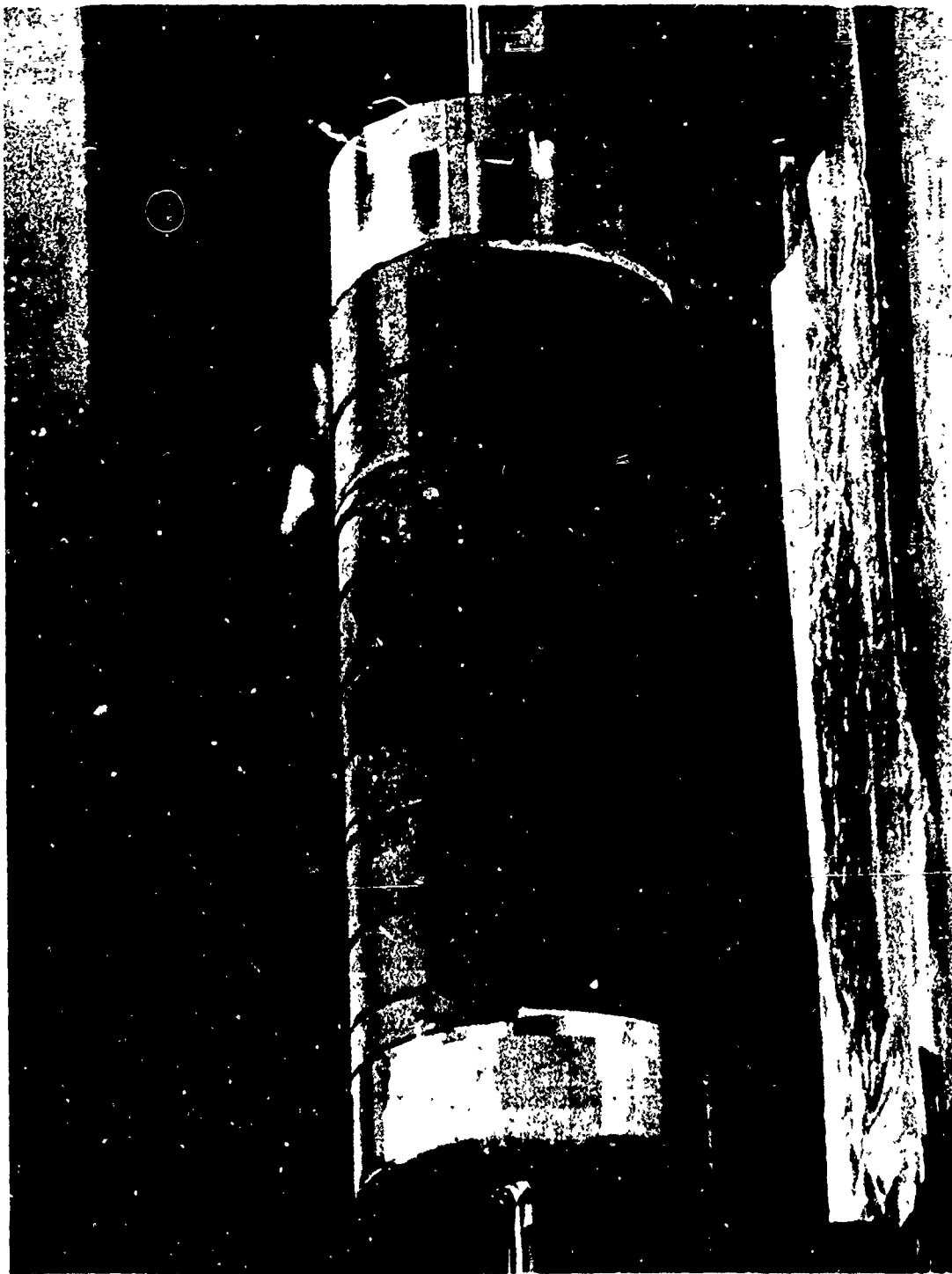
Figure 127. Bias Ply After Stitching and Prior to Final Welding
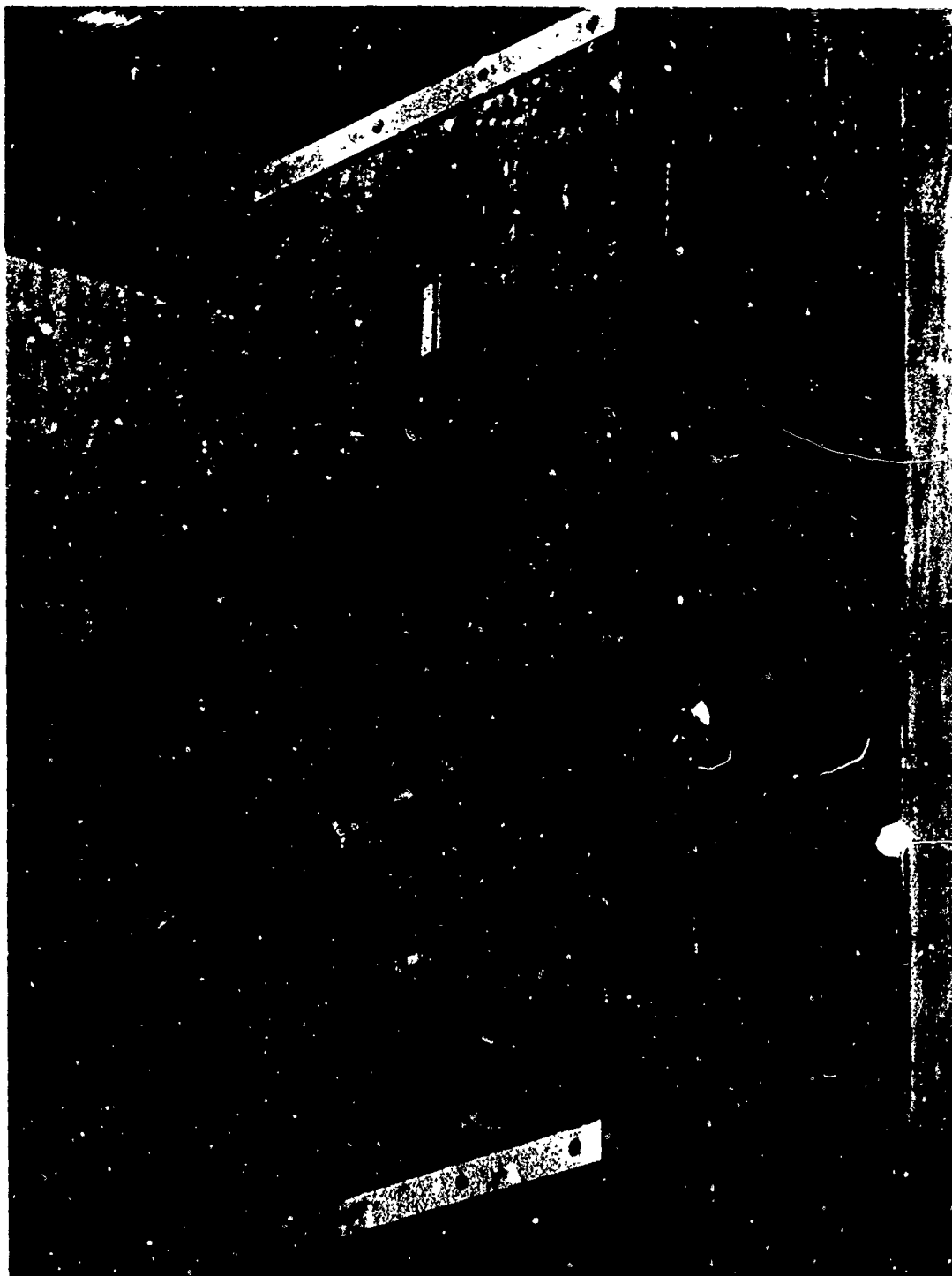
SGC/535

264

Figure 128. Bias Ply in Fixture for Welding Final Seam

SGC/534

Figure 129. Welding Final Bias Ply Joint

SGC/533

266

Figure 130. Completed Bias Ply

SGC/542

267

completed two-ply cylinder, is shown in Figure 121. Figure 131 shows the method in which the welder was used to make the final closure seam of the outer ply of the two-ply cylinder. The completely welded cylinder is shown in Figure 132, along with the Unitek power supply used for spot basting.

The double-ply, 7-inch cylinder was vacuum impregnated using liquid RTV 655 and coated with S-6510 silicone rubber. Wrinkles resulted in the layup of the two plies due to insufficient experience in cutting and basting the fabric patterns. This caused excess RTV 655 impregnant to exist between the fabric layers. Because of the wrinkles it was also difficult to get a uniform coating of the S-6510 stitched to the outer surface.

One problem that was encountered during the impregnation and coating of this 7-inch cylinder was that the fuzzy edges of the metal fabric tended to stick up through the overlaid S-6510. This condition was aggravated during the vacuum bagging causing the fine wires to penetrate the outer coating to a greater extent.

The cylinder was impregnated in the manner discussed in the final fabrication plan (Section 3.10.1.2) using a nylon bleeder screen to help distribute the liquid silicone rubber between the vacuum bag and the fabric. Figure 133 illustrates two views of the final cylinder removed from the tool after the S-6510 silicone rubber had been overlaid and cured. Small patched areas may be noted on one side of this cylinder where the coating was repaired before final cure. The patches adhered and cured properly indicating that it was possible to make repairs in the outer coating particularly if they are observed before final cure.

This cylinder was cured in an unventilated oven which contributed to some discoloration and possibly the lack of adherence of the S-6510 to the substrate in several areas. The lack of smooth fit between the two plies also contributed to some delamination and blistering between the fabric layers. Many of the difficulties were attributable to handling and processing techniques both in layup and welding as well as in impregnation and coating. The split transite mandrel used as a form tool was not sufficiently long to allow a good vacuum seal at the ends during vacuum bagging operations.

Essentially all of these problems were solved in the fabrication of the subsequent 10-inch by 30-inch-long frustum.

3.10.4   FABRICATION OF FRUSTUMS

In addition to the three 7-inch-diameter by 15-inch-long cylinders which were successfully fabricated (see Section 3.10.3), four frustums, 30 inches long and tapering from 1/ inches to 7 inches in diameter, were fabricated from the pilot run of fabric. The first of these was a "learning" frustum using glass fabric instead of metal fabric impregnated and coated with silicone rubber. The three 7-inch-diameter cylinders discussed above were then fabricated. These were followed with a 10-inch-diameter frustum which was impregnated and coated, a 10-inch-diameter frustum which was uncoated, and a
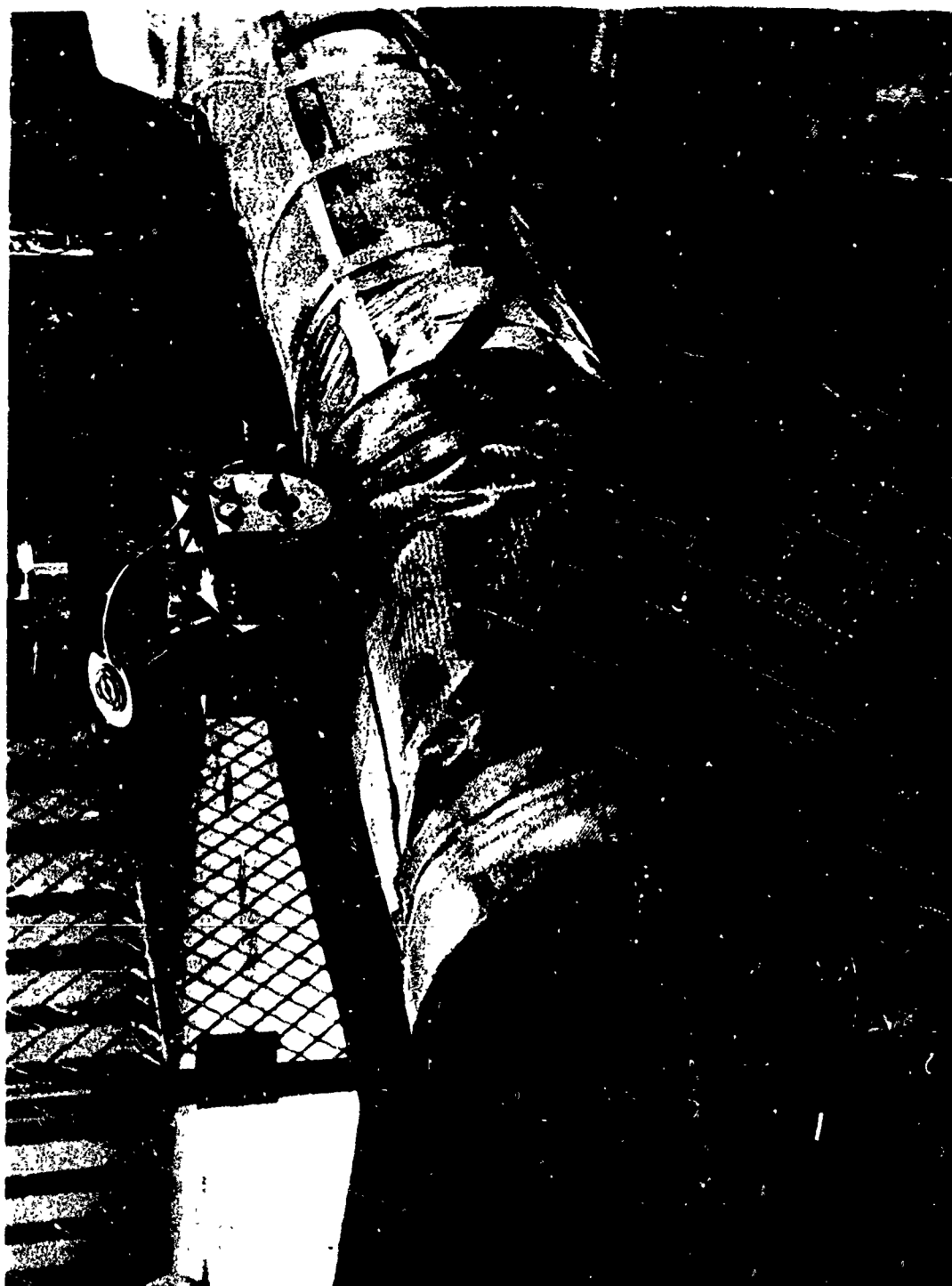
Figure 131. Welder Setup as for Final Closure Seam of Cylinder

335/146

269

Figure 132. Completed Cylinder and Spot Welder Used for Basting

335/141

270
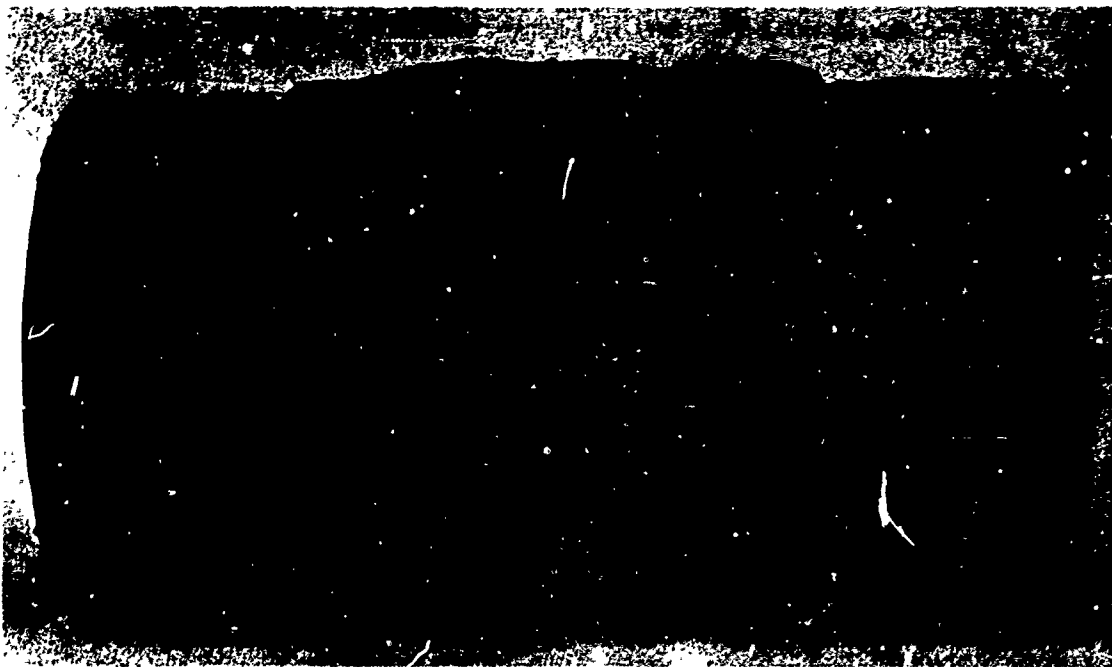
335/193

a. Side

335/189

b. Bottom

Figure 133. Two Views of Pre-Cured 7-inch Cylinder

271

final 10-inch-diameter frustum which was completely impregnated and coated to demonstrate all of the fabrication techniques to be used in constructing the final test frustums to follow.

3.10.4.1 FIBER GLASS-REINFORCED FRUSTUM

To confirm the developed techniques prior to application to metal fabric components, a practice prototype, multi-layer fiber glass frustum was impregnated with RTV 655 and coated with S-6510. As intended, this exercise provided knowledge in the application of the techniques and exposed unforeseen problem areas.

An aluminum mandrel (constructed for fabrication of the metal fabric frustums) was spray coated with release compound. This was overlaid with two layers of clean fiber glass cloth with overlapped hoop and longitudinal seams giving four thicknesses in localized areas. The joints were sewn together with glass thread. A quantity of RTV 655 rubber was degassed at 29 in/Hg vacuum. The structure was impregnated using the standard vacuum bagging techniques at 28 in/Hg vacuum. The impregnation setup with the vacuum bag in place is illustrated in Figure 119.

Difficulty initially experienced with foaming of the impregnation compound during evacuation was resolved in that simple mechanical agitation effectively collapsed the foam and permitted continuous degassing of the compound. A stainless steel screen was employed as a spacer to provide unimpeded flow of the impregnant. A nylon-plastic screen was used on all other frustums and would have been more desirable in this case because of the stiffness of the stainless steel screen, but the plastic screen was temporarily unavailable. Despite the problems imposed by this substitution, no difficulty was experienced in vacuum impregnating the glass fabric.

The peroxide-catalyzed S-6510 was calendered to a 0.040-inch thickness on the polyethylene film from which removal was found to be nearly impossible without the use of a stripping solvent. The methanol solvent used for stripping is reported not to degrade the catalytic or bonding characteristics of the silicone rubber.

The frustum was completely covered with one layer of the S-6510, a segment of approximately 120° was laid-up with a second layer, and a final segment of approximately 90° was laid-up over the second layer. The total thickness laid-up varied between 0.04- and 0.12-inch prior to curing. Bubbles of entrapped air between the layers of S-6510 were removed by hypodermic needles. Some of the bubbles in other small, bubble-free areas were treated as though they were serious imperfections requiring repair. The repair was accomplished by gouging out the "damaged" sections and replacing with fresh layers of S-6510 until the thickness was re-established. Blisters in the "repaired" areas were then corrected with the hypodermic needle. The whole system was vacuum bagged and cured at 250°F for four hours. After the vacuum bag was removed, the assembly was post-cured at 450°F for an additional four hours. The cured frustum was released from the mandrel with the aid of compressed air introduced between the frustum and the mandrel. Figure 134 shows

272
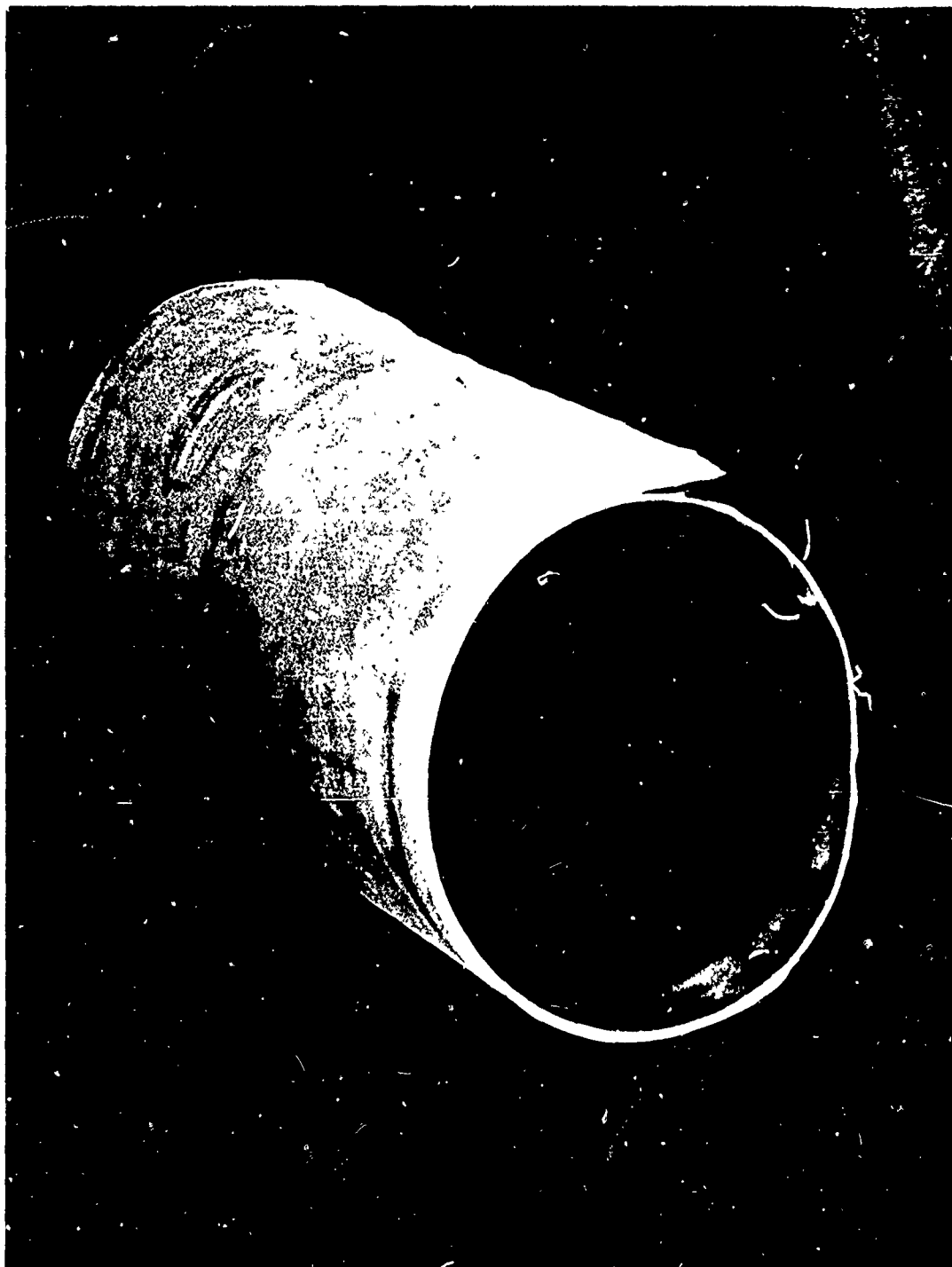
Figure 134. Silicone Rubber – Impregnated and Coated Fiber Glass Frustum

335/136

273

the completed frustum from one end so that the reasonably smooth surface characteristics of the interior and exterior may be seen.

The glass fabric "learning" frustum was fabricated to approximately correct size and thickness but without the reinforcing cuffs or closure-retaining wires at the ends.

3.10.4.2 FIRST PRELIMINARY FRUSTUM

After welding and assembling the two plies of this frustum, the assembly fitted the form tool very well except for some small discrepancies in the cuffs. This permitted a much improved impregnation and lay-up as compared to the 7-inch cylinder shown in Figure 133.

This frustum was vacuum-impregnated with a liquid RTV 655 and overlaid with the S-6510 silicone rubber in thicknesses varying from 0.025- to 0.125-inch. The part was cured in a well ventilated oven and a very satisfactory light-colored appearance resulted. Figure 135 shows the impregnated and overlaid frustum just after the initial 250°F pre-cure but before the extended, elevated-temperature post-cure. Some of the tools and accessories used in the coating process are shown in the foreground of that photo. Extreme difficulty was encountered in removing this first 10-inch-diameter metal fabric component from the form tool after post-curing the silicone rubber. A number of unsuccessful attempts were made to remove the part from the form tool. These included spraying liquid nitrogen into the interior of the tool in an attempt to shrink it, and injecting water, alcohol, and air between the tool and the part. The component was finally removed by inserting a thin strip of steel about 0.025 inches thick between the part and the tool and sliding it around the periphery. In the process, the aluminum tool was scored and some scratching occurred on the inside of the RTV 655-coated surface of the frustum. This technique was not used again.

Figure 136 shows the post-cured frustum after removal from the form and attests to the significant improvement in fabrication techniques. In this view the tangential flap simulating the wing attachment may be seen. The scratching that occurred on the form tool may also be observed.

This frustum was post-cured while still on the tapered aluminum form. The fact that a considerable portion of the rubber shrinkage occurred during post-curing obviously had contributed to the difficulty in form removal. It was at this point in the program that the experiments utilizing the miniature forms and frustums were conducted, as described in Section 3.10.2.1. All subsequent components were removed from the form tool before post-curing.

3.10.4.3 SECOND PRELIMINARY FRUSTUM

Because of the highly successful impregnation and coating of the first preliminary 10-inch frustum, the impregnation and coating operation was not carried out on the second preliminary frustum. This frustum served its purpose as a learning device in the welding operations but was not destined for any further testing or evaluation.

274

Figure 135. Preliminary Frustum After Pre-Curing

Figure 136. Frustum After Removal From Form

335/220

276

3.10.5 FAI·ICATION OF FINAL FRUSTUMS FOR TEST

These frustums were fabricated from the production run fabric, whereas all previous metal fabric components had been constructed from the pilot run metal fabric. The production run fabric was somewhat lighter in weight and about 15 percent lower in tensile strength due to the average filament diameter having been controlled at 1.00-mil rather than the 1.07-mil average of the pilot run fabric. The production run fabric was also more flexible than the pilot run fabric but met the design goal as originally established.

The metal fabric for the first of the ten "final" frustums was cut separately to gain experience in the handling of the lighter weight material. The metal fabric segments for all of the remaining final frustums, serial numbers 2 through 10, were cut from the "production run" bolt at one time. However, the segments were cleaned and packaged in nit·ogen-purged sealed bags only as they were needed. Quality control tensile te t coupon segments were cut from fabric adjacent to the segments and stored with each segment of fabric. The drying operation used on all of this fabric employed hot, dry-nitrogen gas as described in Section 3.10.1.2.1.

The segments of the frustums were basted together for final welding using the Unitek power supply with the hand-held pencil electrode. Two rows of basting spots were used for retention of the wire rings incorporate 1 in the frustum ends. The wire used for the end rings was 0.080-inch-diameter except for frustum number 6.

The reinforcing cuffs were basted and welded only with longitudinal seams. No circumferential basting or welding was used to fasten the cuffs to the main fabric plies or to each other. Positioning of the cuff with respect to the rest of the assembly was done just before impregnation. The fifth, sixth, seventh, and eighth frustums were fabricated without longitudinal flaps (simulated wing attachment) in the cross ply since the capability to make these flaps had been demonstrated previously.

At one point, during the vacuum drying process of the fabric segments for the third and fourth frustums, the fabric was saturated with vacuum pump oil due to an upset in the operation of another connected chamber in the same vacuum system. However, repeated cleaning of this fabric and its associated quality control tensile test coupons with the prescribed cleaning procedure resulted in no loss of weld quality. This indicated that re-cleaning can be performed without deterioration of the fabric.

Welding was completed without serious problems and the results were judged to be satisfactory in appearance and relative fit of the parts. The strength of the joints was excellent, as demonstrated both by the quality control tensile coupons made prior to welding and by the burst test results on the frustums. Welding of a typical frustum is shown in Figure 118.

As with basting, it was found advisable to weld from the center to the end of the longitudinal seams to avoid puckering of the seams. If possible during welding, the row of basting spots was straddled by the two welded seams.

277

The following sections describe the processing details as actually performed on each frustum in the sequence of fabrication. The serial number arrangement starts with the first "final" frustum (made with "production" fabric) designated as number 1. The work was based on the general methods described in the Fabrication Plan, Section 3.10.1.2, although the plan presented in that section represents the most effective final approach developed in the fabrication of all the components.

3.10.5.1 FRUSTUM NUMBER 1

After impregnation, this frustum had a tacky RTV 655 surface even after curing overnight. Since previous tests had indicated that this might have been due to loss or lack of catalyst at the surface, additional RTV 655 was painted on the surface before application of the first layer of S-6510.

Thin, Mylar shrink-tape was applied to the impregnated fabric but it appeared that the RTV 655 had, by that time, set-up too much and very little excess rubber squeezed out. (In the previous fabrication of the preliminary frustum, the impregnated fabric was immediately wrapped with a rubber-backed Mylar tape (not shrink-tape) and a significant amount of the still-fluid RTV 655 squeezed out between the tape wraps.) A few hours later, the tape wrap was removed and the S-6510 silicone rubber coating was applied. It was then vacuum bagged and pre-cured for approximately one hour at 250°F.

This frustum was patched to repair irregularities in its surface after the pre-cure; it was pre-cured again to polymerize the patched areas. The second pre-curing was also for approximately one hour at 250°F. The part was then post-cured at 400°F for 16 hours, without the vacuum bag. Although all of the patched areas appeared to be well adhered and cured, the rubber showed brownish discoloration and obvious patches. There were several fairly prominent ridges on the external surface of the S-6510 coating; these were caused by wrinkling of the bleeder cloth during vacuum bagging. This component performed very well in test, however. Following this, the emphasis was on providing a finished product with better appearance.

On the area of the preliminary frustum under the flap, the bleeder cloth was a Teflon-coated, fiber glass fabric which gave a very smooth appearance. On this frustum there was some concern that the Teflon-coated "Temp-R-Glas" cloth would not lie smoothly due to lack of bias trellising, and the more coarse, but commonly used, type 181 fiber glass fabric was used over the patched areas. This gave a rougher canvas-like surface to some areas of this frustum. Some non-uniformity was noted in the adhesion of the S-6510 coating to the RTV 655, with some areas adhering very well and others appearing to peel or separate.

3.10.5.2 FRUSTUM NUMBER 2

Due to irregularities in basting and welding of the patterns it was difficult to pull this frustum onto the form tool far enough to minimize wrinkles

278

and other areas of loose fit. Consequently, a split hardwood ring, Figure 137, with hook bolts clamped over the end of the form, was fitted over the wire ring and fabric at the end of the part and used to pull the welded frustum onto the form.

After impregnation, it was found that the RTV 655 had set-up too much, in only a two-hour period, for any significant amount of the rubber to squeeze out when it was wrapped with shrink-tape. In an effort to encourage the expulsion of excess RTV 655, the part was immediately unwrapped and a roll of shrink-tape, which had been drilled with radial, staggered, 1/8-inch holes, was used for rewrapping, but still very little of the excess RTV 655 was squeezed out. The holes, however, appeared to cause a series of small bumps on the surface of the RTV 655 and this approach was abandoned.

This second "final" frustum was the first component to have the first layer of 0.025-inch S-6510 pre-cured before adding successive layers of S-6510, followed by another pre-cure. This process, although taking more time for the pre-cures, appeared to be successful in preventing areas of delamination (as fabricated) in the multilayer coating. Appearance of the frustum was improved significantly over that of the first, as shown in Figure 219 which appears in a later section of this report. The double pre-curing permitted a much smoother lay-up, without the problem of attendant blisters in the first layer.

3.10.5.3 FRUSTUMS NUMBER 3 AND 4

These frustums were manufactured without difficulty or special problems. These and all succeeding final frustums were impregnated on lightweight rolled aluminum forms. Two such forms were fabricated. These forms had a longitudinal separation backed by a backing strip and filled with epoxy. These forms were welded only at the ends so that difficulties in getting the form out could be overcome by breaking the spot welds and collapsing the forms slightly for removal. Frustums number 3 and 4 were easily removed from their forms immediately following pre-cure.

It was observed that all frustums and cylinders manufactured up to this time had a few small "islands" (averaging about 1/2-inch in diameter) in which there was practically no coating of RTV 655 on the inside of the compo-nent, while the remaining area was covered with approximately 5 to 25 mils of RTV 655. The fabric in these islands appeared to be impregnated but there was concern that these areas could have been somewhat "starved" of RTV 655 and might contain small pin holes or voids. To assure complete sealing at these points, the islands were filled by applying a small quantity of fresh RTV 655 which bonded satisfactorily and provided a continuous film of inner liner.

3.10.5.4 FRUSTUMS NUMBER 5 AND 6

These two frustums were impregnated simultaneously to establish the technique of impregnating from more than one flask. No significant dif-ficulties were evident. It was necessary to collapse the aluminum mandrel to separate the frustum and form following pre-curing of the fifth frustum.

279
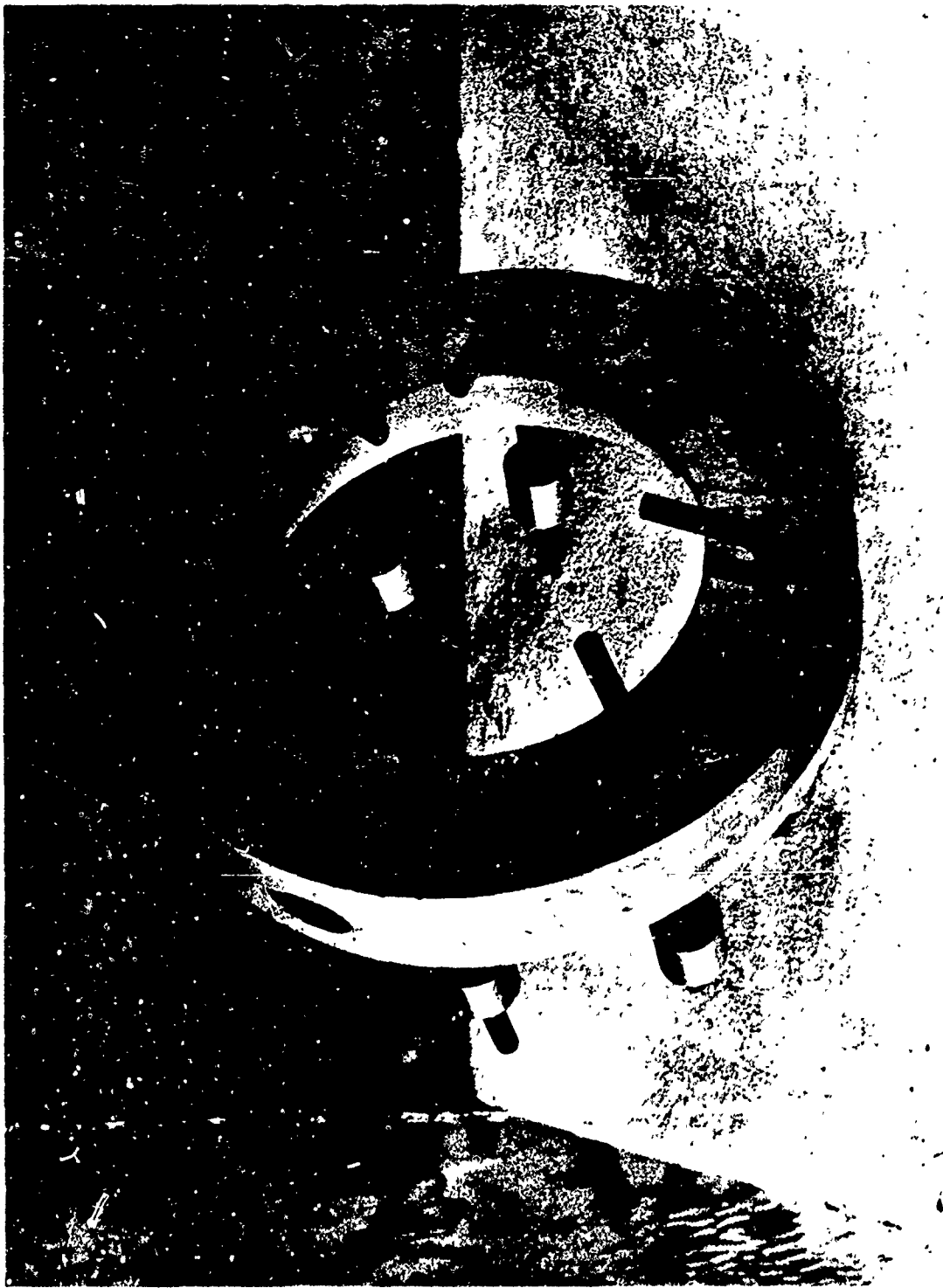
Figure 137. Split Ring for Frustum Assembly

335-293

280

The fifth through the eighth frustums were fabricated without long .dinal flaps. The tests to which these components were assigned did not require the flap and it was felt that sufficient previous experience in fabricating the flap had been achieved.

The sixth frustum was welded with a 0.11-inch-diameter steel wire basted in place. The wire was coated with the Orvus WA release agent prior to being installed. The purpose of this was to permit the withdrawal of the wire after impregnation, coating, and curing, so that a packaging (folding) test could be made on this unit. A 0.08-inch wire was then inserted into the cavity left by the withdrawal of the larger wire. The smaller wire permitted retention of the end closures during subsequent pressure testing. Some difficulty was experienced in removing the larger pre-coated wire) as described in the Test Section. It was found to be coated with tightly adherent rubber, indicating that the Orvus release agent did not perform its function very well.

3.10.5.5 FRUSTUM NUMBER 8

This frustum was fabricated on a freshly polished aluminum form and pre-curing was completed in a pressure autoclave to investigate the possibility of improving the interlaminar bonding of S-6510 and RTV 655. The frustum was coated with all the required thicknesses of S-6510 prior to pre-curing, then was vacuum bagged and subjected to 100 psig autoclave pressure at 240°F for 0.5 hour. After pre-cure, no blisters or imperfections were found - the surface being smooth, uniform, and of excellent appearance.

Repairs of the S-6510 coating were not required between pre-cure and post-cure as had been the case with several previous components. The resultant saving in manhours for repairs more than paid for the cost of autoclaving. In addition to the lack of repairs, the frustum showed a distinct increase in the inner laminar peel strength between the RTV 655 and the S-6510, as compared to the atmospheric pressure (vacuum bag only) cured frustums previously fabricated. This strength was noted in removing the 1.5-inch length of outer rubber from the ends of the frustum to permit proper gripping of the end closure. The outer S-6510 coating tended to tear and break rather than peel away from the substrate.

This frustum was removed with relative ease from the tool without collapsing the tool form as has been required for some of the other frustums. The frustum was put directly into the post-cure using a ventilated, forced-circulation oven at 400°F for 16 hours in accordance with the standard fabrication plan.

3.10.5.6 FRUSTUMS NUMBER 7, 9 AND 10

These components were impregnated simultaneously using three of the seventeen flasks in the special "shaker" assembly for defoaming the RTV 655 liquid rubber during degassing prior to impregnation. The remaining fourteen flasks were filled with water. The setup is shown in Figure 138a.

281
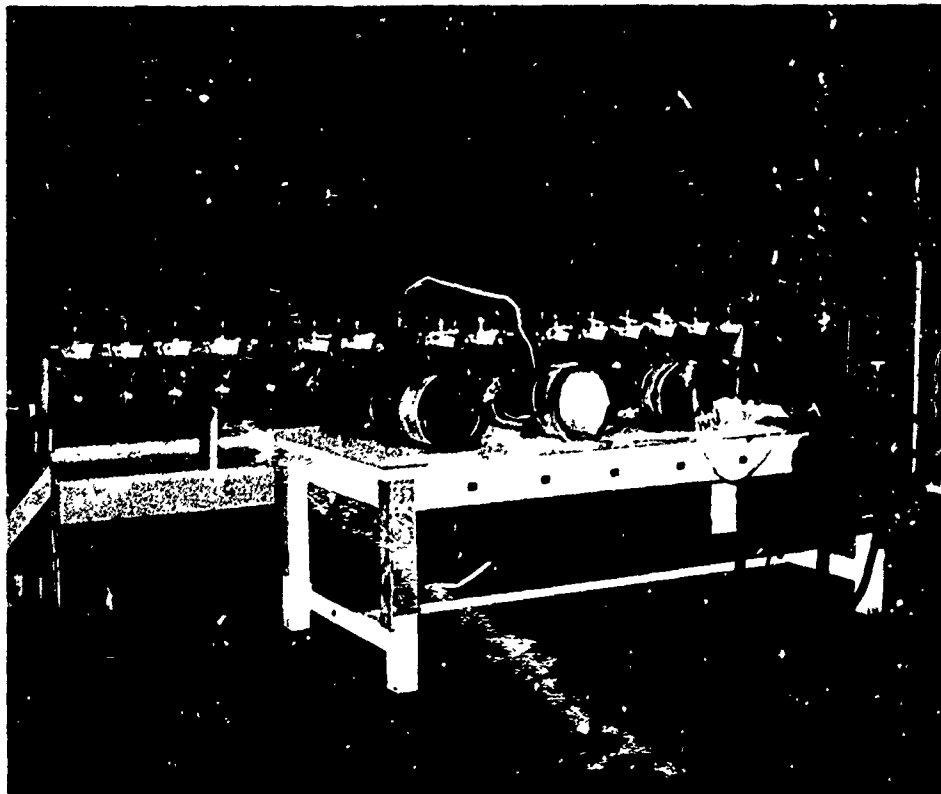
Figure 138a. Impregnation Set-Up
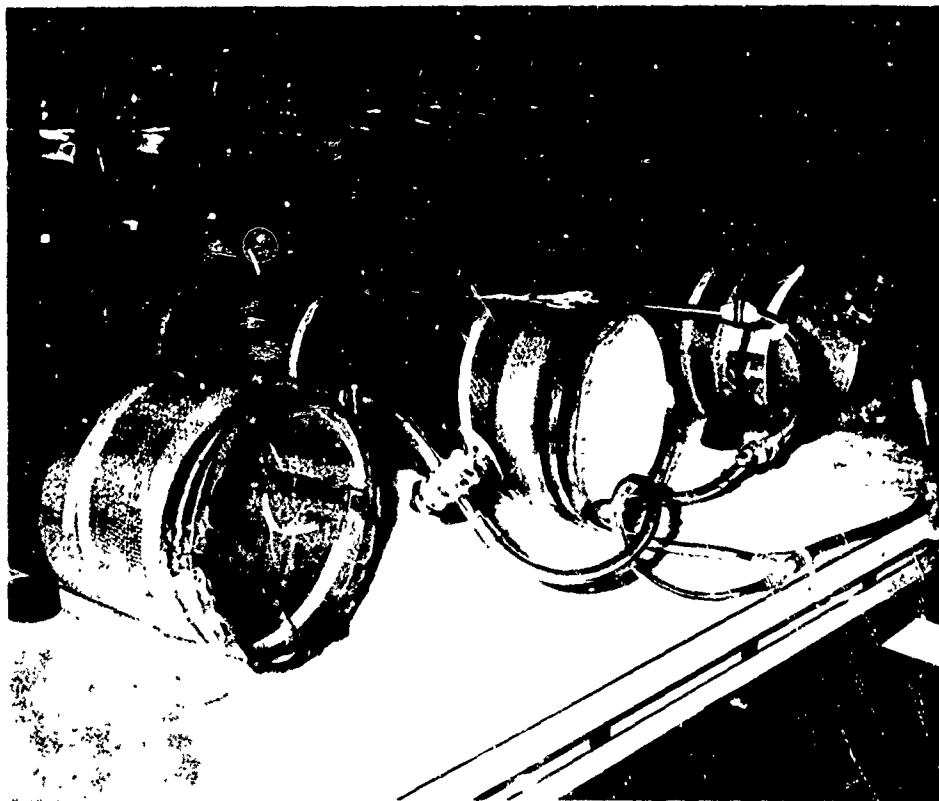
Figure 138b. Close-Up View Showing Varying Rates of Impregnation
(Frustums 9, 7, and 10, Left to Right)

Shaking of the pivoted flask-holding device was performed manually for the approximate 15-minute period required. All three frustums were vacuum bagged using 2-mil polyvinyl chloride film over the usual Teflon-coated "Temp-R-Glas" bleeder cloth which gives a smooth surface to the part.

Different techniques were evaluated for impregnating each of these frustums, with the time required to completely saturate all of the fabric being noted. The shortest impregnation time was 40 minutes for frustum number 10, which had strips of type 181 fiber glass bleeder cloth installed between the PVC vacuum bag and the lapped area of the Nylon screen. Frustum number 7 had no lap in the Nylon screen and no bleeder cloth and required 50 minutes. Frustum number 9, with the Nylon screen lapped but no bleeder cloth strips, required 60 minutes for impregnation. This frustum, however, had the screen lapped 180° away from the impregnant inlet (bottom) and this lack of inlet "header" undoubtedly accounted for the longer time.

The darker area in each of the frustums, shown during impregnation in Figure 138b, is where the fabric had been saturated with liquid rubber. It will be noted that the impregnation is progressing most rapidly in frustum number 10 on the right and slowest in frustum number 9 on the left.

Frustums number 7, 9, and 10 were coated with S-6510 on the same day as impregnation, with the intention of obtaining maximum bond strength by bonding to a fresh, partly cured surface of the RTV 655.

The 0.100- and the 0.125- inch S-6510 areas of frustum number 7 were perforated with a metal roller having many short pin-pointed spikes on its periphery to permit air entrapped between the layers of S-6510 to escape. The part was then placed in a vacuum chamber and the pressure lowered to 12 in/Hg (abs), at which point numerous small blisters (about 1/4-inch-diameter) and one large blister (about 1-inch-diameter) were observed. The blisters were predominantly in the area which was not perforated. The large blister appeared to be causing considerable delamination of the S-6510. When the pressure was restored to atmospheric, the blisters disappeared. The remaining surface was then perforated with the roller, the blistered areas were repaired and the frustum vacuum bagged in preparation for pre-cure.

The entire surface of the S-6510 on frustum number 9 was perforated with the spiked roller. The pressure on frustum number 9 was lowered to 10 in/Hg (abs) in a vacuum chamber. There were no large blisters but several small blisters were evident. The entire surface of the frustum was perforated but this part was not exposed to the vacuum inspection treatment for blisters. It was reasonably certain that this perforating operation was helpful in preventing entrapped air, but care must be exercised to prevent puncturing the impregnated metal fabric underlying the outer S-6510 coating.

During this pre-cure operation, frustum number 7 lost vacuum at 175 psig autoclave pressure during the initial pressure rise. The autoclave was depressurized and the assemblies inspected, revealing a small hole in the PVC vacuum bag of frustum number 7. The leak was attributed to bridging of the vacuum bag and to the high external pressure. The three frustums were

re-bagged with 2 mil-polyvinyl alcohol film and a knit bleeder cloth over the "Temp-R-Glas" cloth. Curing was resumed with pressure at 250 psig and part temperature at 250°F (as measured by thermocouple attached to the metal fabric of one of the parts) for 30 minutes. Frustum number 7 again lost vacuum after 11 minutes at 250°F but it was decided to complete the cure of all of the frustums without shutting down. The use of PVA film apparently had no advantage over PVC for vacuum bagging. (Note, however, the poisoning of the impregnant caused by PVC on the apex, Section 3.10.7.3.) Frustum numbers 7,9, and 10 after pre-curing are shown in Figure 139.

Removal of all three frustums from their respective tools was difficult and necessitated collapsing the tools to remove the parts. None of the three frustums required repair of the S-6510 coating before post-cure and all were of even better appearance than frustum number 8, probably due to the use of the 250 psig autoclave pressure. All evidence of the perforations had disappeared. However, the commonly observed "islands" on the inside were still evident and these were repaired with RTV 655 after post-cure.

3.10.5.7 CONCLUSIONS FROM FRUSTUM FABRICATION WORK

3.10.5.7.1 GENERAL CONSTRUCTION

Because of the taper of the frustums, it was found impractical to make each reinforcing cuff of a single continuous piece of fabric. A better approximation was achieved by using three segments for each reinforcing cuff. The patterns for these cuffs can be seen in Figure 114.

Due to the difficulty in removing the end wires from frustum number 6, preparatory to the folding and packaging tests, a number of different techniques for removing these wires were studied. At the time of folding and packaging frustum number 6, however, it became obvious that removing the wires again would probably damage the frustum to the point that it could not be remounted for the final pressure testing. As a result of this experience, and the fact that the wire was easily folded up in the package, even though it did contribute somewhat to the volume of the package, efforts and plans to remove wires from future components were abandoned.

A technique was developed for attaching thermocouple strips directly to the metal fabric before impregnation. Chromel-Alumel (type K) 26-gage thermocouples with fiber glass insulation were used. The entire lengths of the thermocouple wires were soaked in methyl ethyl ketone to remove the varnish coating. This permitted adhesion of the RTV 655 silicone rubber impregnant to the thermocouple insulation and prevented charring of the organic varnish during the 400° F curing of the silicone rubber. On some of the frustums, thermocouples had been attached to the inside of the inner bias ply as well as to the outside of the outer cross ply. The thermocouples on the inside tended to become damaged in the handling and set-up for test. It was, therefore, planned at this time to have thermocouples only on the exterior of the

284

Figure 139. Frustums 7, 9 and 10 After Pre-Curing

335/267

285

cross ply and buried under the S-6510 coating in the boom and apex. Thermocouple wires were run longitudinally in the frustums, as well as in the boom and apex, through the thicker coating rubber to the end of the part where they emerged between the outer rubber coating and the outer fabric ply near the end closure clamps. This also eliminated the need for connecting internal thermocouple wires to sealed connectors on the outside of the end closures. Thermocouple wires were not run through the metal fabric at any location on any component because this would have introduced a possible leakage path.

In preparing the thermocouple sensing joint, the end of the thermocouple wires were stripped of insulation for about 1/4-inch. The wires were then bent away from each other to form a circle, with the tips of the wires crossing and overlapping. The Unitek spot welder, used for basting metal fabric, was then used to spot weld the two thermocouple wires together and to weld the thermocouple joint to the metal fabric. Care was exercised in handling the part to prevent the thermocouple wires from damaging the fabric or breaking off. Three thermocouples were normally positioned along the "stagnation" line (or side to be heated) on the frustums.

It was found that the cross-ply pieces, wherein some yarns were more or less parallel to the edge of the fabric segments, tended to ravel, particularly if they were handled extensively during lay-up and basting. The raveling could be stopped by using the Unitek spot welder and manual probe to make spot welds approximately every 1/4-inch along the edge of the cross-plied pieces. Although very time consuming, the technique was effective in preventing raveling. It is not possible to use the large, semi-automatic seam welding machine for this purpose because the automatic electrodes do not perform well near the fuzzy edge of the fabric. The high current flow and sparking that occurs tends to damage the electrodes.

3.10.5.7.2 IMPREGNATION AND COATING

It is most desirable to have relatively long pot life of the RTV 655 after mixing the A and B portions, although it is not desirable to increase the viscosity. Consequently, purchase requests for additional RTV 655 stipulated particular cuts or batches of this material with low rate of cure and low viscosity characteristics.

Some difficulties were observed occasionally in getting the RTV 655 to cure properly even though it cured too fast on other occasions. Apparently this was due to slight differences in the fraction or cut obtained from the silicone rubber manufacturer, or it may have been due to contamination or poisoning. Caustics (bases), sulphur, amines, and even such materials as Teflon or PVC may inhibit cure when certain additives or plasticizers are present. The vacuum bag material has been either PVC or PVA. Both of these were tested and proved satisfactory, as was the case with the Nylon bleeder screen which was used. (See Section 3.10.7.3 for unusual difficulties with PVC later in the program.) Even though complete cure does not occur at room temperature, it will occur completely at elevated temperatures during the pre-cure

of the outer S-6510 coating. It is desirable to lay-up the S-6510 before the RTV 655 cures too far because this insures the availability of larger quantities of labile ligands (active ends of molecules) with which the overlaid S-6510 can co-polymerize.

The use of Mylar shrink-tape has proved to be very effective in compressing the protruding strands or filaments of the metal fabric until gelation of the RTV 655 occurs after impregnation has been completed. It also tends to insure a minimum of impregnate since the excess is squeezed out by shrink action. The tape is shrunk using a hot-air heating gun. The net result is to permit the overlay with S-6510 with a minimum amount of localized correction required. This results in a better appearing and probably, a better performing component.

The use of positive autoclave pressure in the curing of some of the frustums resulted in a distinct increase in the interlaminar tear strength between the RTV 655 and the S-6510, as compared to frustums previously fabricated wherein only the pressure exerted by the vacuum bag was used. Apparently, the intimate contact between the two kinds of silicone rubber not only improved the co-polymerization of the two materials but may have also created some mechanical bonding due to driving the S-6510 into the irregular upper surface of the impregnated fabric.

Use of highly polished tool form surface permitted easier removal of the pre-cured part; this was evident by the fact that frustum number 8, which was fabricated on a freshly polished aluminum form and subsequently autoclaved at 100 psig, was removed with relative ease from the tool without breaking the weldments or collapsing the tool form as had been required on some of the other frustums.

During testing at high temperature, heating lamps were not intended to simulate the ablation environment that the vehicle would encounter during actual re-entry since the physical mechanisms of heat transfer are quite different. The heat lamps are intended to heat the metal fabric substrate to the same temperature predicted by the computer analysis of the trajectory. The maximum temperature that the fabric is expected to attain is 850°F, while ablation (i.e., charring of the outer coating) occurs during a ten-minute period starting when the metal fabric reaches approximately 700°F, as may be seen in Figure 18 previously cited.

Some of the heating tests on frustums caused rather severe cracking and flaking away of the S-6510 coating, although none of these heating tests caused the frustums to fail or even leak in the heated area. The tendency of the S-6510 to flake or delaminate appeared to be related to the fact that the 0.125-inch-thick ablative area was composed of five 0.025-inch layers of S-6510. Although the high autoclaving pressures used on the latter frustums appeared to improve the tenacity of the laminates, it was believed that using one homogeneous 0.125-inch-thick layer of calendered S-6510 would eliminate the tendency to delaminate. This was supported by the tests described in the Test Section. The only disadvantage to using a single 1/8-inch-thick layer instead of five separate layers was the inability to lay-up the individual layers in

287

shingle fashion to taper the thickness gradually. If one 1/8-inch-thick coating layer was used it would have to be carried further around than the present five layer area of 0.125-inch maximum thickness and, therefore, the total weight of the component would be increased. Calculations indicated that laying-up a 1/8-inch-thick layer around 90 percent of the boom periphery would increase the weight only a few pounds.

Difficulties were experienced in laying-up the thin 0.025-inch-thick first layer of S-6510 because many imperfections existed in the material as received from the manufacturer. Other imperfections occurred during lay-up due to the lack of tenacity and the tendency to tear as it was being handled. For this reason consideration was given to increasing the thin coating, around 270° of the periphery of the boom, from 0.025 to 0.035 inches. The appearance would be improved because the higher autoclaving pressure, used on the later frustums, pressed the S-6510 coating material such that small irregularities in even the weave of the fabric tended to show through. The calculated increase in boom weight was only six pounds, or about 6 percent. The result of making the ablative area a single 1/8-inch-thick layer and the remaining area a 0.035-inch-thick layer of coating would result in the boom weighing only about 10 percent more. These recommendations resulting from the frustum fabrication program were used in the fabrication of the boom.

3.10.6   BOOM FABRICATION

3.10.6.1   FABRIC PREPARATION

In January 1966 paper patterns were made for the boom bias-ply segments. These were fitted on the boom form and trimmed to exact configuration. The resulting patterns were then transferred to Mylar drafting sheet and cut out. The resulting set of patterns was used to guide the actual cutting of the fabric.

The boom hemispherical and cap patterns were obtained by first making an approximate development of the cap, using twelve identical gore-shaped ("flattened spherical triangles") pieces of Mylar (plus the disc-shaped end patch), assembling these patterns to the form, and checking for fit. Minor modifications were then made to the gore patterns and the assembly was again placed on the form tool and checked. Twelve bias-ply gore segments and the disc were cut from the metal fabric, guided by the Mylar patterns, assembled to the form end cap, and exact shape and configuration again checked. These metal fabric segments were then basted on the special form tool shown in Figure 140a which had a copper conductor fitted to its surface. The result was an end cap basted together from segments, with one side still open for final positioning and fitting onto the end of the boom form tool, as shown in Figure 140b. After this fitting had been completed and the joints basted, the end cap was welded on the semi-automatic welder. The cross ply hemispherical end cap was made in identical fashion but fitted over the finished bias ply cap to assure proper size.

The huge size of the boom cross-ply fabric segments, approximately 4.5 feet by 17 feet (as shown during cutting in Figure 141a, necessitated some

288

Figure 140a.   End Cap and Basting Form
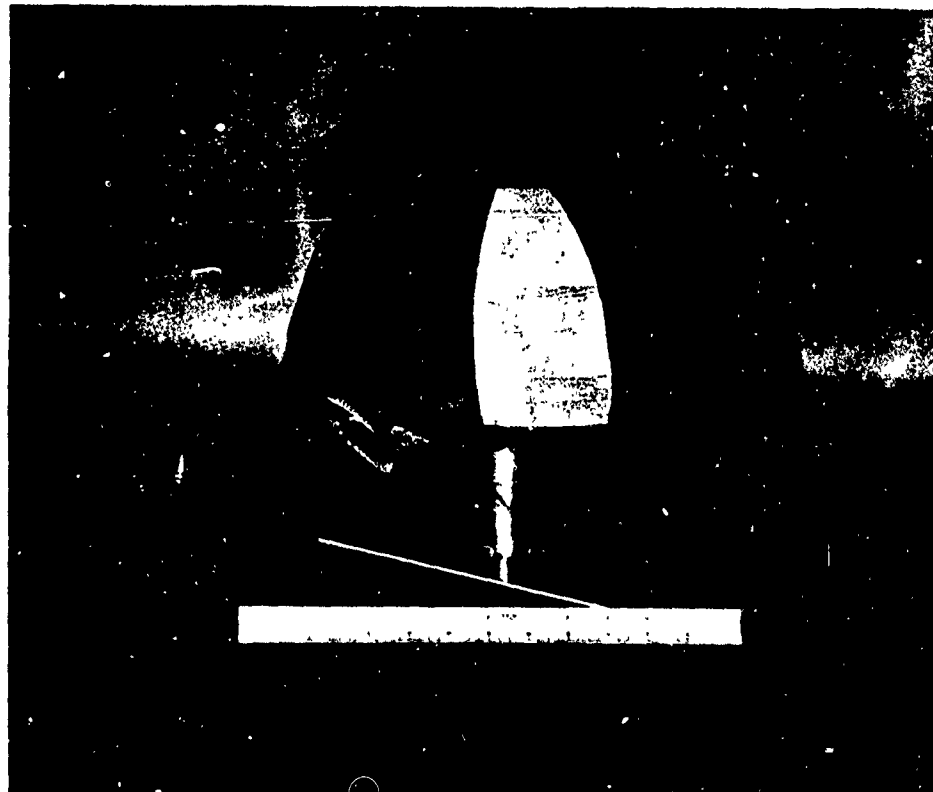
Figure 140b.   End Cap Ready for Basting Final Gore

289

Figure 141b. Cleaning Boom Cross-Ply Fabric
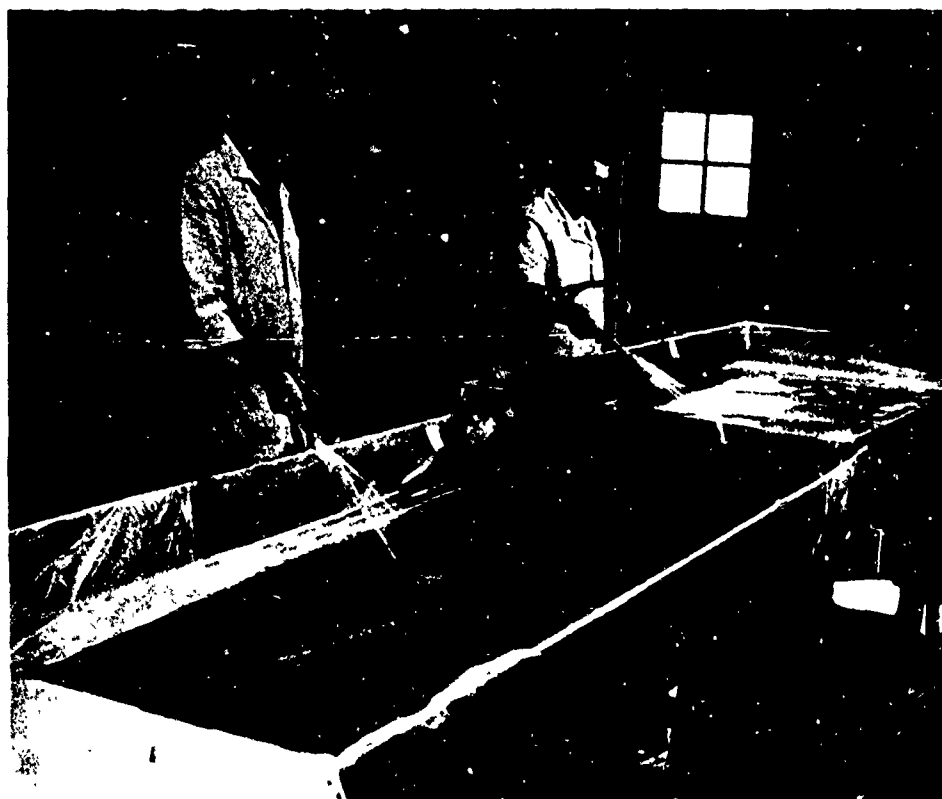
Figure 141a. Cutting Boom Cross-Ply Fabric

rearrangement of the cleaning facility. The cleaning of the boom cross-ply is shown in Figure 141b. In this process, the fabric was advanced lengthwise through the Phos-It wash tank and then the water wash tank, after which these steps were repeated, and the fabric finally rinsed in deionized water.

The fabric was dried in the heated nitrogen drying box and sealed in nitrogen-purged plastic bags along with the quality control weld coupons.

3.10.6.2 WELDING THE BOOM FABRIC

The boom end cap welding required extreme care due to the compound curvature of the part and the need for precise fit in this area. Welding of the bias-ply end cap is shown in Figure 142.

Welding of the large pieces of fabric for the boom was found to be considerably more tedious and time consuming than the work on the smaller frustums due to the large size of the fabric pieces and the need for supporting fixtures, as well as increased maintenance on the welder. When both plies were completely welded and assembled on the form tool the construction quality was not quite as good as on recent frustums, with small wrinkles appearing in one or both plies in some areas.

The longitudinal seams in the bias ply were welded first. The segments of the bias ply, after longitudinal seams were welded, are shown positioned on the boom form tool in Figure 143 for the purpose of locating and basting the circumferential seams. Then the welder heads were set at an angle of 90° with respect to the welder arms and circumferential welds were made, starting with the end cap.

A special device was used with the welder for welding the long, 17-foot welds in the cross-ply fabric. As shown in Figure 144, the two cross-ply pieces were basted together and rolled on a long reel positioned between the arms of the welder. The fabric was then unrolled as it advanced forward between the welder heads. Considerable care had to be exercised by the operators to weld a straight path in the middle of 3/4-inch overlap and to prevent unnecessary wrinkling of the fabric, as shown in Figure 145. Due to the extensive handling of the large pieces of fabric during lay-up, basting, and subsequent welding, the cross-ply pieces (wherein yarns are more or less parallel to the edge of the fabric) tended to fray. The fuzzy edges, where the fabric frayed, caused electrodes to spark and stick at times. Basting of the edge with the Unitek spot welder alleviated the problem of fraying, but was very time consuming, since the spots had to be made one at a time manually at about 1/2-inch or less spacing along the 17-foot edges.

Other problems were encountered, including electrode breakage due to catching of the large, comparatively heavy pieces of fabric on the electrodes as well as sticking of the electrodes. To alleviate the electrode breakage problem, principally of the upper 0.035-inch-diameter electrodes, the fabrication personnel elected to try 0.050-inch-diameter electrodes on top, identical to
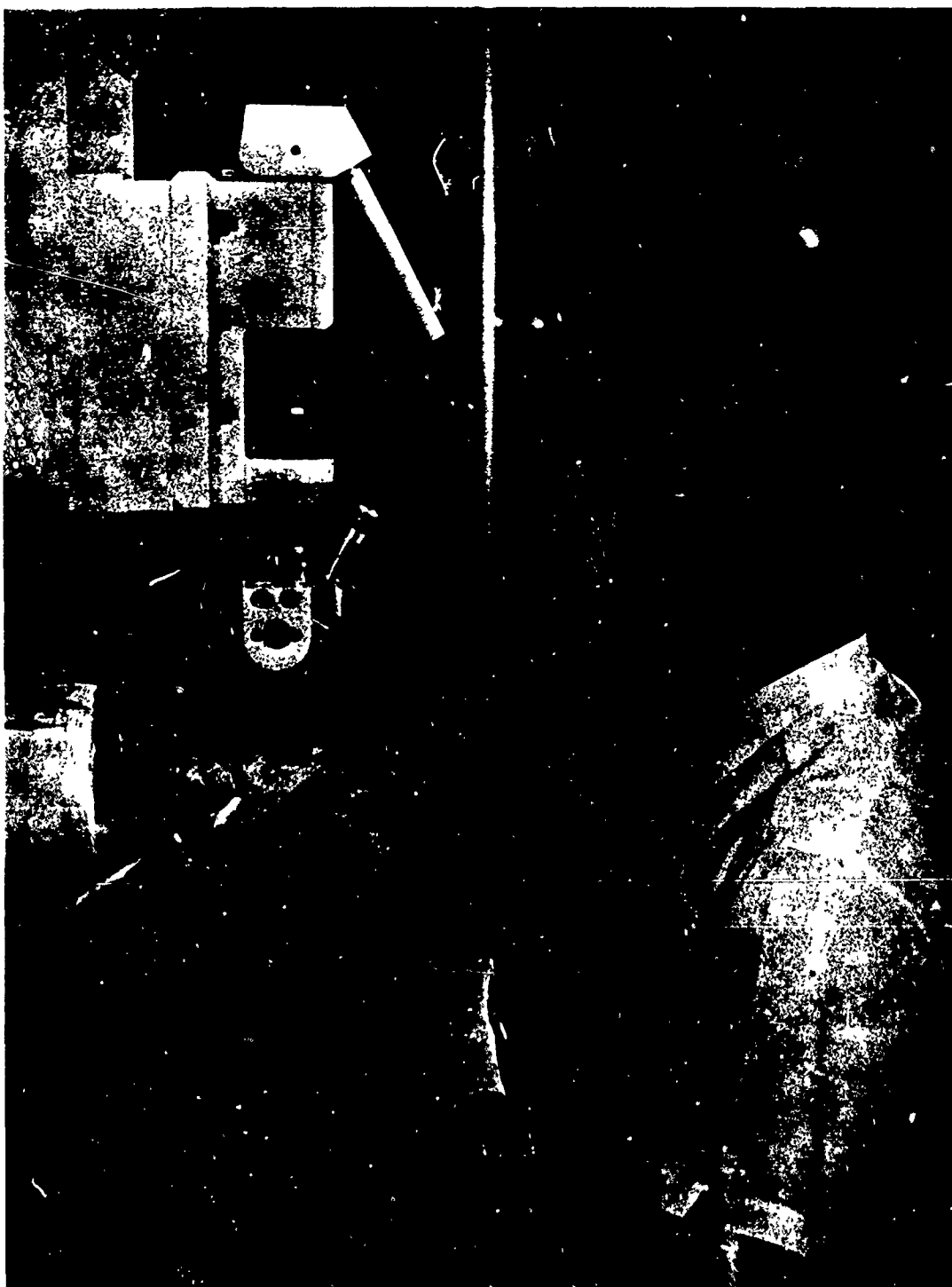
335/277

Figure 142. Welding Boom End Cap

292
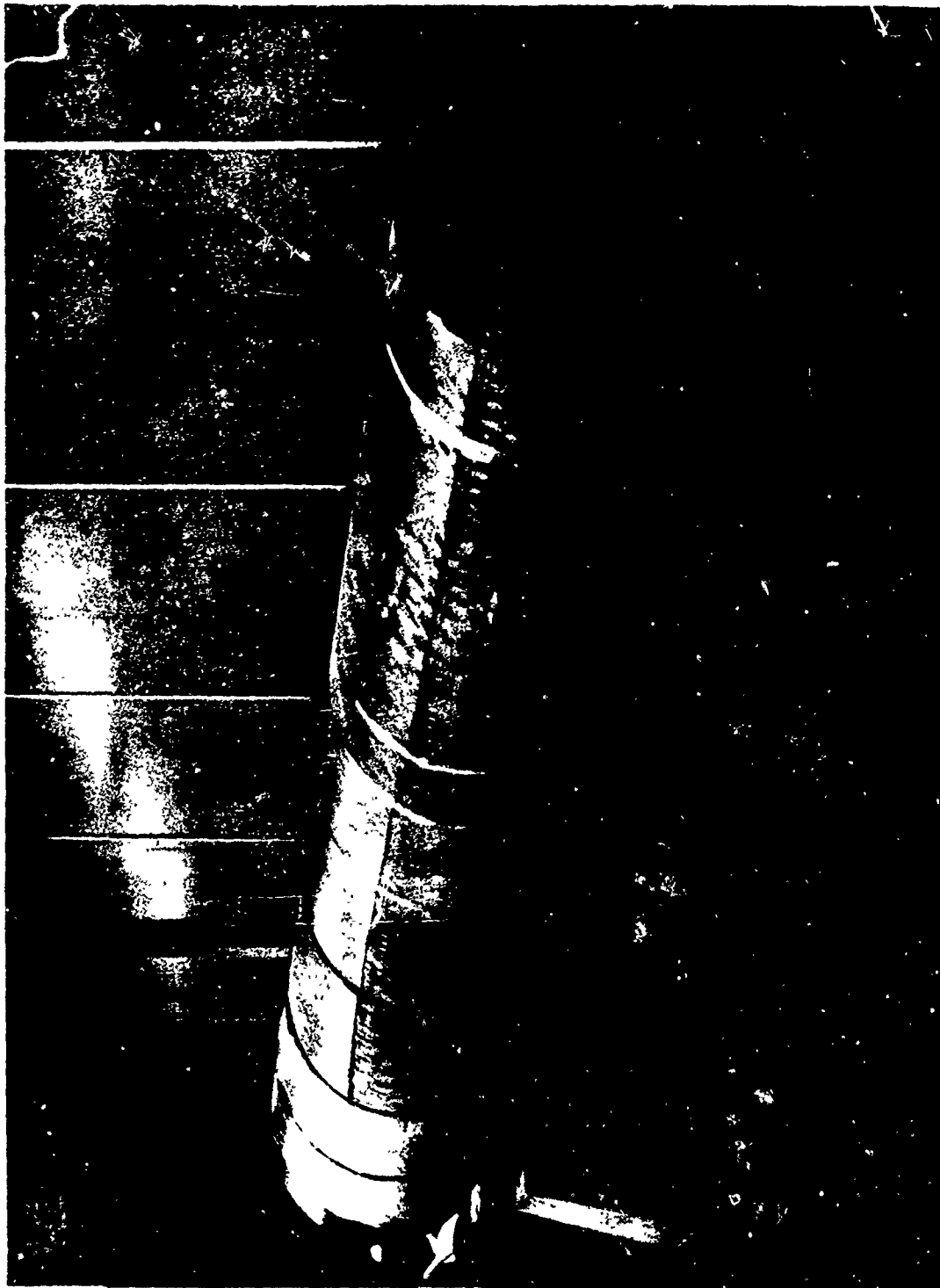
Figure 143. Bias-Ply Segments of Metal Fabric Positioned on Boom Form Tool

335/290A

293
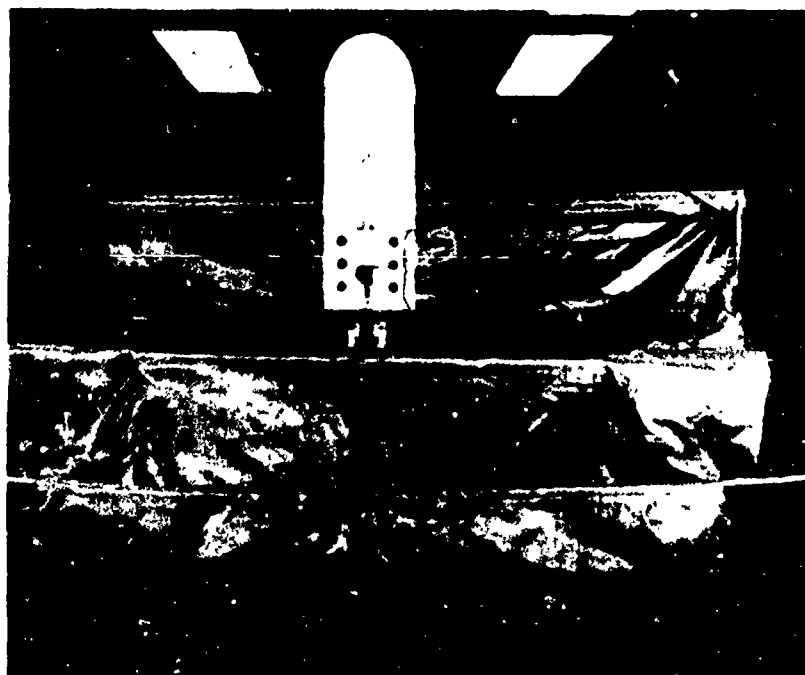
335/394

335/300

Figure 144.   Welding Large 17-Foot-Long by 8.5-Foot-Wide Cross-Ply
Metal Fabric for Boom
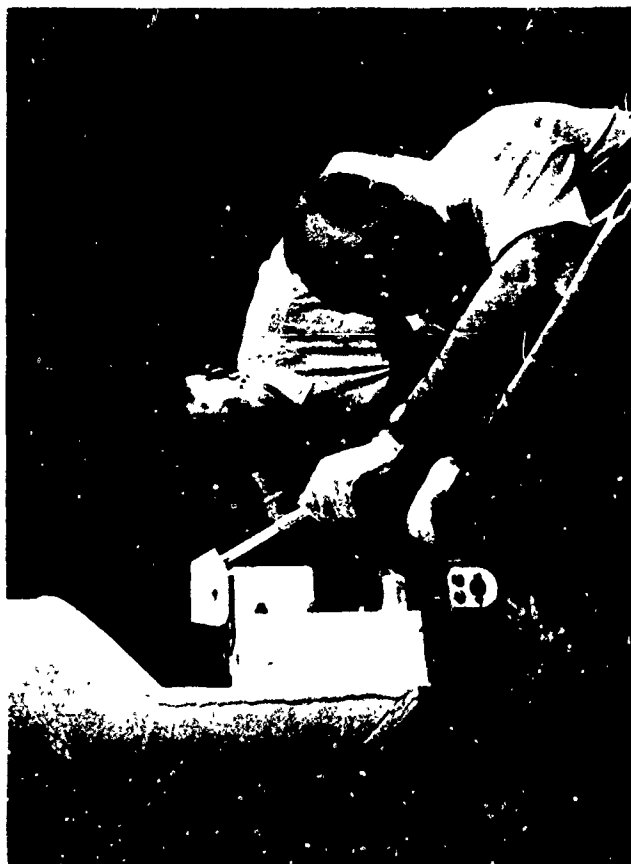
335/295
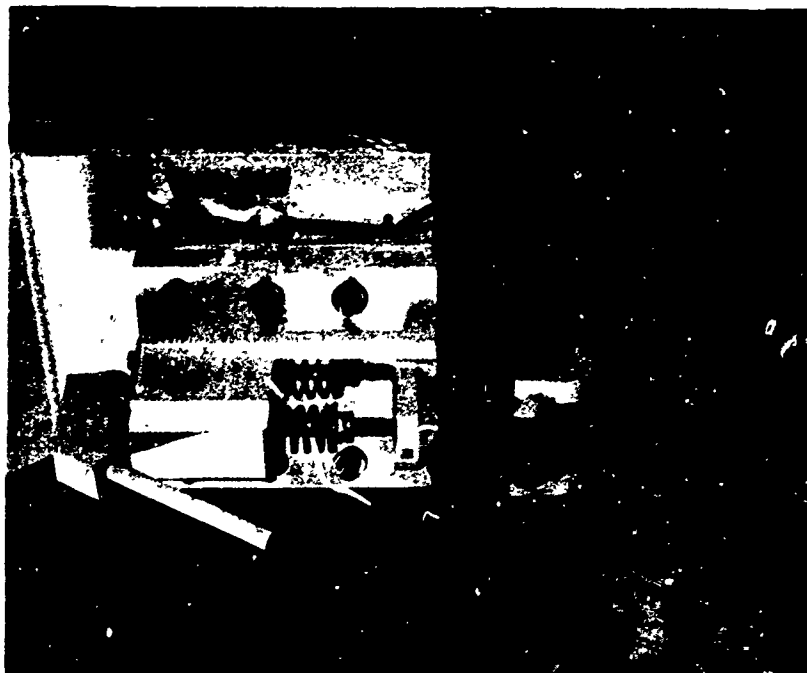
335/298

Figure 145. Positioning Welder Head During Welding of Boom Cross Ply

those on the bottom welding head. Statistical analyses of the coupons, as detailed in Appendix V, indicated that the average of 29 check coupons was 88.8 percent joint efficiency at 90 percent confident level, or 89 percent efficiency by arithmetic mean. As discussed in Section 3.9.3.3, the performance of the welder was improved through the change in electrode diameter and other modifications. The breakage problem of the upper electrodes was significantly reduced by this change.

After the cross ply of the boom was welded, the weld heads had to be turned again to 90°, relative to the welder arms, to weld the cross-ply end cap in place. During the period of readjustment of the welder, the entire cross ply was bagged on the boom form using chromate paste to seal the PVC bagging film and nitrogen to purge the enclosure to protect the cross-ply fabric from atmospheric contamination.

3.10.6.3 IMPREGNATION OF THE BOOM

To improve the possibility of removing the impregnated and coated boom structure from the form after curing, the form was sanded with fine sand paper to produce a 10- to 20-micro-inch surface. Circular wood forms were built to support the boom form tool on the horizontal supporting pipe of the dolly. The supporting dolly (to carry the boom form tool and boom metal fabric structure during impregnatic ., coating, and curing) is shown in Figure 146. This dolly supported the boom form, cantilevered from one end, and had casters designed to ride in the channels of the autoclave in which the curing was performed. The entire dolly was painted with high-temperature aluminum paint and baked at 400°F to assure that no volatiles would be given off by the paint which might contaminate the boom rubber surface during the curing process.

Two form-fitting bags of Teflon film, two mils thick, were used between the metal fabric and the boom form during the impregnation and coating to assist in removal of the structure after curing. It was planned that this would prove two possible separation or release areas between the two Teflon bags (friction coefficient only 0.05) and between the inner bag and the form tool. In addition, five holes were drilled and tapped along the length of the form tool, including one in the end cap, and these were equipped with sealed stainless steel connections accessible ._om within the boom form, to permit pressurizing the underside of the Teflon bag to aid in removal.

The plumbing set-up for boom impregnation was very extensive, involving 17 four liter flasks for liquid rubber, about 200 feet of Tygon tubing, and hundreds of miscellaneous tubing clamps and fittings. The tubing connections provided for evacuating the flask to de-gas the rubber, pressurizing the flask to help force the rubber out during impregnation, draining the rubber from each flask to individual inlets in the boom vacuum bag, and 17 similar vacuum take-offs along the top of the boom vacuum bag, all connected to the vacuum pump. About 70 large-diameter, glass stopcocks were required in this system. A large 40 cfm dual vacuum pump was selected to maintain vacuum on the system

335/295
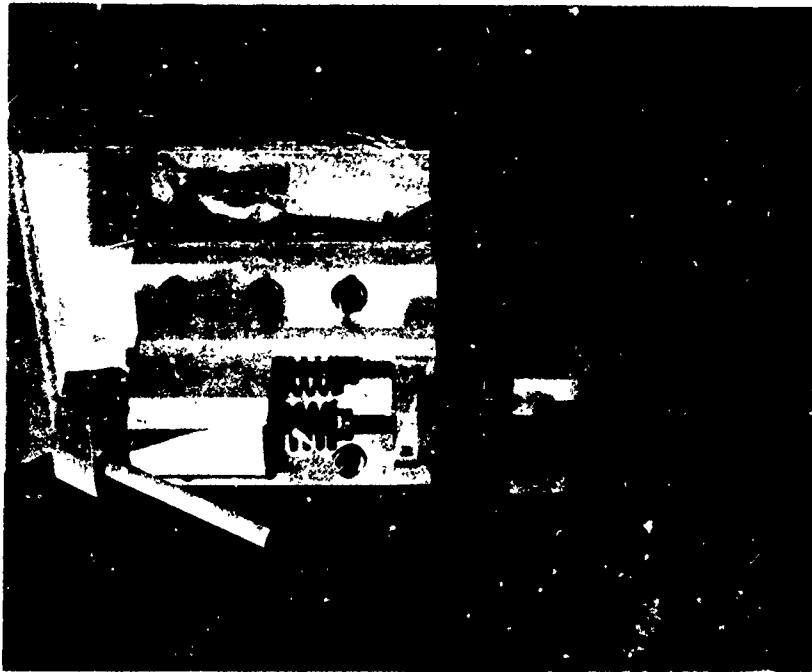
335/298

Figure 145. Positioning Welder Head During Welding of Boom Cross Ply

335/340

Figure 146.   Supporting Dolly for Boom Form Tool

during impregnation. The dual pump afforded added reliability, since a system failure during impregnation would be disastrous. The impregnation must go to completion once it is started due to the fact that the rubber is mixed and will completely polymerize in hours. Views of this plumbing arrangement are shown in Figures 147, 148, and 149. The liquid rubber may be seen soaked into the metal fabric approximately half way up the periphery of the boom in Figure 148 and about three-quarters of the way to the top in Figure 149.

After impregnation, the vacuum bag and nylon screen were removed and the entire boom was wrapped with Mylar shrink-tape, (as shown in Figure 150).to minimize the voids and squeeze out excess RTV 655, in addition to holding down the edges of the fabric at the seams during the curing of the impregnate.

Evaluation of the cure time of the RTV 655 which had been used on the frustums, indicated that the recommended mix of ten parts of component A to one part of component B was providing less than two hours of usable pot life, after which the viscosity increased to the point where it was doubtful whether it would flow through the extensive plumbing system required. With the cooperation of the General Electric Laboratories, Waterford, New York, tests were run resulting in the use of a mixture of two lots of component A (in 1:1 proportion) to lengthen the pot life. The two different lots were guaranteed to have the same physical properties except that one lot had a longer cure period than the other. Use of this mixture, with the usual mix of one part of component B to ten parts of component A, resulted in a significantly longer pot life; as a matter of fact, some difficulties were experienced in getting the impregnant to cure sufficiently to permit overlaying the S-6510, and heat guns were used to accelerate the curing after impregnation.

Additional tests were run with the RTV 655 mixture to assure that the Teflon film, which was used to coat the boom form, and the Teflon "Temp-R-Tape C," which was used to seal the seams in the Teflon bags, would not inhibit the cure of the RTV 655. Tests at both General Electric and Space-General established that no inhibition would occur. The "Temp-R-Tape" is coated with a silicone rubber adhesive.

The impregnation of the boom was started at 4:15 a.m. on 13 April 1966 and concluded at 6:00 p.m. that day.

3.10.6.4 COATING THE BOOM

The lay-up on the boom of the S-6510 silicone rubber was started early on 14 April and concluded at 12:15 a.m. on 15 April 1966. The operation of applying the S-6510 silicone rubber coating is shown in Figure 151. Considerable hand work was required to fill cracks and voids which occur unavoidably in the calendering of the silicone rubber sheet. Figure 151 shows how the "orange peel" seams in the end cap were first faired in with strips of the white silicone rubber to present a smooth surface for the final overlaying of the 0.125-inch-thick ablative coating shown in Figure 152.
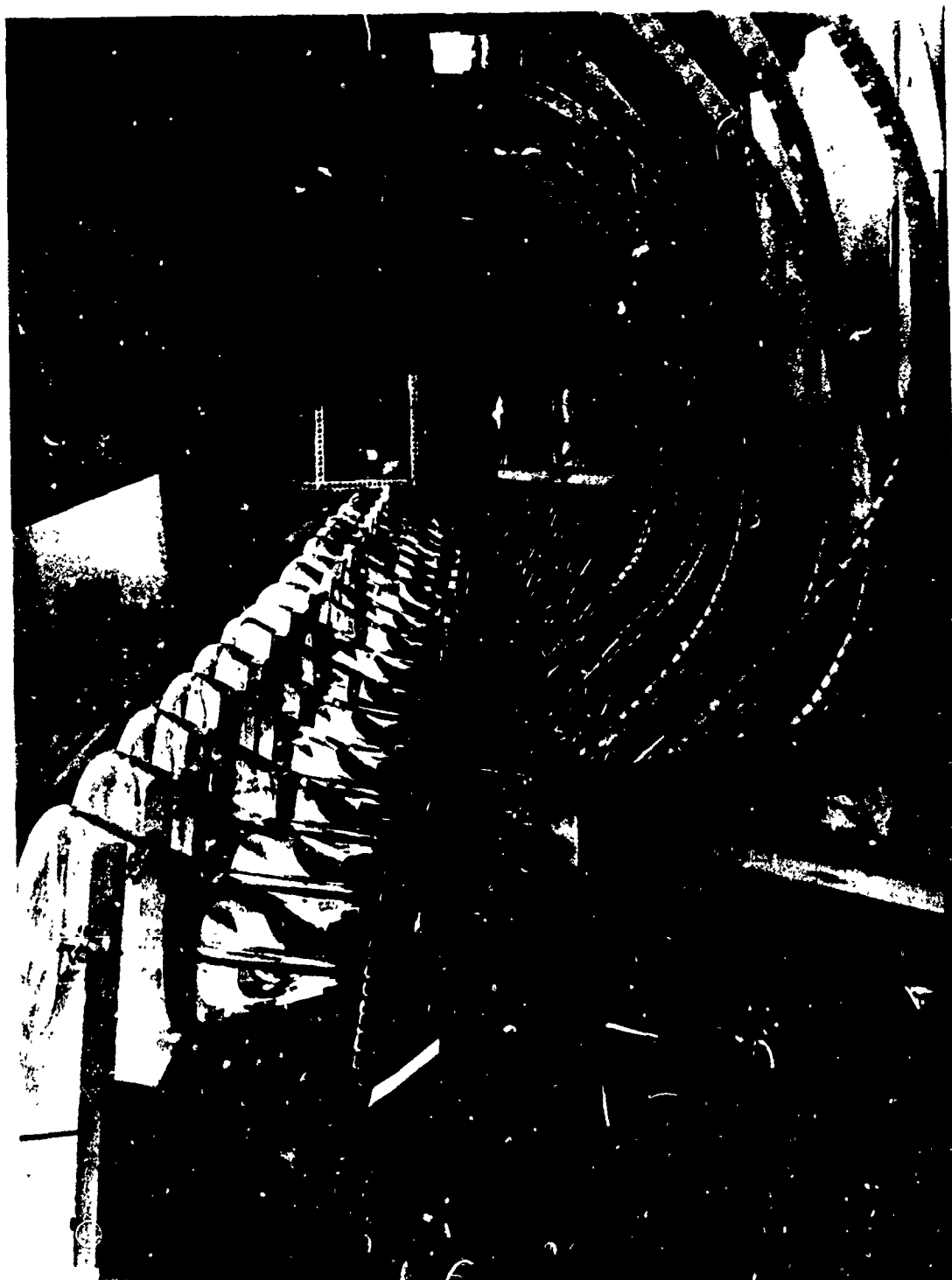
Figure 147. Plumbing Arrangement for Feeding Liquid Silicone Rubber
to The Boom During Impregnation
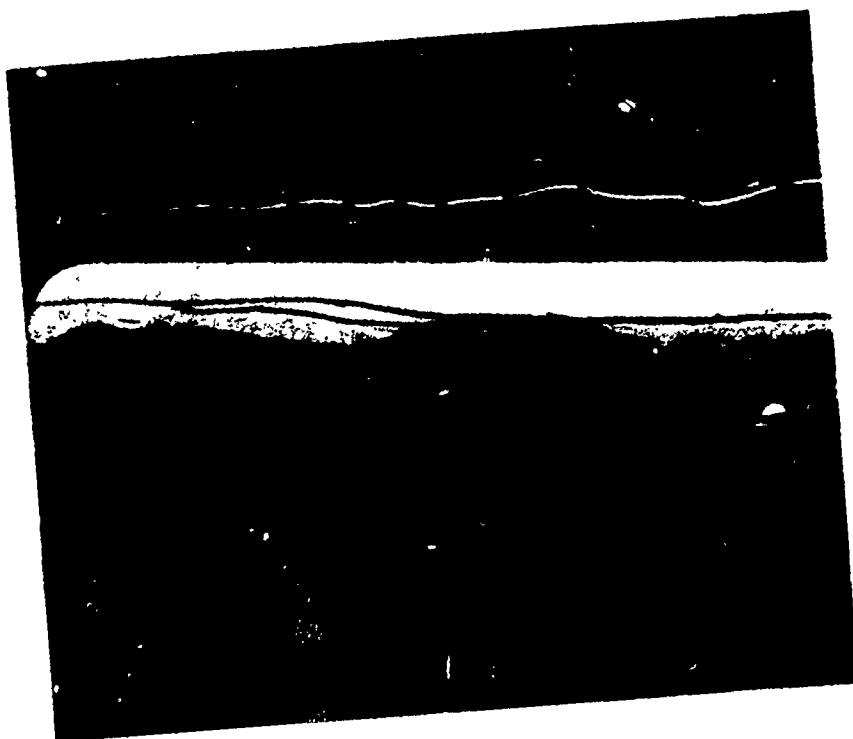
335/354

Figure 148. Overall View of Plumbing Set-Up and Vacuum System
During Impregnation of Boom
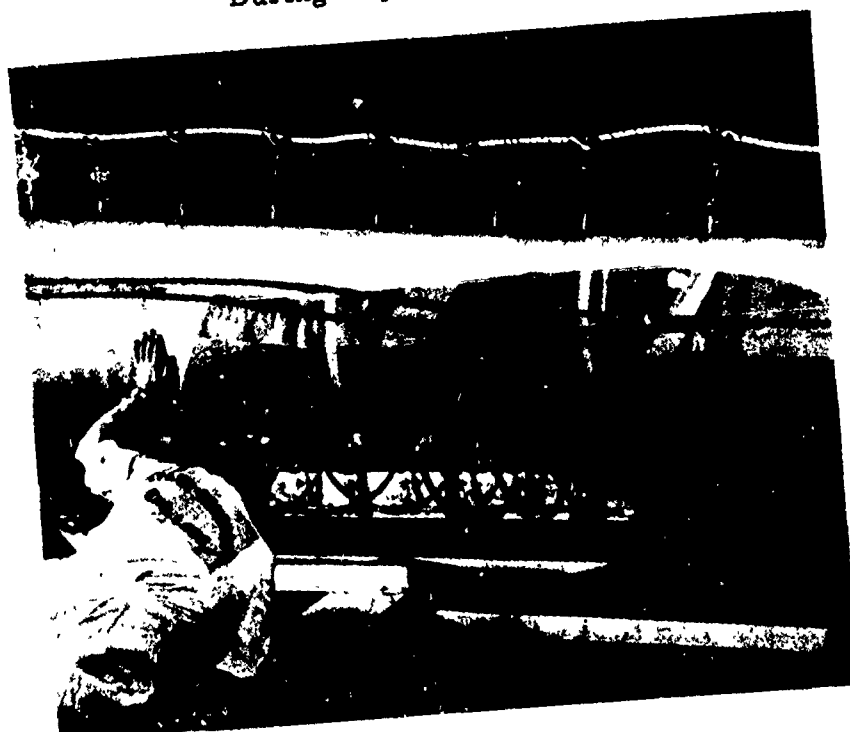
335/356

Figure 149. Saturation of Boom Fabric Shown Approximately Three-
Fourths Complete

Figure 150. Wrapping Impregnated Boom with Shrink-Tape
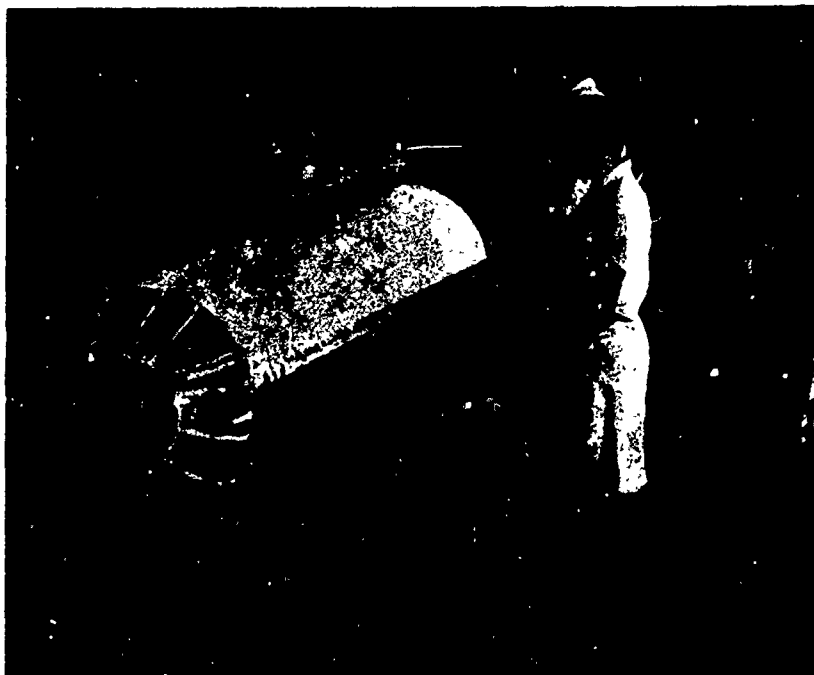
335/307

335/309

Figure 151. Applying S-6510 Silicone Rubber Coating to Impregnated
Boom

302

335/311

Figure 152. Hand Dressing of Boom End Cap Coating

The boom, nearing completion of the lay-up of the outer coating, is shown in Figure 153, with the 0.125-inch-thick coated quadrant of the boom facing the camera. The plastic-enclosed, semi-clean room in which the impregnation and coating was performed may also be seen in these photos. As a result of the development testing involving laminated S-6510 silicone rubber lay-up versus a single homogeneous layer of S-6510, the boom was laid-up with approximately 90° of the periphery having a 0.125-inch-thick single layer (non-laminated) "ablative" area and the remaining three-fourths coated with 0.035-inch of S-6510 silicone rubber.

The entire surface of the boom was carefully covered with a layer of "Temp-R-Glas" Teflon-coated glass fabric to get a smooth finish. The end cap was laid-up with type 181 glass fabric because it was easier to stretch this fabric over the compound curvature surface. The "Temp-R-Glas" fabric was cleaned with methyl alcohol immediately prior to use, and the type 181 fabric was treated with Orvus WA release agent and dried before being applied to the end cap. Over these primary bleeder fabrics, an additional layer of type 181 glass fabric was loosely wrapped. Finally, the entire assembly was covered with a PVC bag to protect it during transportation to the autoclaving facility of Haveg-Rheinhold at Santa Fe Springs, approximately 15 miles from Space-General.

The boom is shown positioned in front of the autoclave in Figure 154, with the outer fiber glass bleeder cloth in place but prior to application of the vacuum bag.

At the autoclaving facility, the boom was vacuum bagged with new PVC material (see Figure 155) after removing the shipping bag. The boom on its supporting dolly was installed in the autoclave at 1:30 p.m. on 15 April 1966, and vacuum applied to the bag as shown in Figure 156. An overall view of the autoclave and instrumentation is shown in Figure 157. Vacuum on the vacuum bag appeared to be holding quite well, although some cycling between 26 and 28 inches of mercury was noted. Although contrary to the 28 inches of mercury minimum vacuum specified in Space-General's specification, inability to reset the subcontractor's vacuum pump instrumentation prompted proceeding with the process. The autoclave operators felt that the vacuum pump could handle the apparent leakage and the autoclave pressurization was started.

At 216 psig, at 2:45 p.m., the subcontractor advised that it was impossible to pressurize higher with the available CO_2 supply and that it would be necessary to turn the autoclave heat on to increase the pressure. Although this also was contrary to Space-General's specification, the process had started and it was decided to continue the operation. The vacuum cycling, as a result of the vacuum pump starting and stopping, became very rapid at 3:10 p.m. when the autoclave was at 242 psig and the temperature was 250°F. At this point the subcontractor advised that the process would have to be shut down to repair the vacuum leak. The autoclave was fully de-pressurized, cooled, and opened at 4:05 p.m. After several hours of trying to locate the vacuum leak without success, the vacuum bag was changed to PVA (polyvinyl alcohol) material on the advice of the subcontractor. After considerable difficulty with leaks in this vacuum bag, the autoclave was again closed and re-pressurized at 2:00 a.m. on 16 April 1966.

304
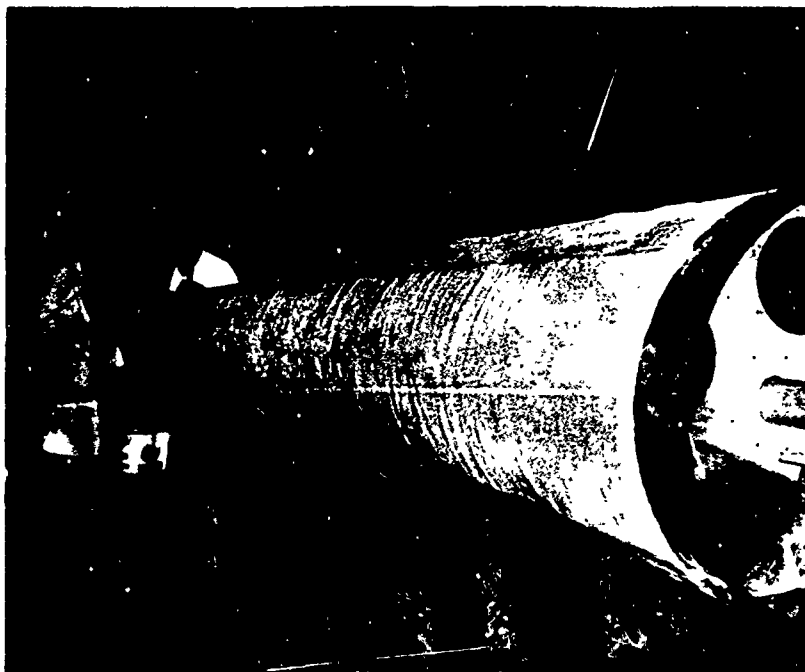
335/361

335/329

Figure 153. Finishing Silicone Rubber Outer Coating of Boom

335/364

Figure 154.   Boom Wrapped with Outer Fiber Glass Bleeder Cloth in
Front of Autoclave and Prior to Covering
with Vacuum Bag
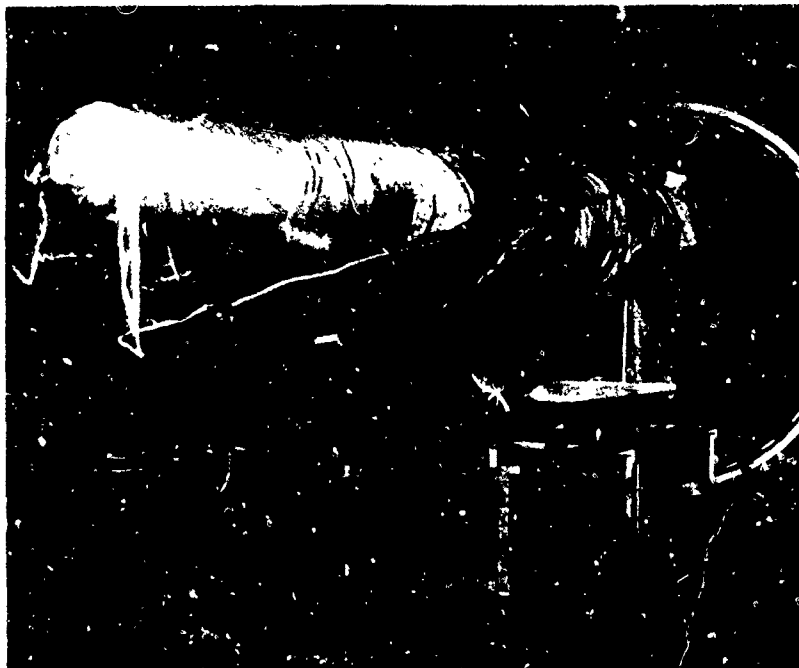
335/366

Figure 155.   Boom with Final Vacuum Bag Covering Reading for Autoclaving

307

335/369

Figure 156.   Boom in Autoclave with Vacuum Applied to Vacuum Bag
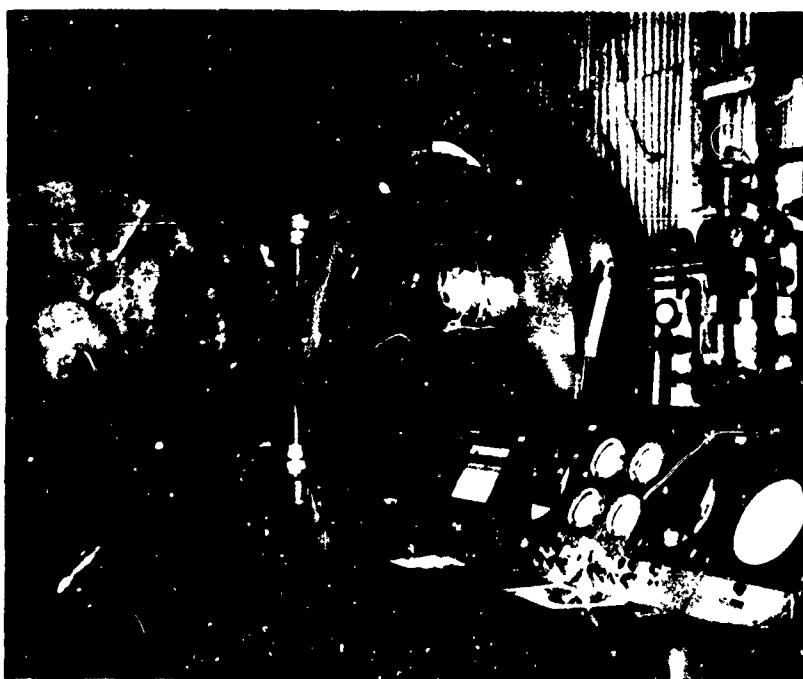
335/368

Figure 157.   Boom Located in Autoclave with Instrumentation in
Foreground

308

The heaters in the autoclave had to be turned on again to increase the pressure to 250 psig. At 4:14 a.m. on 16 April, with a pressure of 242 psig and the boom temperature, as measured by thermocouples installed on the metal fabric, at about 250°F, the 1/2 hour cure period was started. The cure was stopped at 4:45 a.m. and the heat turned off. At 6:33 a.m. the temperature had dropped sufficiently that it appeared safe to start the de-pressurization. At 8:13 a.m. the autoclave door was opened, and the boom was removed at 8:40 a.m. Immediately upon removal, it was noted that several large bumps about 12 inches by 4 inches and 3/4-inch-high existed near the tip of the boom. It was not known at the time whether this was a blistering or de-lamination of the rubber coating or just a bleeder cloth or vacuum bag discrepancy.

The vacuum bagging and bleeder cloth material was removed from the boom on 18 April 1966, and the surface of the S-6510 silicone rubber coating appeared pockmarked with many small 1/8-inch fissures over about six square feet in two areas, especially in the 0.125-inch ablative section. After close inspection by personnel from the Space-General Materials and Processes Department, the interior of the 0.125-inch-thick silicone rubber coating was found to be full of holes (like a sponge) and not well bonded to the impregnated metal fabric. After removal of many of the sponge-like areas, the boom appeared as in Figure 158. A close-up view, Figure 159, clearly shows the sponge-like structure of the coating. It was reasonably obvious that the de-pressurization of the autoclave, after the heating process had started, caused expansion of the volatile products of the curing reaction. It was apparent that all of the 0.125-inch-thick S-6510 quadrant of the boom was unsatisfactory and that the coating operation in this area would have to be repeated. The boom was returned to Space-General for re-work.

Almost a week of tedious peeling away of the coating by two to three technicians, resulted in a nearly "clean" surface, with specks of S-6510 still cohesively adhered to the impregnated metal fabric. Since the end cap had been coated with 0.125-inch-thick S-6510 to help cover the many seams, all of this material was removed also.

The process of repair and replacement of the coating material on the boom is discussed in Section 3.10.8, entitled "Repair Techniques." The small specks of S-6510 and some of the adjoining areas did not appear to be properly cured since they were still tacky. The entire surface of the thin S-6510 coating, as well as the areas where the coating had been peeled away, was sprayed with a toluene solution of 5 percent (by weight) benzoyl peroxide catalyst, since the necessary catalyst had obviously been lost during the autoclaving perturbation.

A fresh batch of 0.125-inch-thick calender S-6510 was obtained to re-coat the boom using additional RTV 655 painted on the area as an adhesive. The cuff areas were again shrink-taped to hold down the fabric edges and the tape was shrunk using the heat gun shown in Figure 160. This photograph also shows the thermocouple wires which passed between the impregnated metal fabric and the outer silicone rubber coating. The thermocouple junctions were spot welded to the outer surface of the metal fabric before impregnation.

309
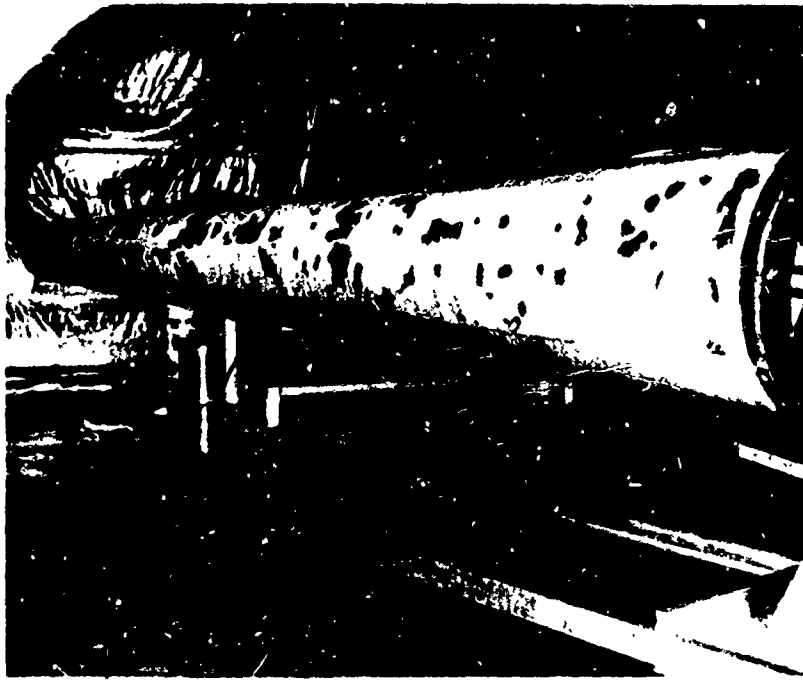
. 335/341

Figure 158. Boom with Portions of Outer Silicone Rubber Coating Removed
to Expose Damage that Occurred During First
Pre-Cure Operation

335/343

Figure 159. Close-Up View of Damaged Boom Coating Showing Sponge-
Like Consistency

310
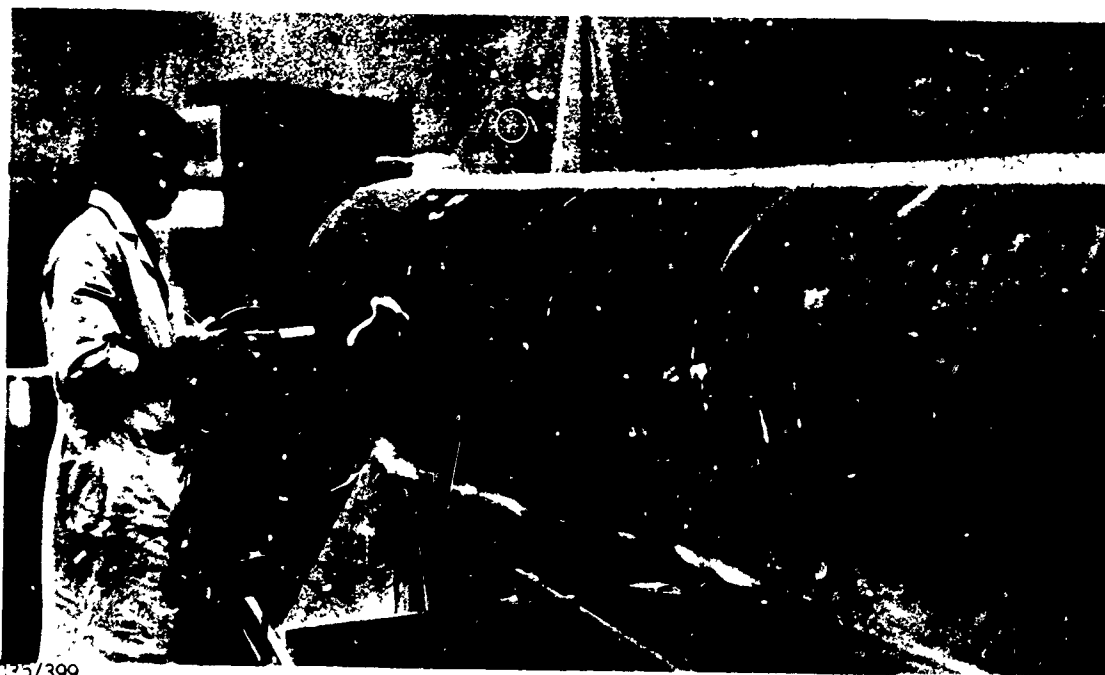
Figure 160.   Heat Shrinking Mylar Tape to Hold Down Fabric Edges
After Recoating with RTV 655
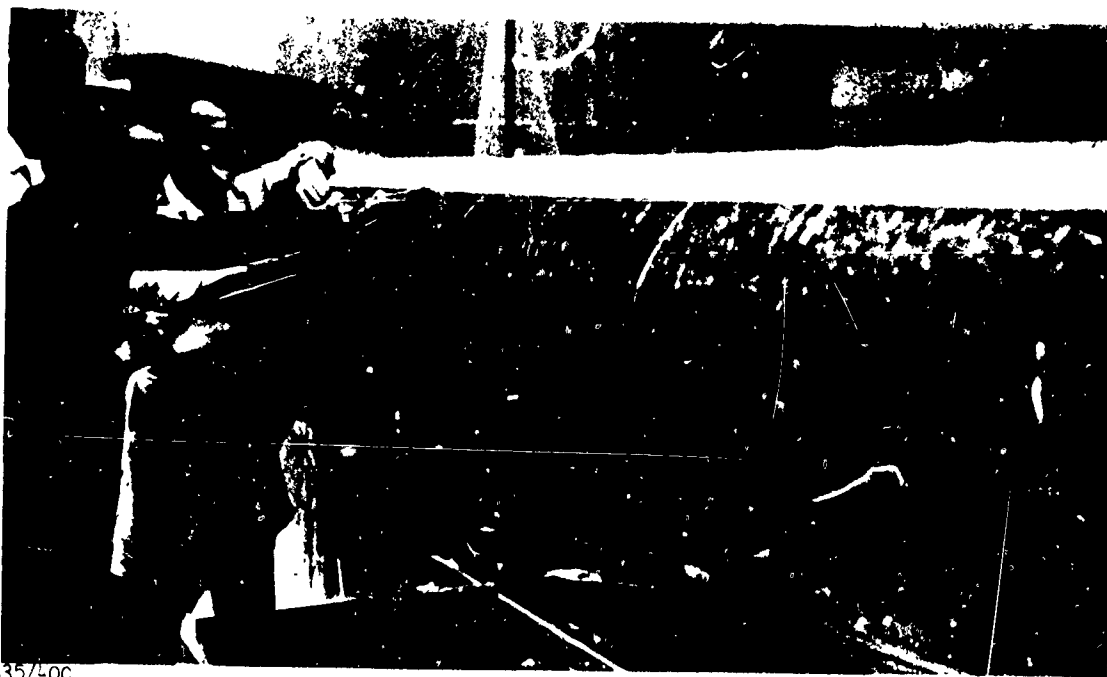
Figure 161.   Applying New Silicone Rubber Ablative Coating

311

The S-6510 was laid down very carefully by rolling it into position to exclude air as shown in Figure 161. All areas were hand dressed and finally covered with "Temp-R-Glas" fabric except for the end cap which was again covered with type 181 cloth treated with Orvus. The boom was again covered and shipped to the Haveg-Rheinhold autoclaving facility at about 11:00 p.m. on 5 May 1966.

The subcontractor vacuum bagged the boom with PVA and, after a test on the vacuum tightness of the bag, the autoclave door was closed and pressurization of the clave began at 2:35 a.m. on 6 May. When the autoclave reached 215 psig, the heat had to be turned on as usual to increase the pressure. The pressure reached 240 psig at 4:08 a.m. with the clave temperature at 250°F. The clave temperature was kept below about 270°F to prevent overheating, and by 5:15 a.m. the thermocouple embedded in the metal fabric at the large end of the boom showed 250°F. It was later found that this temperature was in error due to an instrumentation hookup problem, and the actual maximum cure temperature was about 210°F. A 45-minute cure period was started to insure that all of the boom areas would reach the cure temperature. This longer cure period probably helped to offset the effects of the low cure temperature. The cure was considered complete at 6:00 a.m., at which time the heat in the autoclave was turned off. Since this autoclave has no provision for rapid cooling, the temperature dropped only about 10 degrees in 15 minutes, and the operators were forced to vent the clave to 224 psig to aid the cooling operation. Finally, the clave was de-pressurized and the temperature of the part had dropped to 190° F at 8:20 a.m. when the clave was opened. The part was left sealed in its vacuum bag over the weekend.

On removing the vacuum bag from the boom, the new 0.125-inch-thick S-6510 surface appeared excellent and white, but the old 0.035-inch material remained tan and mottled-to-dark-tan, although it was better appearing than after the first pre-cure probably due to the application of the additional peroxide catalyst. There were a few areas in the old 0.035-inch material which were quite dark, almost purple colored, and still appeared to be uncured, as they were soft and easily marked with a fingernail.

After removal from the pre-cure autoclaving, the boom appeared as in Figures 162 and 163. These photographs show the lighter colored new 0.125-inch-thick coating and the darker colored old coating with the boom in two different rotational positions. Figure 163 also shows the wing attachment flap at the bottom of the boom before trimming off the excess silicone rubber.

The boom seemed to be stuck tightly on the form and for a while concern existed that it could not be easily removed. The internal tube leading to the end cap was pressurized with air at less than 1 psig and the cap area was raised from the form tool approximately one inch. Next, the tube leading to the large end of the boom was pressurized. By pushing on the fabric to distribute the air, all of the areas were loosened from the form tool and the boom slid off easily. The separation occurred between the inner Teflon bag and the form tool. The inner Teflon bag was then pulled easily from within the boom, but the outer Teflon bag adhered to the impregnant, particularly at the end cap. This outer Teflon bag was released from the boom by crawling inside and carefully peeling it away.
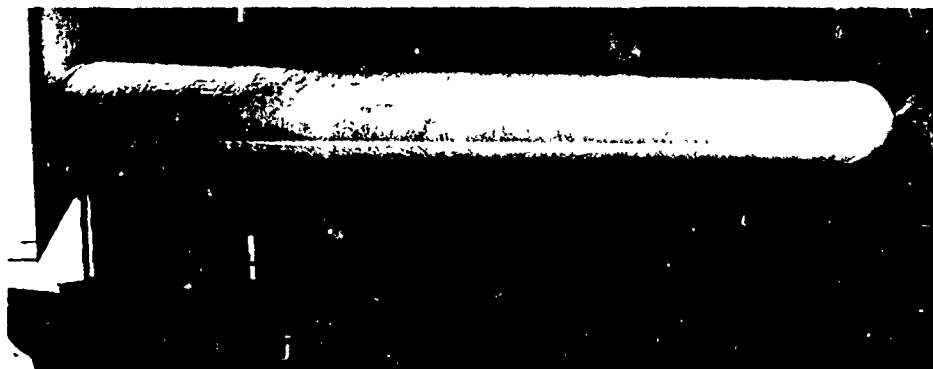
335/414

Figure 162. Boom After Second-PreCure Showing Old and New
Coating Areas
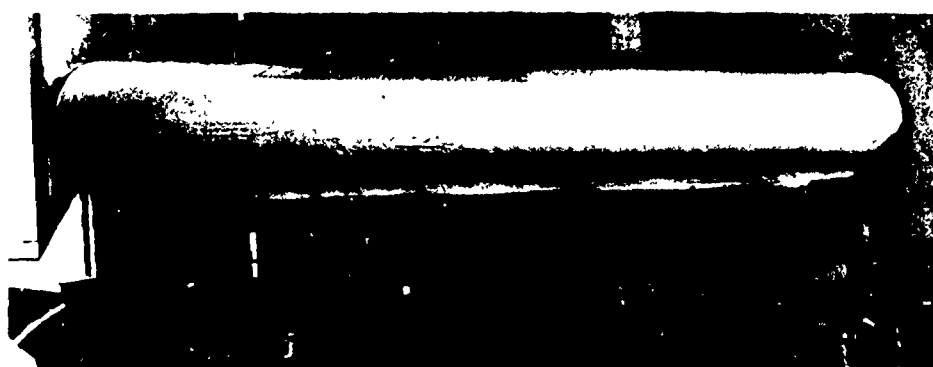
335/415

Figure 163. Boom After Second Pre-Cure Showing Wing Attachment
Flap and New Ablative Coating

335/433

Figure 164. Boom Following Second Pre-Cure After Removal
From Form Tool

313

The boom was very flexible when off the form tool, and there was some difficulty in handling it without creasing, but no obvious damage occurred. The boom is shown in Figure 164 (after removal from the form tool) with a technician holding open the large end showing a rather uniform coating of impregnant on the interior. The thermocouple wires connected to the boom may also be seen in this view.

A steel pipe extension was strapped on the supporting pipe of the dolly to give added length, and the entire pipe length was padded with fiber glass fabric. The boom itself was then hung on the supporting pipe without the form tool. The entire surface of the boom was cleaned with liquid soap and water, rinsed, and dried with white cotton cloths. Practically all of the boom surface was repainted with a 10 percent benzoyl peroxide solution in toluene, to help bleach out the dark areas and cure the small purple-colored areas. These areas were given a double coating of the toluene solution which tend to soak into the rubber and carry the benzoyl peroxide with it.

The entire assembly of the boom hanging on the horizontal pipe of the boom dolly was installed in the subcontractor's large oven, as shown in Figures 165 and 166. The oven had been cleaned out and all organic material removed.

The oven was heated to 250°F and held for one-half hour, then to 350°F for one-half hour, and finally to 400°F $\pm$ 10°F. After 16 hours at 400°F, the oven heat and blower were shut off. It was allowed to cool to 300°F, then the blower was turned on to bring the temperature down to 250°F, at which time the doors were opened.

Inspection of the boom indicated that the final cure had been successful with no obvious bad areas in the coating except for the mottled color of the thin rubber. The boom is shown in Figure 167 immediately after removal from the oven. The second application of catalyst had apparently been successful in curing the dark spots. The purple color disappeared, and all areas now appeared to be completely cured. The boom was returned to Space-General.

Important observations on the autoclaving process which would help prevent the repetition of problems encountered were as follows:

a. The autoclave should be able to get to 250 psig or to the final agreed-upon autoclaving pressure without turning on the main clave heating system. This would assist in the discovery of vacuum bag leaks before the actual chemical reaction of the cure cycle has started. If necessary, the clave could be de-pressurized slowly at any time before heat was applied.

b. There should be a way to cool the clave rapidly. This would slow down any chemical reactions before de-pressurizing in case it is necessary to shut down before the cure is complete. Nevertheless, there would still be considerable risk involved in this.

314

335/425

Figure 165. Boom in Oven Ready for Post Cure with Ablative Area
on Top

335/423

Figure 166. Boom in Oven Ready for Post-Cure Showing Non-Ablative
Coated Area and Wing Attachment Flap
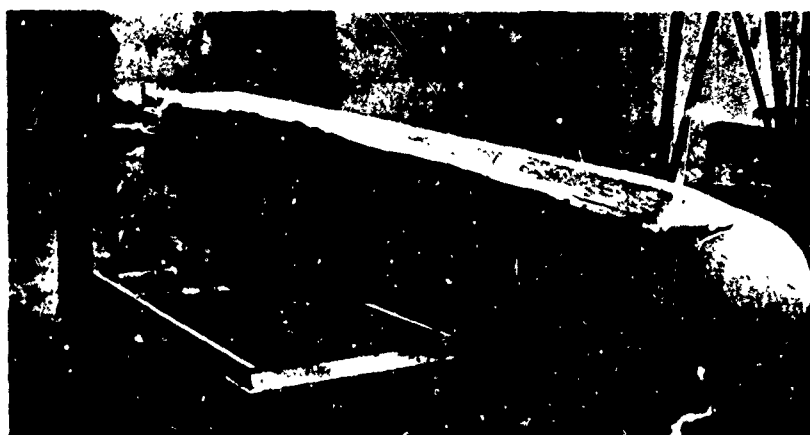
335/440

Figure 167. Boom Being Inspected Following Post-Cure

315

After return to Space-General, the boom was again washed with detergent and rinsed with water, as shown in Figure 168. By using a large fiber glass cloth as a cradle, six men removed the boom from the form tool without creasing it, as shown in Figure 169.

In preparation for testing, the S-6510 coating was removed from the clamping area about 1-1/4 inches from the end of the boom. The overhanging cuff material was trimmed off flush with the end of the boom as had been the practice with the frustums. Superfluous RTV 655 within the outside of the clamping area was peeled off by hand to avoid interfering with the holding capability of the clamps in retaining and sealing the specimen. The clamp ring was installed using only every other clamp, as shown in Figure 170, to permit checking for leaks. At a nitrogen pressure of approximately 0.2 psig, some small leaks, blisters in the external coating, and small areas of inner ply delamination were observed. Most of these areas were in the thin coating near the large end of the specimen and may possibly be attributable to the difficulties encountered in the cure cycle

To hold open the boom for internal inspection and repair work, five form rings of one-half-inch steel tubing in graduated diameters were fabricated.

Inspection of the interior of the boom indicated a superficial layer of RTV 655 impregnant as much as 0.050-inch deep in some places. Several voids in this layer, some of approximately one square-inch in area, were observed where the fabric surface was exposed, but these areas apparently were saturated with impregnant.

Another type of fabrication anomaly consisted of folds in the bias (inner) ply. Small longitudinal folds were noted in several locations with the largest being almost two feet long. These folds were of the order of 1/8-inch-high.

Due to possible contamination from handprints, etc., during removal of the Teflon film and inspection of the interior of the boom, the boom was washed out with water, followed by methyl alcohol, and dried with a purge of warm air. A batch of RTV 655 was prepared and painted on the interior of the boom. The RTV mixture consisted of 350 grams of the quick cure to 200 grams of the slow cure component A and 55 grams of Component B. This mixture polymerized very slowly, and heating lamps were installed in the boom the next day, in addition to a warm nitrogen purge at 100°F to hasten the curing period. Subsequently, the small areas which could not be coated due to the supporting rings were similarly painted with RTV 655. A warm air purge was used to hasten curing during the following day. On finally removing the supporting rings from the boom, two small areas of RTV 655 about 1-1/2-inch by 1-inch adhered to the rings and were peeled away. There is no direct evidence that these areas may have contributed to some of the small leaks that were encountered later.

335/412

Figure 168. Washing Boom Following Post Cure

335/410

Figure 169. Removing Boom from Form Tool for Initial Pressure
Testing

335/434

Figure 170. Installing Boom End-Closure for Initial Pressure Tests

317

3.10.7   APEX FABRICATION

3.10.7.1 APEX PATTERN DEVELOPMENT AND LAY-OUT

The apex form tool shown in Figure 123, Section 3.10.2.3, was
scribed to determine the longitudinal and transverse centerlines. Since the
pattern lay-out drawings, previously prepared, were primarily to determine
the most economical and expeditious utilization of the bolt of fabric, these
lay-outs did not attempt to show the precise geometry (i.e., curved edges)
of the patterns. It was, therefore, necessary to cut oversized pieces of heavy
kraft paper and position them on the apex form to determine the exact location
of the overlay seams. Because of the compound curvature and large size,
aircraft lofting techniques were used. Large sheets of paper were laid out
on a drafting table and, with the use of large ship curves, the exact shape of
each pattern was developed full-scale. The paper segments were then cut
and placed on the apex form tool so that they would fit smoothly without
wrinkles, as shown in Figure 171. The most difficult lay-out and fitting of
the paper patterns came in the small-radius crotch areas between the center
keel and the two outer leading-edge booms.

The patterns were marked to give symmetrically arranged seams
imposing minimum stress concentrations. Each pattern was identified be-
fore being removed from the apex form tool. Both bias and cross-ply pat-
terns were developed in this way and over 200 separate fabric segments were
required for the apex, including the three stub booms. The 32-inch-diameter
by 36-inch-long stub booms are not shown in Figure 171. The paper patterns
were then transferred to the metal fabric broad goods using a ball-point pen to
carefully outline each pattern. The metal fabric was cut and prepared for
cleaning. Each metal fabric segment was identified with a plastic tag and stain-
less steel wire which would not be affected by the cleaning process.

3.10.7.2 CLEANING AND WELDING APEX FABRIC

In a simultaneous and parallel operation, the metal fabric seg-
ments were cleaned after they were laid out and cut. The cleaning procedure
was generally in accordance with the process described in Section 3.10.1.2.
Each metal fabric segment was dried in the warm-nitrogen drying chamber,
placed in a nitrogen-purged plastic bag, sealed, and stored until needed.

Welding of the large metal fabric patterns for the apex was per-
formed without encountering serious problems. The work was time consuming,
however, because of the need to manipulate the fabric carefully and to use fix-
tures and other aids to prevent creasing and wrinkling.

The bias or inner ply of metal fabric was undertaken first. The
pattern arrangement for this ply is shown in Figure 172. Difficulty was en-
countered in handling and laying-up the bias ply because of the tendency of
the fabric to trellis or change shape, elongating in one direction and narrowing
in the other. It was necessary to continuously check all segments of fabric to

Figure 171. Lay-Up of Paper Patterns on Apex Form Tool

319
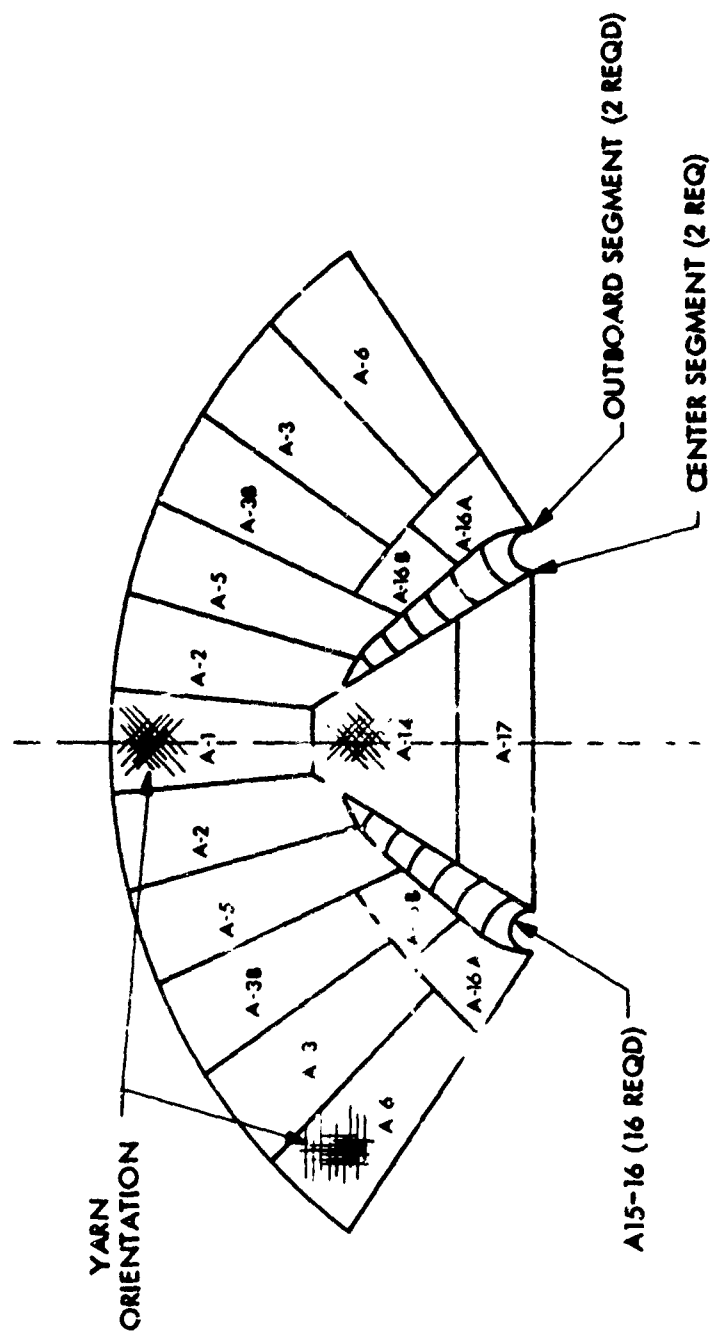
Figure 172. Apex Bias-Ply Pattern Lay-Up

be sure the warp and fill yarns were at right angles, but it was impossible to avoid some wrinkles and packers in the bias ply.

One of the bias-ply seam welds, which joined segments A2 and A5, puckered slightly as shown in Figure 173. One cause of this pucker was undoubtedly the deformation that was occurring due to trellising of the fabric when it was laid and smoothed over the form tool. Another factor that could have caused this was improper orientation before basting. Although basting is done on the form, using copper back-up strips, the compound curvature of each seam and relationship of each yarn to an adjacent yarn is not accurately maintained when the material is passed through the welding heads. To check the possibility of any of these factors being responsible, the opposite symmetrical seam on the other side of the apex was very carefully aligned prior to basting and welded while more accurately trying to control the handling of the part through the welder to maintain the compound curvature. The second seam showed a very slight pucker but not as much as the first seam. It was then decided that the first seam, approximately 24 inches long, would be replaced using another 4-inch-wide strip of metal fabric. This was accomplished but replacement seam also showed a slight puckering, which indicates that there was a possible built-in misalignment of yarns in the fabric on either side of the original puckered area. To help avoid such difficulties on subsequent seams, a ramp-like device was made to fit in the throat of the welder so that the material could be fed downward and between the electrodes, then upward, so that the fabric was assisted in maintaining a pre-set contour.

Typical fitting of the metal fabric in the crotch area is illustrated in Figure 174 which shows the crotch assembly after basting but before welding.

One technique for handling the fabric assembly, as it became more unwieldy with added welded segments, was to use inflated plastic bags made up in various sizes. These were slipped inside the assembly to hold the contoured shape and to prevent the fabric from folding and creasing on itself both before and after a given area was passed through the welder. This technique, as well as the need for good light both above and below the seam being welded, with continual checking of the centering of the seam in the lap joint from above and below, is shown in Figure 175.

As one of the plies neared completion, the use of the inflated bags may be seen in Figure 176 and Figure 177. A close-up of the welding of the long circumferential seams is shown in Figure 178.

Another handling technique was in the use of Mylar shrink-tape to hold the welded metal fabric subassemblies onto the apex form, while the next piece was being basted in place. This technique is illustrated in Figure 179 which shows the outer, cross-ply sections completely welded with the exception of the crotch areas and stub booms. Note that this photograph shows the cylindrical, aluminum stub boom forms in place with metal fabric being located on the center stub boom form.

The cross-ply metal fabric was considerably easier to handle and weld than the bias ply. The only problem with the cross-ply material was that the edges, which were usually cut nearly parallel to the yarns, tended to fray. This

321

3:5/56ư

Figure 173. Welded Seam in Metal Fabric Bias Ply for Apex Showing
Problems Due to Crooked Weld and Puckering
of Fabric

322

255/506

Figure 174. Metal Fabric Segments Basted Prior to Welding for
Crotch Section of Apex

Figure 175. Use of Inflated Plastic Bag to Hold Contour of Apex While Welding

335/562

324

Figure 176. One Ply of Apex Being Welded with Aid of Inflated Plastic Bags to Maintain Proper Contours

335/575

325

Figure 177. Welding on Apex Ply Using Inflated Plastic Bags
for Contour Control

335/578

326

Figure 178. Welding a Long Circumferential Seam in One Apex Ply of Metal Fabric

335/577

Figure 179. Use of Mylar Shrink Tape to Hold Metal Fabric Segments in Place on Form Tool During Basting

535/570

328

problem was overcome, as before, by weld-tacking with a hand-held probe and Unitek power supply, wherever fraying was excessive.

When approximately 75 percent of the bias ply was completed, leaving the inside closure seam through the crotch area unbasted, the bias ply was laid aside. The form tool was wrapped with heavy paper to simulate the thickness of the bias ply and copper shim stock back-up strips for basting the metal fabric were taped onto the form in the areas of the closure seams.

The cross-ply pieces were assembled on the form and basted. Basted subassemblies were removed from the form and taken to the welder to make permanent seams. When the cross ply was completely welded (except for the final closure seams which were basted), the form tool had to be unbolted and removed from within, one piece at a time, as shown in Figure 180. After the closure seams were welded, the form tool was re-assembled within the cross ply as shown in Figure 181. The cross-ply pattern lay-up is schematically shown in Figure 182.

The two metal fabric header strips were then positioned along the outer periphery of the apex and at right angles leading down each side of the center keel-boom extension as shown in Figure 183.

Paper tapes, 1.6 inches wide, had been previously mounted on the form tool to ascertain the exact positioning and length of tape to be cleaned and cut, as shown in Figure 184. It was established that the required metal tape length was 873 feet. Allowing for an extra 10 percent, 960 feet of metal fabric tape was cleaned. Approximately two years earlier in the program, 1,000 feet of tape had been ordered in anticipation of this requirement.

The metal fabric tapes were cleaned and cut to the proper lengths. The tapes were then sewn onto the cross-ply material with small curved and straight upholstery needles using 15-pound monofilament nylon fishing line. This line was only used to hold the metal tape in place while the form was removed and for subsequent handling of the cross-ply assembly. Where the two ends of each tape wrap came together on the peripheral header strip several tack welds were used to hold it in place.

Before using the sewing technique on the apex, tests were run to determine whether sewing the metal fabric with an upholstery needle and nylon line would degrade the strength of the fabric. A sample of 1.6-inch-wide metal fabric tape was stitched with ten needle holes and monofilament nylon line across its width. The line was then removed and the specimen tensile tested. The tensile strength was found to be 462 pounds per inch compared to the tensile strength of parent metal tape of 463 pounds per inch. It was, therefore, apparent that sewing with a monofilament nylon line, using long stitches, had no effect on the strength of the fabric.

The form tool was again dismantled from within. Some of the paper-covered segments of the tool are shown in Figure 185. Some of the fishing line stitching was broken in the process of removing the form tool, but these areas were re-sewn.

329

55756

Figure 180. Removing Form Tool Segments from Within Welded Apex
Cross Ply

330

APEX
CROSS PLY

335/579

Figure 181.   Completely Welded Apex Cross Ply with Form Tool Reassembled
From Within the Metal Fabric Structure

331

OUTER SEGMENT (2 REQD)
A22-7 (18 REQD)
CENTER SEGMENT (2 REQD)
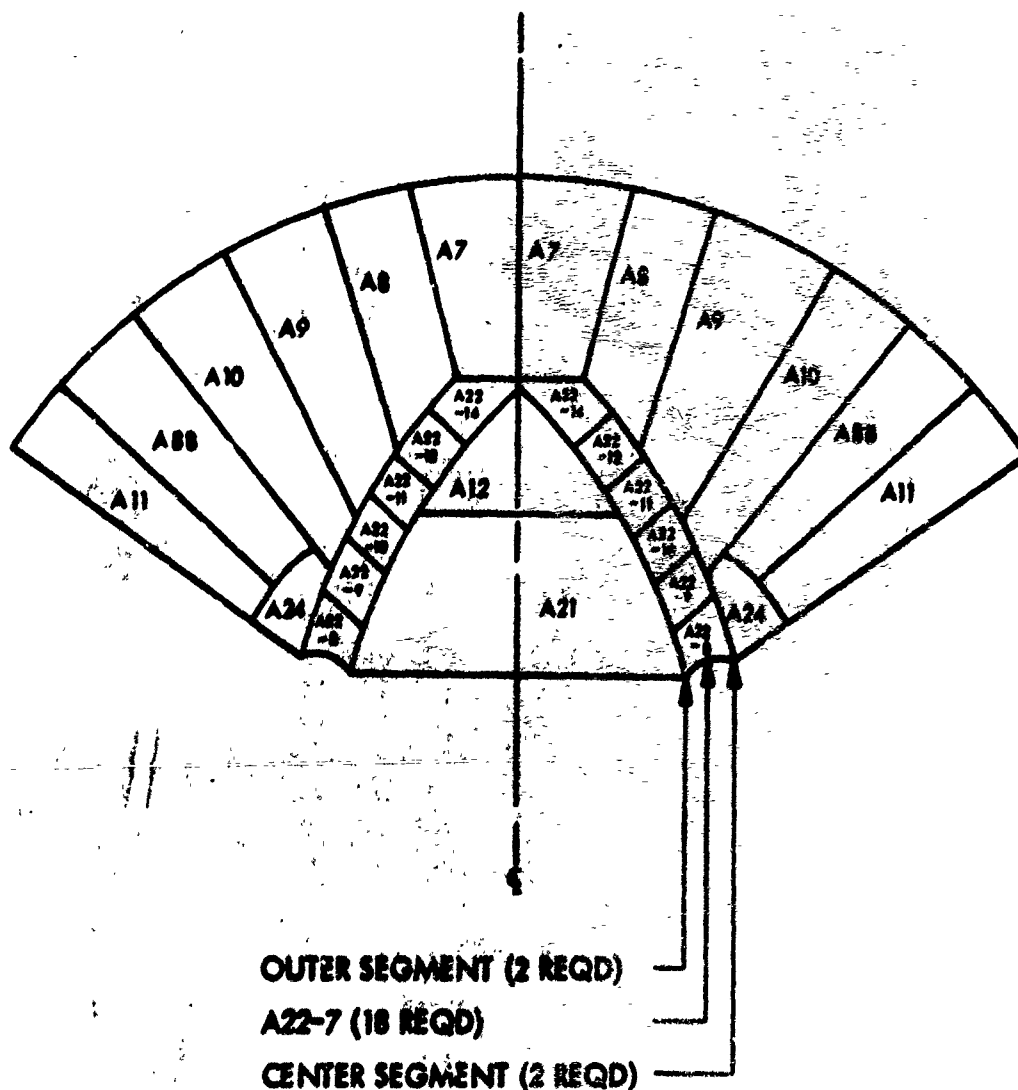
Figure 182. Apex Cross-Ply Pattern and Lay-Up

335/582

Figure 183. Positioning of Metal Fabric Header Strips on Completely Welded Cross Ply of Apex

333

Figure 184. Paper Tapes, 1.6 Inches Wide, Used to Establish Required
Position and Length of Metal Fabric Tapes
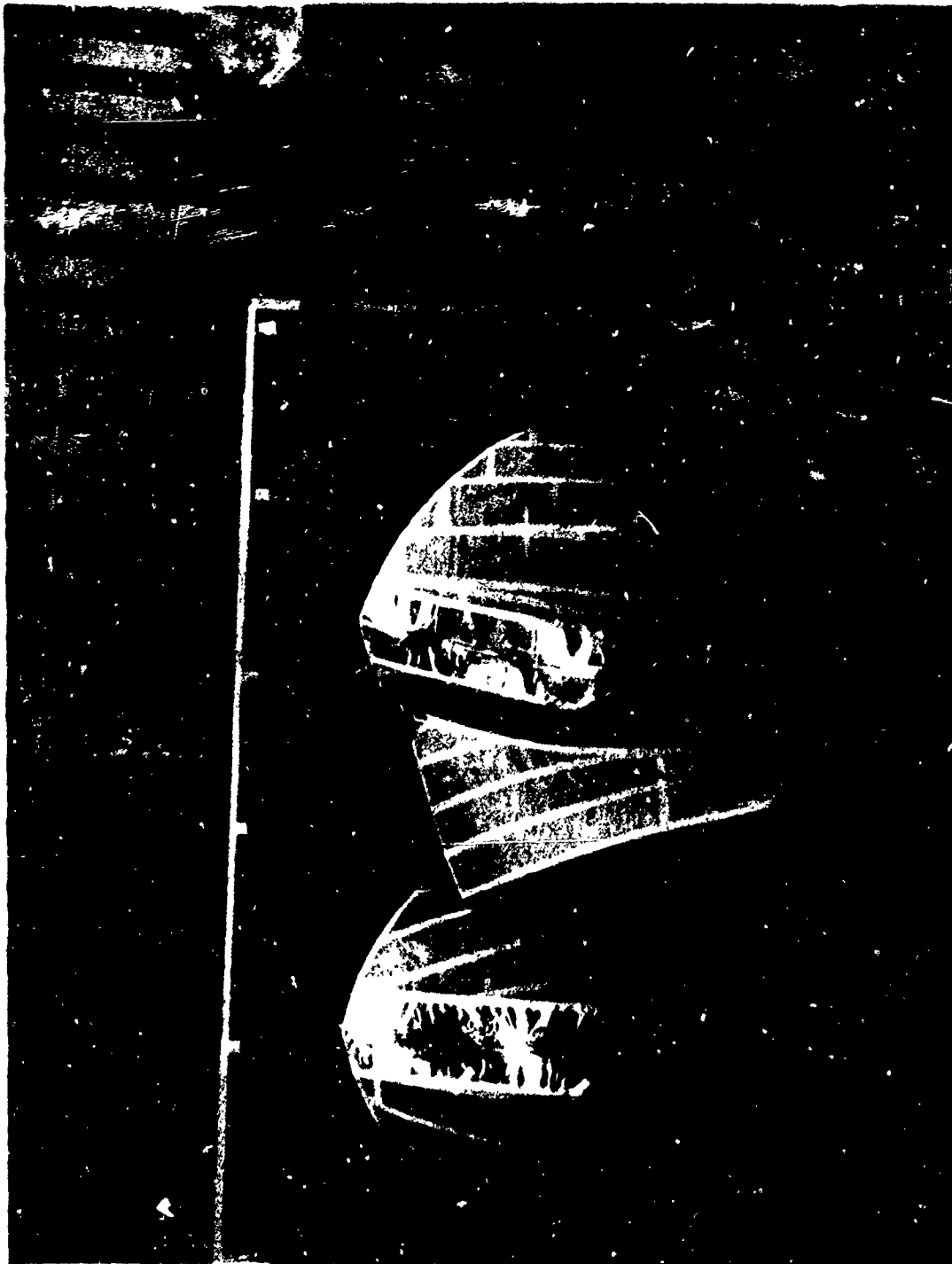
335/297

Figure 185.   Disassembled Sections of Form Tool Showing Paper Covering
to Simulate Inner Fabric Ply

335

After removal of the form tool, the header strips and metal fabric tapes were through-welded to the cross ply only at the header strips where they were basted. This operation is shown in Figures 186 and 187.

The form tool was disassembled from within once more and the closing welded seams in the bias ply were completed. The form tool was assembled again, the bias ply placed on it and basted.

When both plies were completely welded, including the outer ply with all of its tapes, it was decided to clean both plies of the apex assembly with methyl ethyl ketone. Since atmospheric exposure and handling of the apex assemblies had been significantly greater than with other metal fabric components previously constructed, it was believed that cleaning both plies with pure MEK would remove contaminants and prepare the material for better impregnation with the silicone rubber. The cleaning tanks were placed outside the assembly building. MEK was then sprayed over the entire metal fabric surface of the cross ply. After cleaning the cross ply, the lower side of the metal fabric assembly appeared to have dark streaks. The cause of this was undeterminable and it was decided that the ply should be re-cleaned.

The cross ply was cleaned again. The bias ply was then cleaned, using the tank set-up previously discussed with the addition of a stainless steel wire grid to support the fabric just above the cleaning tanks. The MEK was applied to the fabric using a 2.5-gallon can with holes punched in the bottom. Approximately 15 gallons of MEK was used for each ply. After the fabric had dried, both plies were returned to the apex assembly area.

The bias ply was then placed inside the cross ply, and the apex form tool was re-assembled inside both plies. This proved to be a very difficult procedure in that the plies, one within the other, fit very tightly on the form tool. Screw-type jacks had to be used to position some of the form tool segments and some of the clip fasteners on the inside were broken off. These were repaired with epoxy. It took three men more than three days to re-assemble the form tool within the fabric assembly.

After the monofilament lines holding the tape in place were cut and removed, small cross-ply wrinkles were smoothed out and removed. The apex appeared to have several wrinkles in the inner bias ply, however. Two large wrinkles were noted in the crotch areas and two were noted in the center keel boom, just below the tangency point of the apex. Another bulge was noticed approximately 8 inches below and completely around the tangency point on the center-keel boom. Although considerable effort was expended, all of the wrinkles in the inner ply could not be removed because of the extreme tightness of the metal fabric material on the form tool.

The outer cross ply had very good appearance, however. The tapes were also very tight. At this point the apex appeared as in Figure 188.

The clamp retaining wire was positioned at the end of each stub boom and the two-ply material rolled over it and tacked in place. The two reinforcing cuffs were assembled, welded, and slipped over the end of each stub boom. All excess material from the ends of the cuffs was removed by trimming flush.

336

335/599

Figure 186.   Welding Metal Fabric Tapes Through the Header Strips to the
Apex Cross Ply

337

355/597

Figure 187. Positioning Metal Fabric Tapes While Welding Them to Apex Cross Ply

338

Figure 166. Appearance of Final Cross Ply Assembly with Tapes Welded in Place and Form Tool Reassembled Within the Structure

339

All apex welding was accomplished using only the center welding arm. The only change in the welder set-up was to turn the welder head 90° to accommodate certain welds. After the welder became consistently operational, the electrodes were changed only three times during the welding of the entire apex seam spot welds, or approximately 672,000 spot welds. This did not include test coupons, etc. The first set of electrodes welded a total distance of 184 feet. The second set of electrodes lasted approximately 50 feet, since very large pieces of material were welded during this time. A third set of electrodes completed the operation.

3.10.7.3 IMPREGNATING THE APEX

The nylon 1/4-inch mesh bleeder screen and the vacuum bag were installed on the outside of the apex assembly on the form tool.

Chromate-type vacuum paste was applied to all the interior form tool seams. Large cracks in the form joints (over 1/64-inch) were first filled or caulked with PVA film material. A large vacuum pump was then connected and a vacuum pulled on the apex assembly. An adequate vacuum could not be maintained and, after inspection, it appeared that the form tool seams were leaking. More chromate paste was applied to all joints within the form and this improved the vacuum. It was then discovered that the form material itself leaked due to porosity in the epoxy-fiber glass structure of the form members. The entire form tool was then vacuum bagged on the inside with PVC film. The vacuum was improved considerably and there remained only the problem of finding minor leaks. This was accomplished with the aid of a halide leak-detector using a mixture of nitrogen and Freon introduced at low pressure into the vacuum bag.

The apex was then lowered on its supporting dolly to horizontal position and the plumbing for the impregnation operation was completed. The RTV 655 silicone rubber mixture of 50 percent "quick cure" and 50 percent "slow cure" had been tested to determine the usable pot life of the rubber for impregnation and the pot life was approximately 6 hours.

After all of the plumbing and vacuum bagging had been checked for vacuum tightness, 89.1 pounds of RTV 655 liquid rubber mixture was prepared and divided among 18 four-liter flasks with a small amount left over as reserve in case another flask or two had to be prepared. Seventeen of these flasks were mounted on the shaker rack and de-gassed at approximately 29 inches Hg vacuum, using the same foam breaking technique (alternately pulling vacuum and shaking) that had been used or the boom and smaller components. This process, and some of the lines and stopcocks connecting the flasks with the apex, is shown in Figure 189.

During the 30-minute period when the liquid rubber was being de-gassed in the flasks, a vacuum was also pulled on the vacuum bag to de-aerate the metal fabric assembly. The vacuum line leading directly to the flasks was then closed, the flasks (above the liquid) vented to atmosphere, and the valves leading to the apex from the liquid in the flasks were opened. The progress of
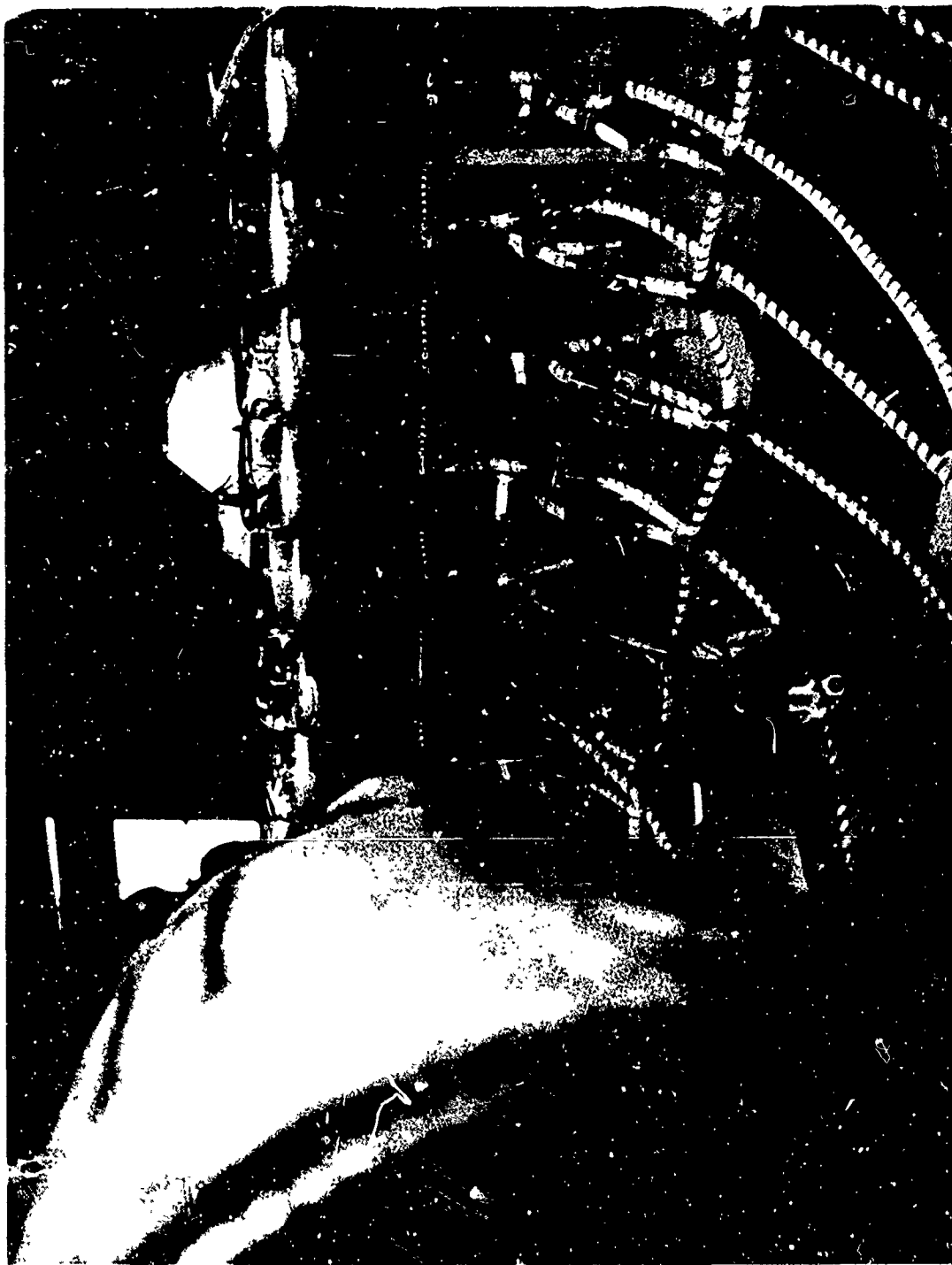
Figure 189. View of Flasks and Lines During Degassing of RTV-655 Liquid Silicone Rubber

335/625

341

The liquid rubber saturating the metal fabric could be observed through the vacuum bag as shown in Figure 190 in which the impregnant has nearly reached the upper vacuum header connections. These upper vacuum connections were placed symmetrically with the lower liquid rubber inlet connections and spaced in proportion to the amount of metal fabric that had to be impregnated. The impregnation process took 2 hours and 40 minutes. At the completion of the process the vacuum bag was removed and the excess RTV 655 was wiped from the metal fabric surface using Teflon scrapers. The entire apex was then wrapped with shrink-tape as shown in Figure 191. It was difficult to wrap the center top and bottom area of the apex in the vicinity of the intersection of the center-keel boom and the toroid since the tape wrap could not be carried around a suitable periphery. However, this area was cross-wrapped from side to side with multiple layers of shrink-tape which were also held with masking tape. The tape was then shrunk using hot air blowers. It tended to pull away from the area just discussed but this did not appear to be detrimental.

Although the RTV 655 should have "set-up" or polymerized by the following day, it was still somewhat fluid and the tape wrap was left on throughout a four-day holiday weekend. After this period it was found that the silicone rubber still had not set-up, and heat was applied to both the inside of the form and outside of the apex assembly using infrared heat lamps on the exterior and hot air blowers on the interior for about 24 hours. This applied heat caused the silicone rubber to set-up somewhat in certain areas but it was not polymerized enough to remove the shrink-tape or the form tool.

A wall of the laboratory was removed and the apex on the form tool was taken to a large, forced-circulation oven in the same building. After heating to 250°F for five hours, it was apparent that the RTV 655 had cured reasonably well.

The apex was set on the center stub boom and the shrink-tape removed. Figure 192 shows the apex after curing and removal of the tape wrap. Figure 193 shows a close-up view of the crotch area and tape wrapping.

The form tool was removed from the cured, impregnated apex with some difficulty. Several segments of the form had to be broken to get them out. Wherever the form tool manufacturer had used the epoxy body putty to fill depressions (see Section 3.10.2.3), the RTV 655 adhered to the form. Actually, a thin layer of body putty tended to break away and adhere to the interior of the apex.

Some observations on the appearance of the apex after removal of the form are as follows: the inside of the apex looked like the outside except for some islands or voids in the superficial RTV 655, apparently due to small wrinkles or areas where the form tool did not fit tightly against the fabric (the fabric appeared to be impregnated throughout, however); there were fewer islands in the cylindrical interior areas of the stub booms due to the better fit of the form tool.

Figure 190. Impregnation of the Apex Showing Progress of the Liquid Rubber Saturating the Metal Fabric Within the Vacuum Bag

343

Figure 191. Wrapping of the Apex with Shrink Tape Following Impregnation and Removal of the Vacuum Bag

335/630

Figure 192. Final Apex Assembly After Curing of Silicone Rubber

335/655

345
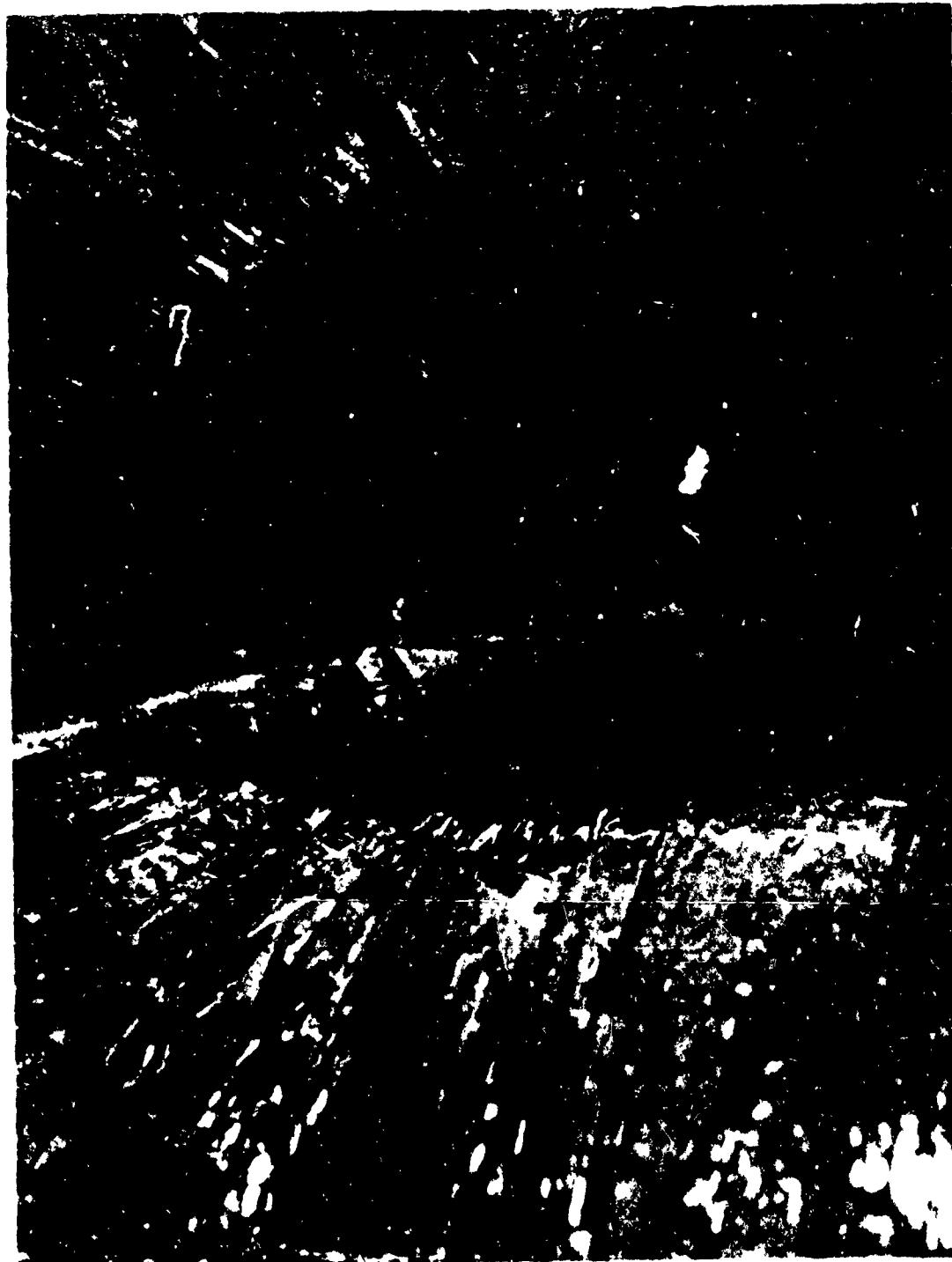
Figure 193. Close View of Tape Wraps in Crotch Area of Apex After Curing of Silicone Rubber

335/656

346

The bias-ply fabric had been pinched in one joint area between the stub boom and the toroidal section causing a severe wrinkle. The crotch areas, having about 25 layers of fabric, were much less flexible than the remainder of the apex, as was suspected. Flexibility in the crotch area was similar to the side wall of an automobile tire. Several small pockets of un-cured RTV 655 were noticed in the crotch areas where the fabric construction was very thick.

Wherever the RTV 655 had been in contact with the epoxy body putty on the interior, it appeared milky and had very little toughness. It could be rubbed off by briskly abrading with the finger tips. The uncured RTV 655 areas, the milky or frosty appearing RTV, and pieces of form and body putty were all cleaned from the inside of the apex. All areas were briskly brushed with a nylon brush to remove any unsatisfactorily cured superficial material. The interior was completely painted with a fresh batch of 2,000 ml of "quick cure" RTV 655. The apex was then placed in the hot-air, forced-circulation oven for 2 hours at 250°. It was supported in such a way that the interior walls did not collapse against each other. After this period in the oven it appeared that the interior was uniformly coated with cured silicone rubber.

The difficulty in obtaining a proper cure with the RTV 655 silicone rubber was very perplexing and the series of laboratory investigations disclosed that the particular batch of polyvinyl chloride (PVC) film used in vacuum bagging inhibited the curing of RTV 655. Although early laboratory tests with PVC film did not indicate any poisoning effect on RTV 655, consultation with General Electric Company indicated that detrimental characteristics may be developed by small changes in the compounding of such plastics. It is believed that a new batch of the PVC film procured for the apex fabrication was sufficiently different from the older material to create this difficulty.

The bias ply alone weighed 29.5 pounds and the cross ply with metal fabric tapes weighed 53.0 pounds, giving a total metal fabric weight of both plies of the apex of 82.5 pounds. The final weight of the impregnated two-ply apex was 115 pounds indicating that approximately 32 pounds of impregnant actually went into the apex construction. The remainder of the RTV 655 used, was necessary as contingency (actually, one flask did leak and had to be replaced with a spare flask) and was residual in the flasks, lines, and vacuum bagging.

Re-direction of this project by the Air Force in conjunction with planning by Space-General, led to the decision that the apex would not be coated with the ablative S-6510 silicone rubber. It was felt that the properties of this coating had been determined as a result of the frustum and boom testing, and that the coating would not contribute measurably to the test results on the apex. It was also agreed that the performance of the metal fabric and reinforcing tapes could be observed better without the coating.

3.10.8 REPAIR TECHNIQUES

One of the objectives of this program was to evaluate repair techniques for the expandable structure system that was developed. During the fabrication work, several occurrences of damage necessitated investigation of methods of repair. In essentially all cases, repairs were effected satisfactorily. Some laboratory work was also undertaken in which intentional irregularities in coupons or small cylinders were repaired by different techniques to ascertain the optimum approach. The materials system developed in this program consists primarily of four successive categories of materials subsystems: the bare metal fabric itself; welded metal fabric structures; silicone rubber-impregnated metal fabric structures, including welded seams; and silicone rubber-coated or laminated structures in which the substrate consists of impregnated and welded metal fabric.

3.10.8.1 METAL FABRIC RECLEANING

Whereas flaws in the weaving of the metal fabric cannot be corrected, the crimp balance, yarn count, and surface quality (freedom from snicks and snags) can be checked during weaving either by removing a small coupon and tensile testing for crimp balance in warp and fill directions, or by examination under 10X magnifying glass and general observation of the fabric surface quality. Once the fabric is woven, however, it is virtually impossible to correct weaving imperfections.

Several experiences during the program in which fabric, which had once been cleaned, was contaminated, indicated that recleaning (using the Phos-It process) was very satisfactory and no significant degradation of fabric strength occurred. At one time a large quantity of fabric that was being vacuum-dryed after cleaning was contaminated with back flow of vacuum pump oil. The fabric was drained of the oil and re-cleaned in two separate washes of hot Phos-It solution, followed by the usual rinsing and drying. This fabric showed no detrimental effects from the repeated cleaning. Subsequent use of the warm-nitrogen-purged chamber for drying the fabric avoided this type of contamination.

Wrinkles or creases in the metal fabric were avoided wherever possible but the severe packaging and folding tests that were performed on the frustums and boom indicated that wrinkles and creases did not degrade the strength of the fabric. Except for appearance and ability to lay-up the fabric on the form tools, it does not appear that wrinkles and creases are of significant importance.

3.10.8.2 REPAIRS USING WELDING TECHNIQUES

As discussed in Section 3.10.6, "Boom Fabrication," and Section 3.10.7, "Apex Fabrication," fraying of the edges of the fabric, particularly where edges were parallel to yarn direction, can be stopped by spacing small tack-welds approximately every 1/2-inch along the last yarn at the edge. This

348

is done with a hand-held pencil probe and the Unitek power supply. This process is time consuming but has the advantage of not introducing any foreign materials into the fabric structure.

The use of silicone rubber as a selvage adhesive, and overcasting with a needle and metal yarn, were investigated but found unsatisfactory.

If a weld is improperly made (such that the segments of fabric do not fit the contour correctly) the only alternative is to cut the section out and replace it with a new patch of metal fabric, properly fitted. The result will be at least one more seam than originally planned, but if the work is done logically, with respect to distribution of loads and avoidance of stress concentrations, the repairs should be reasonably successful. This situation occurred only once during the construction of all of the components in this program. It is discussed in Section 3.10.7.2; the puckered seam in the apex ply that was removed is shown in Figure 173.

No successful method was discovered for the repair of torn or ruptured metal fabric after it had been impregnated with silicone rubber. The removal of silicone rubber from the fabric would be necessary and the fabric would have to be completely cleaned before welding could be performed. The only known means of removing silicone rubber after curing include burning it to a char which would cause severe oxidation of the fine filaments in the metal fabric, and depolymerizing with an alcoholic potassium hydroxide solution. This latter process is slow and probably would not result in cleaning the fabric sufficiently for welding.

Therefore, the only known means of repairing a tear or hole in the impregnated metal fabric would be to overwrap the entire area with a self-supporting, outer-reinforcing structure. It is doubtful whether silicone rubber adhesive alone could be used to effect the patch unless it were only going to be used at low temperature and low loading, compared to the temperatures and loads designed for in this program.

3.10.8.3 REPAIRS USING LIQUID SILICONE RUBBER

The first proof-pressure test on frustum number 10 resulted in a leak and blister about 5 inches in diameter in the vicinity of thermocouple number 4. Two attempts were required to seal this leak by painting RTV 655 liquid rubber on the interior of the frustum, as well as injecting the liquid rubber into the blistered area on the outside to cause adherence of the outer coating. The first attempt involved painting only an 8-inch-square area immediately inside the blister.

When this was unsuccessful, the entire interior of the frustum was painted because it was not known whether the leak originated at some other point and possibly traveled sideways through the fabric. It was found to be quite easy to inject the RTV 655 liquid rubber into the blister area with a large hypodermic needle and work it around the delaminated zone. The frustum was placed on the form tool, wrapped with shrink-tape, and heated to 150°F with a

heat gun. After the second attempt, no significant leaks were observed in the frustum during testing up to 35 psig. The working pressure which the proposed re-entry vehicle would have to withstand is only 11 psig.

In several other instances where leaks occurred, it was recognized that the RTV 655 constituted the main sealing material since, if it leaked, the outer silicone rubber would tend to delaminate into a blister. In most cases, leaks in the components were stopped or significantly reduced by painting the interior completely with a quick-cure mixture of RTV 655, using a clean nylon brush. In at least one case where the surface of the interior had become contaminated with fingerprints, etc., the surface was first washed with methyl alcohol, and dried, before applying the liquid RTV 655 rubber.

3.10.8.4 REPAIRS TO SILICONE RUBBER COATING (S-6510)

The damage incurred by the boom due to the autoclaving problems is discussed in Section 3.10.6.4. If the boom had experienced only fissures and cracks in the surface of the silicone rubber coating, these could have been filled with fresh silicone rubber and the unit re-vacuum bagged and cured. The fresh silicone rubber will cohesively bond to the pre-cured parent material, although a good bond is not obtained after the parent material is post-cured. In the latter case, the only alternative is to seal the post-cured S-6510 with liquid RTV 655, and this is a reasonably satisfactory repair procedure although not producing as strong a bond as the high-temperature curing gum rubber.

After all of the sponge-like coating of the S-6510 had been removed from the boom, small specks of the S-6510 still adhered to the impregnated metal fabric. Since the pre-cure heating had undoubtedly removed all of the catalyst from the rubber, and even the remaining 270° periphery of the 0.035-inch-thick S-6510 appeared to be only partially pre-cured, a solution of 5 percent benzoyl peroxide toluene was sprayed on the peeled area to assure that the specks of S-6510 would have sufficient catalyst to finish curing.

A solution of 10 percent benzoyl peroxide in toluene was brush-coated on the remaining 0.035-inch-thick S-6510. This rubber coating, which was left on the boom, was a mottled-tan color, darker than the usual S-6510 coatings. The application of the benzoyl peroxide lightened the color of the coating. After allowing the toluene to evaporate, a thin layer of de-gassed (at 29.6 inches Hg vacuum) RTV 655 was painted on the peeled area. This RTV 655 consisted of 50 parts of quick-cure component A, 50 parts of new, slow-cure component A, and 10 parts of component B. This coating of RTV 655 did not get sufficiently tacky after several hours and had to be partly cured with hot-air heating guns. When the RTV was sticky to the touch and partially polymerized, the new calendered S-6510 was overlaid as described in Section 3.10 6.4.

Use of a vacuum bag and a high-pressure autoclaving environment improves the bond of S-6510 to the RTV 655. Another advantage of using high pressure (200-250 psig), in addition to the vacuum bagging during pre-cure, is that all areas that have been hand-filled or patched and any small cracks or holes tend to fill and blend out smoothly.

350

As a result of the experience gained, a technique has been developed for removing damaged, and possibly even ablated, outer silicone rubber coating and replacing it with a fresh coating as long as the impregnated metal fabric has not been damaged. Even if the impregnant were charred or perforated in service, it is conceivable that it could be repaired with additional RTV 655, as long as the metal fabric remained undamaged.

3.11 STRUCTURAL COMPONENTS TEST PROGRAM

Originally, the program was intended to include the fabrication and testing of not only small cylinders but also paraglider apex and boom components which were sub-scale, (that is, approximately two-thirds the size of the manned re-entry paraglider). A study of scaling and similarity relationships led to the conclusion that adequate analysis of load distribution at temperature, vibration characteristics, etc., could only be obtained if the fabric (i. e., filament and yarn diameter, strength characteristics, etc.) was precisely scaled to the overall component size. Since this was impossible in this case, it became apparent that the only thoroughly interpretable results would be those from tests performed on full-scale components. A review of the similarity relationships between models and full-scale test articles is presented in Appendix VI. However, sub-scale cylinder and frustum tests can be used effectively to determine the load bearing qualities of the fabric in hoop and longitudinal directions as well as to confirm design and fabrication technology. Furthermore, sub-scale tests can be conducted and compared with full-scale results to develop empirical scaling relationships which can then be applied to sub-scale components or vehicles.

As a result of the studies to determine effectiveness of the test program, the program was revised to include the testing of several 7-inch-diameter by 15-inch-long cylinders, including both monofilament stainless steel cloth and multifilament nickel chromium fabric; ten 10-inch-diameter by 30-inch-long tapered cylinders or frustums; a full-scale boom; and a full-scale apex of nickel chromium alloy fabric. An outline of this test program is presented in Table XXX. It should be noted that both full-scale components, the boom and the apex were planned to be carried through th sequence of tests which they would encounter as parts of an actual paraglider in re-entry flight. As discussed in Section 3.10.7.3, the apex was not coated with the ablative S-6510 silicone rubber and, therefore, was not to be exposed to the high-temperature or post-temperature testing.

3.11.1 HIGH-TEMPERATURE EVALUATION OF SILICONE RUBBER MATERIALS

Having determined the basic construction of the expandable, inflatable re-entry vehicle to consist of two or more plies of metal fabric impregnated with RTV 655 silicone rubber and overlaid with S-6510 silicone rubber, confirmatory tests were conducted to assure that this material system would adequately meet the high-temperature criteria before undertaking the construction of the comparatively expensive and large test components.

351

Table XXX

COMPONENT TEST PLAN

Loading Conditions / Component	Room Temperature							Max. Fabric Temp.						After Cooling					
	1	2	3	4	5	6	7	8	9	10	11	12	13	14	15	16	17	18	19
	Pressure and Permeability	Package	Packaged Vibration (Launch Environment)	Resonant Vibration (Low g Input)	Static Design Loads	Static Load To Failure	Pressure Burst	1	4	5	Cyclic Static Loads (10 Cycles)	6	7	1	4	5	11 6	6	7
Frustum No. 1	x				x	x	x												
Frustum No. 2	x																		
Frustum No. 3	x				x		x												
Frustum No. 4	x	x	x				x												
Frustum No. 5	x							x	x										
Frustum No. 6	x							x	x				x	x					
Frustum No. 7	x										x		x					x	x
Frustum No. 8	x							x				x		x				x	
Frustum, No. 9	x	x		x													x		x
Frustum No. 10	x																x	x	x
FIRST Scale Bo..m	x	x	x		x		x	x		x	x			x	x	x	x	x	x
f Scale Apex	x	x			x		x	x	x		x			x			x	x	x

NOTE: All Frustums are 10" dia x 30"

*Detailed arrangement of failure tests to be established
**350°F

352

3.11.1.1 HIGH-TEMPERATURE, INERT-ATMOSPHERE OVEN TESTS

To determine how the silicone rubber elastomers would perform when exposed to high-temperature testing of the paraglider components in a nitrogen-filled atmosphere, small specimens of silicone rubber were tested in a nitrogen-purged chamber while being heated to high temperature. Table XXXI indicates the temperature of the silicone rubber specimens and the temperature of the oven environment for one of the tests which were run. The temperature of the S-6510 and Y-3350 specimens of silicone rubber, as monitored by a thermocouple inserted in one of the specimens, reached 611°F, while the environmental temperature reached 1096°F. Therefore, it may be concluded that the surface of the rubber specimens was between the two temperatures - probably near 1000°F.

A photograph of the three specimens before and after the oven tests is shown in Figure 194. It was encouraging to note that the specimens did not completely lose their elastomeric qualities although they were coated with a hard, tenacious white char over the partially degraded elastomeric substrate. The Y-3350 material showed a 32.7 percent weight loss and the S-6510 showed a 37.0 percent weight loss during this test. Note that the environment temperature was at 1000°F, or higher, for approximately eight minutes of the total ten-minute test period. Figure 195 illustrates a cross-section of one of the specimens, showing that the interior was a more or less uniform, sponge-like, semi-elastomeric material with a thin layer of char on the surface.

It was reasoned that if a good impregnation of the silicone rubber in the metal fabric could be obtained, high temperature at the metal substrate could be tolerated provided the silicone rubber did not lose all of its elastomeric tendencies and tend to blow out of the interstitial areas of the fabric. The main objective was to insure that sufficient tenacity of the silicone rubber be retained after high-temperature exposure and that the particles will be retained by the metal fabric sufficiently that the gas barrier characteristics and flexibility would not be seriously affected. As a result of this inert-atmosphere oven test, it was concluded that S-6510 and Y-3350 were similar in retention of elastomeric properties and resistance to environmental temperatures of about 1000°F.

3.11.1.2 HOT GAS AND FLAME TESTING

Experiments were undertaken to investigate the thermal behavior of prototype specimens of impregnated metal fabric overlaid with the S-6510 silicone rubber. Computer analysis of the re-entry environment indicated that the "ablation temperature" (the temperature where the elastomer turns into char) of the external rubber coating would be about 1100°F for 15 to 20 minutes during which time the inner surface of the elastomer (metal fabric composite) would experience temperatures of 700 to 850°F (see Figure 18). The outside would be exposed to a space vacuum with the inside of the impregnated metal fabric structure retaining a nitrogen gas pressure of 11 psig.

To simulate these conditions, a fixture was designed which provided a jet of hot nitrogen gas directed at the S-6510 surface of a multilayer impregnated

Table XXXI

SPECIMEN AND OVEN TEMPERATURES VS TIME FOR S-6510 AND Y-3350 SILICONE RUBBER SAMPLES

Time Minutes	Temperature, °F	
	Specimen	Oven
1.0	268	268
1.5	334	401
2.0	464	661
2.5	480	1000
3.0	497	1065
3.5	530	1078
4.0	523	1032
4.5	529	1015
5.0	529	1068
5.5	542	1072
6.0	545	1075
6.5	561	1081
7.0	568	1084
7.5	578	1084
8.0	578	1087
8.5	594	1090
9.0	594	1090
9.5	611	1093
10.0	611	1096

80/286

Figure 194. Silicone Elastomers Before and After Exposure to
1000°F in Inert Atmosphere

355

SG/276

Figure 195. Cross-Section of Specimen After Heating

356

and overlaid sample while a pressure of 11 psig nitrogen was maintained on the opposite side. A view of the disassembled fixture and specimen, complete with thermocouple leads, is shown in Figure 196. The specimen is mounted over the bolts and the ring flange is clamped down tightly so that the specimen acts as its own gasket. Hot gas or flame is then impinged in the center of the open area of the specimen in the ring flange while the 11 psig nitrogen pressure is maintained on the back side.

Leakage of the pressurizing nitrogen was detected with a sensitive flow meter in the gas supply line to the rear of the fixture. Thermocouples were mounted in the specimen composite at the front (S-6510) surface, in between the fabric layer in the RTV 655 impregnant, and at the inner surface.

A typical test gave temperatures as shown in Figure 197. It will be noted that only the period of time during which ablation was predicted in accordance with Figure 18 (i.e., from 900 to 1500 seconds of the re-entry heating period) was simulated in the test. The effect of heating with an acetylene flame in air, however, tended to raise the outer impingement surface 150 to 270°F above the expected "ablation" temperature predicted for the condition occurring during actual re-entry when the metal fabric substrate reached about 850°F. This excess temperature, plus the presence of the extremely greater concentration of oxygen, undoubtedly caused the test to be much more severe, from a temperature degradation standpoint, than the predicted re-entry conditions. Although some leakage occurred in the specimen after sixteen minutes, the leakage rate was very low and the specimens showed no deterioration of the metal fabric and very little deterioration of the RTV 655 impregnant, although most of the S-6510 ablative coating had burned away. Similar results were obtained with a 1000 to 1200°F hot-nitrogen gas stream impinging on the composite samples. It was not expected that the RTV 655 would show such significant resistance in these extremely high temperature tests, although it should be noted that the presence of the metal fabric in the same area as the RTV 655 may serve to conduct the heat away to the supporting fixture and cooler surroundings. Typical appearances of specimen and fixture after testing are shown in Figure 198.

In summary, these tests were very encouraging in that gross leakage did not occur in heating experiments simulating and exceeding the actual re-entry conditions and no apparent deterioration of the metal fabric occurred.

The Dow Corning Company, supplier of the S-6510 silicone rubber coating material, performed a series of ablative heating tests on the S-6510 at the request of Space-General in 1965. This was done to evaluate the possibility of different post-cure conditions on the ablative properties of the silicone rubber. The data are summarized in Table XXXII.

The samples of S-6510 were prepared by curing for ten minutes under pressure at 250°F followed by post-curing as indicated in the foregoing table. The samples were exposed to convective heating at 10 Btu/ft^2 sec for 12 minutes. This closely simulates the heat flux during the ablation period (900 to 1400 seconds of trajectory heating period) as shown in Figure 18. It is interesting to note that the ablation rates of slightly more than 0.1 mil per second, as well as the total ablation during this period, are almost identical to those predicted by the

SGC/884

Figure 196.   Permeability Test Fixture and Specimen
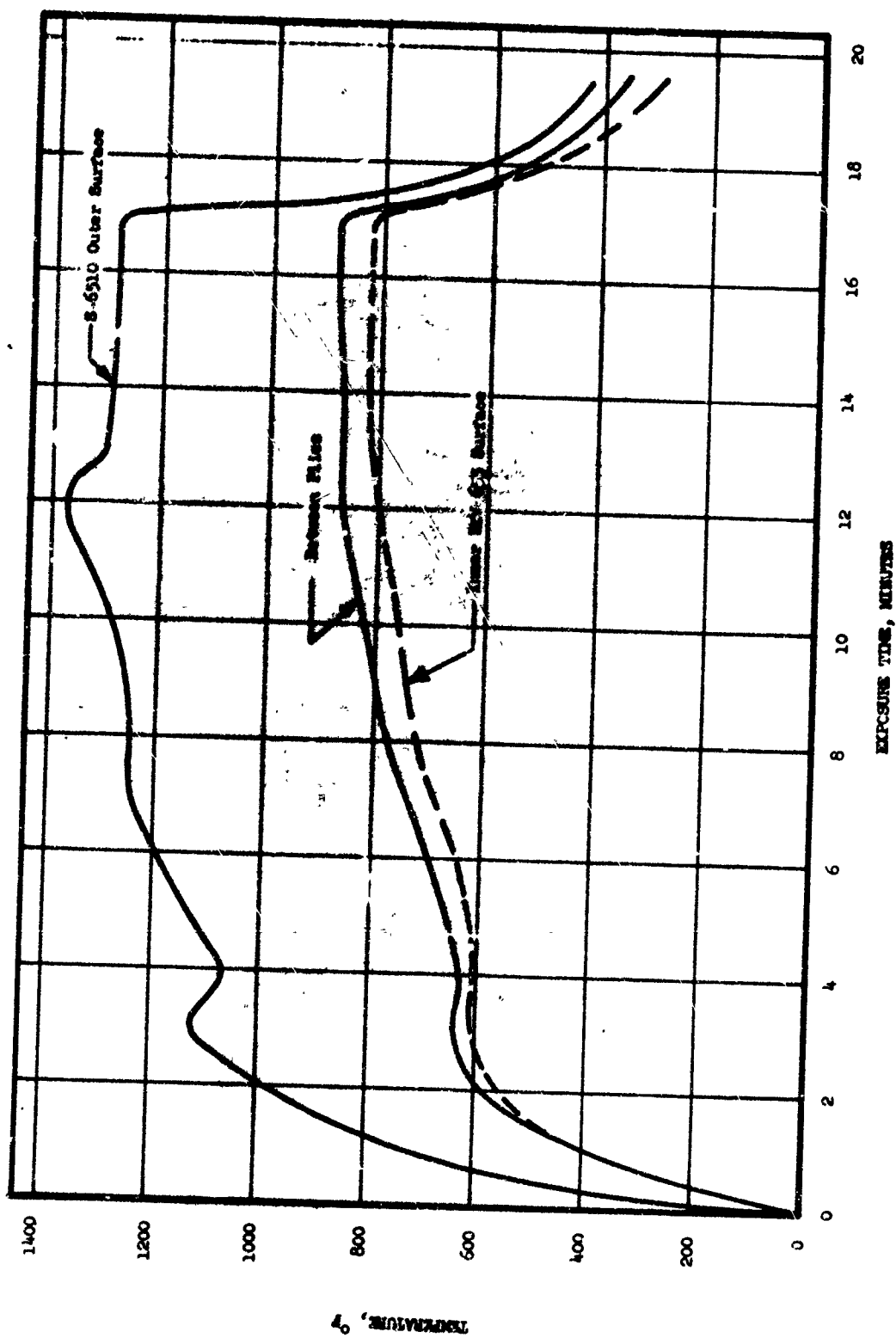
Figure 197. Tests of Thermal Degradation of Metal Fabric/Silicone Rubber Composite Using Torch Flame

359

335/47

Figure 198. Typical Appearances of Specimen and Fixtures Following
Testing

360

Table XXXII

EFFECT OF S-6510 POST-CURE CONDITIONS ON ABLATION CHARACTERISTICS*

		0	48 Hrs. at 300°F	24 Hrs at 400°F	4 Hrs at 480°F
1.	Post-Cure History	0	48 Hrs. at 300°F	24 Hrs at 400°F	4 Hrs at 480°F
2.	S-6510 Thickness (inches)	0.130	0.131	0.139	0.118
3.	Total Ablation (inches)	0.083 +0.001	0.079 +0.004	0.089 +0.009	0.078 +0.003
4.	Ablation Rate (mil/sec)**	0.115	0.110	0.123	0.108
5.	Ablation Surface Temperature (°F)	1460 to 900	1460 to 900	1460 to 900	1460 to 900
6.	T (°F) ***	245	244	244	245

* None of the specimens burned through.

** Equilibrium conditions were reached in 3 to 5 minutes.

***Front-to-back difference at 12 minutes.

computer analysis of the predicted trajectory shown in Figures 44 and 18.
In the latter figure, the calculated ablation rate for the period of maximum
ablation from 900 seconds to 1400 seconds is 0.12 mil per second. The abla-
tion rates determined by Dow Corning ranged from 0.108 to 0.123 mil por
second. The data presented in Figure 18 were based upon plasma-arc testing
performed by Space-General in the Spring of 1964. At that time it was reported
that the plasma-arc data also agreed very closely with the acetylene ter h .est:
performed early in 1964 on this same project. Although the agreeme : between
all these methods of ablation measurement is striking, the most important con-
clusion is that the thickness of S-6510 silicone rubber being used in the proposed
paraglider construction is the right order of magnitude based on the heat flux
predicted in the re-entry environment.

The Dow Corning technical staff concluded that th re was no significant
difference in the ablative characteristics for any of the specimens studied ex-
cept for less reversion experienced with sampler receiving no post-cure. This
indicates that the post-cure history is not critical insofar as the ablative proper-
ties are concerned. Dow Corning did report, however, that both the tensile
and compressive set properties are strongly influenced by the post-cure history.
Because of this latter factor the post-curing of components manufactured for test
in this project will be performed at 400°F for approximately 16 hours to give
maximum physical properties, such as compressive set, to the S-6510 silicone
rubber material.

3.11.1.3 HIGH-TEMPERATURE TESTING WITH INFRARED LAMPS

An insulated plywood enclosure approximately 3 feet square was constructed to test the small, 7-inch-diameter coated cylinders and other similar specimens at high temperature.

A heating lamp was procured in which quartz tubes were heated by internal filaments, radiating a high percentage of infrared energy from the tubes which glow a dull red color. A special design feature of this lamp is that the tube can be mounted quickly so that approximately 4.0 kW of infrared energy will be concentrated on the side of the vertical test cylinder by the parabolic gold-plated reflector. Also, the lamp does not glow so brightly that it interferes with visual observation or photography.

During the heating, the box can be purged with nitrogen to simulate the low oxygen content of the re-entry heating regime (260,000-foot altitude).

This enclosure and lamp assembly was first used with a simulated cylinder made from commercial steel screen and covered with silicone-coated, stainless-steel monofilament fabric. Thermocouples were imbedded in the silicone rubber coating to measure the temperatures at significant points. Prior to and during these tests, the enclosure was purged with nitrogen to prevent oxidation of the silicone rubber. The principal objective of these tests was to determine whether the desired temperature could be reached in a reasonable time and whether there would be a problem with deposition of smoke from the specimen on the lamp reflector. The results showed that the highest fabric temperature reached at the metal cloth substrate was 835°F, with a rubber thickness of 0.103 inches, and that this temperature had stabilized approximately 7 minutes from the start of the heating. Also, there was a considerable volume of smoke from the sample. The smoke was carried from the enclosure by the purging gas without significant deposition on the lamp reflector. Since the desired temperature of the metal fabric substrate is 850°F, the test and the lamp arrangement were considered successful, particularly since both sides of the sample in this case were exposed to the cooling effect of the flowing nitrogen.

In subsequent testing of the 10-inch-diameter frustums, some delamination of the silicone rubber coating was observed. As many as five layers of the S-6510 silicone rubber coating were laminated on an area approximately 4 inches wide along the entire 30-inch length of the test frustums. This area represented the "bottom" or ablative area of the paraglider which would be exposed to the high temperature of re-entry.

The high-temperature tests showed that delamination of the coating had not been structurally detrimental, in that subsequent burst pressures were equal to or greater than those obtained with ambient-temperature test specimens. Nevertheless, to eliminate the possibility of delamination of the silicone rubber layers, a high-temperature test was established to evaluate the five-layer silicone rubber assembly versus a possible single-layer silicone rubber coating of the same total thickness (0..25-inch).

362

One four-inch-square sample was made from a piece of five-layer rubber material obtained from frustum number 6. Another sample was fabricated by the same procedure but using only a single layer of 0.125-inch-thick silicone rubber. These two samples were set in test fixtures and located four inches away from the three-element quartz lamp heat source. The following actual test observations were noted.

The lamps were turned on at zero minutes. The surfaces started to brown at seven minutes and, as shown in Figure 199a, small blisters were observed on the five-layer sample. At eight minutes, the blisters on the laminated specimen had increased to 1/2-inch-diameter. At nine minutes, one blister had a diameter of one inch. Figure 199b shows a small, 1/8-inch blister being formed on the single-layer sample. After 10 minutes, the blister on the five-layer sample was three inches long and one inch wide (see Figure 199c). Figure 199d shows approximately 12 small blisters on the single-layer sample after 13-1/2 minutes of exposure. At 14-3/4 minutes, the five-layer sample blister cracked (see Figure 199e). After 17 minutes, the single-layer sample showed a one-inch crack with no apparent larger blisters forming. This sample is shown in Figure 199f.

The test continued to run for 27 minutes and no other visual changes in either sample were noted. The samples were allowed to cool and then removed for inspection. The results are shown in Figure 200. The five-layer sample showed delamination, cracking, and charring through two of the five layers. The third layer was not charred but was cracked. The fourth and fifth layers, beyond a depth of 0.075-inch, were intact. The single-layer sample charred through about 0.020-inch of material and cracking was visible through another 0.020-inch to a total depth of only 0.040-inch. The latter cracked portion was intact and still resilient. The remaining material thickness was in good condition.

The maximum temperature reached at the fabric substrate on the test samples was 775°F after 28 minutes of exposure. Figure 201 illustrates the time-temperature history.

3.11.2   MONOFILAMENT FABRIC CYLINDER TESTING

One of the monofilament, 7-inch-diameter cylinders discussed was tested and a photograph of the test fixture and a schematic diagram are shown in Figures 202 and 203, respectively.

The general procedure was to install the test cylinder in the test fixture; apply internal nitrogen pressure to the cylinder in incremental steps; measure the cylinder diameter at mid-length at each pressure step; apply bending moment, shear, and torsional loads separately while at each pressure step, and then measure the total deflection of the cylinder at each load condition. The termination of increasing load application at each pressure was determined by observation that buckling was beginning. After completion of these tests, a burst test was performed. Note that this cylinder was lined with a separate latex liner in lieu of silicone coating.

363

One four-inch-square sample was made from a piece of five-layer rubber material obtained from frustum number 6. Another sample was fabricated by the same procedure but using only a single layer of 0.125-inch-thick silicone rubber. These two samples were set in test fixtures and located four inches away from the three-element quartz lamp heat source. The following actual test observations were noted.

The lamps were turned on at zero minutes. The surfaces started to brown at seven minutes and, as shown in Figure 199a, small blisters were observed on the five-layer sample. At eight minutes, the blisters on the laminated specimen had increased to 1/2-inch-diameter. At nine minutes, one blister had a diameter of one inch. Figure 199b shows a small, 1/8-inch blister being formed on the single-layer sample. After 10 minutes, the blister on the five-layer sample was three inches long and one inch wide (see Figure 199c). Figure 199d shows approximately 12 small blisters on the single-layer sample after 13-1/2 minutes of exposure. At 14-3/4 minutes, the five-layer sample blister cracked (see Figure 199e). After 17 minutes, the single-layer sample showed a one-inch crack with no apparent larger blisters forming. This sample is shown in Figure 199f.

The test continued to run for 27 minutes and no other visual changes in either sample were noted. The samples were allowed to cool and then removed for inspection. The results are shown in Figure 200. The five-layer sample showed delamination, cracking, and charring through two of the five layers. The third layer was not charred but was cracked. The fourth and fifth layers, beyond a depth of 0.075-inch, were intact. The single-layer sample charred through about 0.020-inch of material and cracking was visible through another 0.020-inch to a total depth of only 0.040-inch. The latter cracked portion was intact and still resilient. The remaining material thickness was in good condition.

The maximum temperature reached at the fabric substrate on the test samples was 775°F after 28 minutes of exposure. Figure 201 illustrates the time-temperature history.

3.11.2   MONOFILAMENT FABRIC CYLINDER TESTING

One of the monofilament, 7-inch-diameter cylinders discussed was tested and a photograph of the test fixture and a schematic diagram are shown in Figures 202 and 203, respectively.

The general procedure was to install the test cylinder in the test fixture; apply internal nitrogen pressure to the cylinder in incremental steps; measure the cylinder diameter at mid-length at each pressure step; apply bending moment, shear, and torsional loads separately while at each pressure step, and then measure the total deflection of the cylinder at each load condition. The termination of increasing load application at each pressure was determined by observation that buckling was beginning. After completion of these tests, a burst test was performed. Note that this cylinder was lined with a separate latex liner in lieu of silicone coating.

363

Figure 199.   Non-Laminated and Laminated Silicone Rubber Specimens During Heating Test

LAMINATED
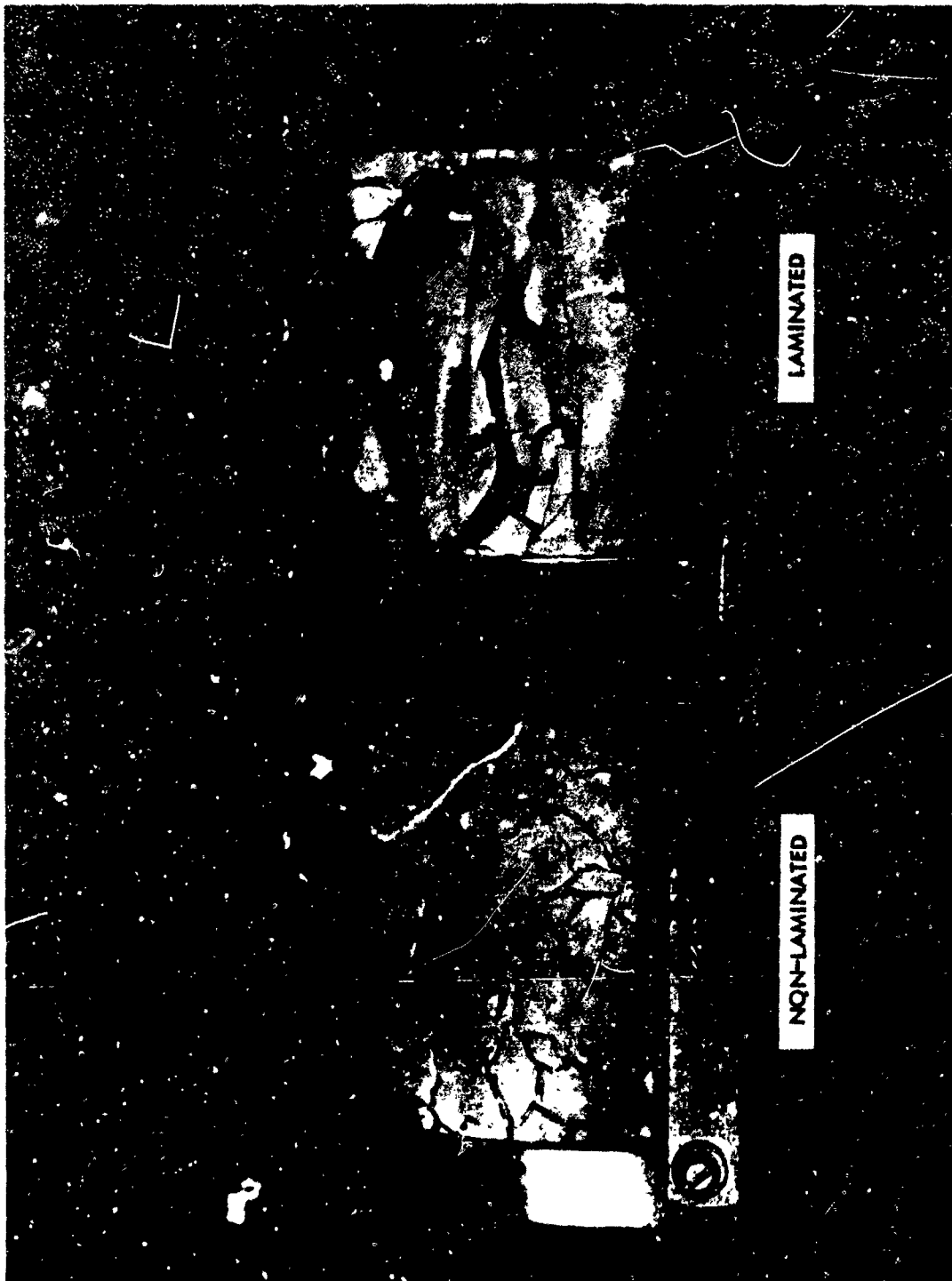
NON-LAMINATED

335/299

Figure 200. Non-Laminated and Laminated Silicone Rubber Specimens
After Exposure to Heating Lamp
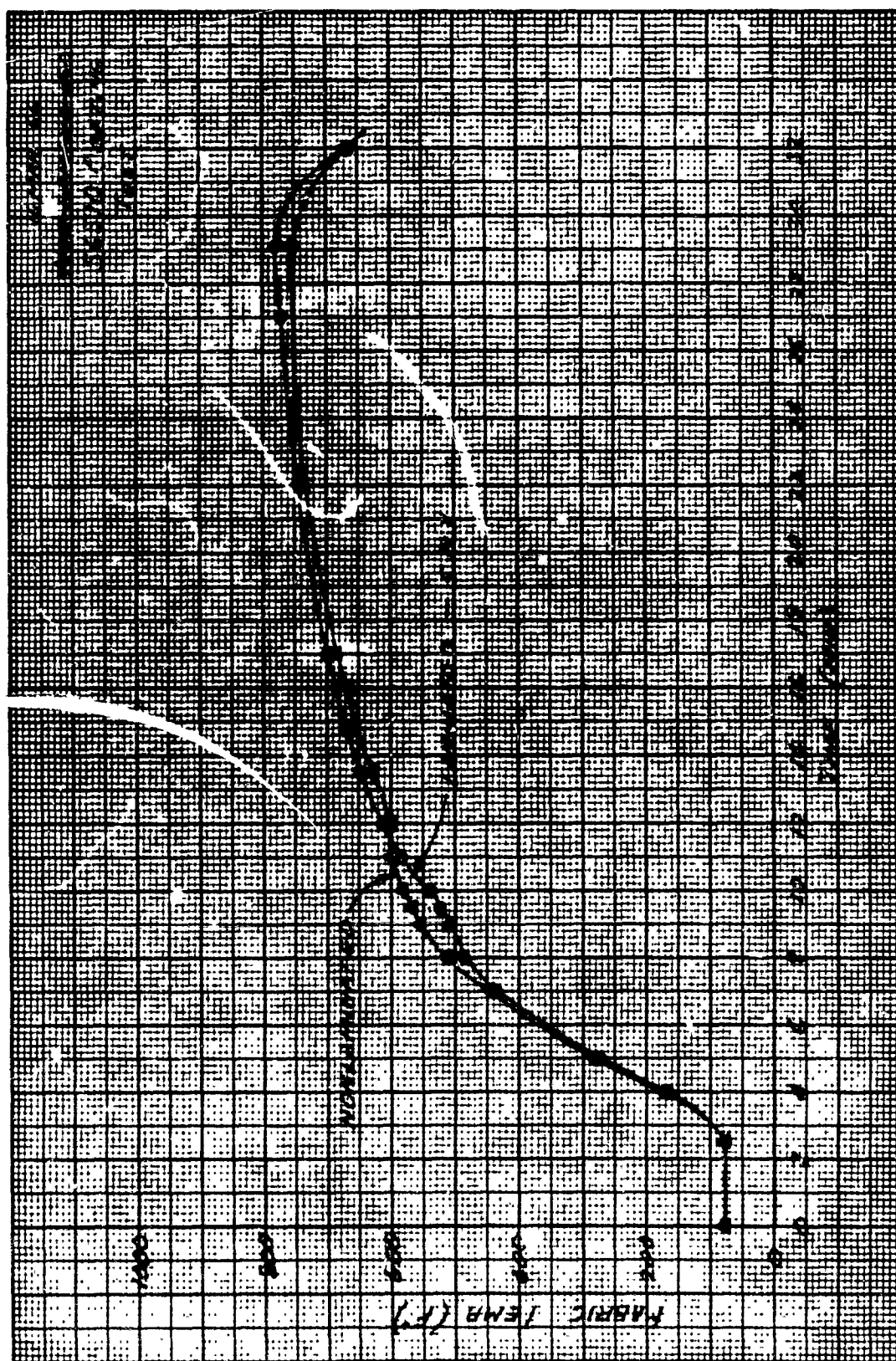
Figure 201. S-6510 Coating Test
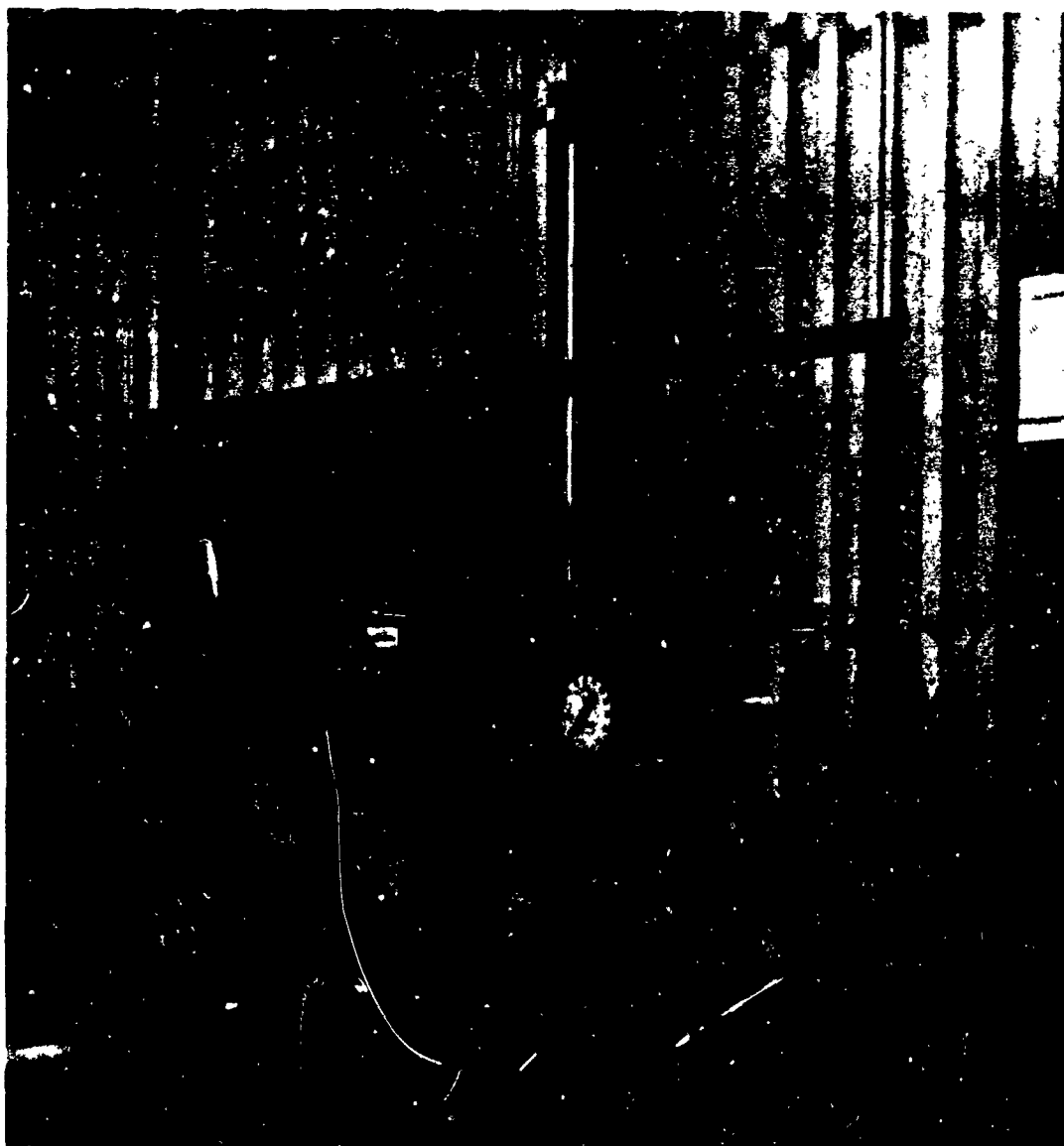
SG/243

Figure 202. Cylinder Test Fixture
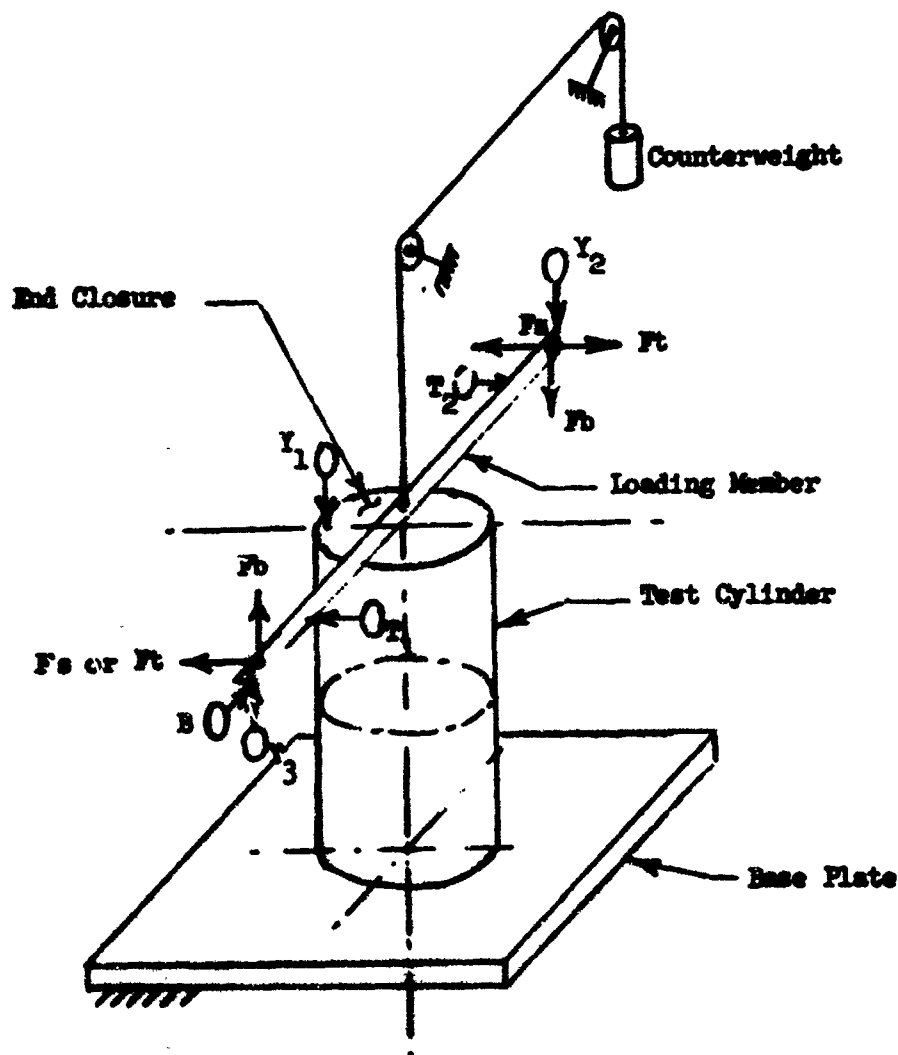
NOTES:

1. Symbols

   a. Forces:
      - **Fb**   1/2 of applied bending force.
      - **Fs**   1/2 of applied shear force.
      - **Ft**   1/2 of applied torsional force.

   b. Displacements (dial indicators):
      - **B**   lateral during bending.
      - T_1, T_2 torsional
      - Y_1 length
      - Y_2, Y_3 bending

2. Forces up to approximately 20 pounds are applied with weights, greater loads are applied with hydraulic cylinders; both are transmitted to the loading bar through cables.

3. Nitrogen gas pressure is introduced to test cylinder through base plate. Pressure is retained by thin latex "dental dam" rubber sheeting, when cylinder is uncoated.

Figure 203   Schematic Diagram of Cylinder Test Arrangement

During testing, the cylinder encountered a joint failure due to separation at a longitudinal weld for about 2 inches near the bottom. This failure occurred at 2.7 psi, while the cylinder was being inflated from 2 to 3 psig. Since the loads had been applied in small increments up to this point, considerable data points were gained prior to this failure. Since the fabric was undamaged, this joint and all other joints in the cylinder were rewelded. It did not appear that going over the same joints with a new series of spot welds caused any degradation of the cylinder.

All the mon, ilament cylinders were not exhaustively tested since they are not the selected material and it was hoped only to gain information applicable to multifilament fabric tests and structural fabric design behavior. For example, considerable knowledge was gained in the technique of assembling cylinders on the test fixture so as to prevent wrinkles during the clamping of the ends. A potential problem existed in the method of retaining the fabric in the end grips since there was considerable slippage at those points. Although the grips did not fail completely, the strength of the band clamps had to be increased to assure that they would hold under the higher pressures to be used with the multifilament fabric. Due to the slippage, longitudinal deflection measurements taken from the upper end closure were not representative.

A special metal tape measure known as a "pi tape" was used to measure circumference growth. This required fitting the tape by hand for each measurement and reading vernier graduations on the tape. This method provided very adequate accuracy. However, at large internal pressures, after the joints were rewelded, it became imprudent to approach the cylinder and the taking of hoop deflection measurements was discontinued at 9.0 psig. Since burst failure did not occur until 16.5 psig, data on considerable additional hoop deflection was not obtained.

Bending, torsion, and shear loads were applied at pressure levels of 1 and 2 psi gauge, and the increase of loads was carried through incipient buckling, (i.e., first evidence of a wrinkle or large waviness) to a condition at which an additional load increment resulted in a sudden increased rate of deflection or a continuing deflection at a constant rate. With evidence of catastrophic buckling as described by either of the foregoing deflection phenomena, the additional load increment was removed and deflection ceased. The ultimate buckling load in each case was at least twice the incipient buckling load.

After the weld was repaired, the bending shear and torsion loadings were again applied at pressure levels of 2, 4, and 6 psig. To avoid damage, the external loads were carefully removed on first evidence of incipient buckling. At 6 psig, during bending loading, a longitudinal seam in the cross-ply material opened for approximately 0.2-inch near the end of the cylinder. The location and type of this failure were exactly the same as previously, but not as extensive. The cause was weld-joint separation. The seam was on the compression side of the cylinder and a slight compression buckle had just begun to show in the area where the joint failed. The loads were immediately removed.

Since the failure was near the end of the cylinder, it was decided to repair it and continue with only pressure testing. The cylinder was then reinforced with glass fiber tape (as shown in Figure 204) to carry the hoop loads

369

Figure 204. Monofilament Test Cylinder Following Burst Test

SG/246

across the rupture. Most of the cylinder, including the critical center portion, was left reinforced. The cylinder was then slowly pressurized and burst at 16.5 psig. The failure initiated fabric failure at the longitudinal seam weld of the cross ply, the seam at which the previous failure occurred.

Analysis of the test results indicates the strength of the cylinder to be 58 lb/in at 16.5 psig. This may be compared with a cross-ply seam strength of 48 lb/in minimum and 54 lb/in average strength of uniaxially loaded tensile coupons. The percentage of the hoop load division between the cross-ply and the bias ply is a function of initial fit between the plies and relative elongations during loading, but would also be affected by prior loading history and any slippage which occurred in the grips, for a given specimen. Hence, it is concluded that the similarity of the actual failure load of this cylinder to that anticipated for the cross ply alone may have been a coincidence.

A report of this test on the 7-inch-diameter monofilament cylinder, including load-deflection curves for shear, torsion and bending, are presented in Appendix VII.

3.11.3 MULTIFILAMENT FABRIC, SEVEN-INCH CYLINDER TESTING

The cylinder test fixture, which was used for testing monofilament cloth cylinders as described in Section 3.11.2, was again set up to provide internal pressurization for the test components as well as external bending, shear, and torsional loads individually and simultaneously.

Typical test equipment used in these tests included the following:

a. The cylinder test facility shown in Figure 205.

b. Mounting and loading jigs, including end closures.

c. Hydraulic cylinders, cables, fittings, pulleys, etc.

d. Hydraulic hand pump, valves, lines, etc.

e. Dry-nitrogen source, regulator valve, lines, etc.

f. Pressure gages (0 to 60, 0 to 300, 0 to 1500 psig).

g. Dial gages (0-to 1.000-inch), pi tape, steel rule, level-protractor, etc.

3.11.3.1 TESTING UNCOATED, SINGLE-PLY, BIAS-AND CROSS-PLY CYLINDERS

A 7-inch bias-ply and a 7-inch cross-ply cylinder were tested separately using internal, thin rubber bladders. These tests were very successful and deflection versus load data were obtained for torsion, shear and
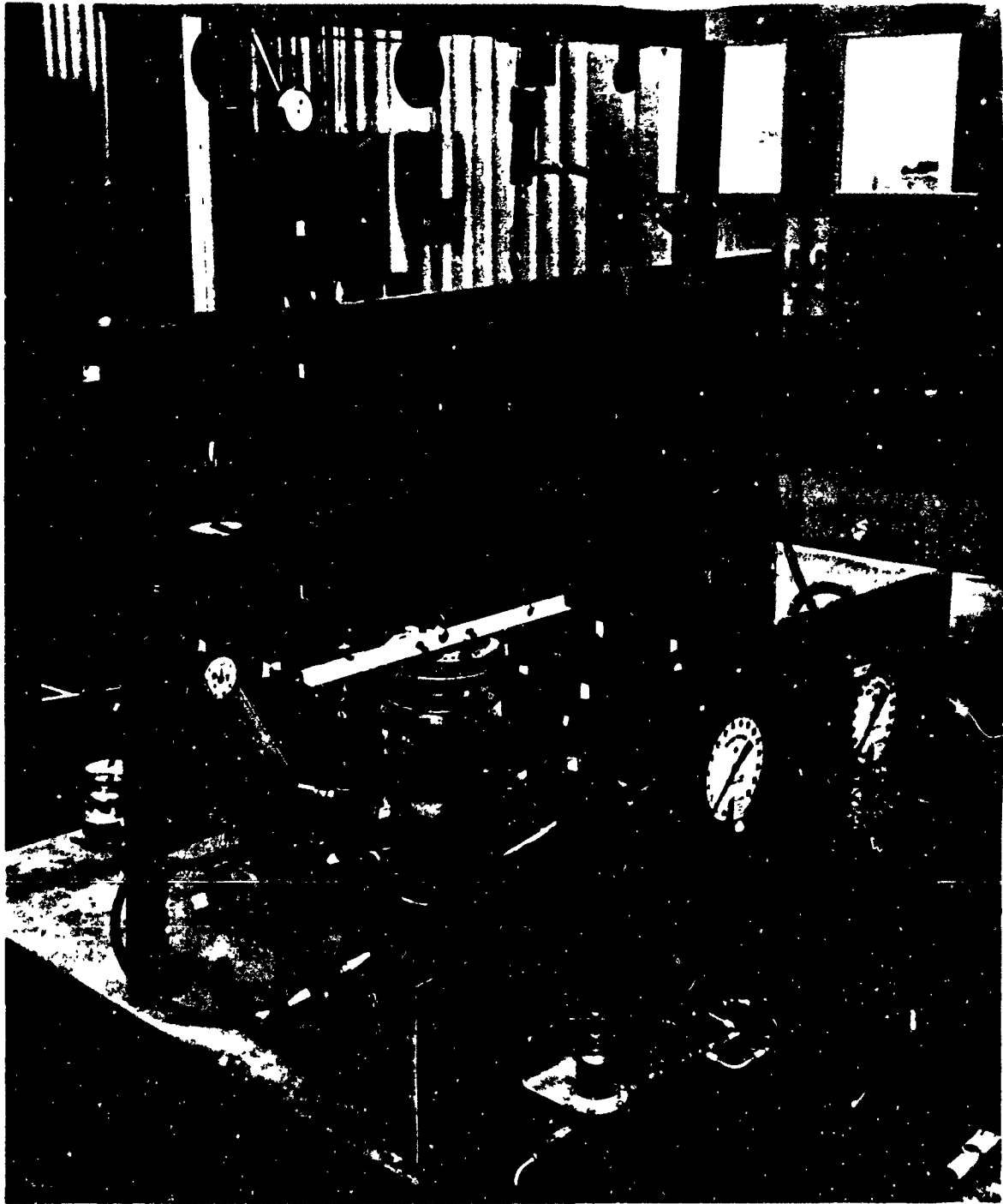
335/156

Figure 205. Test Fixture with Bias-Ply Cylinder Installed

372

bending. These components were some of the "preliminary" test components. Fabrication and test work on these was intended to contribute the necessary experience to assure the success of the remaining formal test program on 10-inch by 30-inch frustums, and the boom and apex.

These cylinders were 7-inch-diameter by 15 inches long. The ends of each cylinder were folded back and welded over a ring made from 0.08-inch-diameter steel wire, so that the cylinder would not pull off the end closure when using a band-type clamp. Each end of the cylinder was covered by a two-ply reinforcing cuff.

An internal bladder was fabricated from natural rubber sheet stock. Top and bottom end closure plates were mounted to the specimens with 5/8-and 7/8-inch-wide hose clamps, respectively. Adequate pressure sealing was verified by low-pressure leak checks. Figure 205 shows the bias-ply cylinder mounted in the test stand at the beginning of the first bending test. Subsequent testing produced deflections beyond the range of the loading system and most of the dial gages. As a result, the loading system was modified to permit greater deflections by an arrangement of pulleys; deflections were measured by steel rule.

The bias-ply cylinder was tested at incremental bending loads (to the maximum values shown in Table XXXIII) at each of three inflation pressures: 5, 10, and 14.3 psig. It was then exposed to incremental shear and torsion loads at the 14.3 psig pressure. The pressure, 14.3 psig, theoretically gives the same stress in bias ply alone as in the 32-inch-diameter and of the two-ply paraglider boom at full inflation pressure (11 psig). Deflection readings were taken at each increment of load until buckling was noted. The torsion moment, however, was limited by slippage of the specimen on the bottom closure plate.

Highest deflections were obtained, of course, at the lower inflation pressures. The deflection of the bias-ply cylinder at incipient buckling at 758 in/lbs bending moment and 5.0 psig internal pressure may be seen in Figure 206. The multiple pulley arrangement required to obtain such deflection is shown in that figure.

Although pure bending cannot be obtained due to the slight angularity that develops in load cables, pure shear is much more difficult to produce. A form of shear, which includes bending, is produced by a single horizontal cable, as shown on the bias-ply cylinder, in Figure 207, at a 207-pound load and 14.3 psig pressure.

The torsional loads were applied by wrapping two opposed horizontal cables around a series of pins mounted in the top closure plate, as shown in Figure 208. This photograph shows the bias-ply cylinder under maximum load of 1020 in/lb at 14.3 psig.

Measurements of the bias-ply specimen showed a pronounced change in shape in the test runs:

373

Figure 206. Pressurized Bias-Ply Cylinder Under Bending Load

374
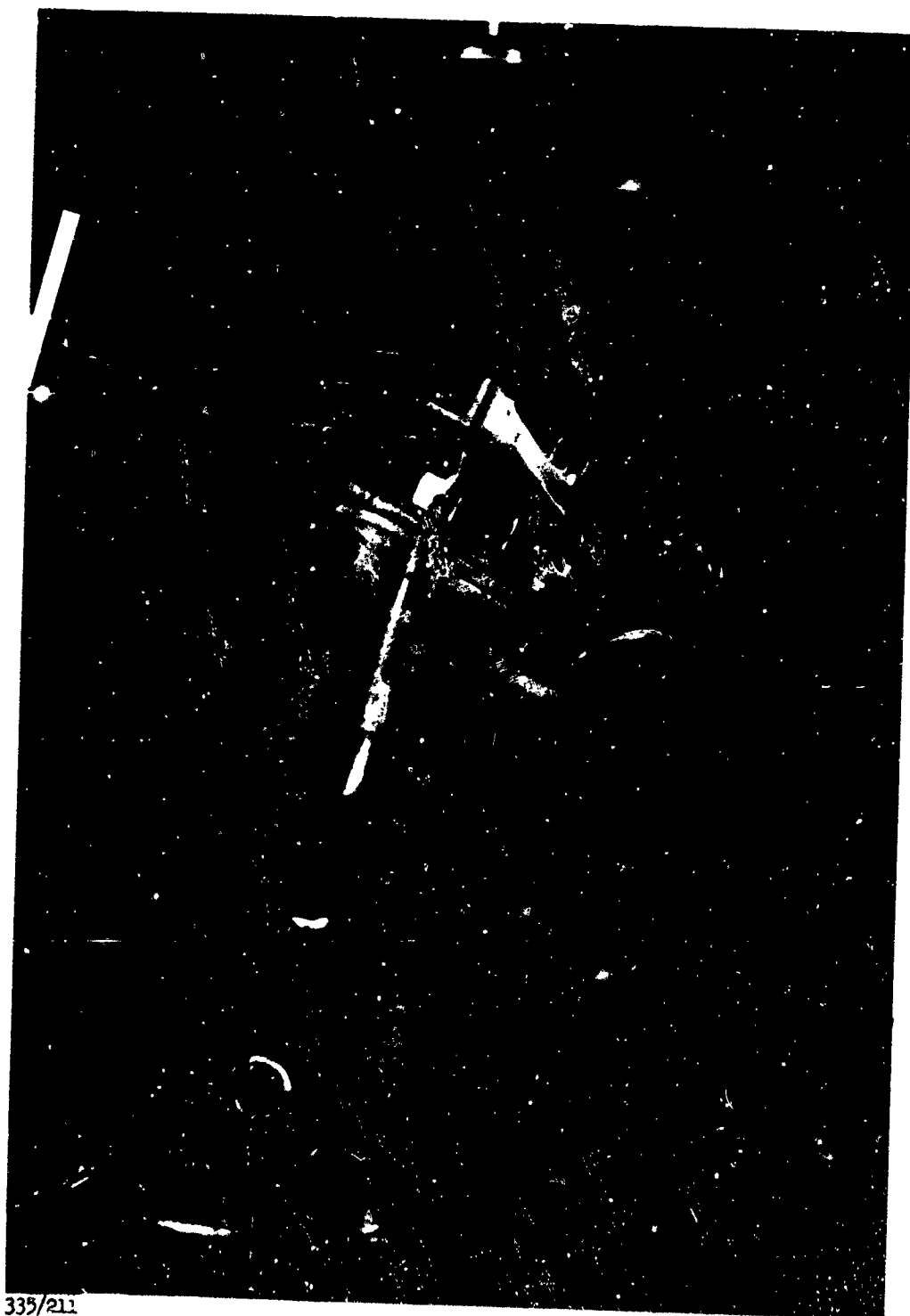
Figure 207. Pressurized Bias-Ply Cylinder Under Shear Load
(207 Pounds at 14.3 psig)

SGC/883

Figure 208. Pressurized Bias-Ply Cylinder Under Torsional Load
(1020 in/lb at 14.3 psig)

Table XXXIII

PEAK DEFLECTIONS OF LOADED END OF THE
BIAS-PLY CYLINDER

Type of Load	Internal Pressure (psig)	Static Load	Total Deflection	
			Translation (in)	Rotation (deg)
Bending	5.0	758 in/lb	2.75	18.0
Bending	10.0	1515 in/lb	2.59	19.8
Bending	14.3	2169 in/lb	2.88	21.6
Shear	14.3	207 lb	4.20	25.0
Torsion	14.3	2040 in/lb	--	2.9[1]

[1] Estimated value. Slippage on test fixture occurred.

a. Permanent Deformations

Mid-Length Diameter   = + 0.476-inch

Quarter-Length Diameter   = + 0.384-inch

Length   = - 0.45-inch

b. Maximum Inflation Deformations

Mid-Length Diameter   = + 0.786-inch

Quarter-Length Diameter   = + 0.581-inch

In contrast, the shape of the cross-ply specimen remained practically unchanged. The rigidity of the cross-ply cylinder under bending load of 2421 in/lb at 24.0 psig, illustrated in Figure 209, may be compared with the considerable bending shown in Figure 206 for the bias-ply specimen. Maximum load and deflection data for the cross-ply cylinder are shown in Table XXXIV. The failure of the cross-ply cylinder which occurred when the pressure was raised to 36.0 psig is illustrated in Figure 210 and shows that the failure occurred in the fabric under the cuff circumferentially at the edge of the band clamp. Failure apparently also progressed on the longitudinal weld seam due to the explosive force of the initial failure at the clamp. A pressure of 36.0 psig theoretically results in the same hoop stress as obtained in the cross ply

377
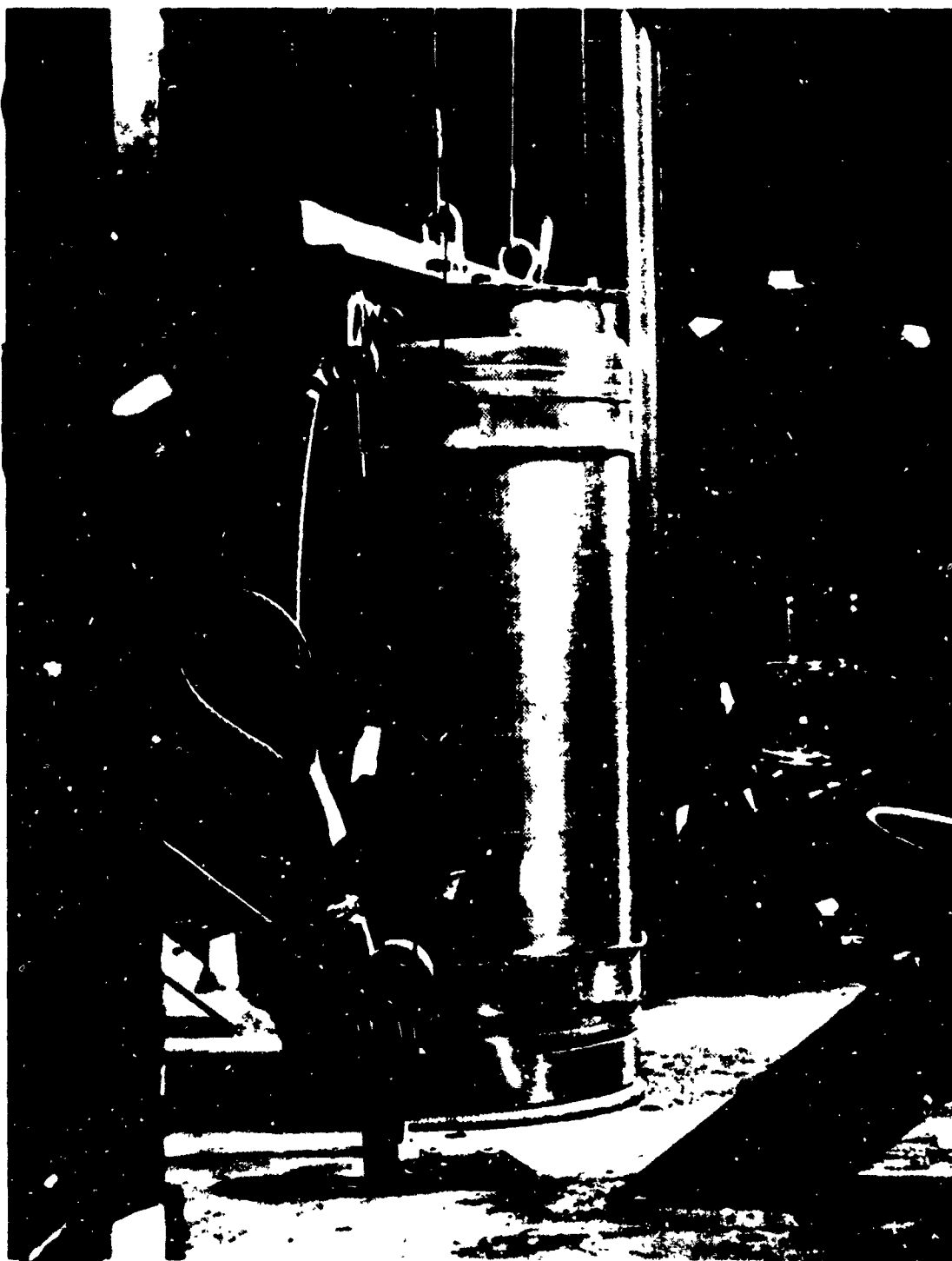
Figure 209. Pressurized Cross-Ply Cylinder Under Bending Load
(2421 in/l b at 24. 0 psig)

378

Table XXXIV

PEAK DEFLECTIONS OF LOADED END OF THE CROSS-PLY CYLINDER

Type of Load	Internal Pressure (psig)	Static Load	Total Deflection	
			Translation (in)	Rotation (deg)
Bending	12.0	1207 in/lb	0.35[1]	0.28
Bending	24.0	2421 in/lb	0.53	0.56
Bending	36.0	1750 in/lb	----[2]	----[2]

[1]Estimated value. Dial gage, actually measured 0.26-inch but was inadvertently "bottomed out" during test.

[2]Specimen failure occurred.

of the proposed paraglider. The fact that the cross-ply specimen burst at 36.0 psig precluded the possibility of putting the two plies together and testing the combined assembly as had been planned.

Both the test data and the general behavior of the specimens during set-up and mounting in the test fixture pointed out these facts:

a. The bias-ply cylinder was pliant in bending and shear but rigid in torsion.

b. The cross-ply cylinder was pliant in shear and torsion but rigid in bending.

c. Internal pressure caused gross deformation (bulging) of the bias-ply cylinder but had little effect on the shape of the cross-ply cylinder.

These conclusions confirmed the basic design approach developed early in the program in which a bias ply and a cross ply of metal fabric would be bonded together to give maximum strength in all three modes of loading: bending, shear, and torsion.

It should be noted that the premature failure of the cross-ply specimen was attributed to severe stress concentrations caused by the method used in closing the open ends of the cylinder. At the time of failure, the load-induced stresses were substantially below the strength of the metal fabric itself

379

Figure 210. Cross-Ply Specimen After Failure

335/169

380

or the weld joints. As a result of this experience, as well as the need for
an improved closure for the tapered frustums, new closures for the ends of
the 10-inch by 30-inch frustums were then designed and fabricated.

3.11.3.2 TESTING OF AN IMPREGNATED AND COATED, TWO-PLY CYLINDER

The objectives of this test were to determine the load carrying
capabilities of a two-ply, multifilament metal fabric cylinder which had been
impregnated and coated with silicone rubber in accordance with the fabrication
procedure proposed for the main paraglider components. This cylinder was
subjected to internal pressure, plus bending, shear and torsion loads followed
by an increase in the pressure and external loads to determine ultimate burst
strength.

In this case, the end closure plates were mounted into the ends of
the test cylinder using Silastic-140 (Dow-Corning) adhesive to prevent leakage
of the pressurizing nitrogen. A protective layer of firm rubber sheet material
was placed between the specimen and the clamping straps to prevent the stress
concentration and the apparent degradation in this area that occurred with the
cross-ply cylinder.

The test setup was, in most respects, the same as that employed in
the previous tests of the individual, uncoated, single-ply cylinders. Impregna-
tion and coating made the specimen less pliable and, therefore, it was more
difficult to install the end closure plates. Adequate sealing was finally achieved
by recessing the plates further into the cylinder ends in order to get the band
clamp area completely inside the wire restraining rings which were installed in
each ply at each end. Both ends were fitted with 7/8-inch-wide band clamps
torqued to 20 ft/lb.

Bending, shear, and torsion loads were applied individually and in
increments until buckling was observed. When no buckling was observed at
maximum possible load, the maximum bending and shear loads were maintained
while the internal pressure was decreased. The pressures at which the maxi-
mum loads formed wrinkles in the specimens were noted.

Table XXXV presents the deflections of the loaded end of the specimen
which resulted from the maximum static loads. These data compare favorably
with those obtained in previous testing of unimpregnated single-ply cylinders.

Following static load testing, the internal pressure was increased at
a constant rate of about 0.8 psig per second until failure occurred at 78 psig.
Failure occurred due to t e top closure plate blowing out. Figure 211 illustrates
the specimen under maximum pressure of 50 psig and maximum bending moment
of 3630 in/lb.

The specimen under maximum shear loading of 207 pounds at 50 psig
is shown in Figure 212.

THIS
PAGE
IS
MISSING
IN
ORIGINAL
DOCUMENT
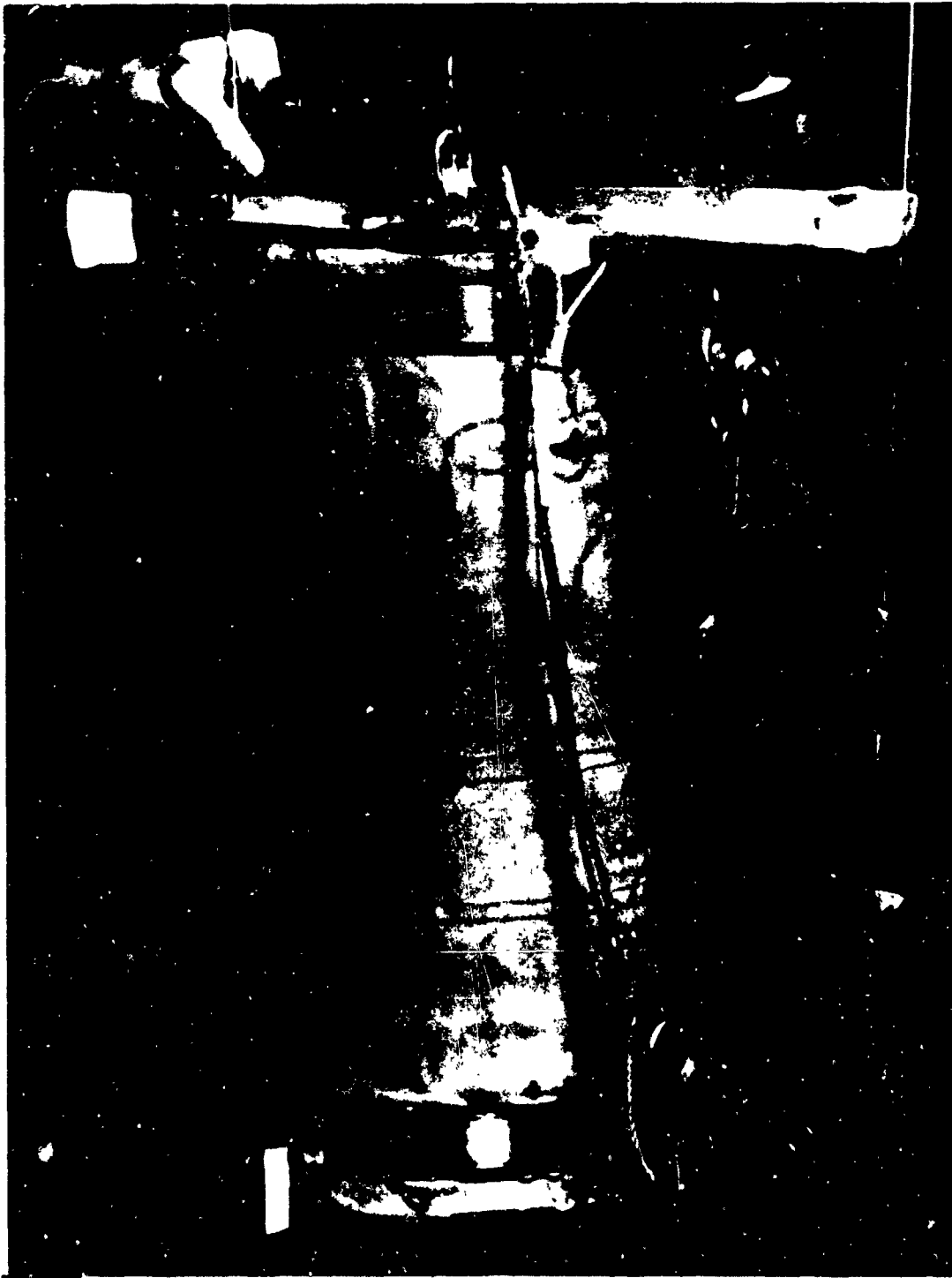
335/217

Figure 211. Pressurized Two-Ply Cylinder Under Maximum Pressure
and Bending Load (3630 in/lb at 50 psig)
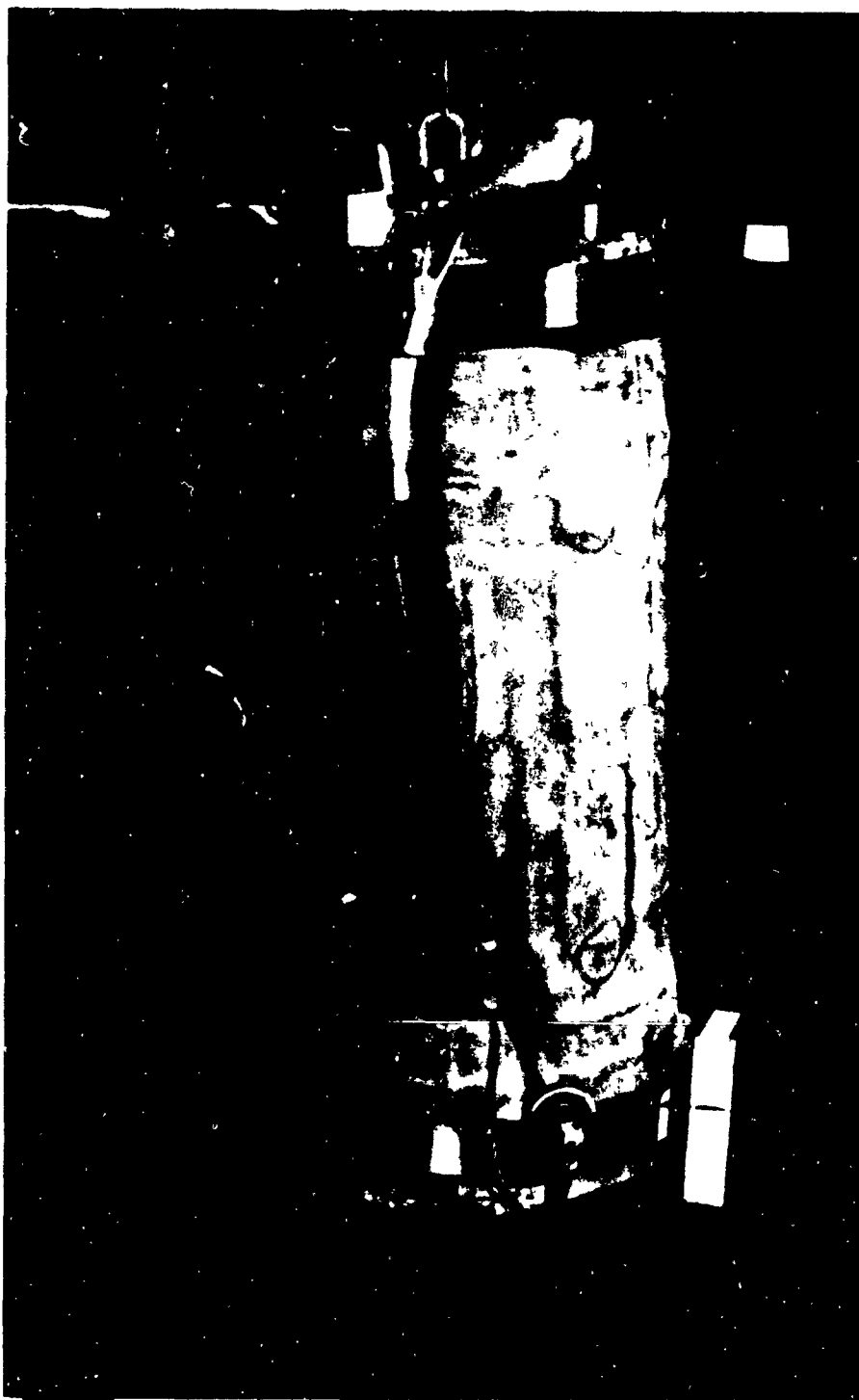
335/218

Figure 212. Pressurized Two 'ly Cylinder at Maximum Pressure
and Shear Load (207 Pounds at 50 psig)

Figure 213. Pressurized Two-Ply Cylinder at Maximum Pressure
and Torsional Load

385

Figure 214. Two-Ply Cylinder After Failure

386

the metal fabric indicated that a two-ply structure in bias relationship should have a hoop strength of 1.4 times (theoretically 1.5 times) that of a single cross-ply structure. The remaining 80 percent factors account for the proposed minimum weld efficiency and the predicted stress concentration factor, respectively. The radius of the small cylinders is 3.5 inches.

Since the design working pressure (corresponding to the full-scale paraglider) for a 7-inch cylinder is 50 psig, the test indicated that the cylinder could stand at least 56 percent excess pressure without bursting. As previously noted, more effective end closure clamping devices were developed so that the maximum strength of subsequent components was determined in actual burst tests. Figure 215 illustrates blisters which developed in the outer S-6510 coating due to obvious pin-hole leakage through the impregnated fabric. Although the S-6510 appears to be homogeneous and leak-free, this property causes small leaks in the impregnated metal fabric matrix to delaminate the outer coating. In each case, the blister was punctured with a penknife after which it retracted to the normal contour of the cylinder and the test was continued while maintaining pressure from the regulated pressurizing nitrogen source.

3.11.3.3 ANALYSIS OF TEST RESULTS ON UNCOATED AND COATED, SEVEN-INCH CYLINDERS

The method of calculating the loads to be applied to the single-ply and two-ply, 7-inch-diameter by 15-inch-long cylinders is presented in Appendix VIII. The deflections obtained at each load level during the test are presented and related to the predicted theoretical performance. About 75 percent of the calculated ideal incipient buckling bending moment was obtained at the point of actual buckling, and the reason for departure from the prediction is explained by corresponding changes in fiber-orientation of the bias-ply fabric.

In the case of the cross-ply cylinder, however, ability to carry 150 percent of the calculated bending moment for incipient buckling was attributed to the individual compressive and bending strength of the longitudinal fibers which are supported by the lateral fibers under hoop stress.

Analysis of the test results on the coated, two-ply cylinder showed that deflections in bending at the point of incipient buckling were greater than buckling deflections of the uncoated, cross-ply cylinder and considerably less than similar deflections of the uncoated, bias-ply cylinder. This difference is attributed to the manner in which the inner bias-ply and the outer cross-ply cylinders share the applied load.

Appendix VIII also presents the calculations for the test loads to be used on the 10-inch-diameter by 30-inch-long frustums discussed in Section 3.11.4. This analysis includes the limit loads to be applied to the full-scale boom.
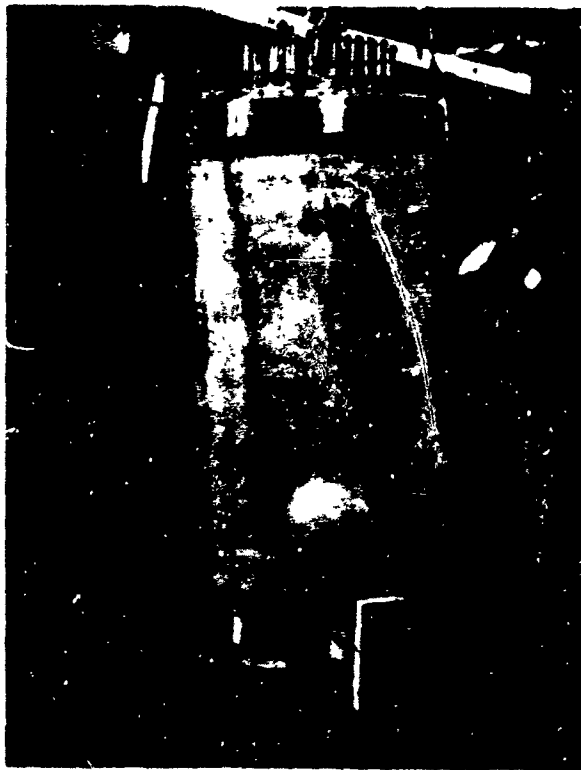
335/222

a. Small Blister

335/216

b. Large Blister

Figure 215. Blisters in Pressurized Cylinder

3.11.4 TESTING OF FRUSTUMS

The plan for testing the frustums is presented in Appendix IX, entitled "Frustum Test Requirement," describing the test specimens, serial numbering, and test setup precautions. The plan also describes the individual tests for permeability and leakage, proof and ultimate pressure, design and ultimate loads, and vibration at room temperatures, high temperature, and post-heating, in addition to instrumentation are given. Charts are provided showing anticipated test conditions. All tests were performed in accordance with this "Frustum Test Requirement" Appendix.

The results in each case exceeded expectations. This indicated that the two-ply bias relationship used as a basis for the metal fabric reinforcing construction in the proposed expandable structure was a very satisfactory technique and that the fabrication method produced very strong, pressure-stabilized structures capable of carrying high loads.

To insure a tight grip over the entire ring at each end of the frustum during pressurization, special end closures were designed and constructed. These used individual, radially-bolted clamps to grip the ends of the frustums. After peeling away 1.5 inches of the S-6510 rubber coating from the impregnated metal fabric, a strip of high-durometer rubber was placed between the finger grips and the metal fabric to prevent abrasion.

3.11.4.1 BURST TEST ON PRELIMINARY FRUSTUM

The objectives of this test were to determine the burst pressure of a 10-inch (tapering to 7-inch)-diameter by 30-inch-long two-ply metal fabric, impregnated and coated frustum, and to verify the functional adequacy of the mounting and loading test fixture assembly. The burst pressure test is the most satisfactory way of testing the adequacy and uniformity of welding as well as general lay-up technology used in an inflated structure.

The test specimen was the first "preliminary" frustum. The frustums had the same taper as the proposed paraglider booms. It was fabricated in two plies in bias relationship from pilot run metal fabric. Steel wire rings were enclosed in the end folds and two-ply cuffs of metal fabric were used at each end of the cylinder to assist in preventing stress concentrations or unrealistic damage due to the end closures. Unlike the coated two-ply, 7-inch-diameter by 15-inch-long cylinder, only one wire was used at each end with both plies rolled over it. This prevented some of the alignment and clamping problems that were experienced with the earlier, smaller specimens. The new end closures, recently designed and fabricated to prevent the ends of the cylinder from pulling out, may be seen in Figure 216. These closures consist of tapered end plates equipped with multiple outer clamps radially bolted to the end plates.

In preparation for testing, the S-6510 silicone rubber coating was removed from an area 1.25 inches long at each end of the specimen. This exposed the outer surface of the outer cuff of the RTV 655-impregnated metal fabric matrix. The end closures were then assembled to the specimen. The top and

389
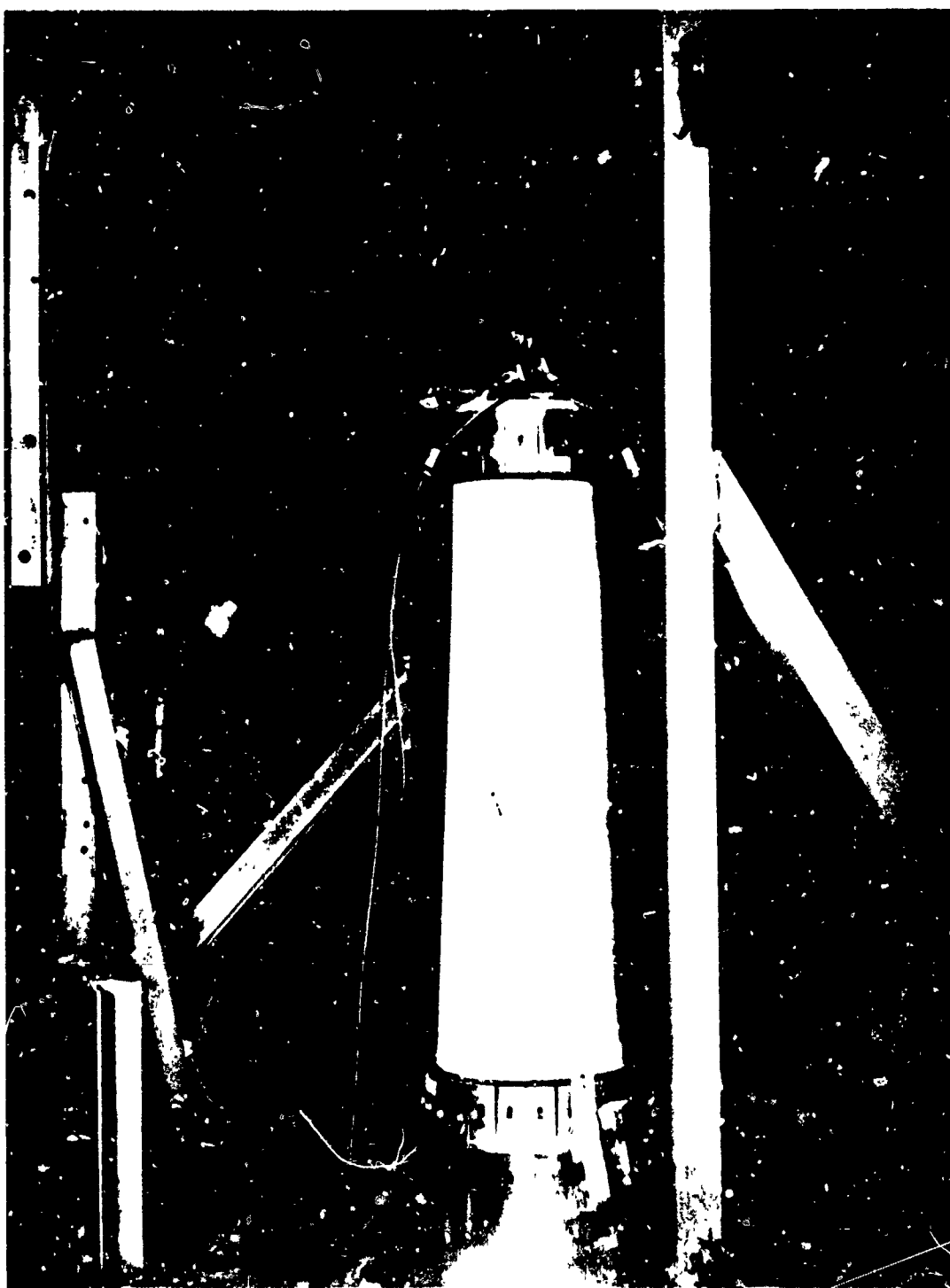
Figure 216.   Metal Fabric Frustum in Test Fixture

bottom clamp screws were torqued to 60 in/lb and 40 in/lb, respectively. A 50 psig leak check showed adequate sealing. The specimen was then installed in the test stand with a counterweight of 20.5 pounds to support the weight of the specimen and the upper end closure. Figure 216 shows the frustum in position for testing.

Using the computation technique similar to that presented in Section 3.11.3 for the 7-inch-diameter cylinder, the expected burst pressure is as follows:

$$\text{Burst pressure} = \frac{400 \text{ lb/in} \times 1.4 \times 0.8 \times 0.8}{5 \text{ inches}} = 72 \text{ psig}$$

In the above calculation the strength of the parent pilot run fabric has been shown to be 400 lb/in average in uniaxial tensile tests. The factor 1.4 allows for the bias-ply load-carrying ability of 40 percent that of the cross ply. It should be noted that the bias ply, if at a perfect 45° angle to the cross ply, would theoretically carry 50 percent as much load in the hoop direction of the cylinder. However, due to the ogee shape of the stress-strain curve, the empirical and relative load carried by the bias ply become 40 percent. The remaining 0.8 factors account for the expected weld-joint efficiency and stress-concentration effects, respectively. The radius of the large end of the frustum is 5 inches.

Internal pressure was increased at a constant rate of about 1.0 psig per second until failure occurred at 76 psig. This 5 percent increase over the predicted burst pressure indicated that not only the original design considerations were sound, but the ability to weld long seams to make an integral pressure vessel was established. In other words, not only could small one-inch wide weld coupons be welded with joint efficiencies in excess of 80 percent, but also medium large structures could be welded while maintaining the same weld efficiency and without building excessive stress concentrations into the structure.

No blister problems occurred as did in the 7-inch cylinder. The failure originated at an external weld seam at the large end of the specimen precisely as analytical theory would predict. Figure 217 shows the specimen after failure. The results of this test were extremely encouraging in that not only was the adequacy of the design and fabrication proven, but the loading and mounting fixtures, including the end closures, performed very satisfactorily. The ends of the frustum were satisfactorily sealed during the entire test and the clamping mechanism, using the radially positioned bolts and individual clamps as seen in Figure 217, inflicted no apparent damage to the test specimen.

The failure occurred suddenly with a loud report and there was no indication of gradual tearing, ripping, or other similar localized degradation contributing to the failure. The test frustum pulled out of the large end clamping device but this apparently happened as a result of the longitudinal seam rupture. This sequence of events was confirmed by high-speed motion pictures which were taken of the test.

391

Figure 217. Preliminary Frustum After Burst Test

3.11.4.2 FRUSTUM TEST 1 (S/N 1) - ULTIMATE LOADS

The first frustum was slightly small in diameter for the end closure and it was pulled onto the end closure using the same hardwood ring and hook bolt arrangement (shown in Figure 137) that was used for pulling frustum number 2 onto the impregnation form during fabrication.

Testing on the first (serial number 1) of the final frustums was extremely encouraging with respect to the loads that this structure could carry. The test was performed to determine the effect of static proof load and ultimate loads on the frustum at ambient temperatures. Simultaneous, torsion, shear, and bending loads were continuously and uniformly applied by a special loading machine. This machine is capable of increasing hydraulic pressures in multiple loading cylinders in constant proportion to one another. Deflection measurements were made at 33, 67, and 100 percent of design limit loads at a design pressure of 35 psig. For safety reasons, the test engineers did not enter the protective, chain-mail-covered enclosure when the loads were increased in excess of the design limit.

The simultaneous loads were increased and the first evidence of incipient buckling was noticed as wrinkles appeared near the small end cuff of the frustum. The wrinkles were about 60 to 70 degrees from the axis of the frustum as shown in Figure 218. The wrinkles occurred at 250 percent of design load limit. This was in excess of the incipient failure loading that was expected and detailed quantitative data are presented in Table XXXVI. The fact that the wrinkles were at this particular angle was not surprising. Pure bending would have created a wrinkle which was about 90 degrees from the axis of the frustum. Pure torsion should create a wrinkle which would be 45 degrees from the axis. The fact that no gross failure of this component, such as bursting or collapse, occurred when loads were continuously increased up to 400 percent of design limit was very significant. It is obvious that the inflated two-ply assembly, impregnated and coated as described, produces a very stable and rigid structure.

After the loads were reduced to zero and reapplied, the wrinkle again appeared at about 130 percent of design load limit. This time the wrinkling was more severe, indicating that the material had definitely been creased at the higher loads and a "memory" of this creasing was being retained. The wrinkle, however, disappeared completely when the loads were reduced to zero while maintaining the 35 psig pressurization.

3.11.4.3 FRUSTUM TEST 2 (S/N 3) - PRESSURE BURST

The second test utilized the third fabricated frustum identified as S/N 3. Frustum 2 was still on its form tool, difficulty being encountered in removing it. This second test was intended to demonstrate the ultimate strength of the structure by pneumatic bursting at room temperature without preloading to determine the basic strength.

The general appearance and workmanship of this frustum was superior to any previous specimen. To expedite the test, the component was sealed to the
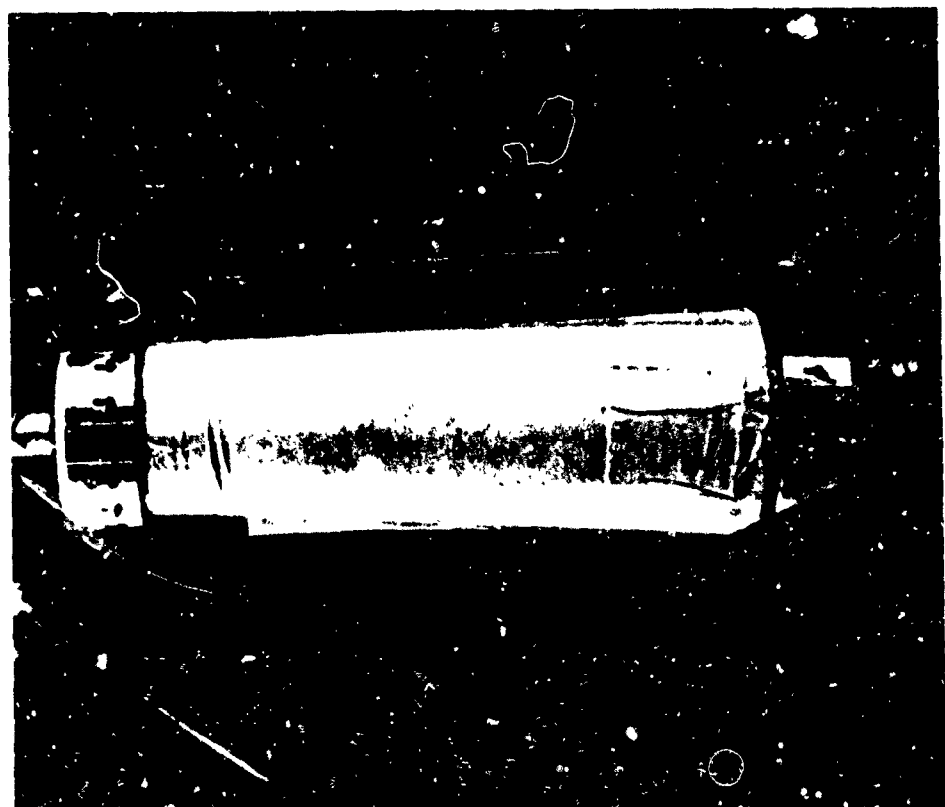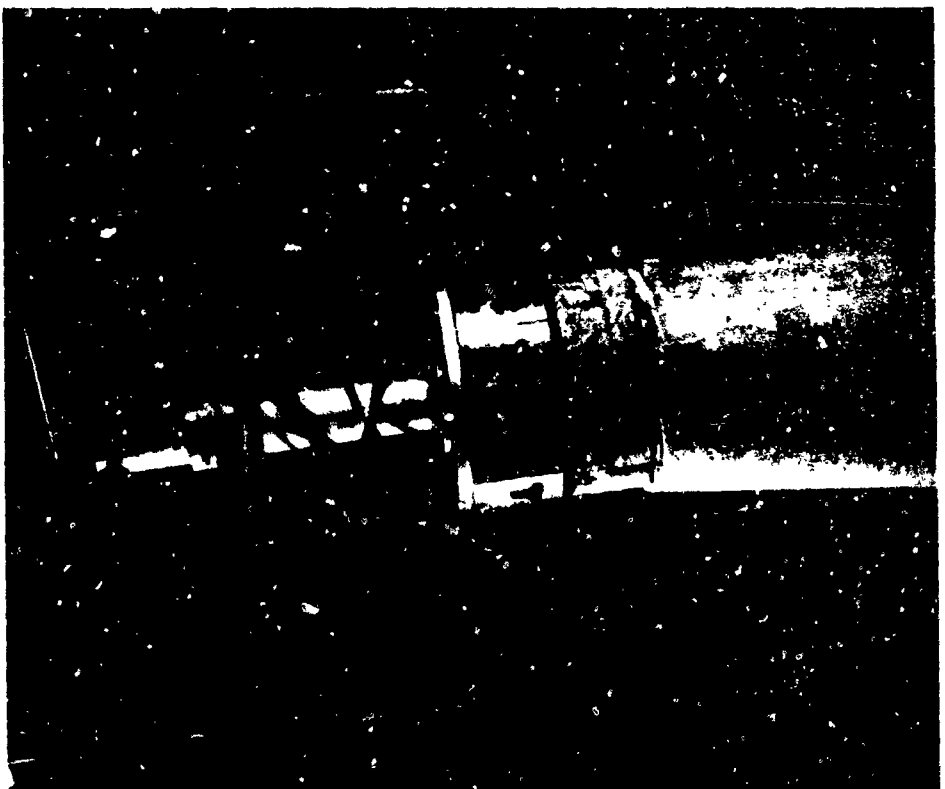
Figure 218. Frustum S/N 1 During Design Load Limit Test (Test 1)

394

Table XXXVI

FRUSTUM S/N 1 COMBINED ULTIMATE LOADS, TEST 1

% of Design Limit Loads*	Deflection Data and Description**
0	
33	Torsional = 0.14°, Bending = 1.47° ***
67	Torsional = 0.32°, Bending = 2.82°
100	Torsional = 0.50°, Bending = 3.85°
250	Buckle Noted Below Top Cuff
300	Loads Held for Photo
400	Loads Held for Photo
0	Buckle Not Evident at No-Load
150	Buckle Noted at Approximately 130%
250	
0	Buckle Not Evident at No-Load
400	Buckle Noted at Approx. 100%
0	Buckle Still Evident at No Load

* 100% of Limit Load:
  Combined Loads at Large End
         344 in. -lb Total Torque
         4710 in. -lb Bending Moment
         103 lb Total Shear Force
  For application of loads refer to Figure 1 of Test Requirement 335R-7 included in the appendix.

** All tests performed with 35 psig internal pressure.

***"Torsional" indicates rotation of top of frustum in the plan view; "bending" indicates rotation of top of frustum in the side view.

395

end closure with RTV 88 (G. E.) which was allowed to cure overnight. The mounting and loading fixture clamp screws were torqued to 100 in.-lb.

Permeability and leak testing was performed. The time required to drop in pressure from 5.0 to 4.0 psig was 26 minutes. Two other tests to determine the time period for the pressure to drop from 10.0 to 9.0 psig resulted in 11.5 and 10.5-minute periods respectively. It was impossible to isolate the leakage at the end of the cylinders from the gas that actually permeates the rubber-coated structure.

The frustum was pressure-tested in the test fixture. No external loads were applied except for the fixture counter-weight of 22.0 which was supporting the weight of the top closure and the frustum itself. The internal pressure was increased at the rate of approximately 1.7 psi per second. At approximately 35 psig, a leak was noted and the pressurization was decreased. When 55 psig was reached, a 2-inch-diameter blister had developed about one-third of the way from the small end and adjacent to the flap. The bleed valve was opened and the specimen depressurized. The blister was punctured to prevent the potential delamination from jeopardizing the test. One loose clamp screw was found and all screw torques were rechecked. The top screws were found to be satisfactory but the bottom screws were at about 75 in/lb. The bottom clamp screws were retightened to 100 in/lb. The reason for the reduction in loading on these screws may have been compressive creep in the rubber under the clamps.

The test was repeated using the same pressurization rate as originally established and the specimen failed with a loud explosive report at 78 psig.

The "design" calculation similar to that given in Section 3.11 4 1, but using the production run fabric strength of 340 lb/in, follows:

$$\text{Burst pressure} = \frac{340 \text{ lb/in.} \times 1.4 \times 0.8 \times 0.8}{5 \text{ in.}} = 61 \text{ psig}$$

As in previous calculations, the factor of 1.4 was allowed for the bias ply load-carrying ability of 40 percent of that of the cross ply in a two-ply structure. The remaining factors of 0.8 account for the expected weld joint efficiency and stress concentration effect, respectively. The radius of the large end of the frustum was 5 inches.

The fact that this frustum burst at 78 psig indicates that the product of the stress concentration and weld efficiency factors is 0.82. The "design" assumption was that this product would be 0.64.

High-speed, 16-mm black and white motion pictures, filmed at 1000 fps, were used to record the failure.

The failure was essentially instantaneous. The large end of the specimen was pulled free of its fixture clamps with the wire ring cutting through both plies of the cloth in certain places. Both plies failed near the large end.

The cross-ply failure ran along a longitudinal seam for about one-third the length of the frustum; it also split sideways for several inches. The bias-ply failure also occurred in this immediate area, not on a seam, but in a 45° direction along the yarns.

3.11.4.4 FRUSTUM TEST 3 (S/N 2) - LOADS AND BURST

The third frustum test used frustum 2 and was intended to determine the effect of external limit loads on the cylinder at room temperature prior to the burst test.

This frustum showed evidence of some wrinkles in the area immediately below the small end cuff. The wrinkled zone was about 1.3 inches long and 250° around the periphery as seen in Figure 219. Considerable abrasion was noted on the inside surface of the RTV 655 at the extreme ends of the specimen. It was unknown whether this damage extended into the inner ply of the fabric itself. This damage and wrinkling obviously occurred during the difficult removal from the form tool.

The test set-up, including the pneumatic system and loading system, was the same as used on the previous frustums. Grid lines making 1-inch squares were laid out with a felt point pen on the entire surface of the frustum. The grid lines were intended to aid the photographic analysis of the deformation of the specimen during application of the loads; however the deformation was so slight that the lines were not of great significance.

Permeability and leak tests showed pressure losses from 5.0 to 4.0 psig in 9.5 and 9.0 minutes, respectively, on two tests. Tests at 10 psig indicated excessive leakage and the clamp screws were re-torqued to 100 in/lb. Subsequent tests from 10.0 to 9.0 psig took 11.4 and 11.3 minutes, respectively. The time required to drop from 35 to 34 psig was 1.5 minutes. At this point a 1-1/2-inch-diameter blister was noted below the top cuff but this did not interfere with the continuation of the test.

With the pressure at 35.0 psig, combined simultaneous loads were applied in increments to 33, 67, and 100 percent of design limit. The minimal deformation at 100% limit load may be seen in Figure 220. These loads were then removed while maintaining the 35.0-psig internal pressure and photographs were taken during a 45-minute period. At each of the load increments, deflection data was taken. A tabulation of the combined loads and the resulting deflection data is presented in Table XXXVII.

The internal pressure was increased at approximately 1.5 psi per second and bursting occurred at 85 psig. This would indicate that the product of the weld efficiency and stress concentration factors was 0.88, using a calculation similar to that presented above for frustum test 2. The failed specimen showed massive damage and the clamp ends were retained in the closure fixture with no discernible damage. Figure 221 shows the burst frustum and mirror broken by the shock wave. As usual the cross ply failed along the side of a longitudinal seam but the extent of the damage to the frustum indicated that the frustum apparently failed in many areas at the same time. The test was considered a significant

397
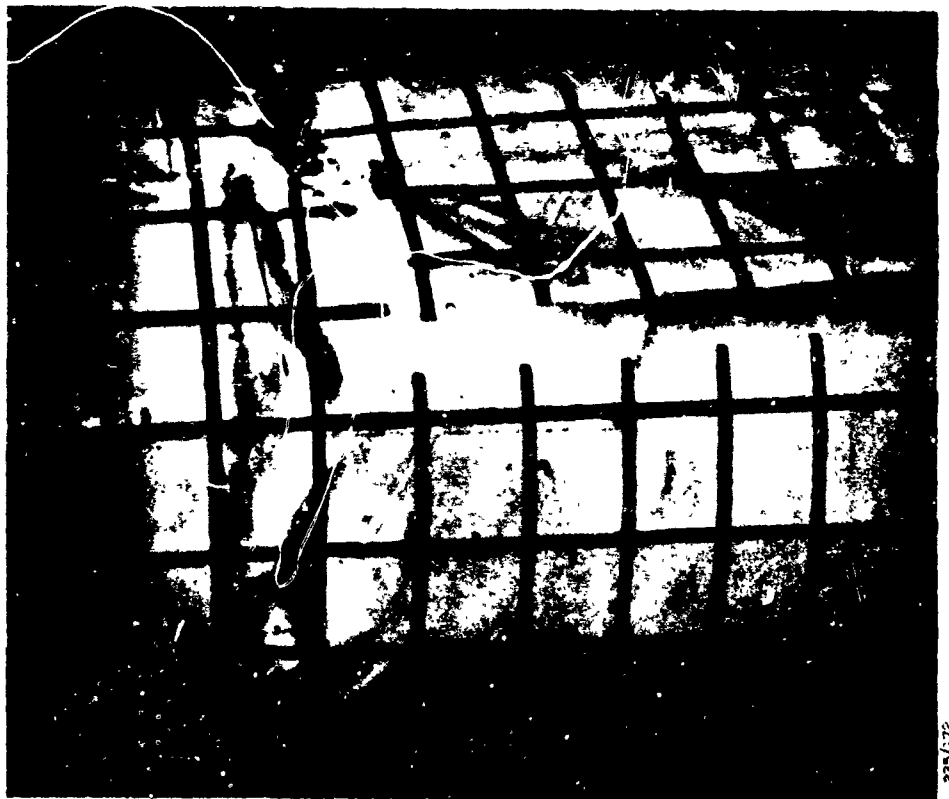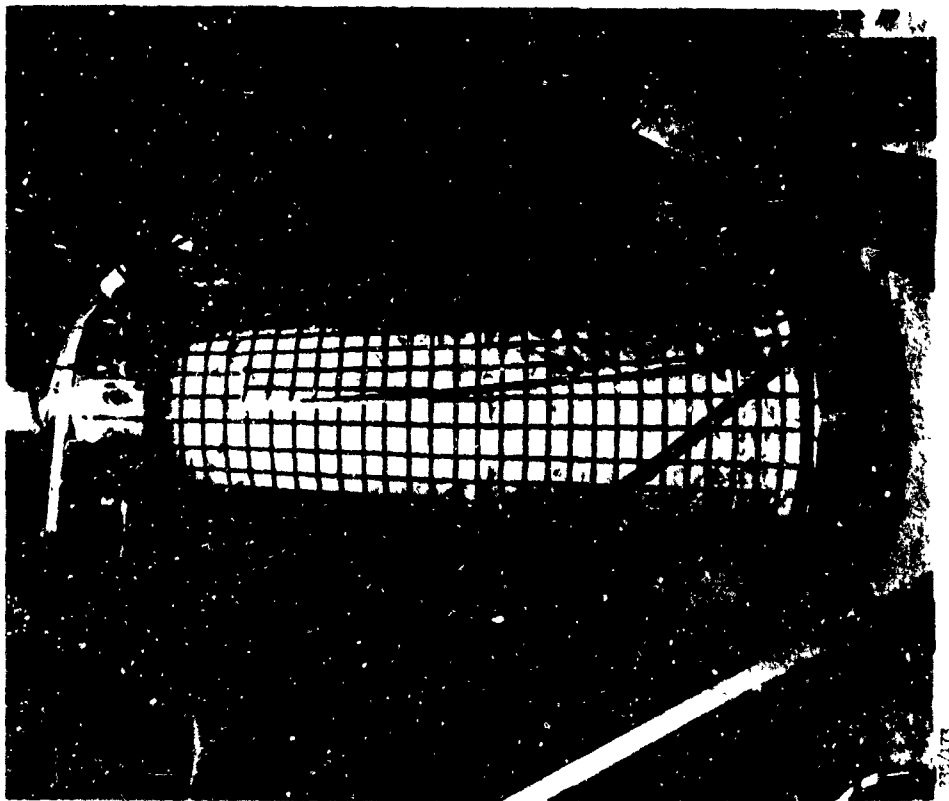
Figure 219. Frustum S/N 2 Prior to Loads Test (Test 3)

398

Figure 221. Frustum S/N 2 After Burst Test (Test 3)
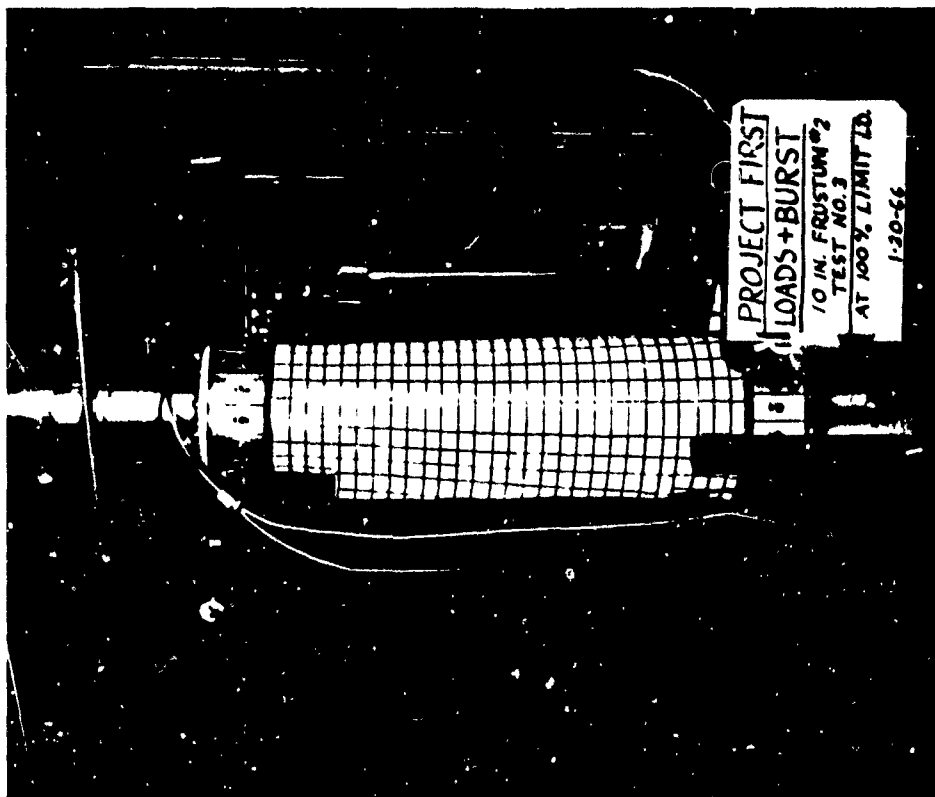
Figure 220. Frustum S/N 2 Under Test at 100% of
Limit Load (Test 3)

399

Table XXXVII

FRUSTUM S/N 2 COMBINED DESIGN LIMIT LOADS, TEST 3

% of Design Limit Load*	Deflection Data and Description**
0	Pressure check. 35 to 34 psig in 1-1/2 min.
33	1-1/2 inch blister noted below top cuff on tension centerline
0	
33	Torsional = 0, Bending = 1.5° ***
67	Torsional = 0.2°, Bending = 2.8°
100	Torsional = 0.27°, Bending = 3.8°
0	Torsional = 0.18°, Bending = 1.07°
0	Increased pressure at 1.5 psig/sec Specimen burst at 84 psig.

* 100% of Limit Load:
 Combined Loads at Large End
 344 in.-lb Total Torque
 4710 in.-lb Bending Moment
 103 lb Total Shear Load
 For application of loads refer to Figure 1 of Test Requirement 335R-7 included in the appendix.

** All deflection tests performed with 35 psig internal pressure.

***"Torsional" indicates rotation of top of frustum in the plan view; "bending" indicates rotation.

success; it showed that a frustum which had been subjected to maximum limit loads sustained no apparent degradation due to these loads, and that it actually burst at a higher pressure than the previous frustum which had not been subjected to external loads. Improved fabrication quality probably accounts for this.

High-speed movies were taken of this burst failure. The mirror permitted observation of the back-side of the frustum.

3.11.4.5 FRUSTUM TEST 4 (S/N 6) - PACKAGING, VIBRATION, AND BURST

This test was intended to determine if compact packaging of the frustum and the vibration of the package, to simulate a rocket launch environment, would affect the ultimate strength of the structure. Frustum No. 6 was used for this test. This frustum was essentially the same as the previous test frustums except that the end wires were coated with Orvus release agent before being welded in the rolled cuff, and the wires were allowed to extend about 3 inches out of the lap joint of the fabric. This specimen was made without the simulated wing flap.

After mounting this frustum, the permeability and leak tests were conducted as usual with the closure clamp screws torqued to 100 in/lb. The test stand was not used for this leak test. Three tests of the time required to drop the pressure from 5.0 to 4.0 psig resulted in periods of 7.2, 8.2, and 8.0 minutes. The times required in three tests for a pressure drop from 10.0 to 9.0 psig were 4.3, 5.0, and 5.2 minutes. The time required to drop the pressure from 35.0 to 34.0 psig was 0.6 minute. No blisters were observed.

Following the leak check, the bolted clamps on the end closure were removed but the closures were left in place to maintain rigidity while the end wires were pulled out of the frustum. The small end wire was removed by hand with considerable difficulty; removal of the large end wire required a hydraulic cylinder using an estimated force of 800 to 1200 pounds.

This frustum was folded by first laying it flat with the bias and cross-ply seams in the center of the flattened component as shown in Figure 222. It was then folded from the small end toward the large end. The dimensions after folding were established by fitting a cardboard box carefully around the folded component as shown in Figure 223. The dimensions of the box were 15.4 inches long by 5.4 inches wide by 1.2 inches high at one end and 2.0 inches high at the other end. The volume of the box was 134 cubic inches. The volume of the material in an impregnated and coated frustum is 65.5 cubic inches. This gives a packaging ratio, relative to material, of 2.0. The volume of the inflated frustum is 1705 cubic inches, giving a package ratio, relative to inflated volume, of 12.7.

The specimen, without the box, was clamped between two 1.0 inch aluminum plates with about 80 pounds of preload and was then mounted on an MB C10 shaker. It was left in this condition overnight, about 17 hours. The dimensions of the folded specimen, when mounted on the shaker, were 1.10 to 1.92 in.

401

335/.8a

Figure 222. Frustum S/N 6 Lying Flat Prior to Folding (Test 4)

335/18

Figure 223. Frustum S/N 6 Folded and Placed in Package (Test 4)
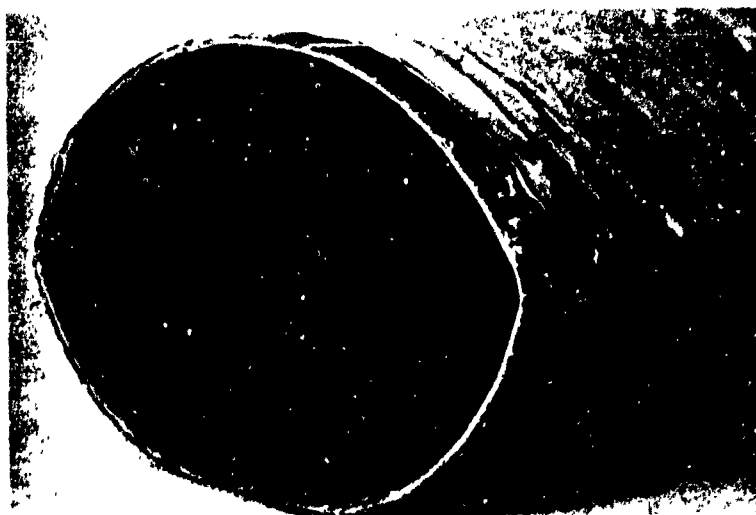
335/189

Figure 224. Frustum S/N 6 Inner Surface Crease After Folding (Test 4)

402

high, small to large side, by 5.44 in. wide by 14.90 in. long, giving 122 cubic inches, or a packaging ratio, relative to material, of 1.86.

The vibration test, reported to simulate the vibration regime experienced by a Saturn V at lift-off, was as follows:

Sinuscidal wave shape with one sweep at three octaves per minute:

5.0 to 18.5 cps   0.154 inch double amplitude

18.5 to 100 cps   2.69 g (constant)

The specimen was removed from the shaker, unfolded, and inspected for damage. Creases from folding remained visible after unfolding the frustum. The most serious damage appeared to be located on the inner surface along the two longitudinal creases. In these areas, the superficial layer of RTV-655 was cracked and ruptured. It appeared that there might have been some intra-ply delamination along these creases which may be seen in Figure 224.

After inspection, the specimen was refolded for additional photographs. It is to be noted that this resulted in two complete foldings on this specimen.

The permeability and leak tests were rerun on this specimen, after replacing the end wires with one gauge smaller wires and mounting the end closures. The frustum, after mounting in the test fixture but before pressurizing, is shown in Figure 225. The leak tests indicated 5.5, 5.8, and 5.5 minutes for the drop of pressure from 5.0 to 4.0 psig, 3.0, 3.6, and 3.6 minutes for the drop from 10.0 to 9.0 psig, and only 0.1 minute for the drop from 35.0 to 34.0 psig. The latter short leak period was due to a very distinct leak which occurred with a percussive sound just as the leak test was being conducted. The leak occurred in an area along the longitudinal fold near the large end of the side where the S-6510 coating is at a maximum thickness. Some delamination of the coating was caused by gas seeping out the end of the coating, but the S-6510 coating did not rupture.

With respect to the leaks in these components, it should be noted that, while 35 psig is required to properly load the sub-scale frustum in hoop and longitudinal directions, the pressure sealing requirement for the RTV-655 is only at the 11-psig working pressure planned for the full-scale vehicle.

The above-mentioned leak was patched with an internal layer of RTV-655 in an area approximately 3 inches wide by 6 inches long and additional leak readings were taken. The times for drop from 5.0 to 4.0 psig were 3.3, 3.8, and 3.6 minutes; the corresponding times for drop from 10.0 to 9.0 psig were 2.3, 2.1, and 2.2, while the drop from 35.0 to 34.0 occurred in 0.4 minute.

After the above testing, the specimen was burst-tested with no external loads except the loading jig counterweight of 22.0 lb. The internal pressure was increased at a rate of approximately 2 psi per second. At 60 psig, a blister began to form in the S-6510 coating. Between 60 and 75 psig the pressure rise rate averaged 1 psi per second. At 75 psig the blister ruptured. Between 75 and 85

Figure 226. Frustum S/N 6 After Burst Test (Test 4)

Figure 227. Frustum S/N 6, Showing Burst Pattern (Test 4)
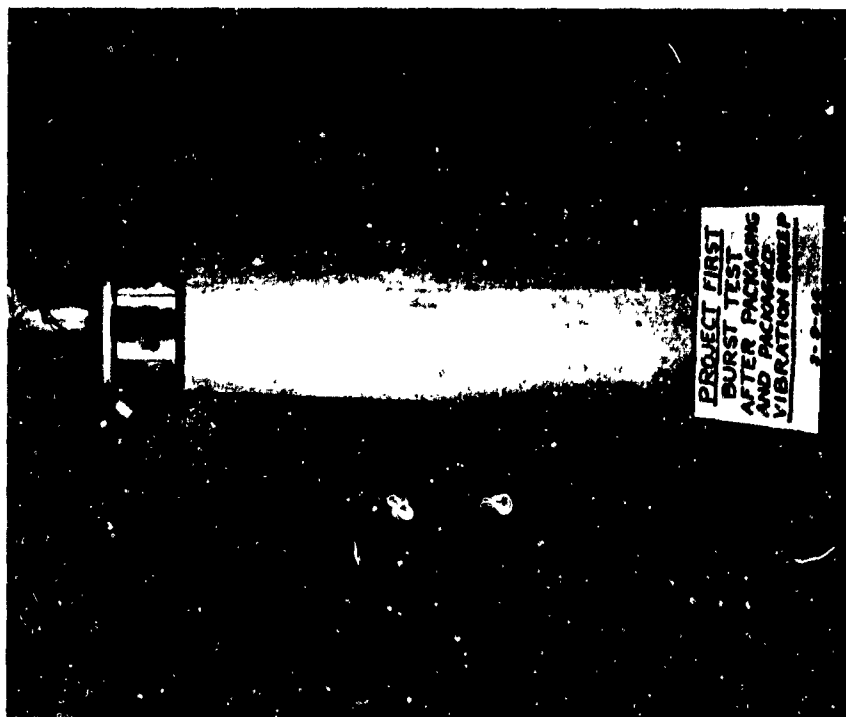
Figure 225. Frustum S/N 6 After Packaging and Prior to Burst Test (Test 4)

404

psig the pressure rise rate averaged 0.5 psi per second. During this time, noises of escaping gas and rubber failure, small "pops", were noted. The pressure rose fr⁻⁻ 85 to 86 psig in 10 seconds, at which tirr e the specimen burst as shown in Figure 226. The origin of the failure could not be definitely established, but it is believed to be somewhere along the external cross-ply seam. As shown in Figure 227, gross failure occurred along the entire longitudinal seam and not in the areas of the folds. Again the high burst pressure with this component indicated that the preloading, packaging, and vibration while packaged had little, if any, detrimental effect on the ultimate strength of the component.

3.11.4.6 FRUSTUM TEST 5 (S/N 8) - LOADS AT HIGH TEMPERATURE

Frustum test 5 used frustum serial number 8. This frustum was the first specimen subjected to an autoclaving procedure for curing the silicone rubber coatings. This process is discussed in Section 3.10.5. Test No. 5 was performed to demonstrate the effect of external limit loads on the frustum at elevated temperature.

The test set-up, including the pneumatic system and loading system, was the same as used on the previous frustums. A three-element radiant heat lamp was used for the high temperature requirement of the test. The temperature of the frustum was monitored by nine thermocouples. Three thermocouples were mounted on the outside of the silicone rubber coating; three were welded to the metal fabric between the outside coating and metal fabric cross-ply; and three were welded to the bias ply on the inside of the frustum. Thermocouple locations are tabulated in Figure 1 of Frustum Test Requirement 335R-7, which is included in the appendix.

The test specimen was proof tested to 35.0 psig. Several small gas leaks at the small end closure fitting were detected. The permeability test was waived so the primary objective of the test could be completed. The test stand including the specimen, loading jig, and heat lamp was covered with a 4 x 4 x 4 ft. polyethylene bag, see Figure 228, and purged with nitrogen gas to eliminate the possibility of a fire due to the extreme heat produced by the heat lamp. Oxygen concentration of less than 1% was verified with an oxygen analyzer. The effective oxygen concentration at the re-entry heating altitude, including velocity pressure effects, will be of this order of magnitude.

With the internal pressure at 35.0 psig, and the preheated lamp, (preheated for three minutes behind a shield) placed in front of the frustum, the specimen was allowed to heat for eight minutes, at which time the metal fabric temperature had stabilized to 550°F. At 11.3 minutes, the combined static loads were applied to the test specimen at a constant rate for 30 seconds up to 250 percent of design limit loads. By this time, the smoke in the test chamber was too dense to permit visual observation of the specimen. To ensure that the specimen had buckled under the high temperature conditions, the loads were increased to 400% for one minute and then reduced to 100 percent for the remainder of the heating period. At 17 minutes, the heat lamp was turned off and the static loads were reduced to zero. During the cooling period, the loads were inadvertently

405

335/221

Figure 228. Frustum S/N 8 on Test Stand with Polyethylene Bag
Enclosure (Test 5)

momentarily raised to approximately 300 percent (through accidental switching on of the loading machine), and then reduced to zero without any apparent damage to the specimen. After cooling, the specimen showed residual buckles similar to those shown on frustum 1. A post-test permeability check showed that the pressure would decay from 35 to 34 psig in 12 seconds. Figure 229 illustrates the temperatures of the nine thermocouples and the design loading sequence of the test specimen.

3.11.4.7 FRUSTUM TEST 6 (S/N 4) - ULTIMATE LOADS AFTER COOLING

Frustum test 6 used frustum serial number 4. The general appearance of this frustum was superior in workmanship. Test 6 was performed to demonstrate an ultimate loads test on a preheated and a cooled test frustum. The test setup was the same as the previous test. Thermocouples were not included in this specimen fabrication; therefore temperature measurements were limited to the external surface of the frustum.

Pressure and permeability tests were conducted on the test specimen. Three tests were performed to determine the time required to drop the pressure from 5 to 4 psig. These tests showed 19.2 minutes, 23.0 minutes, and 20.5 minutes. The time required in each of the three tests for a pressure drop from 10 to 9 psig was 9.8 minutes, 10.2 minutes, and 10 minutes. The time required to drop the pressure from 35 to 34 psig was 2 minutes. No blisters were observed on the test specimen.

An insulation shield was placed between the lamp and the test specimen so that the lamp could be preheated for 3 minutes. With the insulation removed, the specimen, with 11-psig internal pressure, was exposed to the preheated lamp. After approximately 6 minutes, the thermocouple recorded a temperature of about 880°F. The maximum temperature was maintained for 9 minutes; during the last 2 minutes of the period the nitrogen internal pressurization supply was valved off and the following permeability readings were taken. At time 8 minutes, the pressure was 11 psig; this pressure was maintained from time 8 minutes through time 10 minutes. After the last pressure reading was taken, the lamp was turned off and the insulation shield was replaced in front of the test specimen. The maximum temperature recorded was 900°F on the outside skin of the test frustum. Figure 230 shows the time-temperature curves of the test specimen.

The post-temperature permeability test indicated that on the 5 to 4 psig test, the times were 49 minutes, 50.5 minutes, and 50.0 minutes. The times required for three tests for the pressure drop from 10 to 9 psig were 18.2 minutes, 18 minutes, and 18.5 minutes. The time required to drop the pressure from 35 to 34 psig was 1.3 minutes. No blisters were observed on this test, but heat delamination occurred after cooling on the outer 2 layers of the silicone rubber coating as seen in Figure 231, but the temperature may have been much higher than 900°F (see Section 3.11.4.8).

With the pressure at 35 psig and the test specimen cooled to room temperature, the design limit loads were applied from zero to 250 percent. At 177 percent of the design limit loads, buckling was first evident; at 250 percent the buckling was well defined. The load was reduced and, at 50 percent of design

407
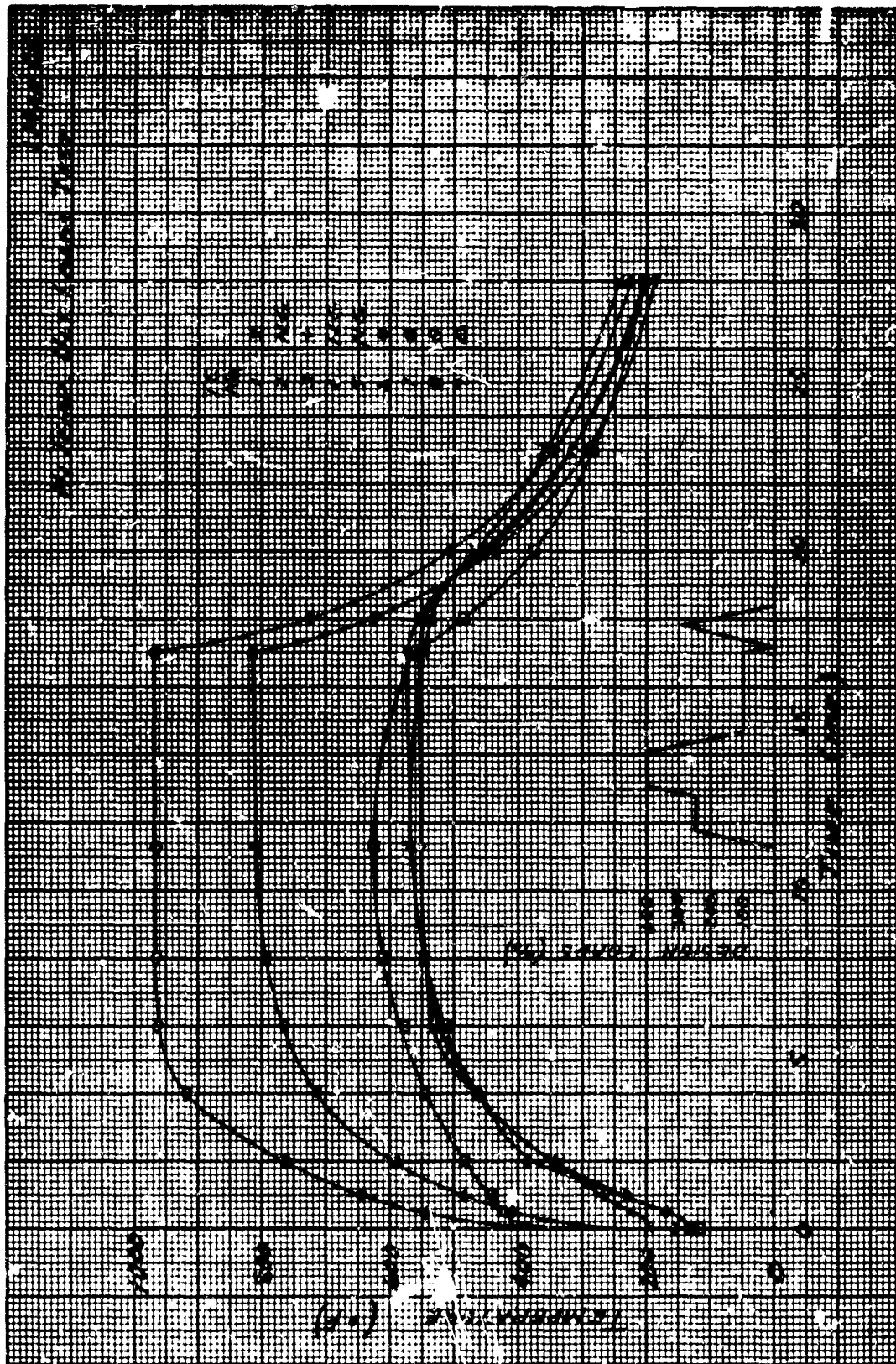
Figure 229. Actual Temperatures and Loads During Test 5 – High
Temperature, Ultimate Loads, Frustum S/N 8
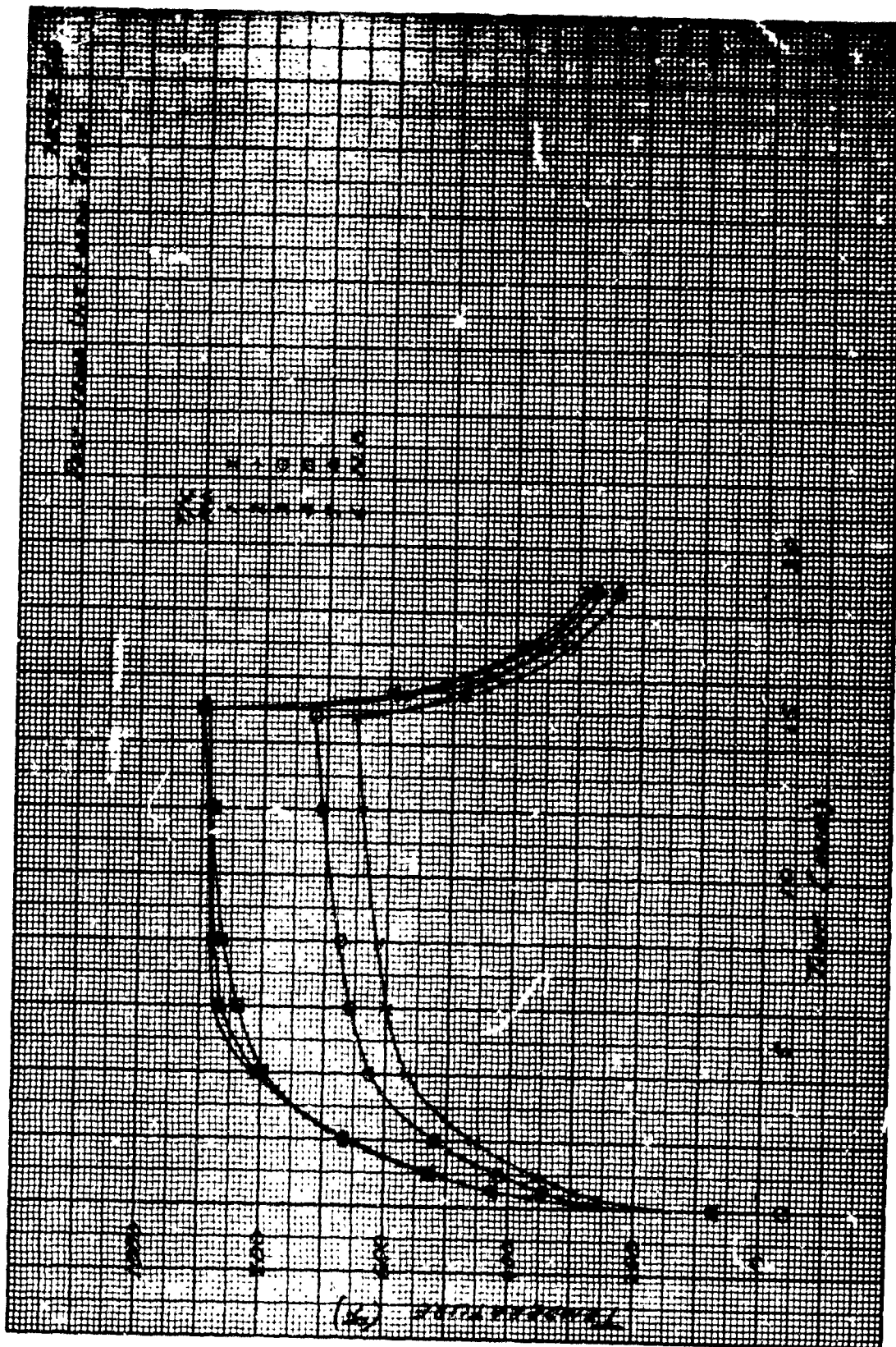
Figure 230. Time-Temperature History for Post-Temperature
Ultimate Loads Tests, Frustum S/N 4, Test 6

Figure 230. Time-Temperature History for Post-Temperature
Ultimate Loads Tests, Frustum S/N 4, Test 6

409
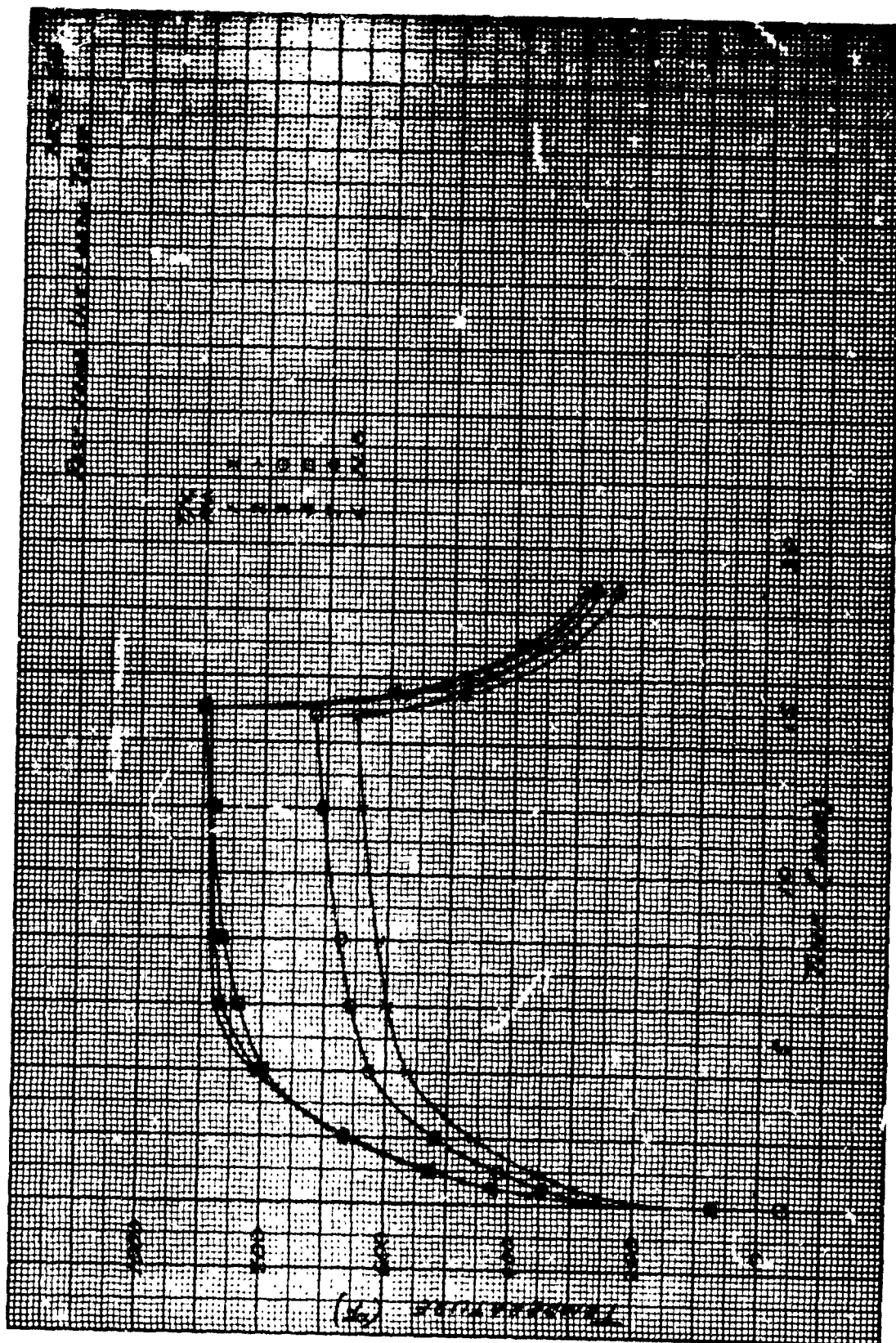
335/264

Figure 231.   Frustum S/N 4 After High Temperature Exposure (Test 6)

410

limit load, the buckling disappeared. The load was again increased; buckling was first evident at 130 percent and well defined at 250 percent. The load was then reduced to zero.

3.11.4.8 FRUSTUM TEST 7 (S/N 5) - PRESSURE BURST AFTER COOLING

Frustum test 7 used frustum 5. This frustum had no flap and had not been autoclaved during the fabrication procedure. Test 7 was performed to demonstrate the effect of exposure to high temperature and then cooling to room temperature prior to bursting the test specimen. Three internal thermocouples were used for this test; they were not welded to the metal fabric but were placed between the outer cross-ply and the silicone rubber coating. The three other thermocouples were installed on the outside of the silicone rubber coating.

A preliminary pressure test indicated that leakage was evident and was causing a small diameter blister. The frustum was removed from the test jig and an RTV 655 coating was applied to the internal surface of the frustum to stop the leak. The test specimen was remounted on the test fixture and a leak check indicated that a seal had been effected.

The pressure-permeability test was then applied to the test specimen. Three tests on the time required to drop the pressure from 5 to 4 psig showed 8.5, 9.0, and 8.5 minutes. The times required in the three tests for a pressure drop from 10 to 9 psig were 3.5, 3.5, and 3.8 minutes. The time required to drop the pressure from 35 to 34 psig was 0.4 minute; no blisters were observed.

The test set-up was the same as for the previous test, with the specimen to heat-lamp clearance of four inches maintained over the full length of the test specimen. The specimen was protected from lamp pre-heating and post-heating by an adjustable shield of insulation. The polyethylene enclosure was purged by nitrogen to less than 1 percent (by volume) of oxygen.

The test specimen was pressurized to 11 psig and, after preheating the lamp for 3 minutes, the heating cycle was started. After 4 minutes of heating, the temperature of the metal fabric was recorded by thermocouple number five at $850^{\circ}F$, at which time the 10-minute period started. Figure 232 shows the time-temperature curve of the test specimen. Note the temperature fluctuations of the thermocouples; these were caused by turning the lamps off and on to control the metal fabric temperature at 800 to $850^{\circ}F$. Internal gas temperature, indicated by thermocouple number 10, reached $330^{\circ}F$. Small blisters on the silicone rubber coating were noted at approximately 5.5 minutes. At 12.5 minutes the nitrogen supply was turned off and a high temperature permeability test was made. The time required to drop the pressure from 35 to 34 psig was 1 minute. The times required on three tests for a pressure drop from 10 to 9 psig were 6.5, 5.7, and 5.6 minutes. The times required to drop the pressure from 5 to 4 psig were 8.7, 8.4, and 7.4 minutes.

After cooling and with no external loads applied, the internal pressure was increased at a constant rate of approximately 0.9 psi per second. Figures 233 and 234 show the frustum at the beginning of this pressurization. Near 50

411
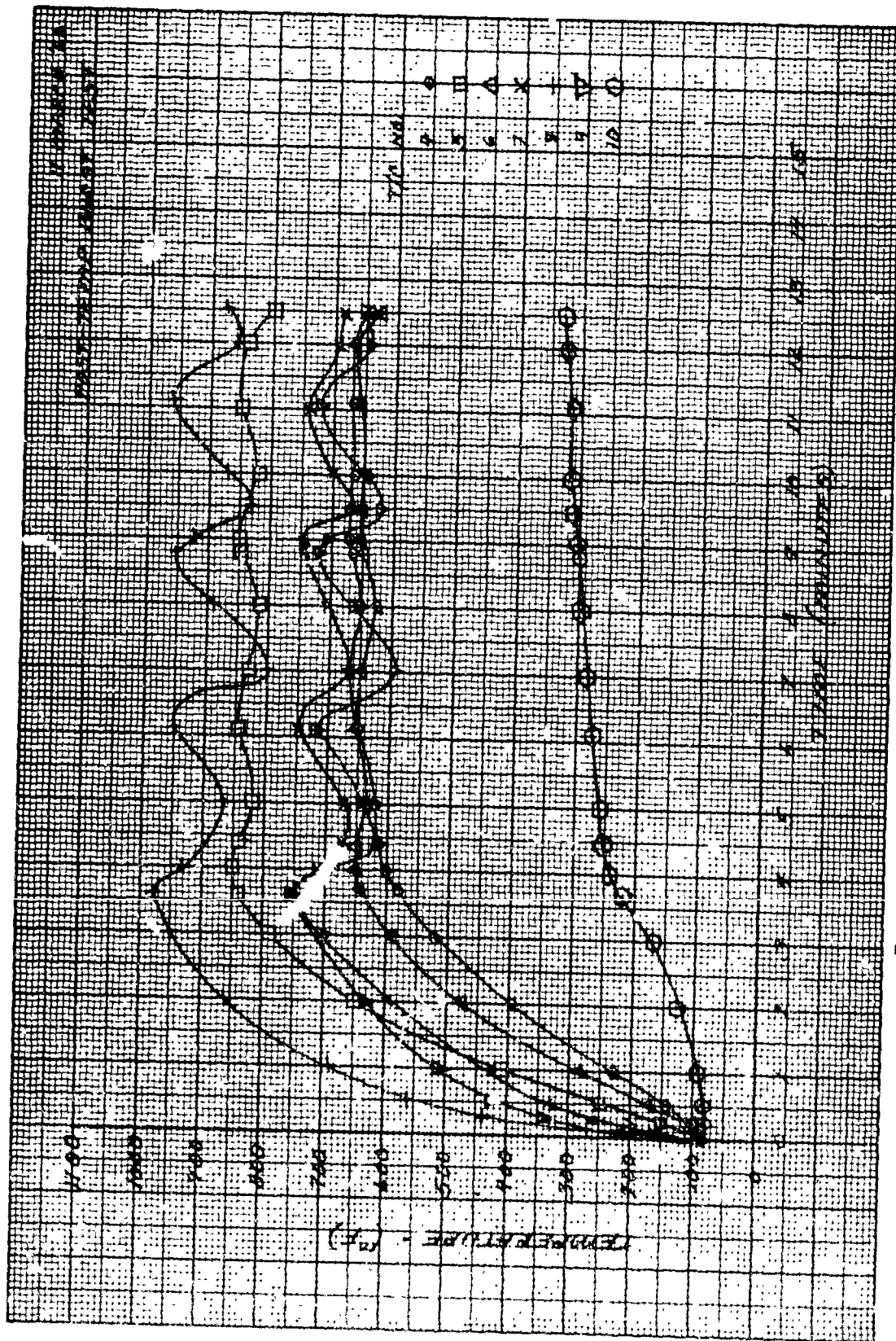
Figure 232. Time-Temperature History for Post-Temperature
Burst Test on Frustum S/N 5 (Test 7)

Figure 234. Frustum S/N 5 After High-Temperature Test, Close View of Heated Area (Test 7)
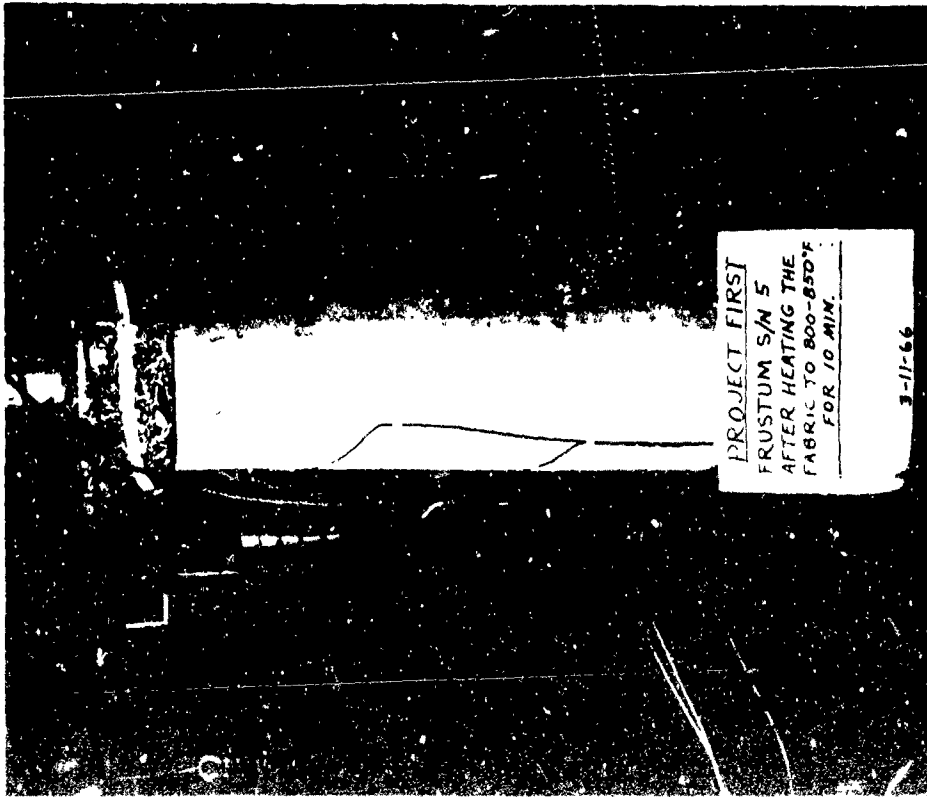
Figure 233. Frustum S/N 5 After High-Temperature Test (Test 7)

PROJECT FIRST
FRUSTUM S/N 5
AFTER HEATING THE
FABRIC TO 800–850°F
FOR 10 MIN.

3-11-66

psig a 2-1/2-inch-diameter blister was observed on a cross-ply seam about 1/3 of the way down from the small frustum end. No noticeable increase in leak rate was detected until failure occurred at 85 psig. The ends of the specimen were still retained by the jig clamps after failure as indicated by Figures 235 and 236.

It will be noted in Figure 236 that the rupture failure did not occur in the heated area (near left side of frustum) indicating that the high temperatures obtained did not weaken the fabric reinforcement's room temperature strength.

Most significant in this test is the high fabric temperature obtained with negligible charring and no delamination (Figure 234). Only two small blisters were evident in the highly heated zone; these disappeared on cooling. Extensive tests conducted between tests 6 and 7 indicated that previous heating tests had the quartz lamp placed too close to the side of the frustums. The particular geometry of the lamp, with a gold plated "parabolic" (approx.) reflector containing three tubular lamps, caused a cold area in the center between two hot areas on the heated surface. Ironically, the thermocouples were always positioned in the center of the lamp exposure zone and therefore apparently were not measuring the maximum temperature seen by the silicone rubber surfaces of Frustums S/N 8 and 4 in tests 5 and 6, respectively. This may explain the more extensive degradation encountered in those tests.

Development tests, using a transite board painted with temperature-sensitive "Tempilaq" paints, indicated the lamps should be 4 inches from the frustum (as used in test 7), rather than the previously used 2 to 3 inches, to give uniform heating.

3.11.4.9 FRUSTUM TEST NO. 8 (S/N 10) - FATIGUE LOADS AND PRESSURE BURST TEST AFTER COOLING

Type J, 26 gage thermocouples were welded at three points to the exterior metal fabric along a line directly under the heating area. Three additional thermocouples were attached to the exterior of the outer silicone rubber coating of this frustum. The frustum, as set up for this test, is shown in Figure 237. Small silicone rubber tabs used for holding the external thermocouple wires in place may be seen in this view. Directly behind the frustum is the insulating shield, behind which the heating lamp is preheated. The simulated wing attachment flap may also be seen extending from the right side of the frustum. The hydraulic cylinders, cables, and pulleys used for applying the combined torsion, shear, and bending loads are also shown in this photograph. The large cables extending from the base plate to the top of the frustum are intended to restrain the upper closure and loading fixture during burst test. The weight of the upper closure is nullified by a counterweight shown to the left of the structure.

The steel shield was added to the test stand to protect the heat lamp during burst test as well as to provide for preheating the lamp behind the shield so that it could then be moved out adjacent to the specimen to obtain the maximum rate of heating during the test. Finally, after the heating test, the lamp could be moved back behind the shield.

414

Figure 236. Frustum S/N 5 Burst Test, Close
View of Heated Zone (Test 7,

Figure 235. Frustum S/N 5 Burst Test Result (Test 7)
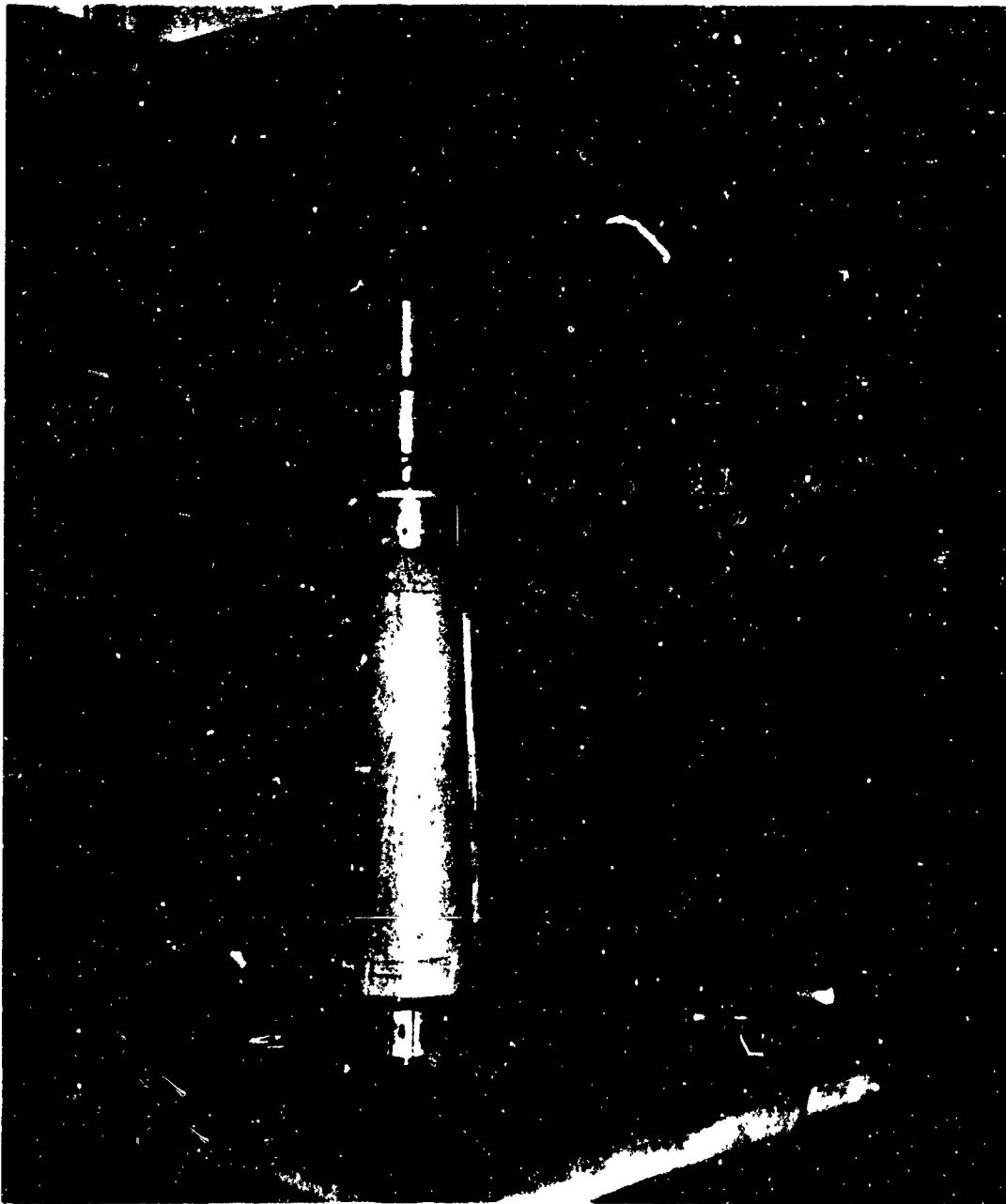
335/290B

Figure 237. Frustum S/N 10 Set-Up for Test 8, Fatigue Loads and
Pneumatic Burst

The test specimen was prepared with the end closures installed. Persistent leaks at the large end closure (not in the component itself) necessitated the application of RTV-88 (G. E.) silicone rubber as a sealant.

The first proof pressure test resulted in a leak and blister 5 inches in diameter in the vicinity of the upper welded thermocouple, T/C 4. The specimen was demounted and coated with two applications of RTV-655 on the interior surface. Subsequent proof pressure test indicated that the leak had been stopped. The time required for the specimen to drop in pressure under shutoff conditions from 5.0 to 4.0 psig was 42, 40, and 42 minutes, respectively, in three tests, indicating a very low leakage rate. Similarly, the time required to drop from 10.0 to 9.0 psig was 27, 28, and 28 minutes. A final test to determine the leak rate at higher pressure resulted in a time of 2.7 minutes to drop from 35.0 to 34.0 psig.

With the specimen pressurized to 11.0 psig (normal working pressure of the re-entry vehicle) and the plastic enclosure purged to less than 1 percent oxygen, the heat lamp was turned on and preheated behind the insulating shield for three minutes. The lamp was moved from behind the shield and aligned with the test specimen with a 4-inch space between the lamp and the ablative rubber coating. After heating for 4 minutes, the specimen began to smoke. At 5-1/2 minutes, very small blisters began to form in the S-6510 coating. The blisters became larger and more numerous as the test progressed.

The specimen did not get as hot as expected but the temperature of the metal fabric substrate in the center of the heated area reached 600°F after heating for 8 minutes. This point was selected to start the 10-minute maximum fabric temperature. Maximum temperature reached at this thermocouple location was 625°F as shown by T/C 5 in Figure 238. Similarly, Figure 239 shows the temperature of the three thermocouples attached to the exterior of the frustum.

While the heat lamp was on, the nitrogen in the specimen continued to expand, and the gas was bled off to maintain 11.0 psig during the first 8 minutes of this test. The high temperature leakage test was conducted during the last 2 minutes of the 10-minute period. With the pressure and bleed valve closed off and the thermocouple on the metal fabric indicating approximately 625°F, the internal pressure increased from 11.2 to 11.3 psig during this 2-minute period.

At the end of the 10-minute period, the lamp was shut off and pulled behind the insulating shield. The specimen was allowed to cool to room temperature before the enclosure was removed for inspection and photography.

Proof pressure and leakage tests of the specimen after cooling indicated the time required for the valved off enclosure to drop from 5.0 to 4.0 psig was 38, 44, and 42 minutes in three tests, from 10.0 to 9.0 psig was 28, 29, and 30 minutes, and from 35 to 34 psig was 1.4 minutes (one test). This is an extremely low amount of leakage and permeation and compares almost exactly with the leakage rates experienced before heating, indicating that little damage was done to the gas barrier properties of the membrane.

The internal pressure was then increased to 35 psig, and the combined limit loads in shear, torsion, and bending were applied with the hydraulic regulator. The regulator had been adjusted to cycle between 0 and 100 percent of limit

417
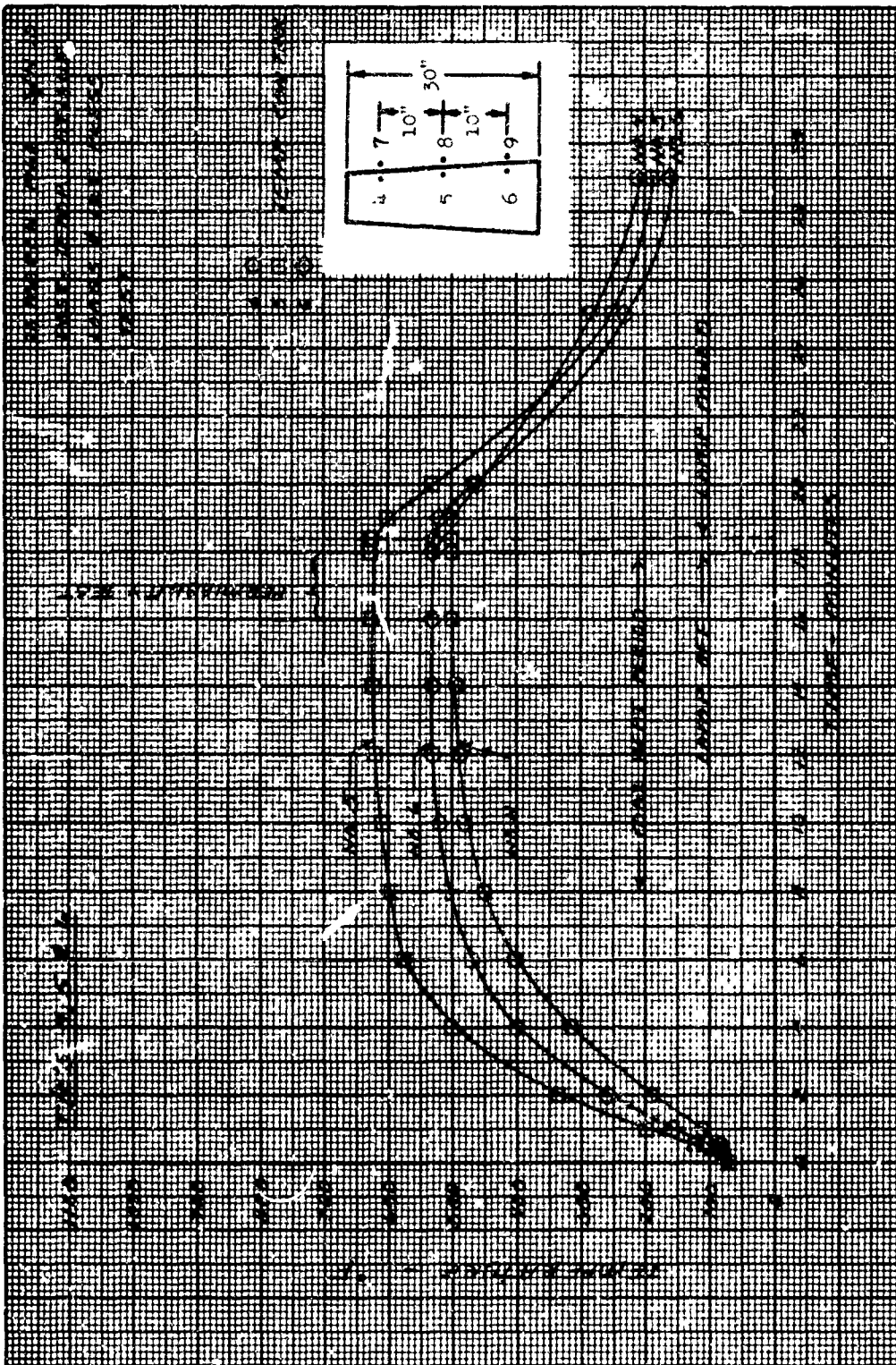
Figure 238. Temperature of Metal Fabric in Frustum S/N 10 During Test No. 8
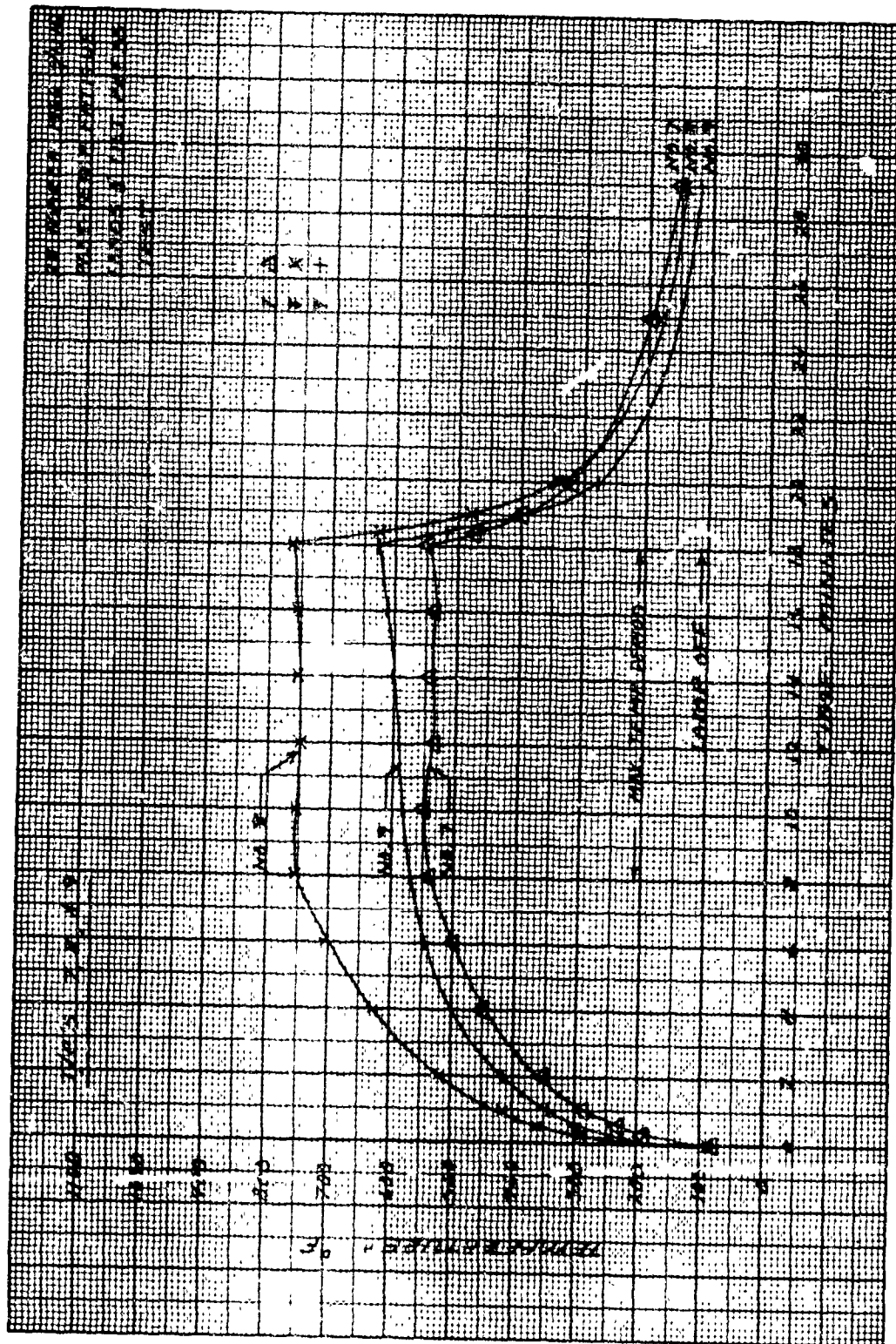
Figure 239.   Temperatures Indicated by Thermocouples Attached to Outer
Surface of Frustum S/N 10 During Test No. 8

load at a rate of one cycle per minute. The values for 100 percent limit load are 344 inch-pounds total torque, 4710 inch-pounds bending moment, and 103 pounds total shear force as established in Table XXXVI and the Frustum Test Requirement 335R-7, Appendix IV.

After ten cycles (ten minutes), the loading system was turned off and the specimen internal pressure was bled to 0 psig. During this test no evidence of buckling or leaking was noted. The appearance of the heated side of the frustum indicated some delamination of the outer coating, but no serious charring, as shown in Figure 240.

The pressurization for burst test was applied with no external loads except the usual counterweight for the upper closure. The internal pressure was increased at a constant rate of approximately 0.9 psi per second. At 70 to 75 psig, a 2-1/2-inch-diameter blister formed about one-third of the way down from the small end on the side of the specimen that had been compressed during the previous bending test. This was opposite the heated side.

Rupture of the frustum finally occurred with an extremely loud explosive report at 102 psig - the highest pressure ever obtained in the burst of a 10-inch frustum. No evidence of leaking, except for the blister, was observed even at the unusually high burst pressure. The ends of the specimen were retained by the jig clamps, and the blister remained inflated after failure as shown in Figures 241 and 242. The rupture did not occur on the heated side.

The extremely high rupture pressure obtained in this test again indicated that the two-ply welded fabric construction is capable of obtaining very high structural integrity. The continued increase in rupture strength with the tests that have been performed is attributed to improved fabrication quality as more systems were constructed. Calculation of the maximum possible theoretical strength obtainable is as follows:

Average Filament Strength: 185,000 psi

No. of filaments/yarn: 49 (dia. - 0.001 inch)

No. of yarn/inch: 58

$$185,000 \times (10^{-3})^2 \times 0.785 \times 49 \times 58 = 414 \text{ lb/in.}$$

Actual fabric strength:[*] warp = 339 lb/in., fill = 375 lb/in.

Translation: warp = $\frac{339}{414}$ = 82%, fill = $\frac{375}{414}$ = 91%

Originally predicted translation was 85%

$$\frac{339 \times 1.5}{5 \text{ inches}} = 102 \text{ psi}$$

---

[*]Based on original tensile tests, Table XXVII

335/289

335/286

335/288

Figure 240. High-Temperature Effect on Ablative Coating of Frustum S/N 10 Du.ing Test No. 8.
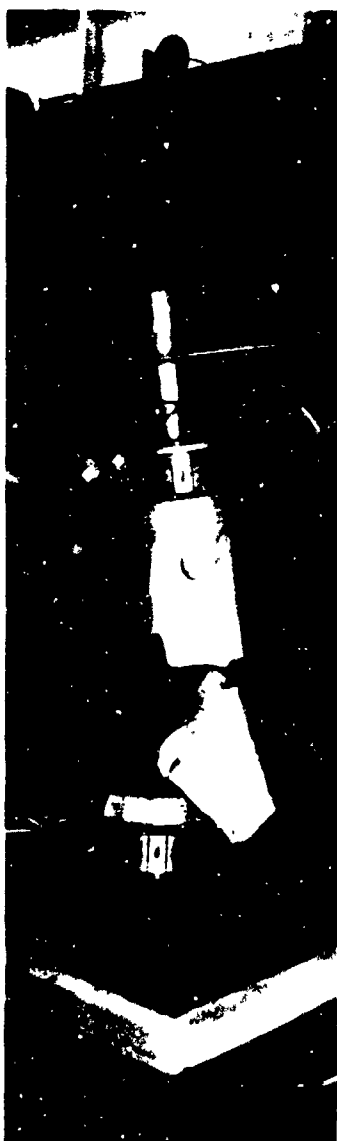
Figure 241. Appearance of Frustum S/N 10 After Bursting at 102 psig (Following Heating and Cyclic Loading in Test No. 8).

Figure 242. View of Heated Side of Frustum S/N 10 After Burst Test.

This indicates that the weld efficiency in this frustum would then have to be 100 percent and no stress concentration effects could exist. Also the factor 1.5 would have to apply for a two-ply construction rather than 1.4 as had been used in previous calculations based on the empirical load-elongation curves. Conclusions drawn from these high results are as follows:

a. It appears that this frustum, which had been autoclaved at 250 psig, may have added strength due to the rubber.

b. Biaxial or pressurization loading may give higher strength than uniaxial tensile tests as a result of:

(1) Increase in strength due to reduced slip and cutting of transverse yarns.

(2) The rubber contribution in biaxial load, which may be significant due to compressive effects.

c. This frustum was coated inside twice with extra RTV-655.

A further conclusion from this test would be that high temperatures and cyclic loading do not degrade the strength of the metal fabric structures.

3.11.4.10 FRUSTUM TEST NO. 9 (S/N 7) - PNEUMATIC BURST AT HIGH TEMPERATURE

This frustum had no simulated wing attachment flap and no built in thermocouples. This specimen was autoclaved at 250 psig along with frustums S/N 9 and 10. It was of excellent uniform construction. The purpose of this test was to determine the ultimate strength of the frustum while at high temperature without having been exposed to previous loads. The test specimen was prepared and mounted to the end closures in the usual manner.

Proof pressure and leakage tests indicated the time for pressure loss from 5.0 to 4.0 psig was 56, 58, and 59 minutes in three tests; from 10.0 to 9.0 psig the time was 25, 27 and 28 minutes; and from 35.0 to 34.0 the time was 1.0 minute (one test).

The usual type J thermocouples were attached externally to the specimen at three locations in the maximum heated area.

This specimen was pressurized at 35.0 psig to develop the same stress that would be reached in a 32-inch-diameter structure at 11.0 psig. The plastic test enclosure was purged with nitrogen to less than 1 percent oxygen and the heat lamp was turned on and preheated for 3 minutes behind the shield. The heating period commenced when the lamp was moved from behind the shield and aligned with a specimen with a 4-inch clearance. During the heating period, the internal gas pressure was maintained at 35.0 psig by bleeding off nitrogen.

Blistering of the S-6510 coating was first noted at 5 minutes of heating with thermocouple No. 8 indicating about 700°F on the surface of the specimen. The surface temperature was at 735°F at 6.1 minutes. This point was selected to start the "maximum fabric temperature." During the succeeding 8 minutes, the temperature gradually increased to 810°F maximum as shown in Figure 243.

The curve for thermocouple No. 10 shows the temperature of the nitrogen gas inside the frustum.

At 8 minutes, the internal pressure was increased at a rate of 1.4 psi per second. When the pressure reached about 55 psig, the lamp was moved behind the shield and turned off. The pressure rose from 35 to 91 psig in 40 seconds, at which point failure occurred with a loud explosive report. At the time of failure, the maximum fabric temperature was approximately 490°F.

The reason for moving the lamp behind the shield before bursting the specimen was to protect the lamp since one more heating test utilized the same lamp.

No leaks were observed before failure. It could be concluded that this is attributable to the high autoclaving pressure and excellence of the fabrication quality of this frustum. This specimen was retained on the mounting jig during failure. A view of the ruptured frustum within its inert atmosphere enclosure is shown in Figure 244. A hole was blown in the rear of the plastic enclosure by the shock wave. A closeup view of the ruptured frustum is shown in Figure 245.

The results of this test again indicated that high heat similar to that encountered in the re-entry exposure causes no significant degradation in the strength of the structure. The burst pressure of 91 psig may be compared with the 78 to 102-psig range of burst pressures experienced on other frustums.

3.11.4.11 FRUSTUM TEST NO. 10 (S/N 9) - FATIGUE LOADS AND PNEUMATIC BURST AT HIGH TEMPERATURE

The final frustum test No. 10, on frustum S/N 9, was completed after some difficulties were encountered with leaks. This frustum had no simulated wing attachment flap, but had three type J, 26 gauge thermocouples welded to the inside of the bias ply and three similar thermocouples welded on the outside of the cross ply among the stagnation (maximum heating) line. In addition, three outside thermocouples were fastened to the exterior surface in the heated zone. This frustum had been autoclaved at 250 psig along with frustums S/N 7 and 10. The construction of this frustum was not quite as high quality as some of the others (i.e., S/N 7 and 8), as it had some surface irregularities in the rubber and some fabric wrinkles.

The test specimen was prepared for mounting in the usual manner. The end closures were installed and the clamp screws torqued to the normal 100 inch-pounds preload. RTV-88 (G. E.) was used as a sealant at the large end closure.

423
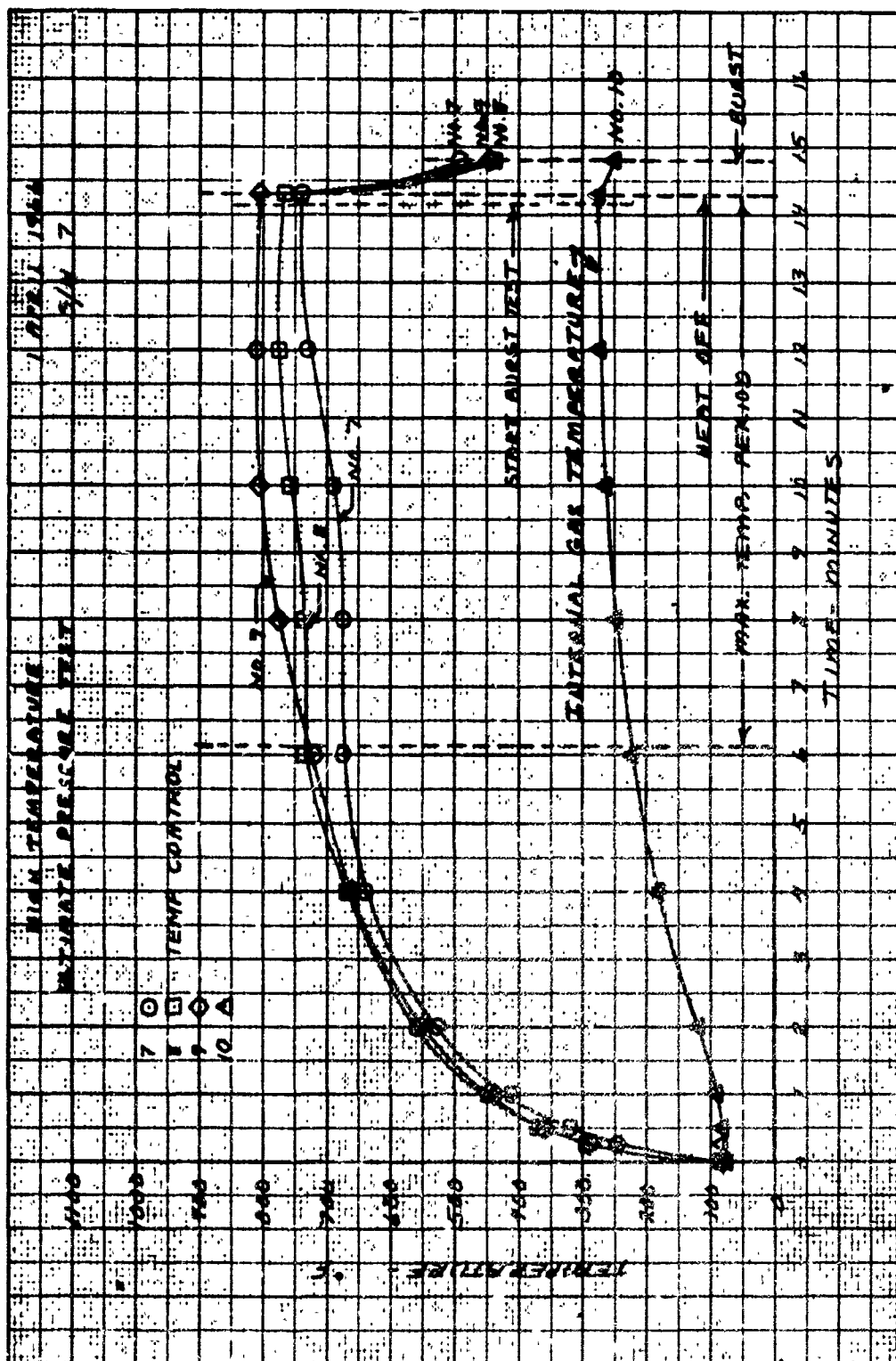
Figure 243. Surface Temperatures and Internal Gas Temperature
of Frustum S/N 7 During Heating Cycle of Test No. 9

Figure 245. Close-Up View of S/N 7 After
Rupture at 91 psig
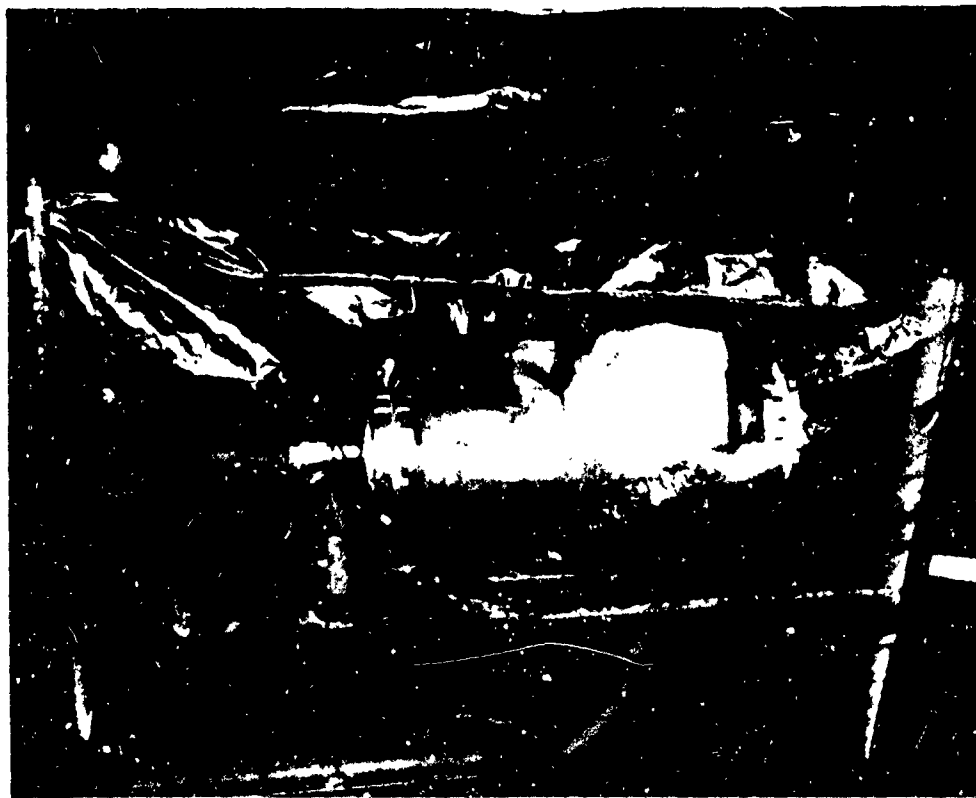
335/315

Figure 244. Frustum S/N 7 in Plastic Enclosure
After Bursing in Test 9

335/316

The first proof pressure test indicated a leak in the area of the small end cuff. Pressurizing nitrogen escaped through a small hole in the S-6510 coating at the inboard edge of the cuff and also at several points around the extreme end of the specimen underneath the clamps.

Two patching attempts were made using RTV-655 coating on the inside of this frustum. After each of these attempts, the frustum still leaked in the same areas. It appeared that the leak must have been originating at some obscure location and traveling sideways through the fabric and rubber matrix. Finally, to expedite the test without encountering further expense, a thin rubber bladder was made and installed in the frustum. This bladder was dental dam material identical to that used as a bladder for pressurizing the 7-inch x 15-inch uncoated cylinders. To protect this thin natural rubber bladder from high heat, a 1/8-inch sheet of red silicone rubber, 6-inch x 20-incn, was placed between the inside of the frustum and the rubber bladder on the heated side. This silicone rubber insulator was not fastened in place, but simply held in position by the pressurization of the inner bladder.

With this arrangement, leak testing of this frustum showed 83, 85, and 82 minutes to drop from 5.0 to 4.0 psig in three tests; 29, 28, and 28 minutes to drop from 10.0 to 9.0 psig; and 3.5 minutes to drop from 35.0 to 34.0 psig. These were the usual tests with the enclosure valved off from the main nitrogen pressurization supply.

After the leak tests, the clamp screws were re-torqued to 100 inch-pounds as some were found to be as low as 75 inch-pounds.

The loading system was identical to that previously used for combined bending, shear, and torsion loads as on test nos. 1, 5, 6, and 8.

The plastic enclosure was installed over the test space. The test space was purged of oxygen to less than 1% as verified by a gas analyzer. The heating cycle commenced when the preheated lamp was removed from behind its shield and aligned 3.5 inches from the test frustum. During the heating cycle, the internal gas pressure was maintained at 35.0 psig by bleeding off nitrogen. After heating for a few minutes, smoke began to develop in the chamber and Figure 246 shows the heating lamp in operation with smoke beginning to obscure the view.

After heating for 8.6 minutes, the control thermocouple welded to the outer cross ply in the center of the heated side of the frustum indicated a fabric temperature of 680°F as shown in Figure 247, in which thermocouple Nos. 4, 5, and 6 are those welded to the exterior ply of the fabric. Figure 248 gives additional temperature history for thermocouple Nos. 7, 8, and 9 which were fastened to the exterior of the rubber surface directly in line with the lamp. Since the heating period is to commence when the fabric temperature reaches approximately 700°F, this point at 8.6 minutes was selected to start the 10-minute fatigue loading period. At 18.6 minutes and 10 load cycles to 100 percent limit load of 1 minute each, the thermocouple indicated a fabric temperature of 775°F. The loading was discontinued but the heat lamp remained on and in place.
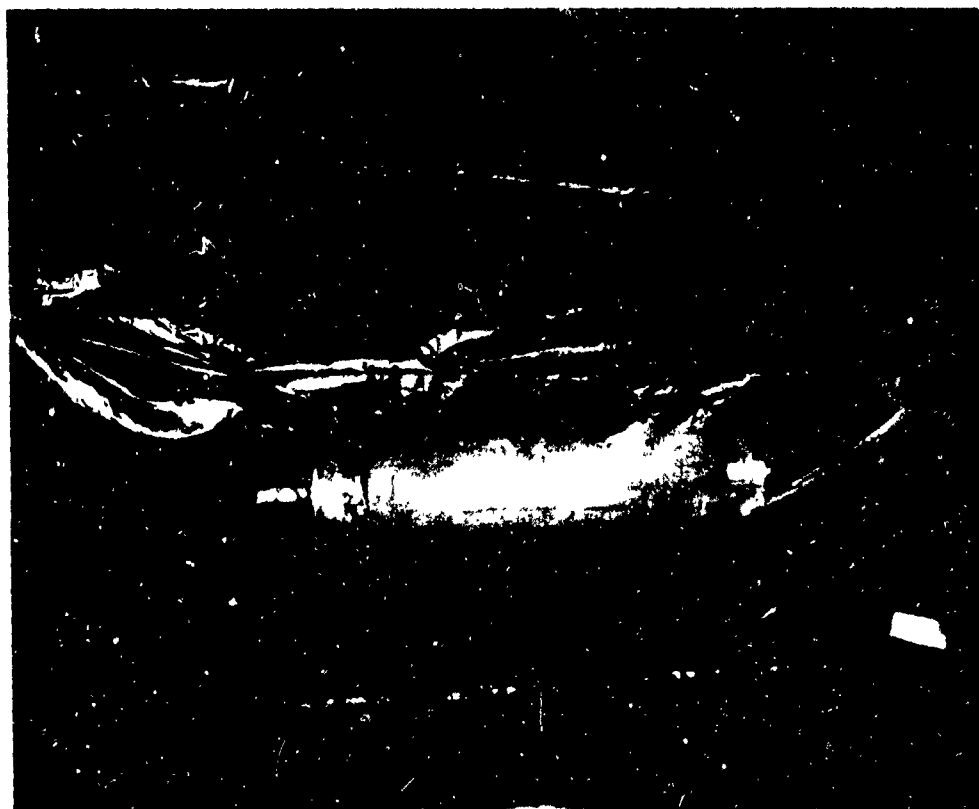
335/320

335/317
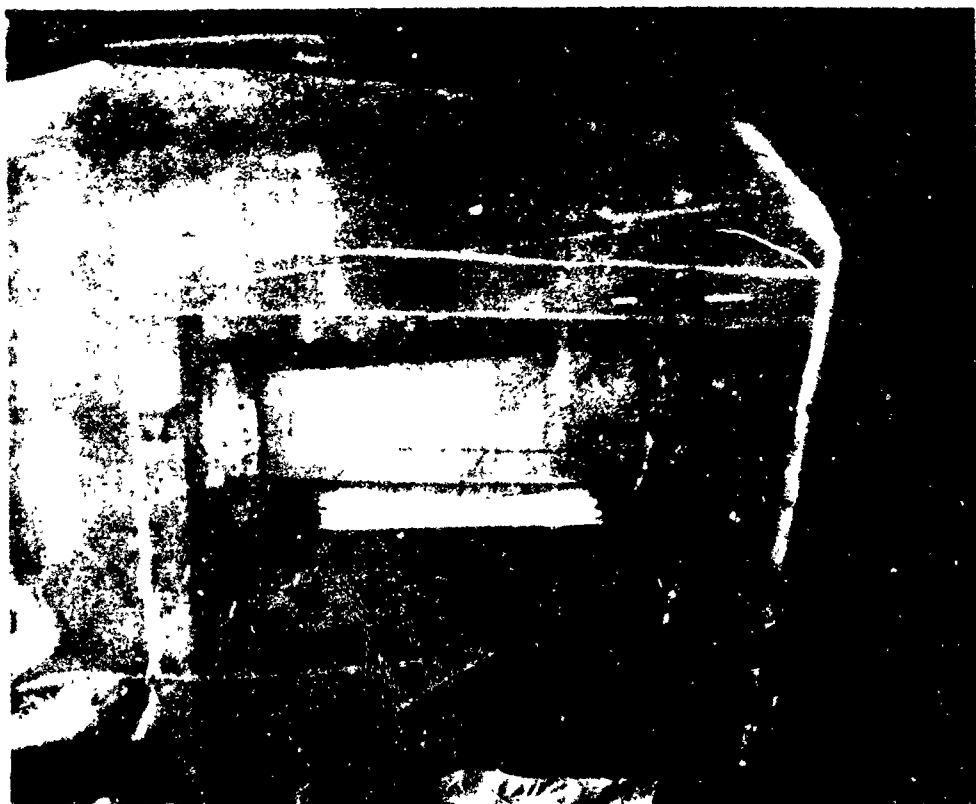
Figure 246. Frustum S/N 10 During Heating with Quartz Lamps, Showing
Development of Smoke Produced by Charring of
Ablative Surface
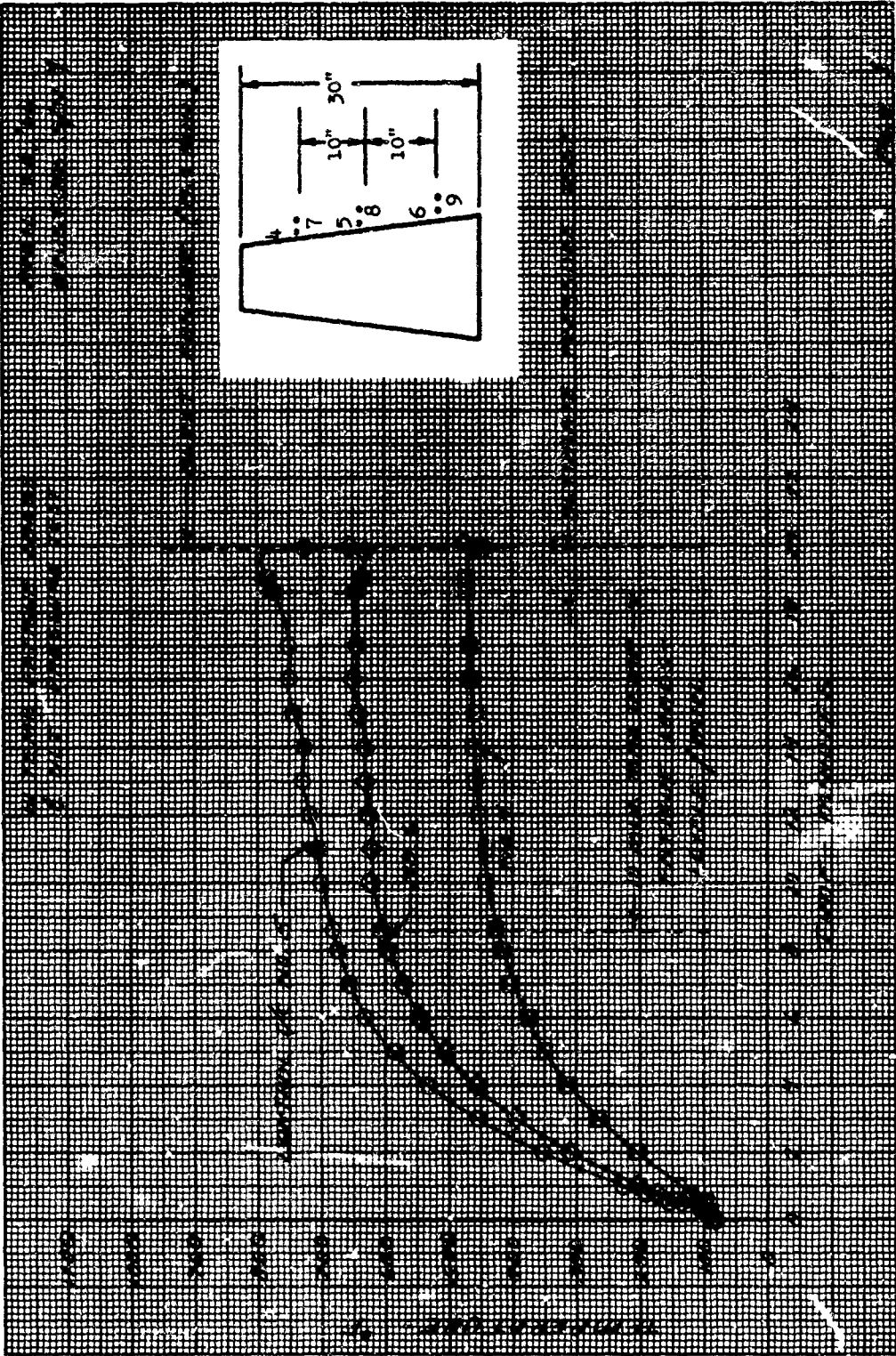
Figure 247. Metal Reinforcing Fabric Temperatures of Frustum
S/N 9 During Heating Cycle of Test No. 10
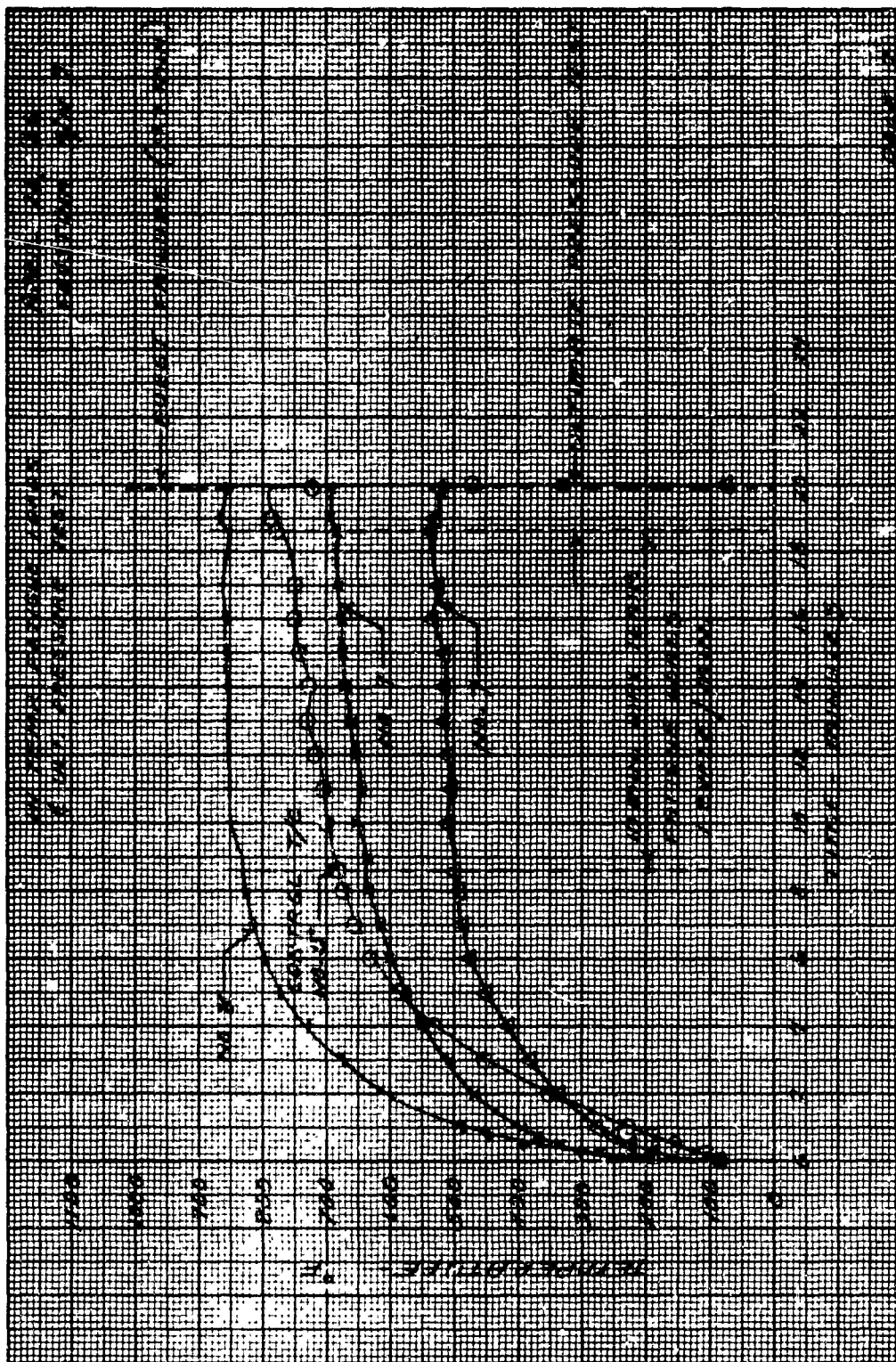
Figure 248. Surface Temperatures of Frustum S/N 9 During
Heating Cycle of Test No. 10

Internal pressure was increased at the rate of 1.2 psi per second. At 90 psig, the control thermocouple indicated a fabric temperature of approximately 790°F. Failure occurred at 19.9 minutes at an internal pressure of 97 psig. The specimen was still being heated when it failed. The shock wave from the explosion shattered the three quartz light bulbs and damaged the lamp reflector and housing as shown in Figure 249. Pieces of the charred rubber from the heated side were also spread about in the enclosure. The previous high temperature burst in test No. 9 was run after the lamp was put behind its protective shield but the lamp was allowed to remain in place for this test since no further use was contemplated for this lamp and a high fabric temperature was desired for this final test.

The appearance of the frustum after burst is shown in Figure 250. As usual, rupture occurred along an outer longitudinal seam of the cross ply but in this case the rupture extended almost from one end of the frustum to the other. The usual circumferential tearing also occurred, with the bias ply tearing along a 45 degree axis. Good adhesion between the plies was indicated, however. The vertical tube shown within the frustum is the nitrogen pressurization tube arranged so that the makeup gas is added at the top to offset the collection of hot internal gases which might affect the sealing ability of the top closure.

Figure 251 shows the overall setup of the test room with the frustum and test stand at the rear left and temperature and pressure readout instrumentation located on the bench at the right. At the extreme right is the multiple-channel hydraulic loading machine which permits the application of bending, shear, and torque loads in constant proportion to one another. The box containing the window in the foreground was used in early tests on small 7-inch cylinders and other coupons as an inert atmosphere enclosure during preliminary heating tests. At the extreme right of the picture the Team slip tables may be seen mounted to the supporting mass in preparation for supporting the base of the boom during the forthcoming tests on the large boom.

No leaks were observed in the frustum during the heating, loading, and pressurizing before failure. Heat damage to the S-6510 coating was moderate.

3.11.4.12 SUMMARY OF FRUSTUM TESTING

Neither loads nor high temperature history appeared to degrade the strength of the frustums either while at high temperature or after cooling to room temperature. Similarly folding and creasing accompanied by packaged vibration did not degrade the structural integrity. Leakage through the RTV-655 impregnated two ply metal fabric appears to be the greatest problem although some of the frustums did not leak at all. Both frustums S/N 9 and 10 presented leakage problems, apparently due to unidentifiable pin holes through the metal fabric impregnant. Frustums S/N 7, 9, and 10 were fabricated at the same time and were the first and only three frustums to have the S-6510 silicone rubber coating perforated with a pin-point roller and then autoclaved during pre-cure at 250 psig. Of these, only S/N 10 was not exposed to a vacuum inspection treatment for blisters prior to pre-curing. There is no evidence that the perforation process is responsible for the leakage problems.

430

PROJECT FIRST
ULTIMATE STRENGTH
TEST ON FRUSTUM #9
AFTER 10-0 TO 100%
LIMIT LOAD CYCLES AT
700-800° FABRIC
TEMP. BURST AT 97 PSIG
AT 790°F 790°F TEMP.

335/403

Figure 250. Close-Up View of Frustum S/N 9
After Bursting in Test 10

335/405

Figure 249. Frustum S/N 9 After Heating, Loading,
and Final Pneumatic Burst at 97 psig and 790°F
Fabric Temperature in Test 10
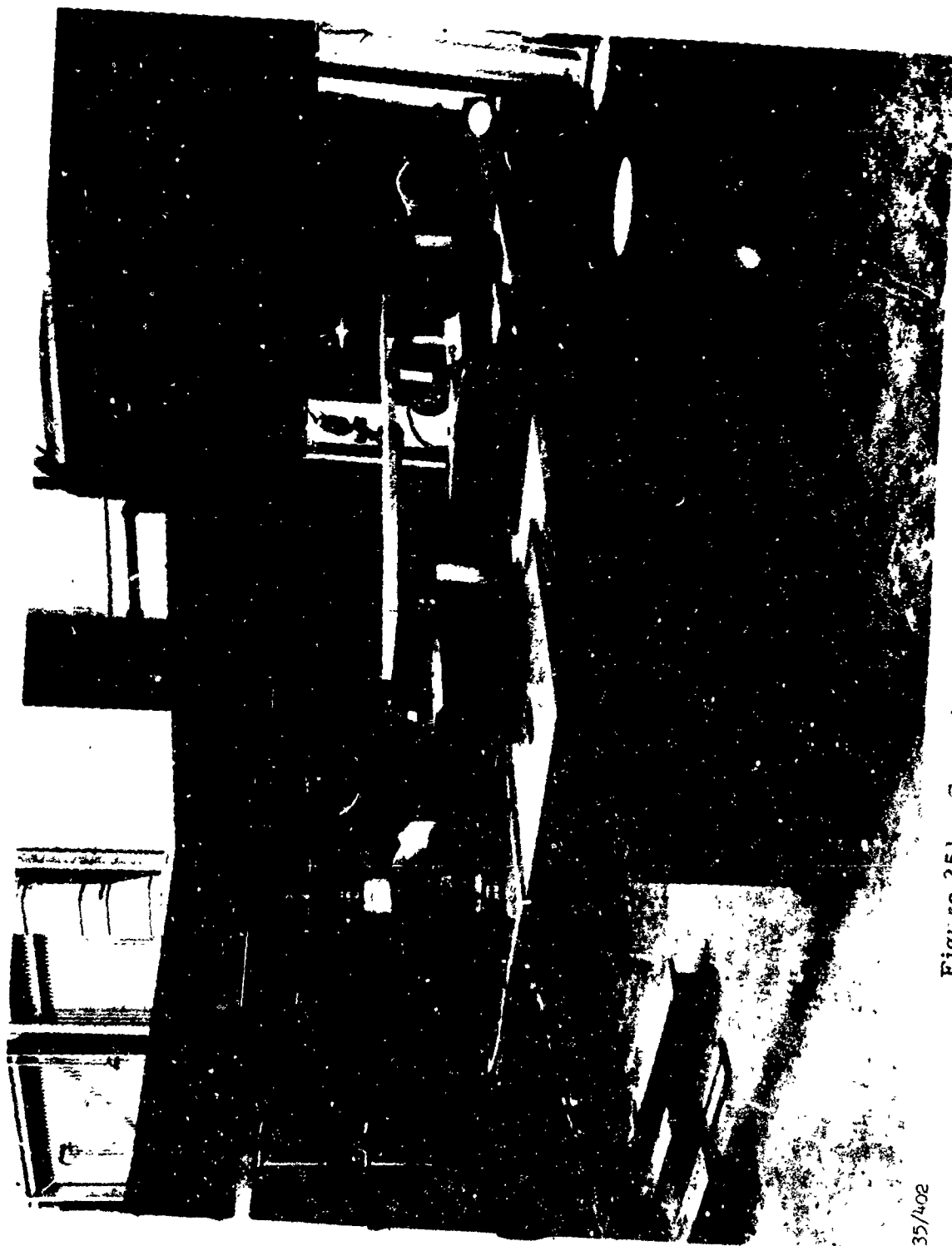
Figure 251. Expandable Structures Test Laboratory

335/402

432

Frustum S/N 8 was not perforated, but was autoclaved at 100 psig. All of the other frustums were pre-cured only in a vacuum bag while being exposed to the required temperature in an atmospheric oven. No leak problems were encountered with frustums S/N 8 and only one leak had to be repaired in frustum S/N 7.

Frustums S/N 9 and 10 had thermocouples welded to the metal fabric. Some concern has existed over the use of the type J thermocouple using a constantan copper-bearing alloy because of the possibility that this might poison the polymerization of the RTV-655 silicone rubber. Frustum S/N 8, however, also had thermocouples buried in the impregnant frustum S/N 7 had no internal thermocouples. There was no particular evidence that the leaks were predominantly in the vicinity of the thermocouples in frustums S/N 9 and 10.

Frustum S/N 7 had the most severe, potentially deleterious cure history due to the vacuum bag leaking while it was being cured along with frustums S/N 9 and 10, but S/N 7 was one of the best components fabricated.

The boom, discussed in Section 3.11.5, also had a number of very small to medium size leaks. On all frustums, as well as the boom, the fabric had been handled with white nylon gloves from the time it was cleaned to the time it was vacuum bagged for impregnation. The boom, however, required greater handling and longer exposure to atmospheric contaminants than any of the frustums, although the amount leakage per square foot of boom surface was not greater than in the case of the frustums.

Solution of the enigma that some of these structures leak and others do not remains to be solved, but one answer may be to place more emphasis on the careful handling of the fabric to maintain cleanliness even after welding. The sensitivity of the RTV-655 to poisoning, as discussed elsewhere in this report, as well as wide differences in cureability of the different lots of RTV-655, are two of the greatest deterrents to obtaining a good impregnation and a satisfactory-cure. The development of stronger, tougher liquid silicone rubber or similar high temperature compounds with less sensitivity to poisoning, would be important in this regard.

All of the frustums after testing are shown in Figure 252. All of the frustums were damaged due to destructive testing either by bursting and/or high temperature heating. Some of the frustums; such as S/N 6, had pieces cut out after the component test for further evaluation of heating lamps, etc. Thermocouple wires may be seen still attached to some of the frustums. The simulated wing attachment flap may be seen on frustums S/N 1, 2, 3, and 10. The scorch area due to high temperature testing may be noted on S/N 4, 5, 7, and 10. All of these frustums were 30 inches long by 10 inches in diameter at the large end tapering to 7 inches in diameter at the small end.

A log of fabrication and test dates, test information and results and pertinent remarks for each of the frustum tests is presented in Table XXXVIII.

335/490

Figure 252. Silicone Rubber Impregnated and Coated Two-Ply Metal
Fabric Frustums After Destructive Testing

431

Table XXXVIII

FABRICATION AND TESTING INFORMATION

Test No.	Serial No.	Date Welded	Date Impregnated	Date Cured	Date Post-Cured	Test Date	Test Information and Results	Remarks
P-1	P-1	11/3/65	11/5/65	11/10/65	11/11/65	12/16/65	**Pressure Burst Test.** Burst at 78 psi on cross ply seam on large end of fracture. Leak detected at range of 25 to 29 psi.	Plies run metal fabric.
1	1	12/27/65	12/27/65	12/30/65	1/2/66	1/13/66	**Static Proof Loads Test at Room Temperature.** Combined loads to 100% of design limit at 35 psi internal pressure in-creased to 150% of limit loads before buckling oc-curred. Proceeded to 400%, reduced back to zero, then up to 150% (wrinkle/buckle started. Repeated loading produced set in fabric.	Production run metal fabric (as in all subsequent components). No thermocouples in specimen.
2	3	1/7/66	1/10/66	1/11/66	1/13/66	1/18/66	**Pressure Burst Test.** Re-peat test as on P-1. Blister 2" dia. noted near flap at 50 psi. Depressur-ized punctured blister. Re-pressurized to burst at 78 psi. Burst on cross ply seam at large end.	No thermocouples.
3	2	1/6/66	1/6/66	1/10/66	1/18/66	1/20/66	**Proof Pressure and Burst Test.** Run combined loads to 100% of design limit loads at 35 psi, then pressure burst (no static load) at 84 psig.	No thermocouples. Fabric wrinkled during fabrication prior to testing.
4	6	1/25/66	1/26/66	1/28/66	1/31/66	2/9/66	**Packaging and Package Vibra-tion + Pressure Burst Test.** No heat. Leakage rate very low. Folded fracture approx. 1345-1/2x1-1/2. Vibrated specimen. Unfolded. Repress to 35 psi and leak devel-oped at fold line. RTV-655 applied. Pressure burst test at 66 psig. Noted leak-age prior to burst.	No Flap. No Thermocouples.

435

Table XXVIII (Continued)

FABRICATION AND TESTING INFORMATION

Test No.	Serial No.	Date Welded	Date Impregnated	Date Cured	Date Post-Cured	Test Date	Test Information and Results	Remarks
5	8	1/27/66	2/11/66	2/12/66	2/23/66	3/1/66	**High Temp Loads Test.** Pressure check OK. Radiant heat, 6 min. temp stabilized at 970°F, 17 min. fabric temp was 550°F. Specimen loaded at 11.3 min. to 250% of design limit load. Proceeded to 400%, then down to 100%. After cooling evidence of buckling at small end near cuff.	6 thermocouples welded, 1st autoclaved unit. No flap. Small leaks at small cuff.
6	4	1/17/66	1/18/66	1/20/66	1/21/66	3/8/66	**Post Temp Ultimate Loads.** Temperature cycle to 900°F on outside skin. Exposed to pre-heated lamps for 15 min. 5 min. to stabilize. Post temp. combined loads showed (35 psi internal pressure) buckling at 117% and pronounced at 250%.	5 thermocouples outside only. Fabrication quality and appearance excellent. No leaks.
7	5	1/25/66	1/20/	1/28/66	1/31/66	3/14/66	**Post Temp Burst Test.** Preliminary pressure test showed leakage. Then 6" dia. blister formed. RTV-655 applied to internal surface to stop leak. No-bonded blister. No leaks. Tested to 890°F 10 min. burst test at 85 psig.	3 thermocouples contacting metal fabric. 3 thermocouples outside. No flap.
8	10	2/1/66	3/3/66	3/8/66	3/12/66	3/18 - 3/29/66	**Post-Temp. Fatigue Loads & Pressure Burst Test After Cooling.** First pressure test showed leakage. After RTV coating, specimen did not leak. Max. fabric temp. reached 625°F. After cooling, 10-100% limit load cycles applied. Burst pressure 102 psig.	3 thermocouples welded to fabric and 3 on outside (wrong side). Autoclaved at 250 psig. Leak seal. One.
9	7	1/25/66	3/3/66	3/8/66	3/10/66	3/29 - 4/1/66	**Pressure Burst at High Temp.** Heated surface 755 to 810°F for 8 min. Burst at 91 psig with outside temp. 440°F.	3 thermocouples external. No flap. Autoclaved at 250 psig. No leak prior to burst.
10	9	2/1/66	3/3/65	3/8/66	3/10/66	4/28/66	**Fatigue Loads & Pressure Burst at High Temp.** Leaked and repaired 3 times, rubber liner installed to stop leaks. Burst at 97 psig at 900°F after 10 min. exceeding 690°F fabric temp. and 10 high temp. 100% limit load cycles.	6 thermocouples welded to fabric. No flap. Autoclaved at 250 psig. Leak problems.

3.11.5 TESTING OF THE FULL-SCALE PARAGLIDER BOOM

3.11.5.1 BOOM TEST PREPARATION AND PLANNING

The test specimen is a full scale left side, leading edge boom (SGC drawing number 1109452). It is made of production run multifilament metal fabric in two plies arranged in 45-degree bias relationship. The open end was formed by folding both plies back over a Teflon coated 0.072-inch-diameter steel wire ring and the fabric was spot welded as described in Section 3.10.1. 2.3. Two reinforcing cuffs, 4 and 6 inches long, were placed over the 32-inch-diameter end of the boom with the smaller cuff outside. These cuffs were welded with short longitudinal welds to make them complete rings of fabric, but they were not welded to each other or to the parent fabric of the boom. They are, however, held in place by the silicone rubber impregnation and coating.

The total weight of the boom was 101 pounds. The final dimensions of the boom were:

Inside (large end) diameter	31.4 in.
Inside (small end) diameter at point of tangency with end cap	12.6 in.
Length from large end to point of end cap tangency	17 ft-4 in.

The above dimensions were taken at the working pressure of 11 psig, and the fabric and rubber thickness subtracted to obtain inside measurements. As will be shown by subsequent data, the dimensions of the boom did not significantly change with pressurization.

The holding ring fixture for the large end of the boom had 48 small 2-1/2 inch x 2-1/8 inch aluminum clamps that were radially bolted to the holding ring to bear down on the protective cuff of the boom, the boom being retained by the wire ring within the fabric.

The lamp frame structure supporting the heating lamps for the high temperature boom test was suspended from an overhead structure. The high temperature lamps were connected in a series parallel arrangement to the 480-volt, 200-ampere, 3-phase electrical service.

The boom flap loading, to be performed during static loads test, simulates re-entry wing loads and air loads on the boom itself on the full scale paraglider. The resultant of the combined loads was a force of 340 pounds to be applied along the flap through spaced steel grommets using a load distribution fixture or "whiffle tree". The whiffle tree was proof loaded to 400 percent of the static limit load of 340 pounds. Experiments on techniques for installing the grommets in the wing flap attachment were performed to assure that loading cables would not pull out. A typical coupon of actual coated fabric material is shown in Figure 253.
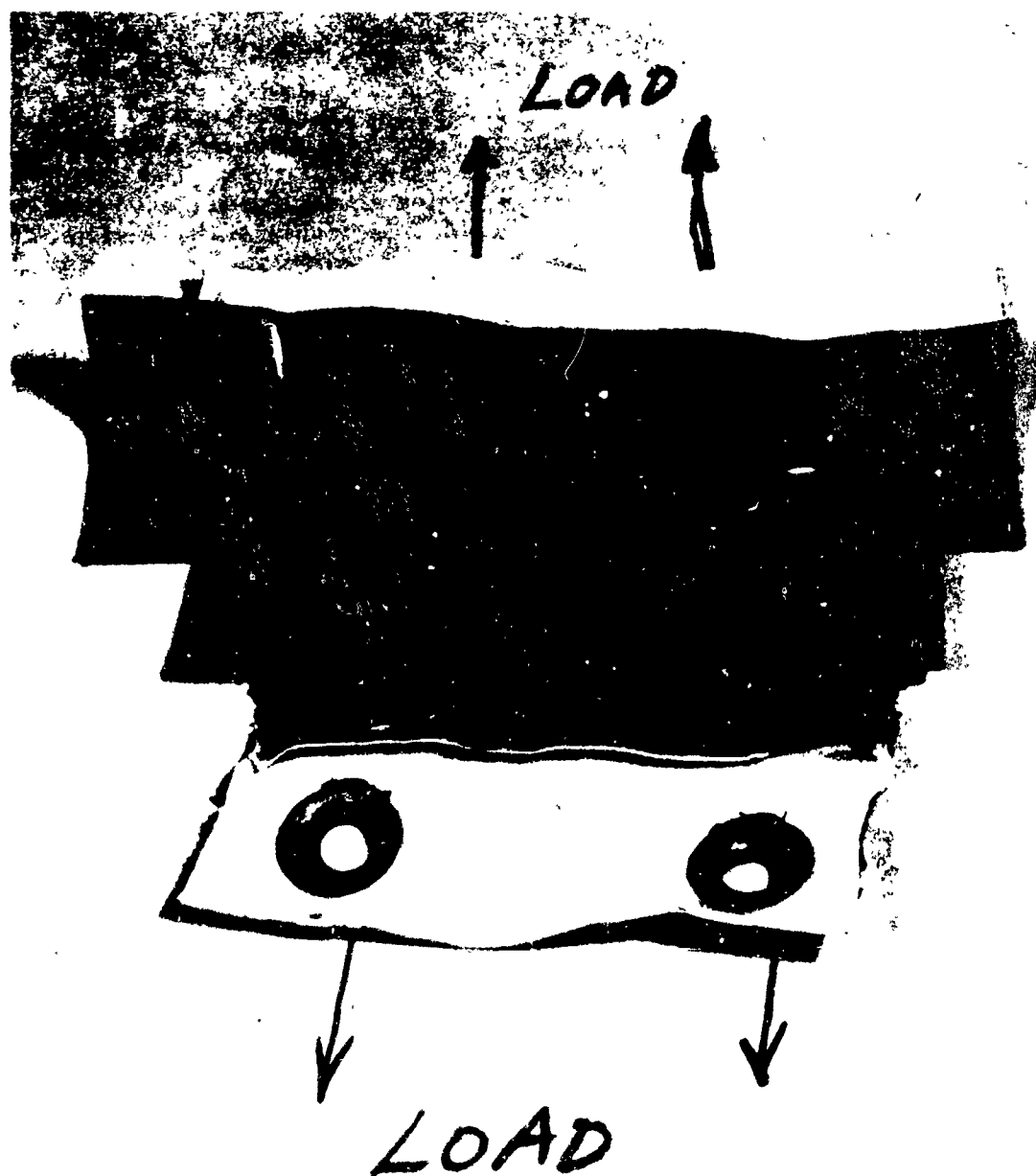
335/479

Figure 253. Typical Impregnated and Coated Metal Fabric Specimen
Used for Development of Load Attachment
Techniques for Boom Testing

The test plan for the complete room temperature and high temperature testing on the boom is presented in Appendix X of this report.

The re-entry paraglider boom static test loads to be used were based on the aerodynamic loads presented in Section 3.2 (also see Appendix VIII). The boom was mounted "upside-down" and the test load of 340 pounds was applied downward on the boom flap at an angle of 17 degrees from the vertical and raked aft at an angle of 8 degrees 22 minutes as shown in Figure 3 of the Test Plan, Appendix X.

The resonant vibration test on the boom was accomplished by vibrating the cantilevered specimen at the vertical plate of the supporting fixture. This plate was supported on four vertically mounted Team tables which may be seen at the left in the photograph of the test laboratory, Figure 251. These tables were enclosed, hydraulically operated slip plates which restricted all lateral and transverse movement, and allowed vertical vibration motion only.

To determine the boom assembly resonant vibration criteria, a preliminary examination of the frequency spectrum was made. Data from NASA SP-23 were used for this portion of the survey. Buffet wake frequencies from 0 to 240 cps were indicated for bluff body configurations. This is appropriate for this application because, at an angle of attack of 70 degrees, a bluff body is presented to the flow.

The magnitude of the oscillation was estimated from experimental data contained in the NASA documents that were reviewed. Using an incremental root mean square pressure coefficient ($C_{P_{rms}}$) from NASA TM X646, an estimate was made of the magnitude of the oscillation of a buffet wake. This magnitude was compared to the maximum pressure coefficient attainable hypersonically. This ratio indicated that a magnitude of 5 to 10% of the total load on the vehicle should be used.

As a result of this analysis, a frequency range of 0 to 250 cps with a magnitude of $\pm$ 10% of the vehicle load was used for testing the paraglider boom.

3.11.5.2 PRESSURE PROOF TESTS AND DIMENSIONAL MEASUREMENTS

Preliminary proof pressure and leak testing of the boom is described in Section 3.10.6.4 of this report. Due to the small leaks found, the boom was demounted from the closure and the interior was recoated with RTV-655 as described in that section.

These tests were in accordance with paragraph 3.3 of the Test Plan in Appendix X. The boom was mounted on the holding fixture and cantilevered from the supporting mass as shown in Figure 254. In this photograph, the heat lamps may be seen suspended overhead. Also small white tabs may be seen affixed to the top and bottom of the boom and a mechanic's scale is lined up with the end of the boom. These were measurement points for determining deflection and diametrical growth characteristics during initial pressurization. The mounting plate and slippery tables were held in fixed position by two wood supports as

439
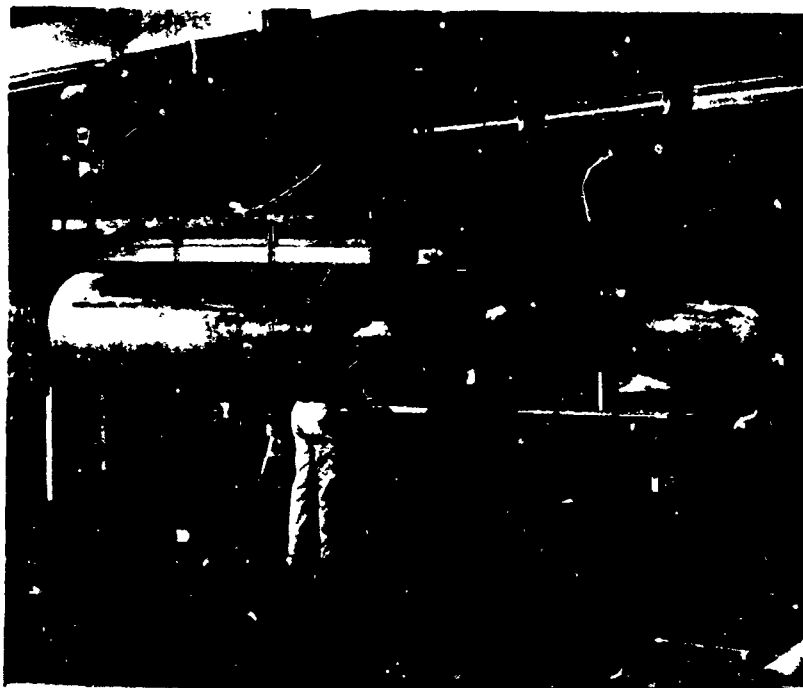
335/471

Figure 254.   Boom Inflated and Mounted on Supporting Fixture
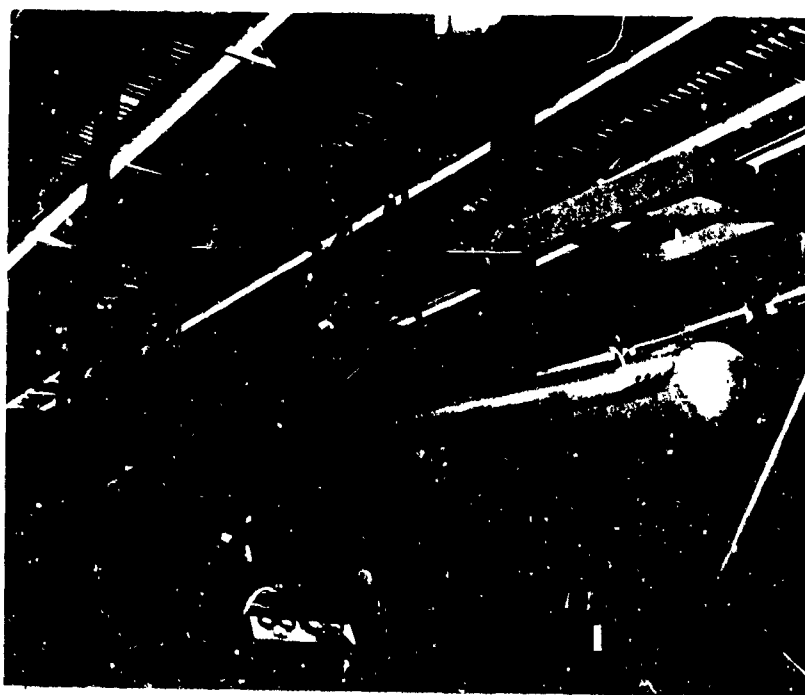
335/469

Figure 255.   View of Boom Inflated and Cantilevered from Supporting
Fixture, with Heat Lamps in Position

shown at the left side of the photograph. Another view of the boom from a low angle, showing the heat lamps more clearly, is shown in Figure 255.

During pressurization, a K&E Paragon tilting level with optical micrometer and a 15-foot vertical tooling bar, with accuracy to 0.001 inch, were used for vertical measurements and a K&E transit was used for horizontal deflection measurements. This instrumentation is shown in Figure 256.

Deflection readings were taken at 2.0-psi pressure increments from 1.0 to 11.0 psig, and final readings were taken after depressurization to 3.0 psig. The results of reducing the test data are shown in Table XXXIX. Diameter measurements 1-2 were at a location 50 inches from the base of the boom, 3-4 at 100 inches, 5-6 at 150 inches, and 7-8 at 200 inches or 8 inches from the point of tangency of the end cap. Deflection measurements 9 and 10 are in the vertical and horizontal directions, respectively, at the tip of the end cap.

After the deflection measurements were complete, the boom was inflated to 5.0 psig and the internal pressurization gas supply was shut off. The time required for the boom pressure to drop from 5.0 to 4.0 psig was 25.8 minutes, which is a low rate of leakage when compared to the leakage rate of the frustums. The volume of the boom is about 48 cubic feet while the volume of a frustum is about 1 cubic foot and the boom has 104 square feet to the frustum's 5.55 square feet. Therefore it would be reasonable to expect that the time required for the boom pressure to drop 1 psi from a given pressure would be about 2/5 of the time required for frustum pressure to drop the same amount at the same temperature. An analysis of the leakage rates is presented in Section 3.11.7.

3.11.5.3 BOOM PACKAGING AND VIBRATION TEST

Testing of the boom by folding into the smallest possible package, followed by vibration exposure simulating (Saturn V) launch environment, followed by unfolding and re-inflating for leak testing, was performed in accordance with paragraph 3.4 of the Test Plan in Appendix X.

The boom was laid out on the floor with the imbedded thermocouple wires and most of the thick S-6510 coating on the top surface. This would place the longitudinal seams of the bias and cross plies in the flat upper and lower surfaces rather than at the creased edges.

The boom was rolled up by first flattening and folding back the hemispherical end cap and then rolling from that end as shown in Figure 257. Although the wire ring in the large end of the boom was Teflon-coated to permit pulling it out, it appeared flexible enough not to interfere with the packaging so that it was not removed, but was bent at the folds to a radius of approximately 3/8 inch. The rolled boom was secured with canvas straps as shown in Figure 258. Due to rolling from the small end, the ends of the rolled boom had conically shaped void areas. Several reasons for packaging the boom in this way are as follows:

441

335/472

Figure 256. Optical Instrumentation Used to Measure Boom Dimensional
Changes at a Safe Distance During Initial Inflation

442

Table XXXIX

DIMENSIONAL MEASUREMENTS OF BOOM DURING INITIAL PRESSURIZATION

Pressure (psig)	Boom Diameters[a] (in.)				Tip Deflection[b] (in.)	
	1-2	3-4	5-6	7-8	9 (Vert.)	10 (Hor.)
1.0	27.19	22.44	18.33	13.63	0	0
2.0[c]	27.23	22.50	18.37	13.73	2-1/16	3/8
3.0	27.26	22.53	18.40	13.73	2-1/4	3/8
5.0	27.28	22.57	18.42	13.71	3	9/16
7.0	27.31	22.57	18.42	13.73	3-1/4	5/8
9.0	27.31	22.62	18.45	13.77	3-1/4	11/16
11.0	27.35	22.58	18.40	13.68	3-7/16	3/4
3.0	27.27	22.56	18.40	13.73	2	9/16

(a) Corrected for 0.50" paper marker height

(b) Relative to 1.0 psig position

(c) Measured on previous day
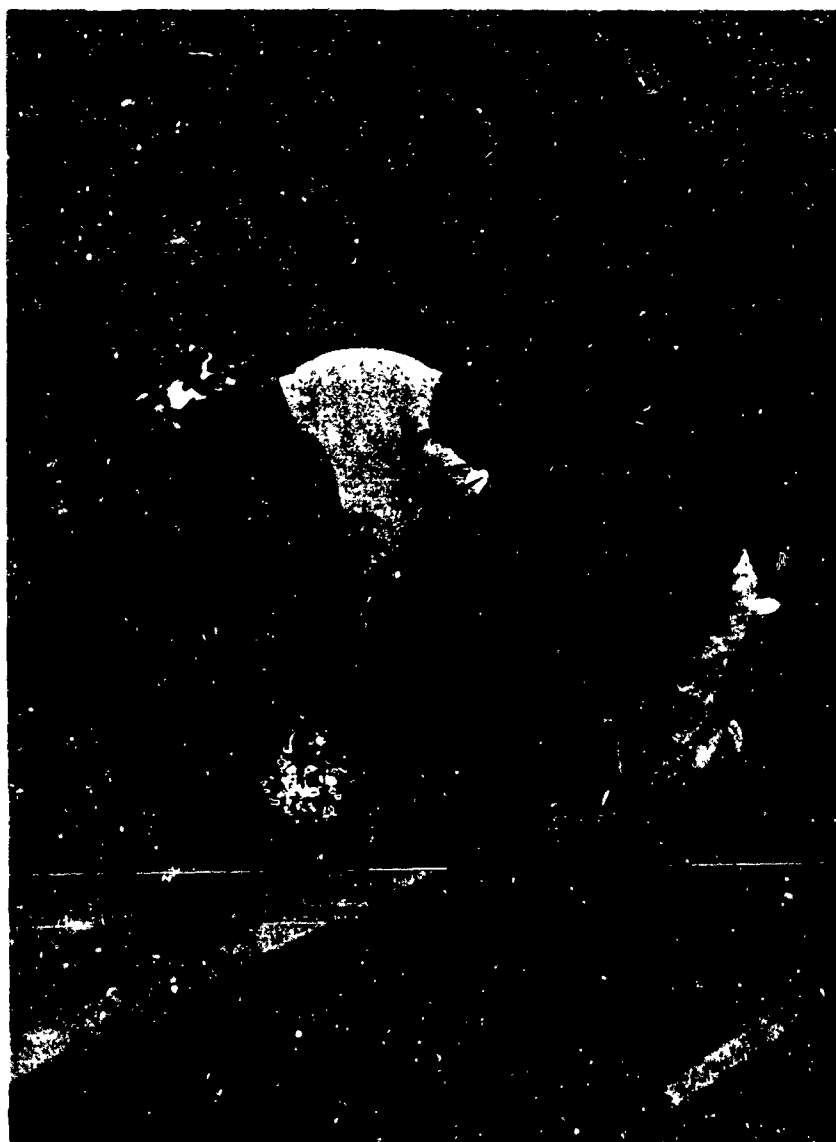
335/456

Figure 257. Rolling Boom for Packaging Test

335/458

Figure 258. Boom Rolled and Ready to be Packaged in Canister for Vibration Tests (Weight 101 pounds)

445

a.   In the case of an actual paraglider vehicle, the booms would probably be folded back against themselves and laid flat against the rigid crew canister in the center keel. This would be a less drastic folding test than the one actually performed.

b.   If the booms of an actual paraglider were to be compactly rolled or folded, the process would have to start at the small end.

c.   Rolling is preferred to zig-zag or accordion folding because less complex creasing occurs, especially in large end of the boom where the greatest stress occurs.

d.   During inflation in space, the boom would probably deploy just as satisfactorily if rolled as for any other technique of packaging.
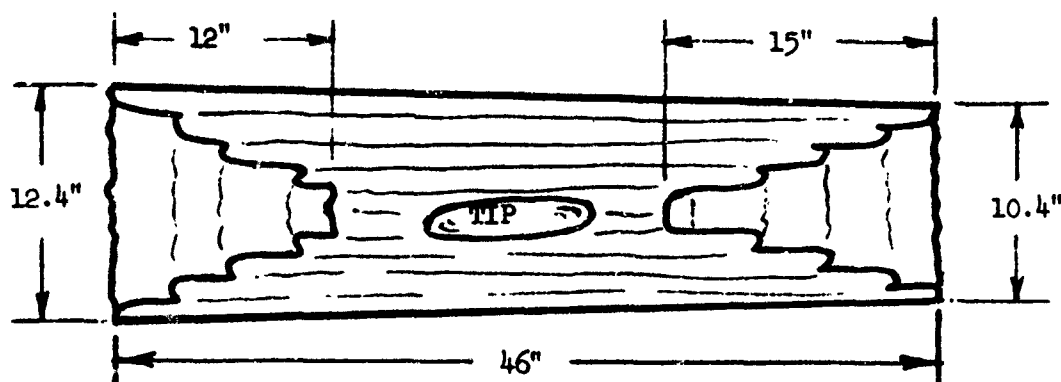
Figure 259.   Schematic of Cross-Section of Rolled Boom Showing
Dimensions.   (Approximate Volume 2.35
Cubic Feet)

The actual dimensions of the rolled boom are shown in Figure 259. The volume occupied by the rolled boom is 2.35 cubic feet. The inflated boom is 48.25 cubic feet. Therefore the packaging ratio relative to inflated volume is 20.5. The volume of the actual material in the boom is 0.76 cubic foot. The packaging ratio relative to material volume is therefore 3.1. The packaging ratio for a frustum (30 inches long x 10 inches in diameter tapering to 7 inches in diameter) was 12.7 relative to inflated volume and 2.0 relative to material.

The rolled boom was wrapped with 1 to 3 layers of quilted packing paper as shown in Figure 260 to produce a cylindrical shape. This covering was held in place with glass-fiber tape. The boom was then placed within a

446

Figure 260.   Wrapping Boom with Quilted Paper to Prevent Chaffing During
Packaged Vibration Test

Figure 262.   Protecting Ends of Rolled Boom in Canister with
Polyurethane Foam

Figure 261.   Boom Being Placed in 14 x 48 Inch Metal Canister

447

14-inch ID x 48-inch-long galvanized sheet metal container as shown in Figure 261. Polyurethane foam was used to fill the conical voids and to protect the ends of the boom from being abraided against the ends of the container as shown in Figure 262.

The package vibration test was conducted at Component Evaluation Laboratory, El Monte, California, a few miles from Space-General. Details of this test are described in the CEL report No. 4727 presented in Appendix XI. A photograph of the boom in its container mounted on the MBC-210 shaker is included in the CEL report. The packaging end of the boom was tied to the shaker table by an 18-inch-long 4-inch-steel channel and two 5/8-inch-diameter tie rods. Sweeping at 3 octaves per minute, the sinusoidal input was held at 0.154-inch double amplitude from 5 to 18 cps, and 2.69 g from 18.5 to 100 cps.

Initially an electronic problem in the vibration equipment resulted in an erratic wave shape with some shocks of unknown magnitude being applied to the specimen.

The day after the vibration test, the boom was removed from its container and unwrapped. It showed no apparent damage on unrolling as shown in Figures 263 and 264, although the creases were visible on the inside of the boom as may be seen in Figure 265. An electrical continuity check, however, of the thermocouple wires showed thermocouple numbers 1 and 3 to be open circuits, apparently having been broken in folding or vibrating.

At this time, only the leaking areas noted and marked on the boom during the earlier pressure tests were sealed on the inside of the boom by painting localized areas with RTV-655. The sealant was allowed to cure over the weekend.

After remounting the boom on the test fixture and inflating, the leak rate from 5.0 to 4.0 psig was found to be 5.7 minutes and from 11.0 to 10.0 psig was 3.2 minutes. It was concluded that the increased leak rate indicates that additional leaks had developed due to packaging and vibrating, but the leaks were not considered serious enough to interfere with future testing.

3.11.5.4 BOOM STATIC LIMIT LOADS TEST

The boom remained mounted and inflated after the last leak test, reported in Section 3.11.5.3. Small aluminum discs were attached to the deflection measurement points with RTV-731 and F-88 as shown in Figure 266. The deflection of points 1-4 were measured with dial gauges while the deflection of points 5-16 were measured with an extensometer transducer as shown in Figure 267.

The boom pressure was established at 11.0 psig and the recorder channels were zeroed. The loads were applied as shown schematically in Figure 268. Concrete weights were stacked on the ram mounting brackets or the floor to react the loads.

335/443

Figure 263.   Unrolling Boom After Packaged Test

444

335/444

Figure 264.   Appearance of Boom After Unrolling, Following Packaging
and Vibration Tests

335/446

Figure 265.   Interior Appearance of Boom After Packaged Tests

450

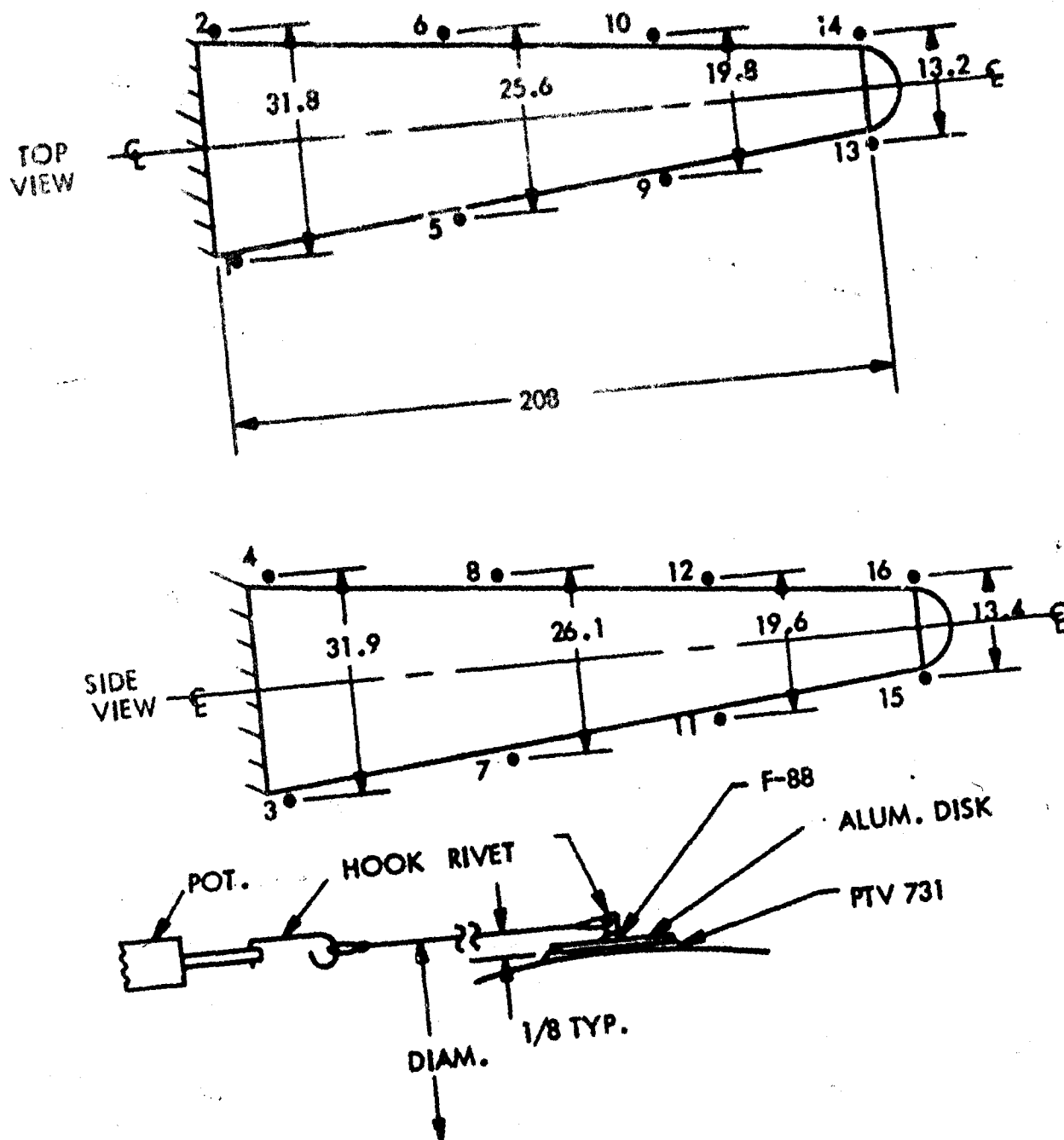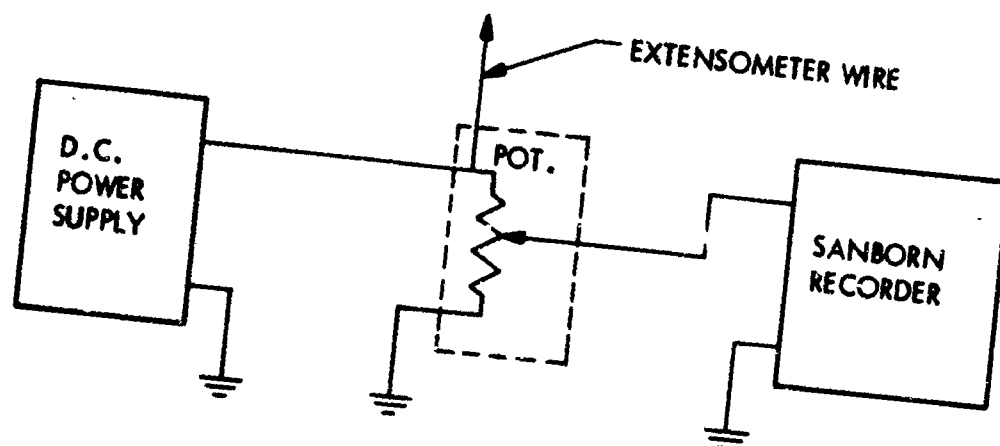Figure 266. Boom Deflection Instrumentation Points for Static Limit Loads Test

INSTRUMENTATION SCHEMATIC:

PNEUMATIC SYSTEM:
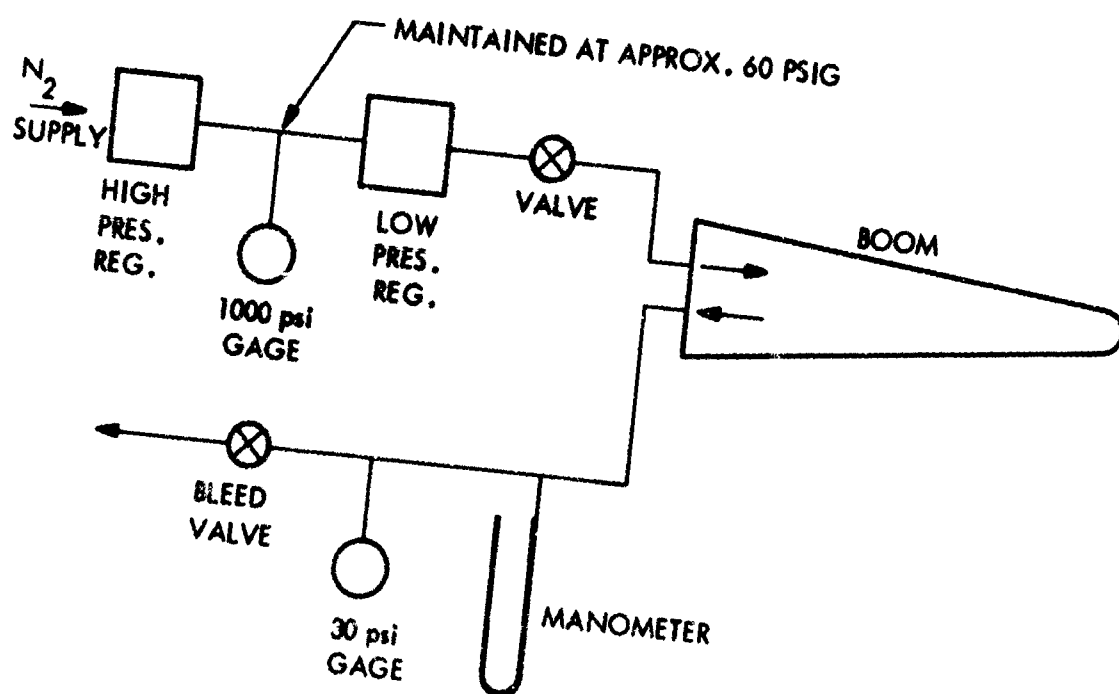
Figure 267. Boom Load Test, Instrumentation and Pneumatic System Set-Up

452
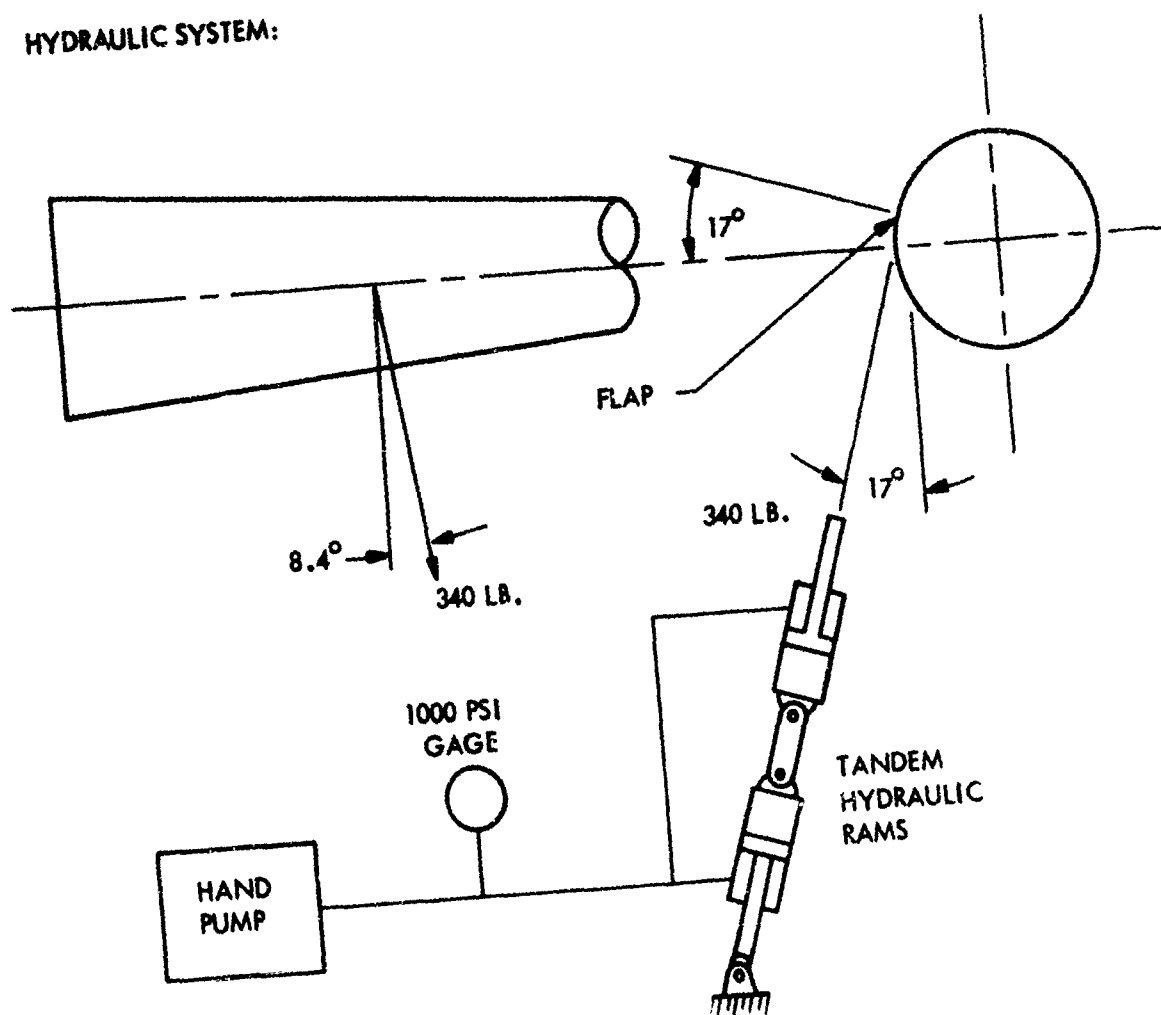
HYDRAULIC SYSTEM:

100% LIMIT LOADS:
(AT SUPPORTED END OF BOOM)

TORSION MOMENT   = 3,760 IN-LB
BENDING MOMENT = 42,183 IN-LB
SHEAR FORCE   = 340 LB

Figure 268.   Boom Load Test, Hydraulic System

453

The combined limit load was raised to the 100 percent values listed in Figure 268 and then lowered to zero percent in 20% increments. Deflection data were taken at each increment. Figure 269a graphically presents the deflections at three points: 68 inches from the mounted end, 138 inches from the mounted end, and at the end cap tangency point (208 inches from the mounted end). These locations are shown in Figure 266.

The curves in Figure 269a show the hysteresis effect or set in the boom as the loads were reduced to zero from 100%. Figure 269b is a cross plot of Figure 269a and presents a curve for the deflections at 100% load, 40% load, and the residual hysteresis set in the boom at zero load, as a function of the distance along the boom from the mounting fixture. The maximum deflection of the boom was 6.8 inches at the point of tangency of the end cap or 208 from the mounting fixture. The boom is shown at maximum deflection in Figure 270. No evidence of incipient buckling or any other form of structural failure was observed.

The four dial gauges, measuring in thousandths of an inch, at deflection points 1-4, showed no deflection during the entire test.

3.11.5.5 VIBRATION TESTING OF THE BOOM AT ROOM TEMPERATURE

The vibration test equipment was set up as schematically shown in Figure 271a in which the hydraulic system for the vertical slip tables described in Section 3.11.5.1 is shown, and the actuator system for the vibration of the boom is also shown. Figure 271b presents a schematic of the instrumentation and control system which was used.

Piezo accelerometers were mounted on the specimen as shown in Figure 272. The complete vibration instrumentation system was calibrated at 1.0 and 10.0 g from 2.0 to 250 cps with an electromagnetic shaker prior to mounting the accelerometers on the specimen.

All vibration test runs were made with the boom pressurized to 11.0 psig with nitrogen.

The fundamental natural frequency of the boom was found to be approximately 3-4 cps by manual excitation of the specimen at its free tip. A model survey was made in the frequency range of 2 to 250 cps with inputs of 0.1 g below 10 cps and 0.25 g above 10 cps. Apparent resonances were indicated by peak crystal outputs at the following frequencies:

3.6 cps	81. cps
16. cps	96. cps
37. cps	139. cps
60. cps	156. cps
64. cps	224. cps
70. cps	

The elapsed time to discover these apparent resonance points was 30 minutes.
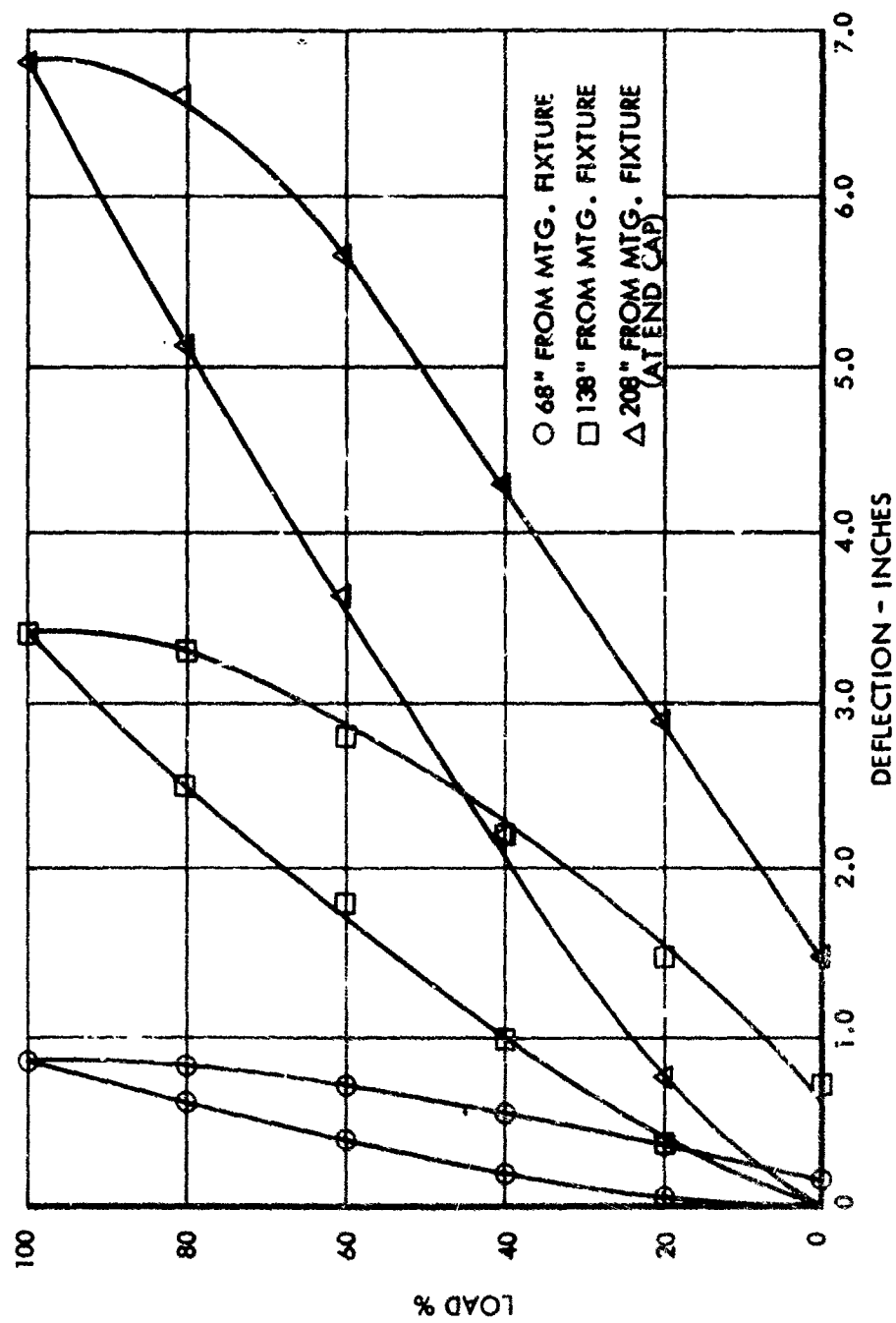
Figure 269a. Boom Deflection During Static Loads Test

455
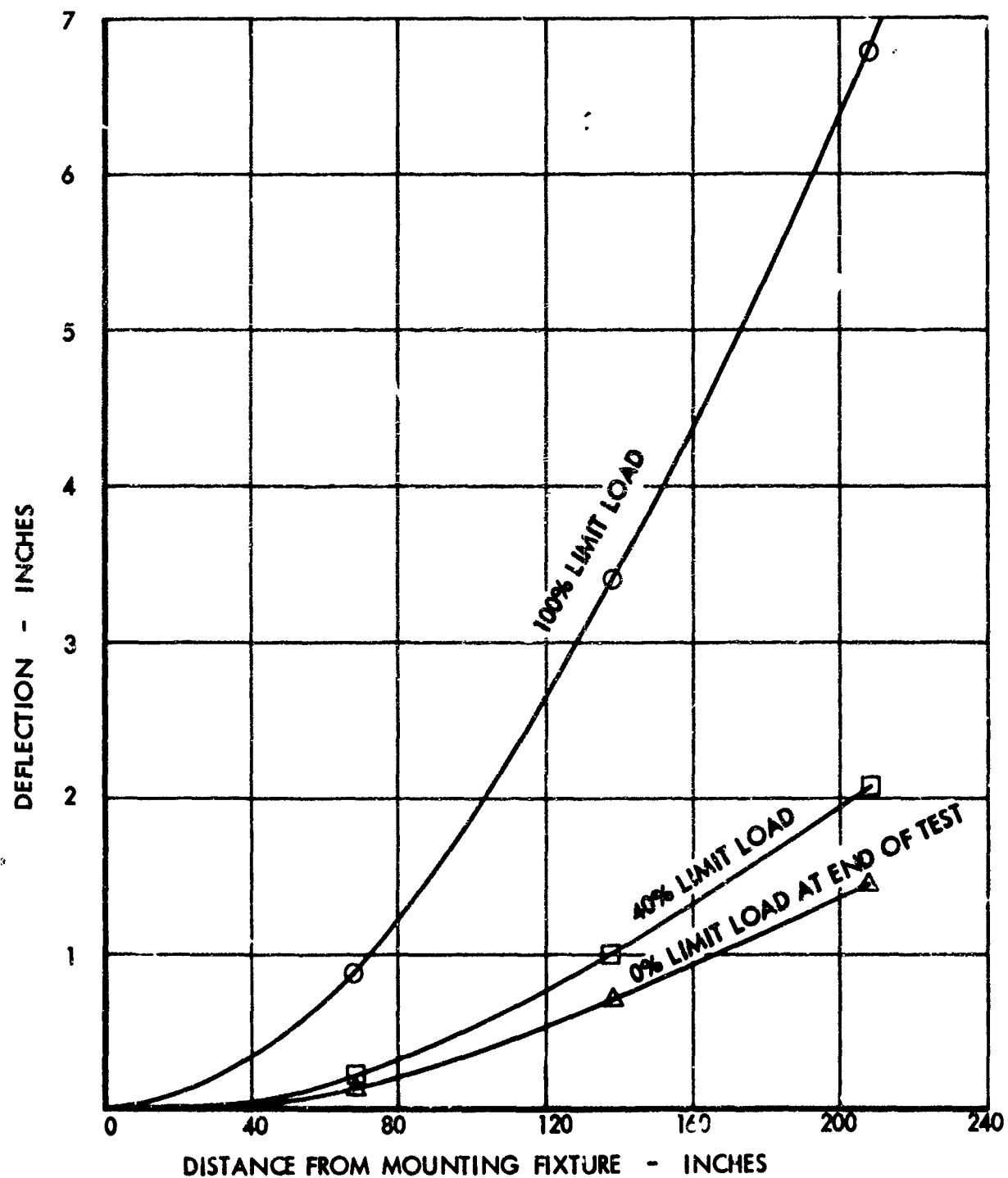
Figure 269b. Deflection Along Length of Boom at Various Loads

Figure 270. Boom at Maximum Deflection

335/484

457

HYDRAULIC SCHEMATIC:
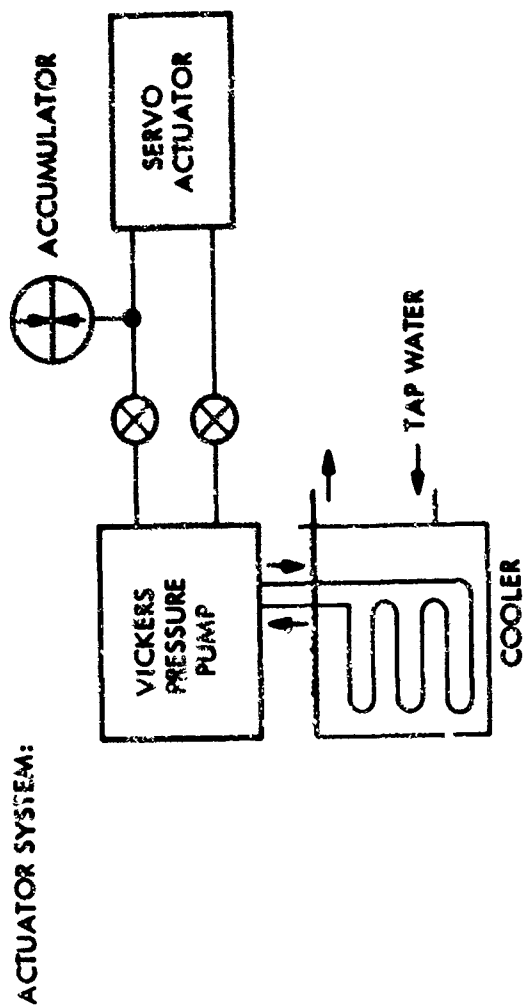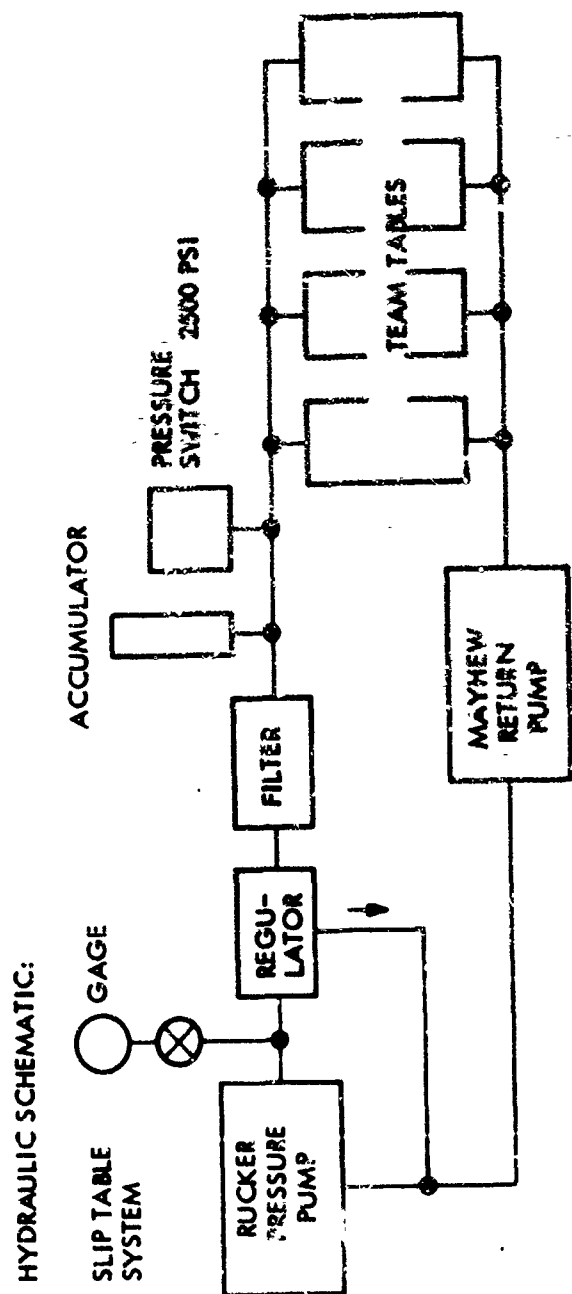
ACTUATOR SYSTEM:

Figure 271a. Boom Vibration Test Equipment Setup

Figure 271b. Boem Vibration Test Instrumentation and Control Schematic

459

CRYSTAL LOCATIONS:

NOS. 1 & 5 = MOD 2213C
NOS. 2, 3 & 4 = MOD 2221
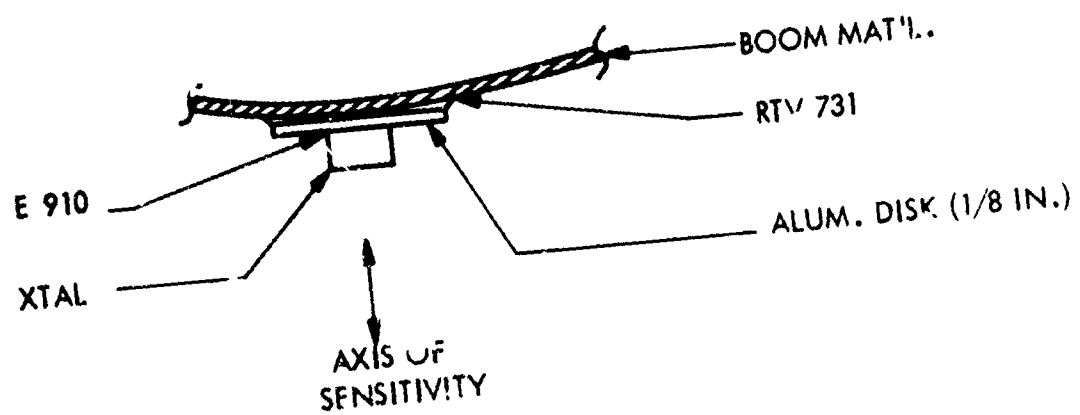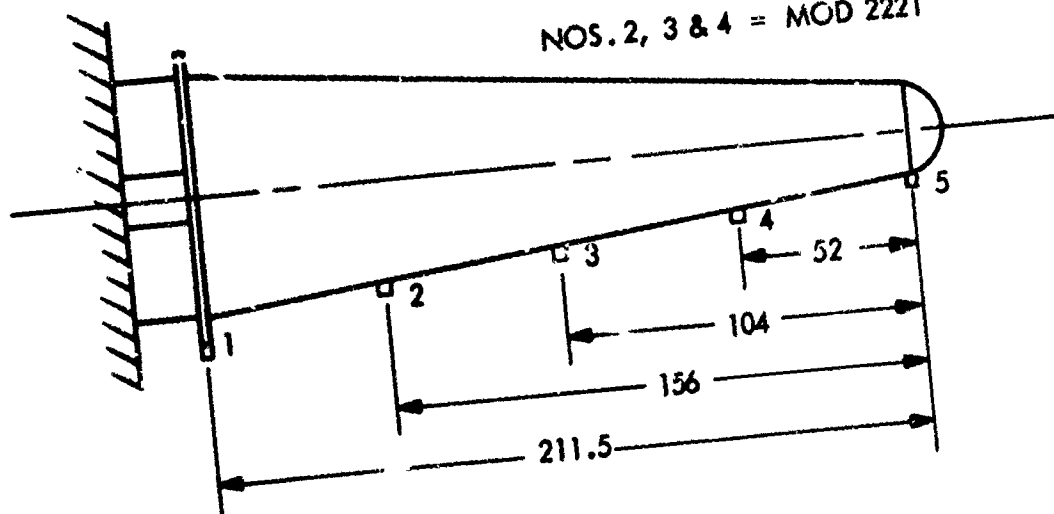
Figure 272. Boom Vibration Test Sensors

A resonance in the servoactuator hydraulic system was noted at 24-25 cps. Frequent adjustment of the actuator pressures were required to obtain sufficient excitation level and minimize undesirable excitation by this shaker resonance.

Acceleration data were recorded during a sweep from 2 to 250 cps with maximum input of 0.25 g. Elapsed time for this run was 15 minutes. The VMS frequency was 0.33 and 1.0 cps.

A position potentiometer was installed on the mounting jig plate as an input level monitor for use at low frequencies because of distortion in the input crystal signal in this range.

Discrete frequencies were investigated from 2.0 to 10.0 cps at 0.15 to 0.25 g but data quality was poor due to the shaker resonance. This run required 42 minutes.

The discrete frequency run was repeated after increasing the accumulator pressure from about 200 to 500 psig. This run required an additional 10 minutes. The data are reported in Table XL.

Table XL

AMPLITUDE OF BOOM TIP AT DISCRETE FREQUENCIES

f	Accel.	Double Amplitude	Notes
2.0 cps	.15 g	.74 in.	Input Monitored by Potentiometer
2.5	.15	.44	Input Monitored by Potentiometer
3.0	.25	.53	Input Monitored by Potentiometer
3.4	.25	.42	Input Monitored by Potentiometer
3.6 (f_1)	.25	.37	Input Monitored by Potentiometer
3.8	.25	.33	Input Monitored by Potentiometer
4.2	.25	.23	Input Monitored by Potentiometer
4.6	.25	.23	Input Monitored by Potentiometer
5.0	.25	.19	Input Monitored by Potentiometer
5.5	.25	.16	Input Monitored by Potentiometer
6.0	.25	.13	Input Monitored by Crystal
7.0	.25	.10	Input Monitored by Crystal
8.0	.25	.075	Input Monitored by Crystal
10.0	.25	.048	Input Monitored by Crystal
12.0	.25	.034	Input Monitored by Crystal
16.0 (f_2)	.25	.019	Input Monitored by Crystal

An attempt was made to record mode shape information photographically with and without strobe lights. This effort was not completely successful due to the combined effects of a large specimen and small displacements. The best results were obtained by marking the near side centerline of the boom with black tape as shown in Figure 273. This photograph shows the complete laboratory setup of the vibration test including the instrumentation at the left and the hydraulic actuator directly under the mounting fixture at the large end of the boom. A closeup view of the instrumentation is presented in Figure 274. Details of the hydraulic actuator system and slip table mounting are shown in Figure 275.

Although exact mode shapes cannot be discerned, the extent of the vibration can be seen in Figure 276 which is a time exposure, and Figure 277 which is a triple exposure. Figure 278 is a double exposure which appears to have caught the boom at the extremes of its amplitude. The photographs in these figures were taken at 16 cps. The 3.6 and 16 cps modes were investigated using photographic techniques with the shaker vibrating the boom for approximately a total of 30 minutes.

Analysis of the data showed the first four natural resonance modes occurred at 3.6, 16, 38, and 68 cps. In addition to the natural modes, other vibration modes of spurious nature were noted at 60, 64, and 156 cps. These spurious modes exhibited noticeably higher transmissibilities. The largest value noted was over 30 inches per inch at 156 cps. It is believed that the recorded data does not represent the true motion of the longitudinal axis of the specimen, especially at the 156 cps resonance point. Anomalies due to mass unbalance, cross-plane/cross-sectional or local resonances, and even the presence of the transducers, are probably present in the data and are significant when modal displacements are small.

A leak rate test was made at this point. The time required to drop in pressure from 11.0 to 10.0 psig was 1.9 minutes and from 5.0 to 4.0 psig was 3.6 minutes. Leakage was increasing as a result of the extensive vibration to which the boom was exposed.

An electrical continuity check of the thermocouple wires was made and now numbers 2 and 6 were found to be open (in addition to numbers 1 and 3 which were damaged in the packaging test). Thermocouples numbers 4 and 5 were still good and showed about 36 ohms.

3.11.5.6 HIGH TEMPERATURE TESTING OF THE BOOM

A number of problems were encountered with the infra-red heating lamps in that the gold plated steel reflectors tended to warp and the gold plating flaked off. After many days of experimentation and evaluation of the problem with the heat lamp vendor, polished aluminum reflectors were provided which appeared to be satisfactory in a number of preliminary tests, although Space-General had spec'ied the gold plated steel type.

462
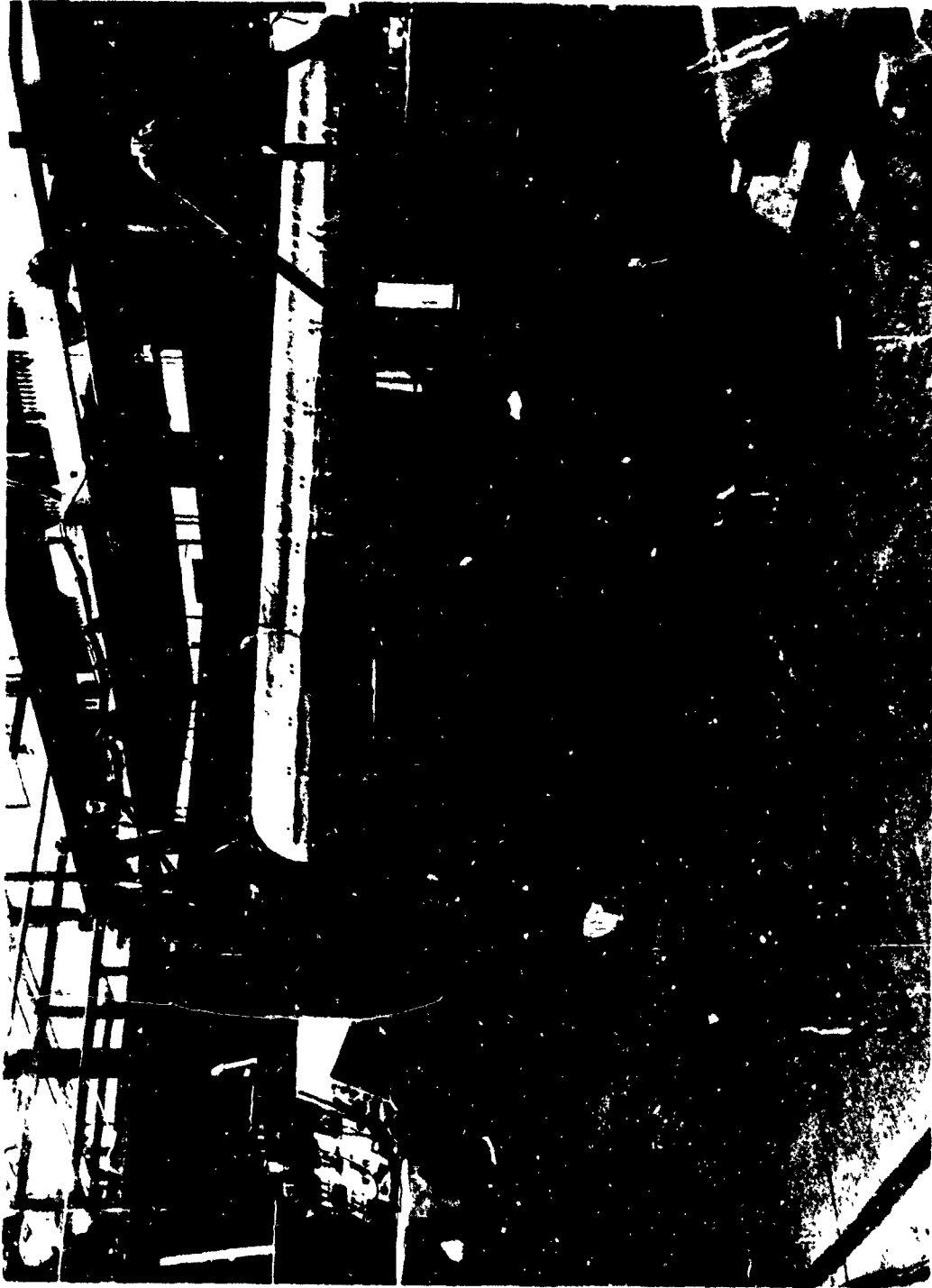
Figure 273. Laboratory Setup for Boom Vibration Test

335/498

Figure 274. Closeup View of Boom Vibration Test Instrumentation

464

335/500

Figure 275. Hydraulic Actuator System and Slip Table Mounting

465
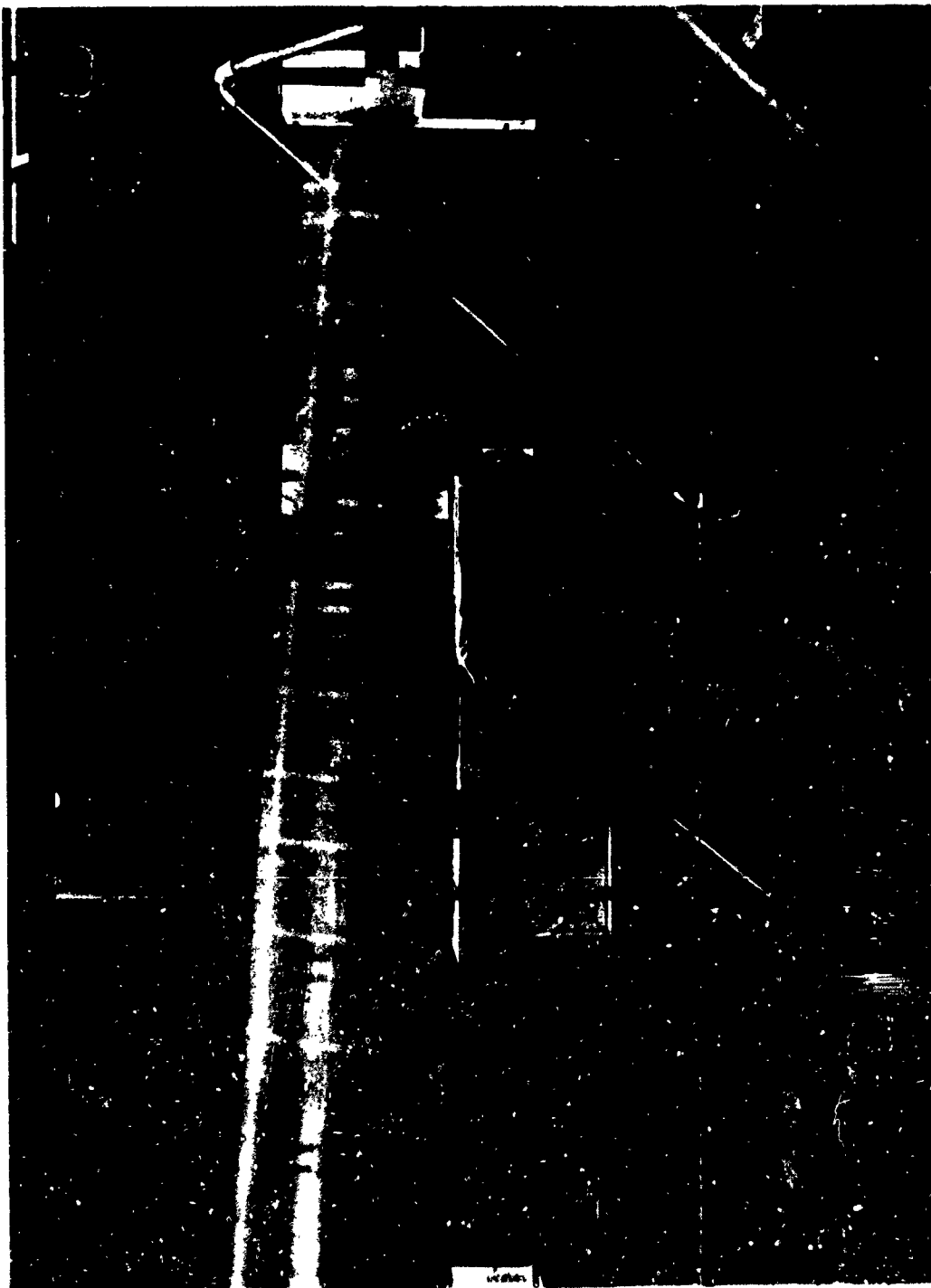
Figure 276. Boom Vibration at 16 cps, Time Exposure

3-35/1499

466

Figure 277. Boom Vibration at 16 cps, Triple Exposure

467
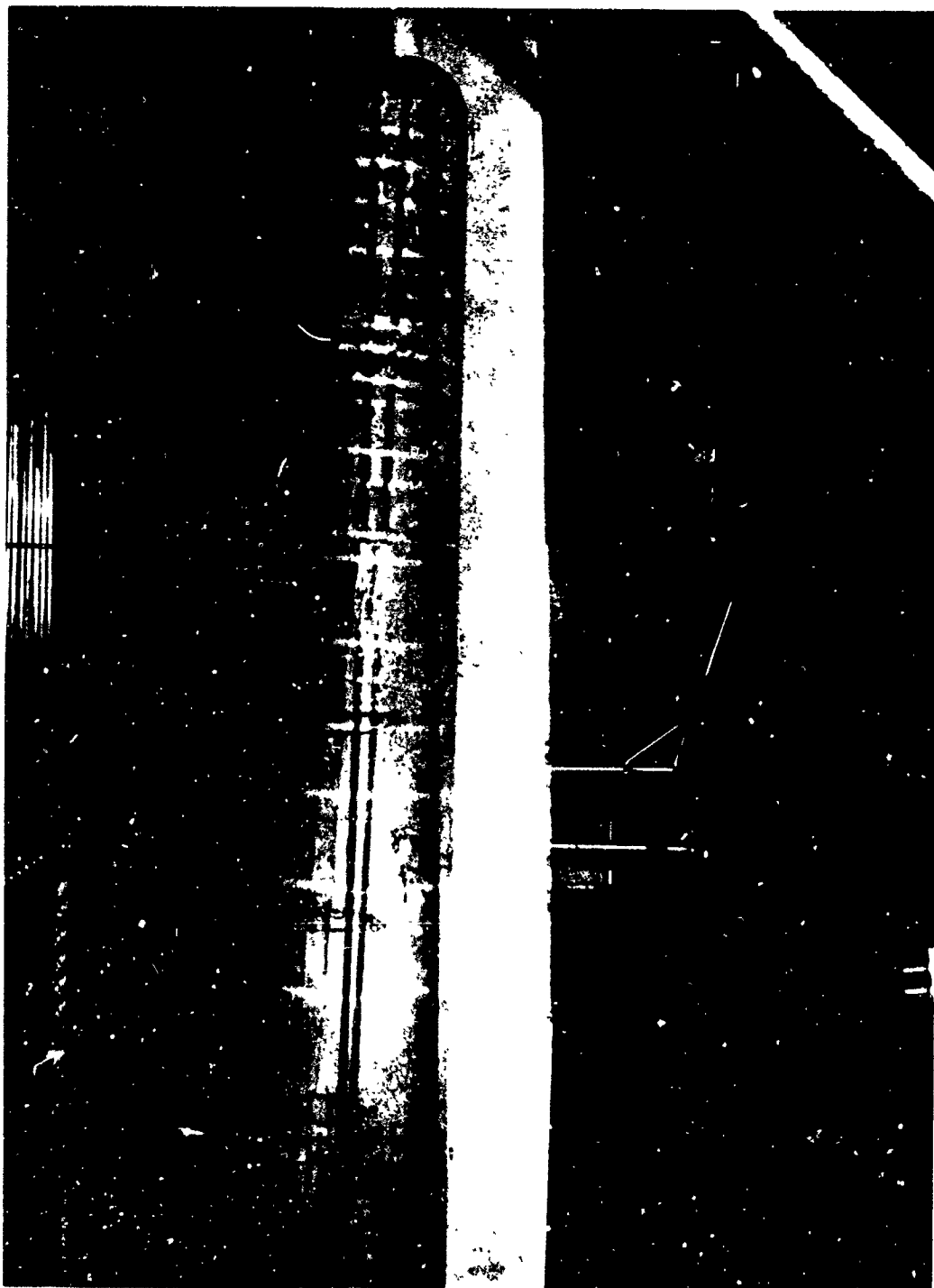
Figure 278. Boom Vibration at 16 cps, Double Exposure

335/493

468

The whiffle tree loading arrangement shown in Figure 270 was installed again in order to distribute the fatigue loads in accordance with paragraph 3.8 of the test plan, Appendix X.

The hydraulic loading system as shown in Figure 268 was also reinstalled. For this test, the hand pump was replaced by an Edison model GFC load regulator and hydraulic power supply. The regulator was set to cycle the load between 0 and 100% at one cycle per minute. The 100% limit load values were designed to develop the torsion, bending and shear conditions listed in Figure 268 and in Table I of Appendix X.

Vertical deflection at the tip of the boom was measured by a real type rectilinear potentiometer (Lockheed model 1022A) using the instrumentation setup shown in Figure 267. The pneumatic pressurization system was also identical to that diagrammed in Figure 267.

The slip table and servoactuator hydraulic system were unchanged from the arrangement shown in Figure 271a except for the removal of the oil cooler which was not required for this short test run. The VMS and its associated equipment were not required because of the low frequencies used. The vibration jig position potentiometer was monitored on a meter and not recorded.

An inert atmosphere was required during the high temperature testing period in order to prevent combustion of the silicone rubber and actually simulate the low oxygen partial pressure of the high temperature regime of the re-entry environment. A pipe framework was constructed around the testing area and used to support transparent 6 mil polyfilm sheet. A portable heat sealer and plastic tape were used to make joints in the film. The enclosure was 10 ft. by 20 ft. by 11 ft. high and it was found that it took 45 to 60 minutes to nitrogen purge the atmosphere in the enclosure to less than 1% oxygen.

Five banks of heating lamps were mounted on a wooden frame as shown in Figure 255. The position of this frame was adjusted over the specimen so that the inflated boom was 8.0 inches below the lamps at the large supported end and 6.0 inches below the lamps at the small end. In order to confine the radiant heat to the thickly coated area of the specimen, auxiliary shields were fitted to the sides of the heater chassis.

A functional check of the vibration equipment and crystals was made at ambient temperature with 11 psig boom pressure and 0.25 g input level. The second mode, f_2, was found to be at 15.6 cps. There proved to be adequate clearance between the reflectors and the specimen. The time that this test added to the total vibration history of the boom was 0.8 minutes.

The mounting clamps screws on the large end of the boom were retorqued to 125 inch-pounds after it was found that a few of the bolts were as low as 100 inch-pounds (which may have contributed to the increased leakage rates previously discussed).

With the whiffle tree and actuator rams attached to the boom and the boom tip extensometer connected, the boom was ready for high temperature testing. A double thickness of fiberglass cloth and asbestos paper was placed over the area of the boom to be heated. Wires leading to the outside of the enclosure were attached to this insulation blanket so that it could be pulled off the boom at the proper time. The purpose of this blanket was to insulate the boom while the heater elements were preheating. The heater elements were turned on for a few seconds in order to check the insulating effect of the blanket and also to verify operation of the thermocouple instrumentation. At this time thermocouple No. 4 was found to be reading erratically low. This left only one thermocouple operative. The enclosure was sealed and nitrogen purged to less than 1% oxygen. An oxygen absorption (pyrogallol) instrument was used to analyze the atmosphere in the enclosure.

The heat lamps were turned on and preheated for 1.0 minute. When the insulating blanket was pulled off of the boom, the heating cycle commenced. Thermocouple No. 5 (the remaining good thermocouple) on top of the boom at 90 inches from the mounting fixture, immediately showed an increase in temperature.

After heating for 2.4 minutes, thermocouple No. 5 indicated a metal fabric temperature of 700°F. This point was selected to start the 10 minute fatigue loading. Smoke was beginning to fill the enclosure.

As the fabric temperature approached the desired maximum, the internal nitrogen pressure began to rise rapidly. Even with the pressure bleed valve fully open the boom pressure reached 11.8 psig before it could be controlled by shutting off the pressurizing nitrogen supply. Thereafter the proper pressure 11.0 psig was maintained by using a lower supply rate.

The heating lamp power was manually switched off and on to maintain the fabric temperature in the range of $800-850^\circ$F. During the fatigue loading period, a dense white smoke filled the enclosure and completely obscured the boom from view.

Toward the end of the period, a 2-ft. diameter hole melted in the top of the polyfilm enclosure emitting large billows of smoke. Until then, nitrogen flow from the purge line had maintained a positive gauge pressure within the enclosure, thus preventing oxygen infiltration. However, after the hole developed, escaping hot nitrogen and smoke created a chimney effect which resulted in a negative pressure within the enclosure and an indeterminable amount of oxygen infiltration. Observers noted no signs of active combustion within the enclosure, however.

At 12.3 minutes, the tenth load cycle was finished. The loading system and the boom tip deflection potentiometer were quickly disconnected from the specimen by withdrawing a longitudinal rod from the small rings in the whiffle tree and pulling a disconnect wire on the potentiometer from outside the enclosure. The slip tables and hydraulic servoactuator were activated at 14.0 minutes. By 15.5 minutes into the test, the second modal frequency, f_2, had been found to be 14.3 cps and the shaker was turned off.

At 16.2 minutes both the pressure and bleed valves were shut off. The boom pressure was manually read and recorded at 0.5 minute intervals for 2 minutes (5 readings). During this time the pressure dropped from 10.8 to 10.3 psig within internal gas temperature holding at 260°F.

After heating intermittently for 18.2 minutes, heat lamps were turned off for the last time and the test run ended. The specimen was allowed to cool down to room temperature before the enclosure was opened for inspection and the nitrogen purge shut off. Thermocouple No. 5 was recorded for 15 minutes after the test run was finished.

Table XLI is a log of the high temperature test and Figure 279 is a graph of the temperature history of the metal fabric and the internal gas related to events during the test.

Figure 280 shows the boom tip vertical deflection during the application of the 10 cyclic fatigue loads.

Data on all the vibration tests are presented in Section 3.11.5.7 along with the post-heating vibration tests.

Inspection of the interior of the enclosure after cooling disclosed that all of its contents were coated with a fine, white powder, obviously a form of silica which normally results from high temperature heating of silicone rubber even in the absence of significant oxygen. The powder may be seen in Figure 281 which also shows the shields on the heating lamps.

Several of the 24-gauge polished aluminum lamp reflectors had been seriously damaged by the heat. Two reflectors were completely destroyed allowing molten aluminum to fall onto the top surface of the boom. The melted reflectors are shown in Figure 282 and the extensive charring and significant damage caused by the molten aluminum are shown in Figures 283, 284 and 285. Some of the molten aluminum had actually run off of the boom and solidified on the floor. The remaining extensive charring of the boom may be seen in Figure 286.

The metal fabric was completely exposed in several large areas near the large end of the boom. However, in these exposed areas, the surface of the metal fabric appeared undamaged and it was still impregnated with RTV-655 which also appeared to be in good condition.

The charring of the boom was far more serious than had ever been experienced on high temperature frustum testing at the same temperature levels. It is believed that the horizontal configuration of the boom, the heat shields on the lamps, the infiltration of oxygen due to the hole in the enclosure, and the melting of the aluminum reflectors onto the surface of the boom all contributed to the extensive destruction of the S-6510 silicone rubber coating. Since the molten aluminum ran off the exposed impregnated metal fabric surface, it is obvious that this surface must have been at 1100°F or higher. It is remarkable that the impregnated metal fabric was undamaged.

471

Table XLI

HIGH TEMPERATURE BOOM TEST LOG

0	Lamps on, asbestos and glass cloth cover on boom
1	350°F metal fab. temp. Removed cloth & asbestos
1 1/2	500°F metal fab. temp.
2	600° metal fab. temp., visible blisters, smoking started
2 1/2	700° metal fab. temp. load cycle started
4 1/2	850° metal fab. temp., 11.8 psi boom pres., lamps OFF
6	810° lamps ON
9	850°F
11 1/2	840°F
12 1/2	Load cycling complete - tree rod out
14	Start vibration test
14 1/2	860°F
15	Vibration continuing
15 3/4	Vibration OFF
16 1/4	10.8 psi start pres. perm. test
16 3/4	10.4 psi
17 1/4	10.4 psi
17 3/4	10.3 psi
18 1/4	10.3 psi
18 1/2	Test complete
19 1/2	10.2 psi
22	9 psi 560°F metal fab. temp.
27 1/2	300°F metal fab. temp.
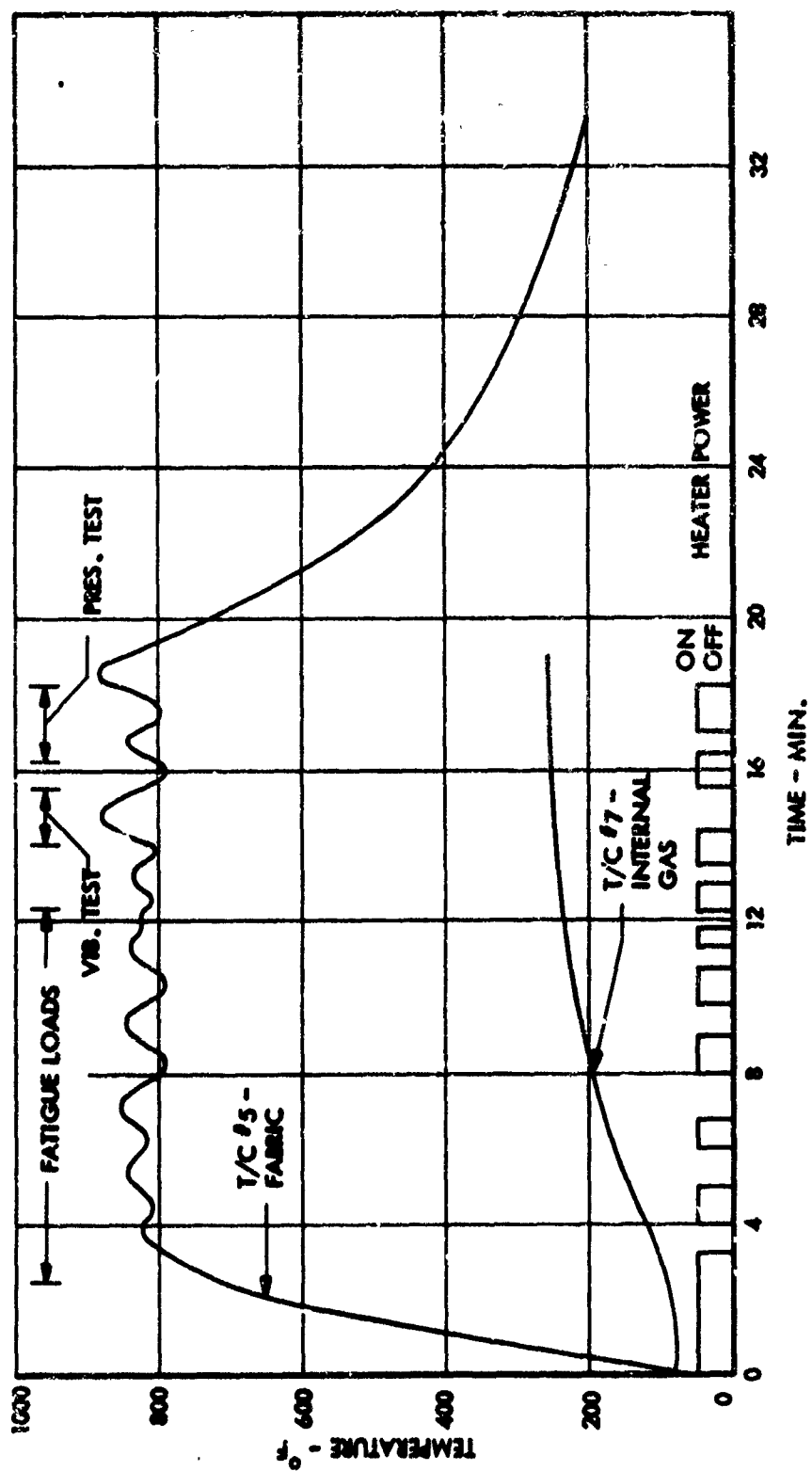
Figure 6.9. Boom Fabric and Gas Temperature During High Temperature Test

473
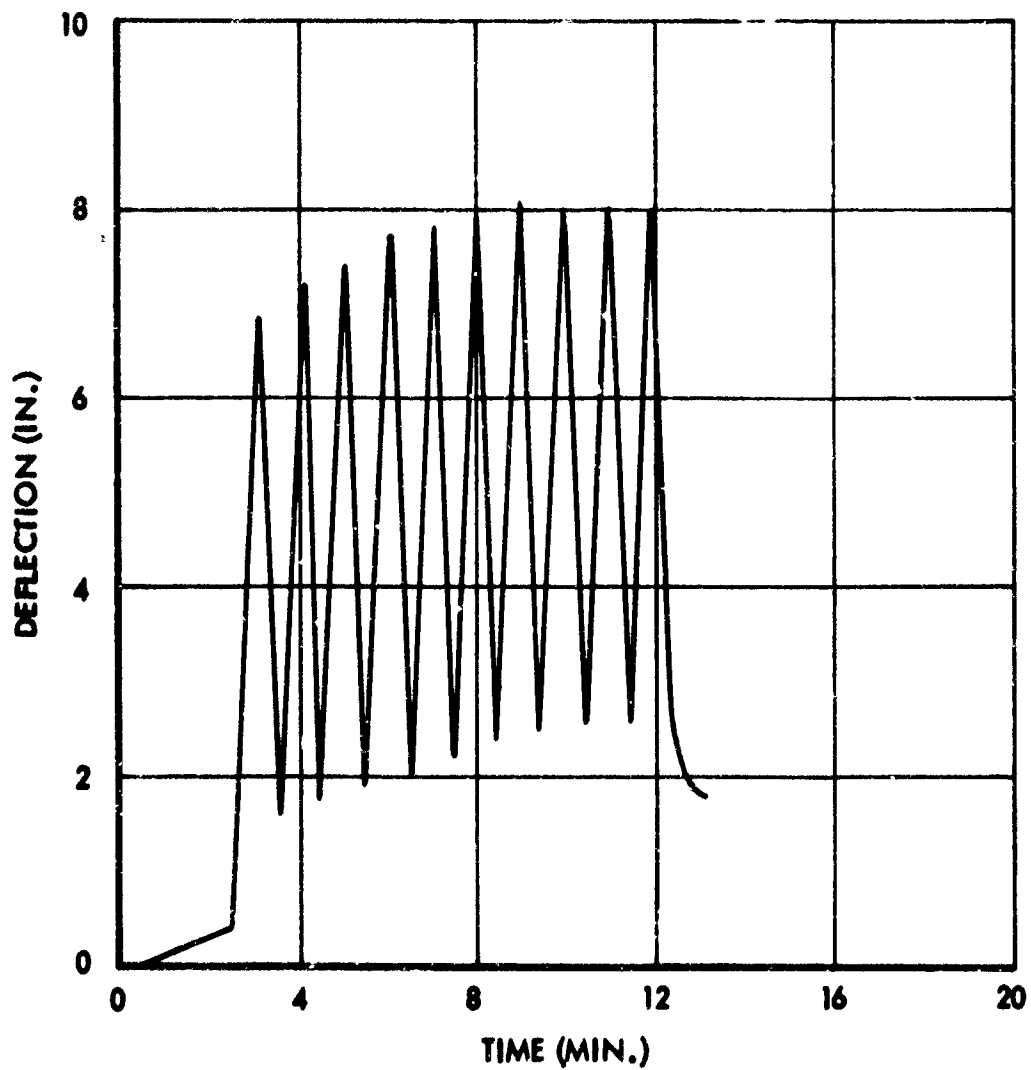
Figure 280. Vertical Deflection of Boom Tip During High Temperature
Test, Cyclic Fatique Loads

Figure 281. Interior of Boom Test Enclosure After Completion of High
Temperature Heating Test

335/526

475

Figure 282. Melted Aluminum Reflectors After High Temperature Test
on Boom-Note Quartz Heating Tubes

476

335/242

Figure 283. Appearance of Boom Surface After High Temperature Heating
Test Showing Charring and Damage Due to Molten
Aluminum from Melted Reflectors

Figure 284. Charring and Damage Due to Molten Aluminum During High Temperature Testing of Booms

335/543

478

Figure 285. Damage to Boom Surface Coating of Silicone Rubber Due to
Molten Aluminum

335/537

479

Figure 286. Charring of Boom Surface During High Temperature Heating Tests

335/540

The failure of the heating lamp reflectors was caused by a combination of several factors. Although difficulty may have been avoided if the reflectors had been gold plated steel as used with the frustums, the reflectivity of the surface was impaired by the smoke residue resulting in increased heat absorption. Heat absorped by the smoke coated reflectors also detracted from the heating of the boom causing the lamps to have to be on longer to obtain the correct boom temperature. Since the lamps were sloped downward toward the tip of the boom to obtain the proper clearance giving the required temperatures, as based upon test data, the hot gases and smoke concentrated at the high end of the lamp assembly. The smoke and the molten aluminum did not damage the quartz heating tubes.

A leak test, at this time in the testing, showed the boom to be remarkably leak free considering its condition. The time required to drop in pressure from 5.0 to 4.0 psig was 5.5 minutes and from 11.0 to 10.0 psig was 2.7 minutes.

3.11.5.7 POST-HEATING TESTS ON THE BOOM

The vibration equipment was identical to that used previously, see Figure 272, except that crystal number 3 and crystal number 4 were removed. The remaining setup was also the same as for the previous tests. The heater lamp framework was lifted up against the overhead beam and secured so as to be out of the way. Internal nitrogen pressure was maintained at 11.0 psig.

The tip of the boom was deflected manually and quickly released. The resulting free vibration frequency was found to be 3.97 cps. The vibration decay data thus obtained was used to calculate the fraction of the critical damping or the damping ratio at 3.6% of critical.

The resonant frequencies of the crystals, their mounting materials, and adjacent boom structure were measured by tapping the boom next to the crystals. It was found that crystal No. 2 was 118 cps, and No. 5 was 180 cps These frequencies do not coincide with the resonant peaks found in the modal survey test prior to heating.

The second modal frequency, f_2, was found to be 15.9 cps with 0.25 g input. As the vibration of the boom was started, some of the loose pieces of charred coating were shaken off onto the floor.

The combined limit loads were cycled between 0 and 100% at one cycle per minute for 10 cycles as described for the high temperature testing in Section 3.11.5.6 except that no heat was applied to the boom. Vertical deflections at the tip of the boom were measured by the same potentiometer previously used. One extra load cycle was imposed on the specimen at 1/4 of the usual rate in order to find any change in deflection due to load rate. No change was noted. The vertical tip deflections during this cyclic load tests are shown in Figure 287. The specimen showed no adverse effects from this test other than the shaking loose of some of the charred coating. Two views of the boom surface are shown in Figures 288 and 289.

481
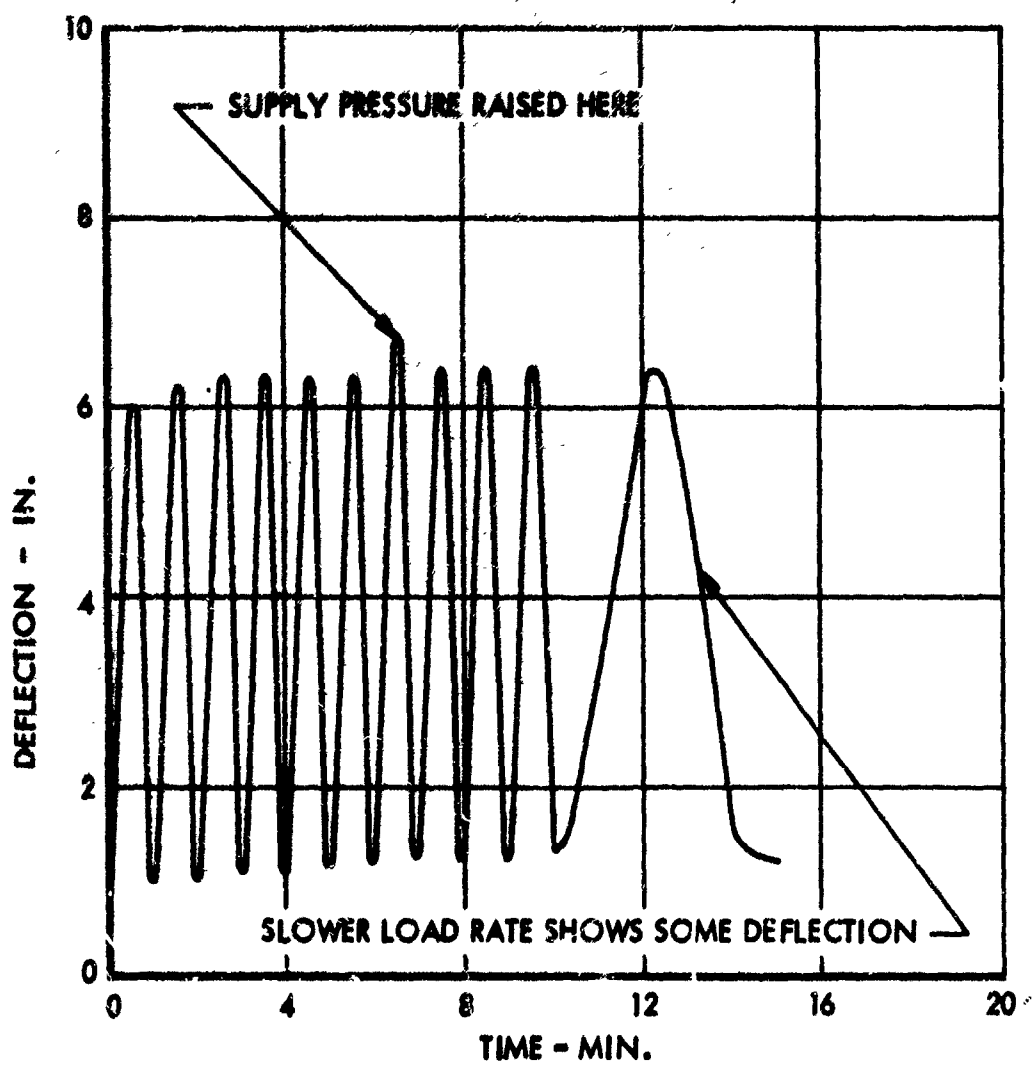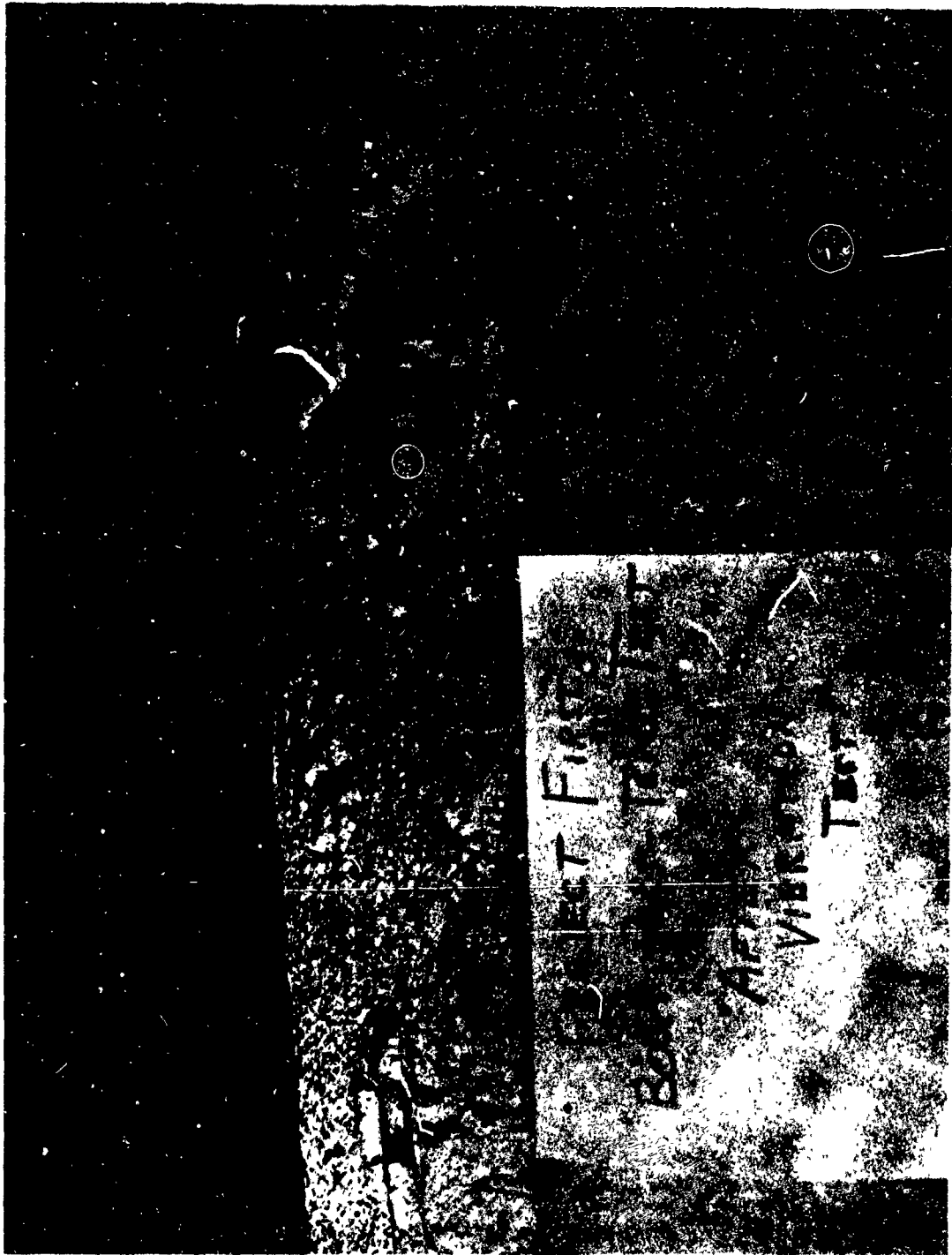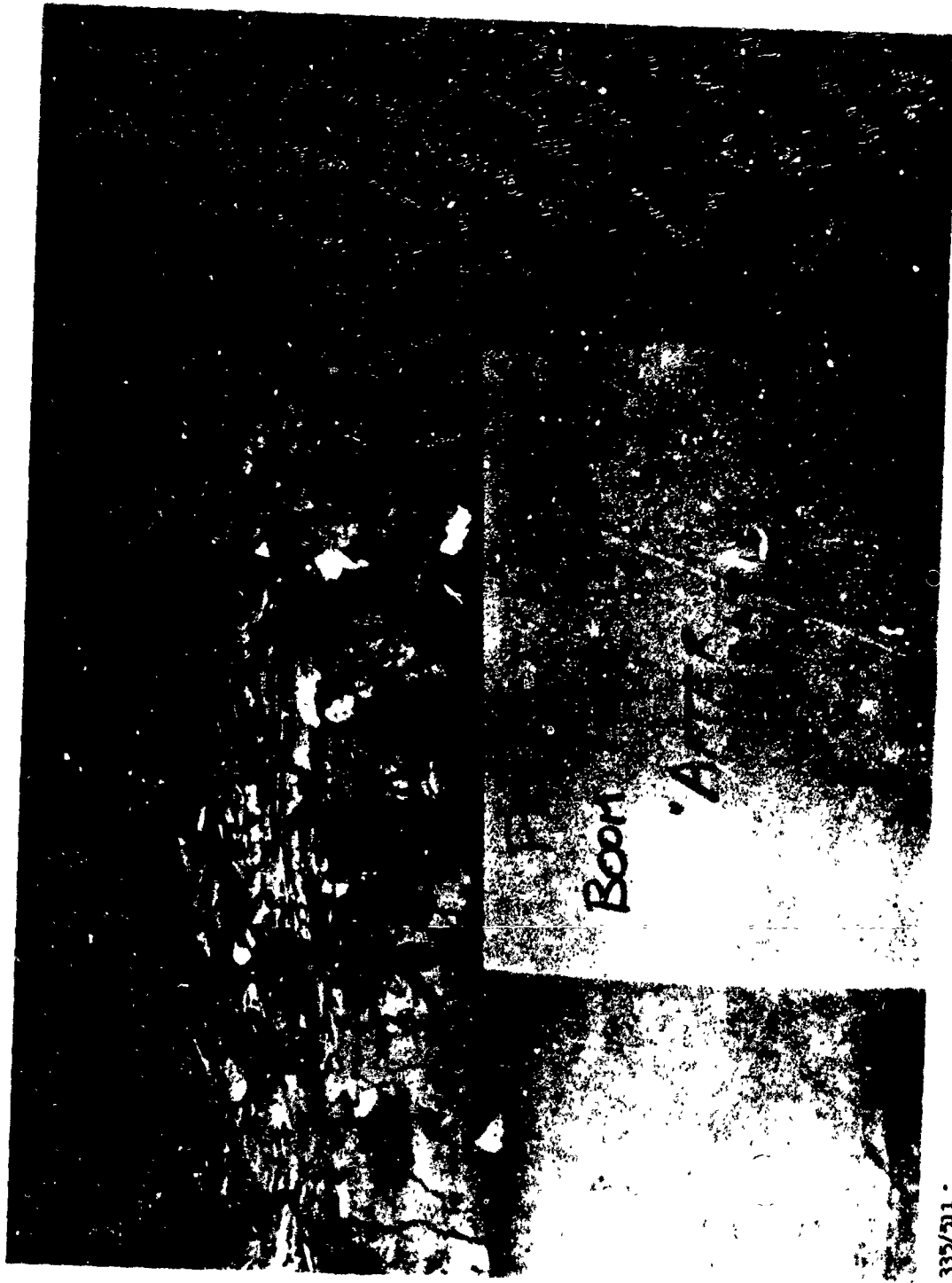
Figure 287. Vertical Tip Deflection During Boom Post-Heating-Fatigue Test

482

Figure 288. View of Charred Boom Surface After Application of Post-Heating
Vibration and Cyclic Loads

Figure 289. Project FIRST Boom Post - Temperature Test.

335/511

484

A leak test was run again, at this time, showing rather surprising freedom from leakage considering the drastic environment to which the boom had been exposed and the condition of the surface coating. It took 4.8 minutes for the pressure to drop from 5.0 to 4.0 psig and 2.5 minutes for the pressure to drop from 11.0 to 10.0 psig.

The ultimate load test on the boom in accordance with para. 3.12 of the Test Plan, Appendix X, was conducted using the whiffle tree, hydraulic power supply and load regulator as in the previous test. In order to provide sufficient deflection capability, four additional hydraulic rams (six total) were installed in series and the complete hydraulic system was calibrated to 300% of the combined limit load against a BLH 1000-pound load cell. The rams were mounted horizontally to a nearby test stand and connected to the whiffle tree with a steel cable and direction-changing ball bearing pulley. The load was applied at the same angles to the boom as shown in Figure 268.

Boom tip deflection was recorded on a Sanborn recorder from the output of a reel type rectilinear potentiometer (Lockheed model 1022A) as in Figure 267.

The clamp screw torques were checked at 125-inch-pounds since a few were found to be at 110-115 inch-pounds.

The internal nitrogen pressure of the boom was raised to 11.0 psig and the Edison loading regulator was started at a loading rate of about 35% per minute. This rate was maintained until the specimen began to buckle at 240% of limit loads. At this time, the load was held constant for photographs. A series of pictures from 0% to 240% load are shown in Figure 290. A closeup view of the wrinkles or buckling occurring in the compression side of the boom is shown in Figure 291.

During the photography, a blister developed about 4 feet from the tip of the boom on the compression side. It had grown to about 10 inches diameter by the time it was punctured by a technician with a knife blade.

Shortly thereafter, the internal pressure began to decrease. The pressurizing gas regulator setting was increased in an attempt to hold 11.0 psig, but the specimen immediately collapsed onto the floor, having pulled out of all the clamps except a few at the bottom. The decrease in pressure was obviously due to the specimen beginning to pull out of its mounting. The result is shown in Figures 292 and 293.

As a result of the boom pulling out of the clamp ring, it was torn adjacent to the clamp ring on the compression side as shown in Figure 294. Since no way is known of repairing such a tear in impregnated fabric, the tests were necessarily concluded without being able to run a burst test on the boom. However, all of the proposed data called for in the Test Plan, Appendix X, had been obtained.

A graph of the deflection of the boom tip as related to other events during this test is shown in Figure 295.

335/552

A

335/553

B

335/554

C

335/555

D

Figure 290.   Views of Boom During Application of Combined Shear, Bending
and Torsion Loads from 0% to 240% of Design
Limit Loads

486

335/249

Figure 291. View Showing Incipient Buckling in Lower Surface of Boom with Application of 240% of Combined Limit Loads

335/551

Figure 292. Boom After Pulling From Its Mounting Fixture During Final
Loads Test

488

335/550

Figure 293. Collapsed Boom After Pulling Out of End Closure Clamps
During Final Ultimate Loads Testing

489

Figure 294. Tear in Large End of Boom Due to Pulling Out of Fixture
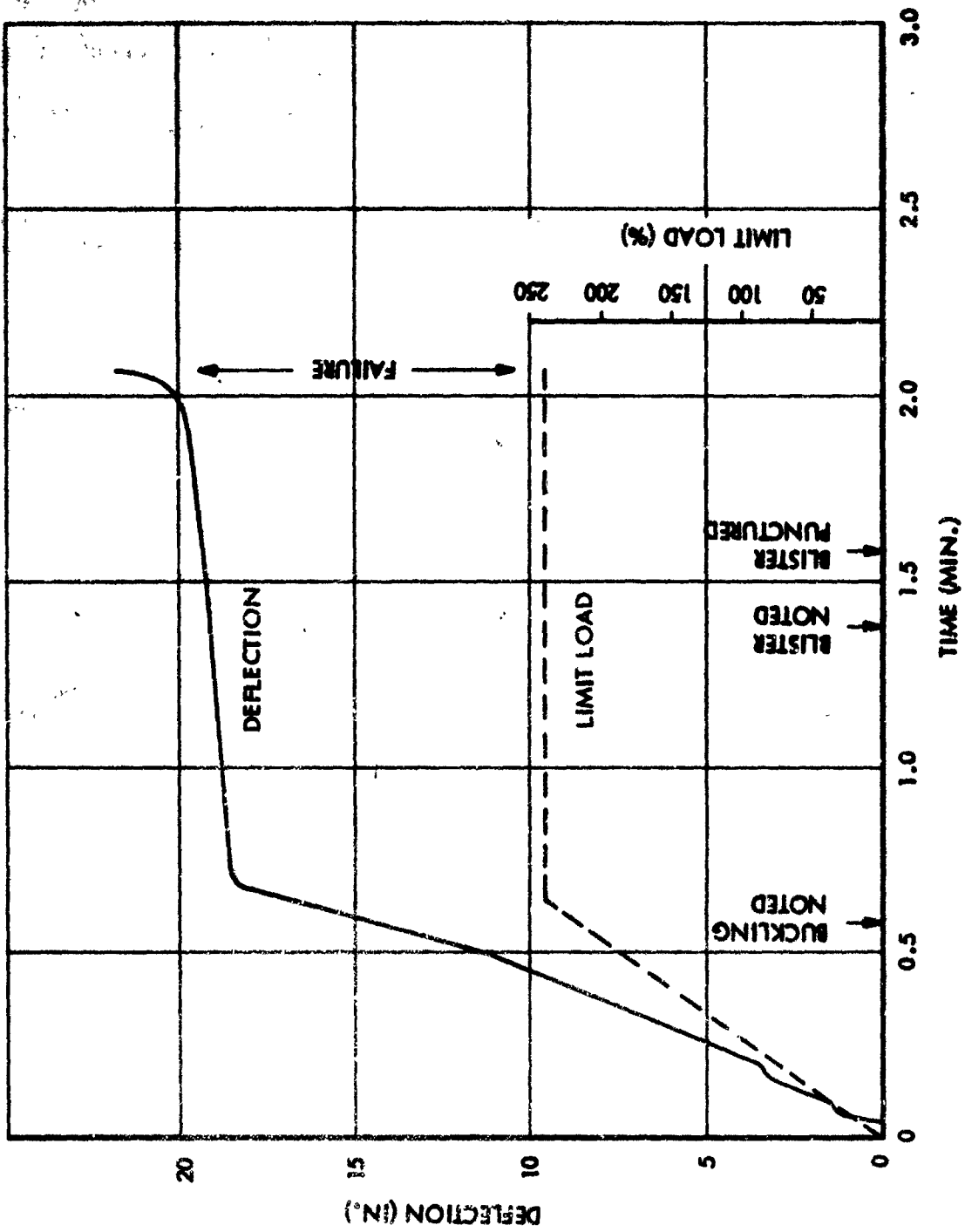
335/559

490

Figure 295. Boom Tip Deflection During Ultimate Load Test

491

3.11.5.8 SUMMARY OF VIBRATION AND PERMEABILITY LEAK TESTING

Final analysis of the mode shapes as recorded by the crystal transducers during preheating vibration tests on the boom disclosed the normalized deflection curves for normal mode shapes at 3.6, 16, 38, and 68 cps as shown in Figure 296. Figure 297 illustrates the spurious mode shapes discovered as 60, 64, and 156 cps.

At the second modal frequency of 14-16 cps, the preheating, high temperature, and post-heating vibration tests produced normalized deflection data as shown in Figure 298.

The total time to which the boom was exposed to Vibration was 159.3 minutes.

Table XL11 lists the times for all frustums and the boom to drop in pressure during permeability and leakage tests. The calculated standard leakage rate is also presented for the 10-9 psig pressure loss tests. This pressure range of 10 to 9 psig is near the 11.0 psig design inflation pressure for the paraglider. It should be noted that the leakage through the clamped joints at the end closures probably was more responsible for variations in the data than leaks or permeation through the impregnated and coated fabric. The results cannot be classified as permeability (or leakage) information on the fabric structures as such, therefore.

Table XLII also presents burst pressures for the frustums and makes note that the frustum (S/N 1) and the boom both encountered incipient buckling at about the same relative load, 240-250% of design limit.

3.11.6 TESTING OF THE APEX

3.11.6.1 APEX TEST PREPARATION AND PLANNING

The test specimen was a full-scale, toroidal apex assembly with 32-inch diameter by 36-inch long stub booms. It was made of production run miltifilament, metal fabric with the customary two plies in 45° bias relationship. In addition, the apex was tape wrapped as described in Section 3.10.7 to reinforce the highly loaded crotch areas between the leading edge booms and the center keel boom. These wraps of metal fabric tape built up to about 25 layers of fabric in the crotch areas.

The open ends of the apex had the two basic plies folded back over a Teflon coated 0.072-inch diameter steel wire ring with the fabric spot welded to itself to retain the wire ring, as in the boom assembly. Two reinforcing cuffs, 4 inches and 6 inches long, were placed over the 32 inch diameter ends of the apex stub booms with the smaller cuff outside and flush with the end of the stub boom. As in the boom, these cuffs were not welded to each other or to the parent fabric of the boom. They were, however, held in place by the RTV 655 silicone rubber impregnation material. The total weight of the apex as completed was 115 pounds.
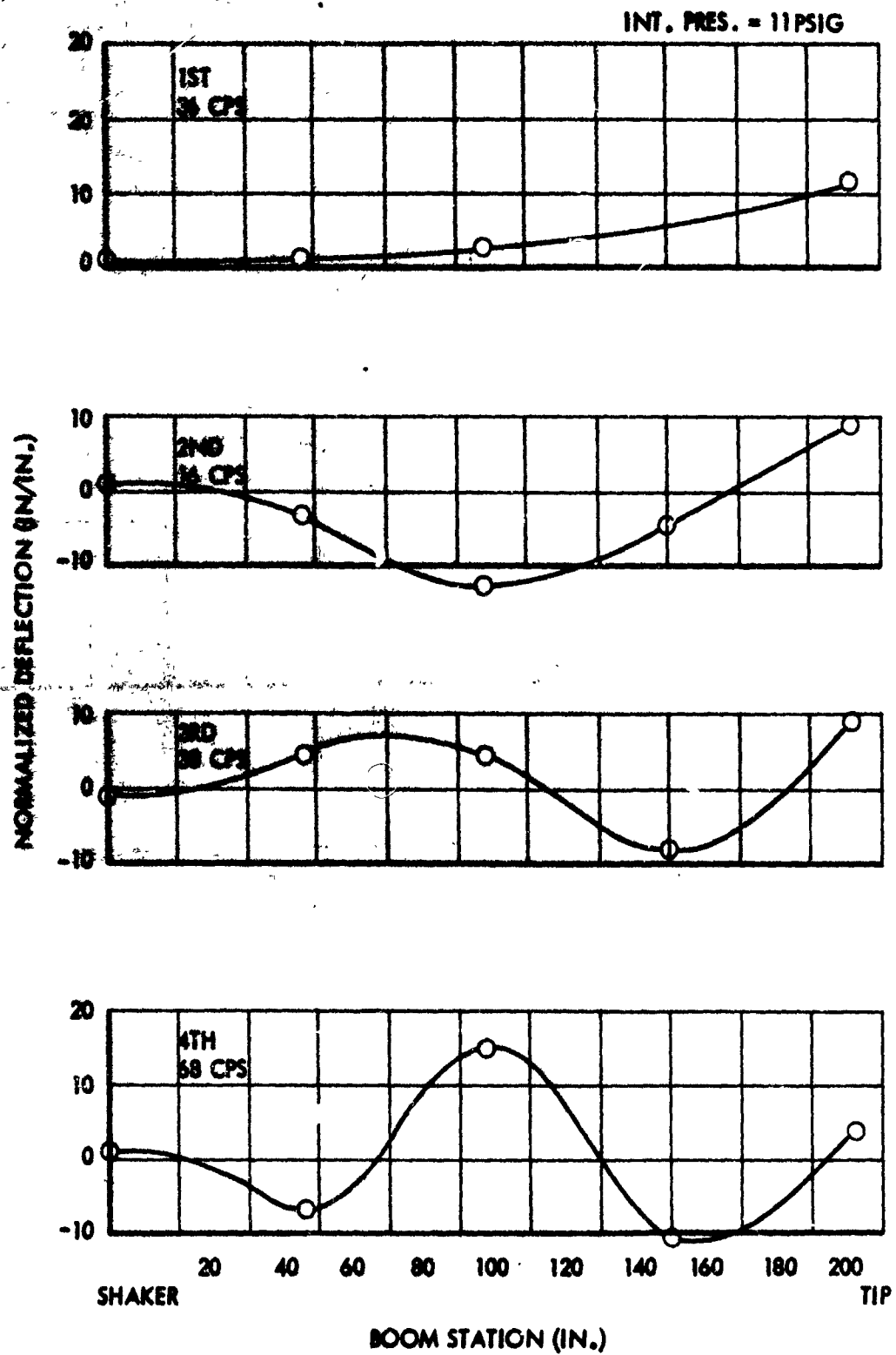
492

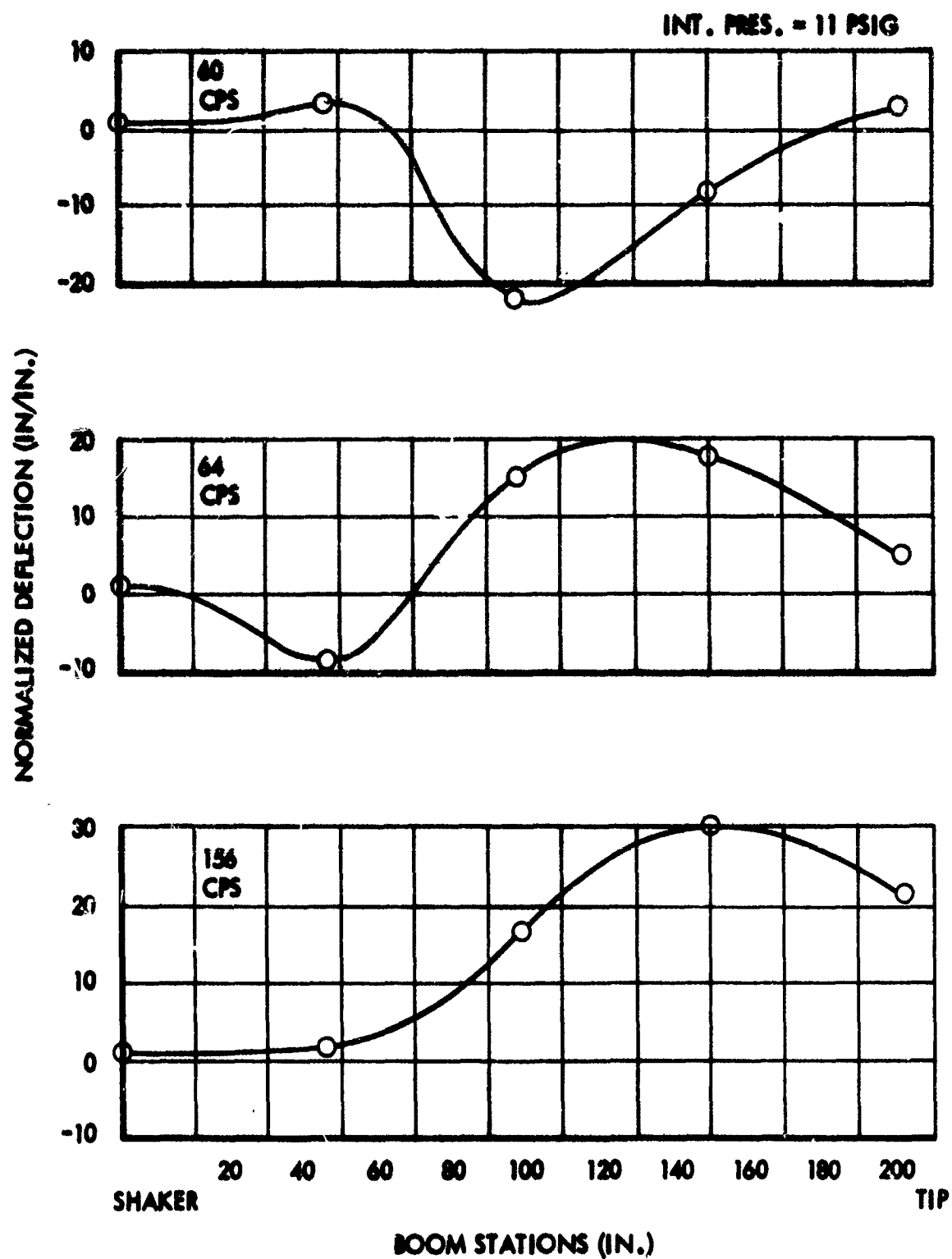Figure 296. Normal Mode Shapes of Boom During Vibration Testing

493

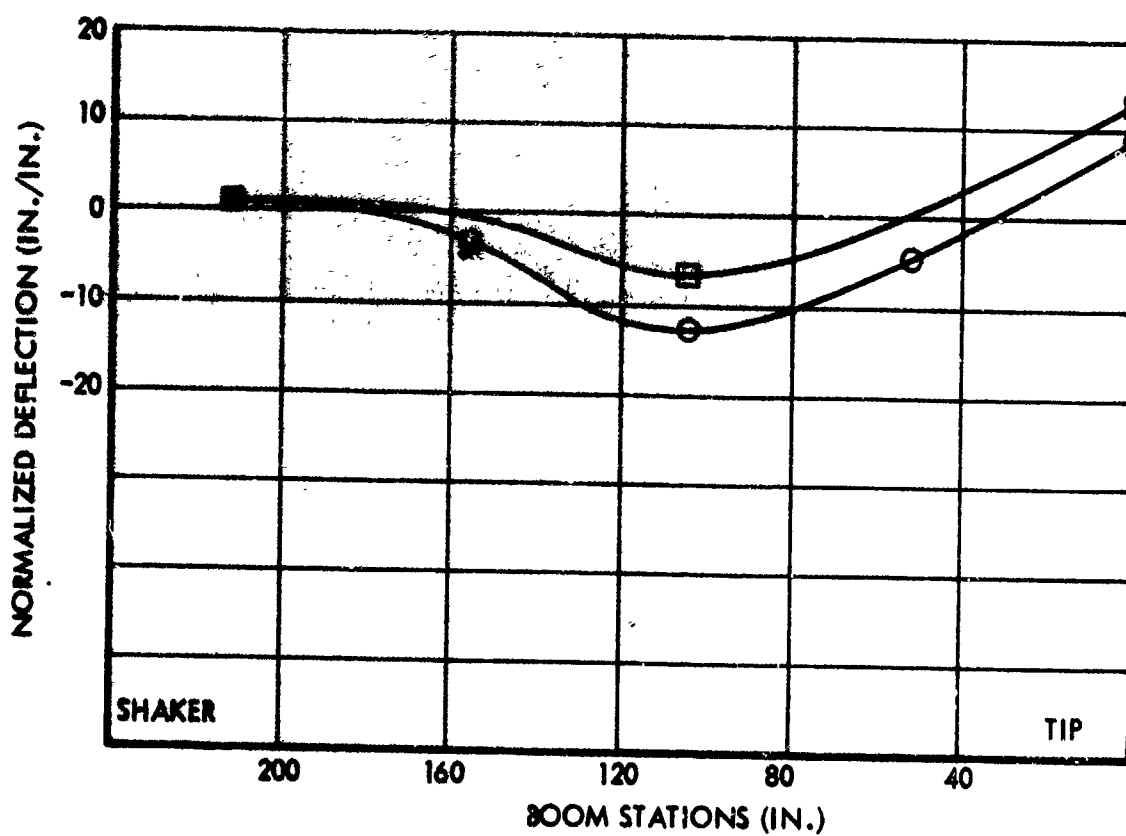Figure 297. Spurious Mode Shapes of Boom During Vibration Testing

Figure 298. Boom Vibration Mode Shapes (at Room Temperature and High Temperature)

495

Table XLII

PERMEABILITY AND LEAKAGE CHARACTERISTICS
OF INFLATED TEST COMPONENTS

Fracture Test No.	Fabrication Serial No.	Time (min.) for ΔP[1]			Total Leakage Rate for 10-9 psig std cu ft/sq ft, hr	Net Leakage Rate for 10-9 psig std cu ft/sq ft, hr[19]	Buckling Load[?] % of Design Limit	Burst Pressure
		5-4 psig	10-9 psig	35-34 psig				
P-1								
1	1	26.0	11.0	1.5	0.098	0.035	250	78
2	3		11.4		0.084	0.033		84
3	2							
4[3]	6	7.8	4.8	0.6	0.134	0.111		84
4[5]	6	5.6	3.4	0.1[4]	0.189	0.164		
	6	3.2	2.6	0.4	0.232	0.240	see text	
5	8							
6[6]	4	20.9	10.0	2.0	0.064	0.041		
6	4	12.8	10.3	1.3	0.104	0.112		
7	5	8.7	3.6	0.4	0.170	0.145		
7[7]	5	8.1	5.9	1.0	0.179	0.200		85
8	10	41.3	27.7	2.7	0.054	●		102[10]
8[9]	10	31.3	29.0	1.4	0.042	●		91[11]
9[12]	7	57.7	26.7	1.0	0.024	●		97[13]
10[12]	9	83.3	28.3	3.5	0.053	●		
		25.8	14.5 (ave)		0.273			
Booms							240[17]	
Boom [14]		5.7	3.2		1.24			
Boom [15]		3.6	1.9		2.95			
Boom [16]			4.0		0.73			
Boom [17]		5.5	2.7		1.47			
Boom [18]		4.8	2.5		1.58			

(1) Average time where more than one test performed
(2) At "design load and pressure" of 35 psig for fracture
(3) After packaging and vibrating
(4) Distinct leak occurred
(5) After "smiling" leak
(6) After heating to 900°F
(7) With fabric at 700°F
(8) Approximate internal N₂ temperature 330°F
(9) After heating to 760°F
(10) After heating to 760°F and cycling loads

(11) At 410°F after heating to 810°F
(12) With internal bladder
(13) At 790°C
(14) After packaging and vibration
(15) After inflicted vibration
(16) Metal fabric at 850°F, internal N₂ at 260°F
(17) After cooling. Loads applied with 11 psig internal design pressure
(18) After post-heat loads
(19) Total leakage less leakage attributed to end closure leakage

496

Three closure clamp ring fixtures for the apex stub boom ends were exact duplicates of the boom holding ring fixture and used small aluminum clamps radially bolted to the holding ring. These clamps were tightened down on the double cuff of the stub booms of the apex over the wire retaining ring and protective rubber insert.

A complete test plan for the ambient temperature testing of the apex is presented in Appendix XI of this report although all of the tests could not be carried out, as discussed subsequently. The apex was mounted upside down and the test load of 340 pounds was to be applied downward on the end of each leading edge boom at an angle of 25° 30' rotated inward from the vertical plane through the stub boom axis and raked aft 8° 22' with this load applied at 6.13 inches from the center line of the stub boom. The same loading effect would be imposed on the apex assembly as if the entire boom and wing assembly were intact during re-entry flight.

To implement the proper application of the boom and wing loads, cylindrical extensions of 20 gauge galvanized sheet metal ducting 88 inches long and 12 inches in diameter were attached as extensions to the closure plate on each leading edge stub boom. These tubes were fabricated using the standard Pittsburgh sheet metal lock in the longitudinal seam and this seam was reinforced by riveting at 6-inch intervals.

3.11.6.2 INFLATION TESTS ON THE APEX

The two large extension cylinders were bolted to the leading edge stub boom closure plates. The apex was then mounted by the central keel boom closure plate to the structural test block. With the outer closure plates, extension tubes, and counterbalances installed on the extension cylinders to support their weight, the apex was inflated with 0.5 psig nitrogen pressure. The apex appeared as shown in the photograph, Figure 299.

Excessive leakage was discovered through the impregnated metal fabric skin of the apex, and after evaluation it was decided that an inflatable rubber bladder would have to be made and installed in the interior of the assembly. The rubber bladder was fabricated of thin natural rubber dental dam material as shown in Figure 300. This was inserted within the apex and the center keel boom holding fixture was then reinstalled and the apex assembly was remounted onto the structural test block.

The proof pressure test started at 1.0 psig and advanced in 1.0 psi increments, holding for 2 to 3 minutes at each increment. A cord was tied from the top of the closure plate on one stub boom to the top of the closure plate on the other stub boom. There had been some previous indications that the stub booms might move inward toward each other and a slackening of this cord would indicate this movement.

The inflated apex is shown being inspected in Figure 301.
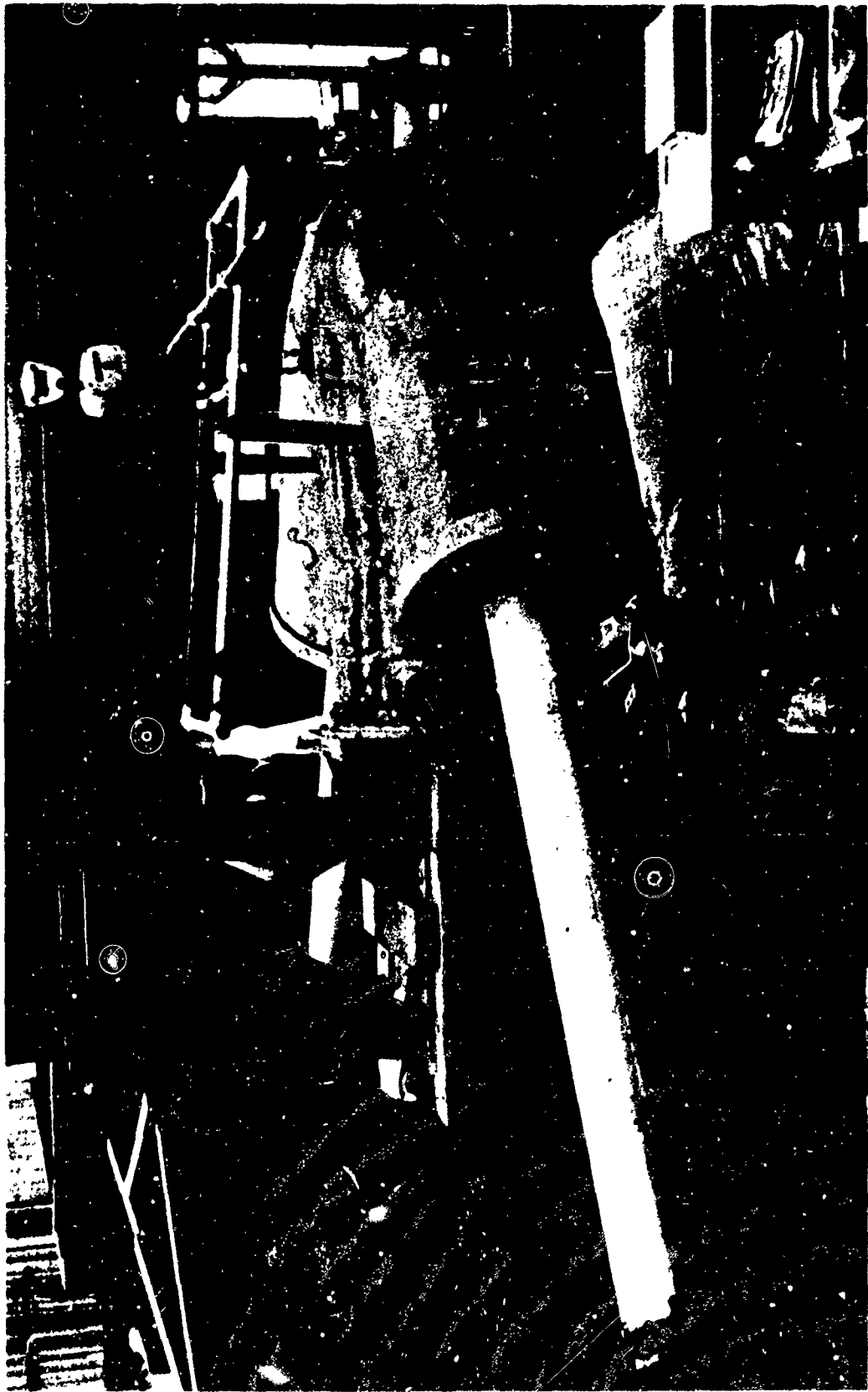
Figure 299. Apex with Extension Tubes Mounted on Test Stand and Inflated with 0. 5 psig Nitrogen

335,69±

498

Figure 300. Rubber Bladder for Apex During Leak Check
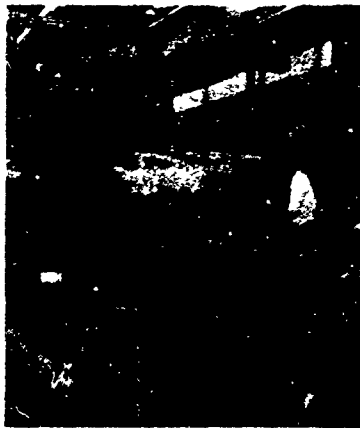
335/667

Figure 301. Inflated Apex Being
Inspected on Test Stand

335/670

Figure 302. Apex After Rupture
During Pressure
Testing

335/672

Figure 303. Close-up Views of
Ruptured Area of
Apex

335/671

Figure 304. Close-up Views of
Ruptured Area of
Apex

500

Some bulging was noted at 1.0 psig where the metal fabric tape wraps stopped and the stub booms became tangent to the toroid. At 2.0 psig, the cord slackened approximately 0.5 inch indicating that the booms did move toward each other slightly. The pressure was increased to 3 psig and then to 4 psig and held for 3 minutes. The only change was that the cord became taut indicating that the leading edge booms were again moving outward.

The pressure was increased to 5.0 psig and the time was recorded for the pressure to drop back to 4 psig. This pressure loss for the bladder lined apex took 5.1 minutes. The pressure was then increased to 5.0 psig again and held for 1 minute.

Upon increasing the pressure to 6.0 psig, a slight noise or rumble was heard, and the pressure was held for an additional 3 minutes. It was believed that this noise was the rubber bladder slipping into equilibrium position within the apex. The pressure was increased to 7.0 psig; the cord was still tight, and this condition was held for 3 minutes. When the pressure was increased to 7.2 psig, an additional rumble or noise was heard from within the apex assembly and again it was assumed that the bladder folds were moving, particularly since the bladder was T shaped and did not exactly conform to the toroidal shape of the apex. The pressure of 7.2 psig was held for 2 minutes and then increased to 8 psig and held for an additional 2 minutes. The cord was still tight.

Upon increase of the pressure to 8.8 psig, an additional small noise was heard and this pressure was held for 0.5 minutes. The pressure was then increased to 9 psig and after holding 1 minute at this pressure the apex ruptured with a loud report along the right side of the keel boom near the area of the right crotch. When the apex ruptured and collapsed it appeared as shown in Figure 302. Closeup views of the ruptured area are shown in Figures 303 and 304.

One tear went completely around the apex center keel stub boom starting approximately 10 inches on one side of the header strip proceeding around the crotch area and 4 inches beyond the opposite header. The lowest tape on the center keel boom was torn loose at the weld on the header strip as may be seen in Figure 305.

The tapes in the opposite crotch were undamaged except for one which was also torn loose at the weld on the center keel boom header. The tear down the center keel boom started below the crotch area and progressed down to within 10 inches of the cuff as shown in Figure 306.

The opposite crotch was also torn in the cross ply just within the first tape wrap between the stub boom and the crotch as shown in Figure 307. A view of the three lateral reinforcing tapes on the inside of the torn crotch is shown in Figure 308.

The center keel boom was also torn along the tangency weld joint of the cross ply for approximately 12 inches. The plies were delaminated around the torn areas and there was indication of inadequate bonding between the two fabric layers. The RTV 655 was not clear but cloudy or milky appearing. Some

501
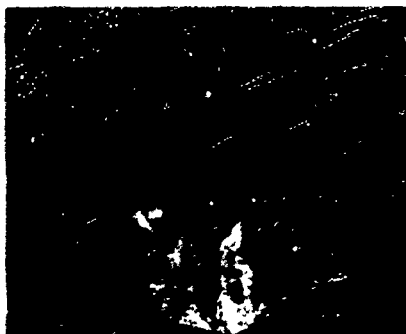
335/689

335/686

335/678

Figures 305, 306, 307 and 308.   Views of Torn Crotch Areas of Apex
After Pressure Test Rupture

areas appeared slightly green colored as if green chromate vacuum paste may have contaminated the RTV 655 during impregnation.

The apex assembly was then layed out as shown in Figure 309 for folding and packaging to determine package volume. It was progressively folded as shown in Figures 310, 311, and 312. Although about 6 inches longer than the rolled and packaged boom, the apex folded into a package somewhat smaller in diameter than the boom as was evidenced by fitting it into the boom packaging can (14 inch O.D. by 48 inches long) as shown in Figure 313.

Some observations prepared by the Space-General Structural Engineering Department on the failure of the apex are as follows:

a.   The failure appears to have initiated in the cross-ply (near a weld seam) at the horizontal tangency center line of the keel stub boom and the crotch radius.

b.   Failure was initiated on both left and right sides of the keel boom indicating reasonably symmetrical loading.

c.   Since the tear was predominantly circumferential around the keel boom, the failure was due to a meridional (longitudinal) stress.

d.   The bias ply was fabricated with some wrinkles as reported in Section 3.10.7.2 (these were evident in the torn specimen); therefore, it could not have assumed its share of the load unless the silicone coating acted as a structural bonding agent.

e.   The silicone coating appeared irregular and of doubtful strength, probably due to the difficulties in obtaining a proper cure as discussed in Section 3.10.7.3.

f.   The three longitudinal reinforcing metal fabric straps attached to the interior of the bias ply may have carried part of the longitudinal load at the reentrant corner prior to cross ply failure. These straps were intact after failure (see Figure 308). On one side of the keel stub boom, the bias ply tore around the ends of the strap. On the other side of the keel stub boom, the bias ply was intact. Therefore it appears that the bias ply failed subsequent to the cross ply.

g.   It appears that failure at the top of the keel boom could have initiated prior to progression of the reentrant corner tear to the top. This could indicate a high stress area at the top which became critical when failure at the reentrant corner reduced the cross sectional area of the boom structural fabric.

h.   The failures appear to have initiated and progressed predominantly along weld seams. The fabric failure was typical of other components indicating that weld strengths were probably adequate.

503

335/699

Figure 309. Apex Laid-Out
for Folding

335/700

Figure 310. Folding Apex
Initial

335/701

Figure 311. Folding Apex
Final

335/704

Figure 312. Apex Folded and
Held with Straps

335/706

Figure 313. Folded Apex Fitted Into Boom Packaging Can to Show
Relative Size

i. Since the failure occurred at 9.0 psig, the nominal circum-
ferential (hoop) membrane load in the keel boom would be
9 x 16 = 144 pounds per inch. The nominal meridional
(longitudinal) membrane load would be 72 pounds per inch.
These are well below the normal fabric and welded joint
load carrying capability so significant stress concentrations
must have occurred.

Section 4

CONCLUSIONS

High-strength, high-temperature metal fabrics can be designed, woven, and applied to the construction of complicated space structures which also have many other applications. Such metal fabrics can be welded with a new, special, semi-automatic seam welder which is capable of producing flexible joints of about 70 percent or higher joint efficiency relative to the strength of the parent fabric. Impregnation or saturation of this fabric with silicone rubber by suitable vacuum techniques can produce a void-free matrix which will not blister or delaminate when exposed to vacuum, has high resistance to heat transfer, and prevents abrasion between the metal filaments during packaging or flexing in use. This impregnated metal fabric substrate is capable of being coated with high-temperature ablative, compatible silicone rubber compounds to protect the structural reinforcement in high-temperature or re-entry environments.

The results of the tests on the numerous components, from subscale to full-scale, indicate that both small and large, complex metal fabric reinforced expandable structures can be successfully fabricated by the techniques which have been developed.

Technologies developed in the project are applicable not only to a re-entry vehicle for both manned and payload return but to many other space, air, land, and sea used. These include re-entry decelerators; parachutes and other drag devices; inflatable afterbodies; high-strength space, and land and sea station structures; expandable rocket nozzles; high-temperature, high-strength protective space suits; blast- and radiation-resistant enclosures; bullet- and shrapnel-protection suits and enclosures; inflatable buoys for deep-sea rescue and recovery of large objects such as submarines; inflatable deep-sea buoyant structures; deep-sea vehicle fairings, and numerous other less exotic used such as high-temperature tire reinforcement (and even uses in arthitecture and interior decorating).

It is hoped and anticipated that this new materials and fabrication technology will open a new realm of applications to make man's life more comfortable and his explorations more successful.

REFERENCES

1. Jensen, et. al., <u>Design Guide to Orbital Flight</u>, 708, McGraw Hill Book Co., Inc., New York, 1962.

2. Penland, J. A., "A Study of the Aerodynamic Characteristics of a Fixed Geometry Paraglider Configuration and Three Canopies with Simulated Variable Canopy Inflation at a Mach Number of 6.6," NACA TN D-1022, 1962.

3. Chapman, D. R., "An Approximate Analytical Method for Studying Entry Into Planetary Atmospheres," NACA TN 4276, May 1958.

4. Gammal, A. A., "Charts for Determining Earth-Atmosphere Re-entry Characteristics," Aeronutronics, Ford Motor Company, WADC Contract AF 33(616)-5928, 15 October 1959.

5. Harris, J. T., "High-Temperature Metallic Fabric for Re-entry Applications," SAE Paper 590, October 1962.

6. Watrons, D. L., "SCR Pulse-Power Supply for Resistance Welding," Technical Paper 63-1447, IEEE Transactions for Communications and Electronics, July 1964.